UNIVERSITY OF LIVERPOOL

PROTEOMIC AND METABOLOMIC SIGNATURES OF ARTHROPATHIES

Thesis submitted in accordance with the requirements of the University of Liverpool for the degree of Doctor in Philosophy

By

James Ross Anderson

March 2019

Contents

Acknowledgements

Firstly, it is an honour for me to thank my primary supervisor Professor Mandy Peffers. Throughout my PhD Mandy's extensive knowledge of cartilage biology and mass spectrometry, encouragement, guidance, support, limitless enthusiasm and ability to push me outside of my comfort zone has been invaluable. Thank you also to my co-supervisors, Professor Pete Clegg for his profound knowledge of cartilage biology and advice throughout my PhD, Dr Luis Rubio-Martinez for all his support and extensive knowledge on joint sepsis and Professor Lu-Yun Lian for her expertise in NMR.

During my time in Liverpool it has been a privilege to work in the musculoskeletal biology group where I have felt extremely well supported and met some fantastic people. In particular I would like to thank Jade, Danae, Panos, Aibek, Kirsty, Ben, Katie, Phil, Megan, Helen, Eithne, Simon, Alan, Yalda, Aggie, Kiran, Luke, Fai, David, Nathalie, Sumaya, Rhiannon, Danielle, Lina and Sarah for their friendship and help.

Within the NMR centre I would like to give my sincerest gratitude to Dr Marie Phelan who is a true unsung hero. A huge thank you to Marie for teaching me everything about NMR, including sample preparation, the underlying science and statistics and the frustrating world of Linux coding! Thank you to Marie also for her unwavering patience with me! Thank you to Mr Rudi Grosman who has been a brilliant NMR companion over the last few years and I am hugely grateful for all his computer and coding assistance!

At the Centre for Proteome Research, University of Liverpool, I would like to thank Professor Rob Beynon for allowing me unlimited access to mass spectrometers and processing software and allowing me to integrate with his group and present regularly at their lab meetings - providing lots of great ideas! Thank you to all the students and staff within the group for their help, in particular Dr Phillip Brownridge, Dr Deborah Simpson, Dr Catarina Franco and Ms Lynn McClean for all their advice and fixing the mass spectrometer on various occasions!

For statistical help with this project I would like to thank Professor Andy Jones and,

in particular, Dr Eva Caamaño-Gutiérrez and Dr Arturas Grauslys for teaching me the dark art of ‘R’.

Thank you to Ms Valerie Tilston for processing and staining all histology slides used within this thesis.

Thank you to my advisory panel, Professor Rob van 't Hof and Dr Richard Barrett-Jolley, for all their advice during my PhD and off-topic conversations too!

Thank you to F Drury & Sons Abattoir, The Hong Kong Jockey Club, The Philip Leverhulme Equine Hospital, The Royal Liverpool Hospital and Maastricht University Medical Centre for provision of samples which have been invaluable for the completion of this thesis.

In addition to academic support, I would also like to say a big thank you to friends that I made during my MRes year, Tasha, Cat, Luke and Marisol, for their great sense of humour and coffee breaks. I am eternally grateful to my mum and dad who have been a tremendous support to me throughout my life and have fully backed all my decisions during my slightly winding career path. Thank you to them also for so often making the trip up to Liverpool to visit which has always been greatly appreciated. I am also hugely thankful to my girlfriend Gen for allowing me to write, largely undisturbed, at home, regular lunchtime coffee breaks and for having patience with me after coming home grumpy after overnight abattoir trips and during my nervous weekends running mass spectrometry! Thank you too to Gen’s mum Val for keeping me fed and watered during my countryside writing weekend escapes. Thank you also to the latest addition to the family, Merlin, my domestic short haired lover from Liverpool, for providing necessary distraction.

Thank you to The Horse Trust for generously funding this PhD studentship and to the University of Liverpool Technology Directorate and University of Liverpool Veterinary School for additional project funding and travel grants.

Abstract

Osteoarthritis (OA) and rheumatoid arthritis (RA) are the most common arthropathies in people, causing limited mobility, pain and subsequent reduction in quality of life, resulting in a substantial impact on human society. Conditions affecting articular joints are also common in horses, including OA, osteochondrosis (OC) and synovial sepsis. Despite their high prevalence and clinical relevance, diagnosis, staging, monitoring and determining an accurate prognosis remain a challenge. Thus, there is a need to identify reliable biomarkers of disease. The development of 'omics' technologies, such as metabolomics and proteomics, has provided global analysis of biological tissues and fluids, enabling discovery of disease biomarkers and providing a greater understanding of their underlying pathogeneses. Within this thesis, protocols for collection and processing of synovial fluid (SF) for nuclear magnetic resonance (NMR) metabolomic and liquid chromatography-tandem mass spectrometry (LC-MS/MS) proteomic analysis have been optimised. Lys-C endopeptidase pre-digestion greatly improved on-bead tryptic SF protein digestion when used in conjunction with randomised hexapeptide ProteoMiner™ beads for low abundant protein enrichment. Equine OA was stratified using metabolomic and proteomic SF profiles, identifying a panel of markers which may be applicable to grading OA severity. This is the first study to undertake computational integration of NMR metabolomic and LC-MS/MS proteomic datasets of any biological system. This thesis is also the first study to use a multi 'omics' approach to simultaneously investigate the metabolomic profile of *ex-vivo* cartilage and metabolomic/proteomic profiles of culture media using the TNF-α/IL-1β *ex-vivo* cartilage OA model. A panel of metabolites, proteins and neopeptides were identified which were differentially abundant within an early phase of this OA model and may provide further information on the underlying disease pathogenesis. Comparing human OA and RA SF identified that the metabolic pathways that differed most were glycolysis, amino acid biosynthesis and taurine and hypotaurine metabolism. This thesis has also identified a panel of metabolites and proteins within equine SF which can distinguish synovial sepsis from nonseptic joint pathologies, with glucose the principal metabolite discriminator.

Abbreviations

1D	One-dimensional
2D	Two-dimensional
ABC	Adenosine triphosphate-binding cassette
ACR	American College of Rheumatology
ADAMDEC1	A metalloproteinase domain-like protein decysin-1
ADAMTS	A disintegrin and metalloproteinase with thrombospondin motifs
API	Atmospheric pressure ion source
ApoA1	Apolipoprotein A1
ApoA2	Apolipoprotein A2
ATP	Adenosine triphosphate
B_0	External magnetic field
BAP	Bone alkaline phosphatase
BLAST	Basic local alignment search tool
BMP7	Bone morphogenetic protein 7
C1, 2C	Collagen type I and II cleavage
C2C	Collagen type II cleavage
CD14	Cluster of differentiation 14
CHAPS	3-((3-cholamidopropyl) dimethylammonio)-1-propanesulfonate
CID	Collision-induced dissociation
Col CEQ	Collagen CEQ epitope
Col I	Collagen type 1
COMP	Cartilage oligomeric matrix protein
CPII	C-propeptide of type II collagen
CPMG	Carr-Purcell-Meiboom-Gill
CRP	C-related protein
CS	Chondroitin sulphate
CS846	Chondroitin sulphate epitope 846
CTXI	C-terminal telopeptide of type 1 collagen
CTX-II	C-telopeptide fragments of type II collagen
CV	Coefficient of variation
DAPC	Discriminant analysis of principal components
DC	Direct current
DDA	Data-dependent acquisition
DE	Differentially abundant
Delta Di0S	Delta-disaccharide 0S
DIP	Distal interphalangeal
DMARD	Disease-modifying antirheumatic drug
DMEM	Dulbecco's modified Eagle's medium
DMMB	Dimethylmethylene blue
EBI	European Bioinformatics Institute
ECM	Extracellular matrix
EDTA	Ethylenediaminetetraacetic acid
EIF2	Eukaryotic Initiation Factor 2

ELISA	Enzyme-linked immunosorbent assay
ENE2A	Equine neutrophil elastase 2A
ESI	Electrospray ionisation
ESI-LIT	Electrospray ionisation-linear ion trap
ESR	Erythrocyte sedimentation rate
FCS	Foetal calf serum
FDR	False discovery rate
FID	Free induction decay
FP	Femoropatellar
FT	Femorotibial
GAG	Glycosaminoglycan
GC/TOF MS	Gas chromatography/time-of-flight mass spectrometry
GC-MS	Gas chromatography-mass spectrometry
GH	Glenohumeral
GLUT	Glucose transporter
h	Planck's constant
H & E	Haematoxylin and eosin
HA	Hyaluronic acid
HCD	Higher-energy collisional dissociation
HDL	High density lipoprotein
HKJC	Hong Kong Jockey Club
HPLC	High performance liquid chromatography
HRMAS	High resolution magical angle spinning
HSQC	Heteronuclear single quantum coherence
hUNC-93A	Unc-93 homolog A
IC	Intercarpal
IGF	Insulin growth factor
IGFBP6	Insulin-like growth factor-binding protein 6
IL	Interleukin
IL-1β	Interleukin-1β
kDa	Kilodalton
KEGG	Kyoto Encyclopedia of Genes and Genomes
KS	Keratan sulphate
LBP	Lipopolysaccharide binding protein
LC	Liquid chromatography
LC-MS	Liquid chromatography-mass spectrometry
LC-MS/MS	Liquid chromatography-tandem mass spectrometry
LTF	Lactotransferrin
m	Magnetic quantum number
m/z	Mass-to-charge ratio
MALDI	Matrix-assisted laser desorption/ionization
MCP	Metacarpophalangeal
MFT	Medial femorotibial
MMP	Matrix metalloproteinase
mRNA	Messenger ribonucleic acid
MS	Mass spectrometry
MSI	Metabolomics Standards Initiative

MT	Meniscal tear and concurrent OA
MTP	Metatarsophalangeal
M_{xy}	Transverse net magnetisation component
M_z	Longitudinal net magnetisation component
NFE2L2	Nuclear factor (erythroid-derived 2)
NMR	Nuclear magnetic resonance
NSAID	Nonsteroidal anti-inflammatory drug
OA	Osteoarthritis
OC	Osteochondrosis
PBS	Phosphate buffered saline
PC	Principal component
PCA	Principal component analysis
PCR	Polymerase chain reaction
PFA	Paraformaldehyde
PGE_2	Prostaglandin E_2
PLS-DA	Partial least squares discriminant analysis
POD	Palmar/plantar osteochondral disease
ppm	Parts per million
PQN	Probabilistic quotient normalisation
QTOF	Quadrupole time-of-flight
RA	Rheumatoid arthritis
RF	Radiofrequency
RRM2	Ribonucleotide reductase M2 polypeptide
SF	Synovial fluid
sGAG	Sulphated glycosaminoglycan
SDS PAGE	Sodium dodecyl sulphate polyacrylamide gel electrophoresis
S-lens	Stacked-ring ion guide
TC	Tarsocrural
TCA	Tricarboxylic acid
TFA	Trifluoroacetic acid
TIC	Total ion count
TIMP	Tissue inhibitor of metalloproteinase
TNF-α	Tumour necrosis factor-α
TOF	Time of flight
TSP	Trimethylsilyl propionate
UPLC	Ultra-high performance liquid chromatography
VIP	Variables of influence
γ	Gyromagnetic ratio
ΔE	Change in energy state

1. Introduction

1.1. Arthropathies

Arthropathies encompass all joint diseases, with these conditions commonly leading to limited mobility, pain and subsequent reduction in quality of life (Aşkın *et al.*, 2017; Ji *et al.*, 2017). Arthritis is a generic term for inflammatory joint disease, comprising the majority of arthropathies, with osteoarthritis (OA) and rheumatoid arthritis (RA) having the largest impact on human society (Fusco *et al.*, 2017). One-third of people in the UK aged over 45 (approximately 8.75 million) require treatment for OA with an estimated prevalence for RA of 0.5-1% of the adult population within developed countries (Davis and Matteson, 2012; Reynard and Loughlin, 2012; Scott *et al.*, 2010). Conditions affecting the articular joints are also common in horses, resulting in loss of function, pain and/or subsequent inability to work, all of which represent economic and welfare concerns (Anderson, Phelan, *et al.*, 2018). These pathologies include OA, accounting for 60% of lameness seen in horses, osteochondrosis (OC) and synovial sepsis, which can be life-threatening (Caron and Genovese, 2003; Summerhays, 2000). Despite their high prevalence and clinical relevance, diagnosis, staging, monitoring and determination of an accurate prognosis remain a challenge and thus there is a need to identify reliable biomarkers of disease (Anderson, Phelan, *et al.*, 2018). The development of 'omics' technologies, such as metabolomics and proteomics, has provided global analysis of biological tissues and fluids, enabling discovery of potential disease biomarkers as well as providing a greater understanding of their underlying pathogenesis (Carlyle *et al.*, 2018; Wang, Zhang, *et al.*, 2012).

1.1.1. Synovial Fluid

The synovial membrane, which lines the inner layer of the joint capsule, consists of a one-cell thick layer of synoviocytes, within a hyaluronic acid and collagen matrix, and is responsible for the production of synovial fluid (SF) (Gibson and Rooney, 2007; Mahendran *et al.*, 2017). Although primarily acting as a lubricant within the joint, containing molecules with low-friction and low-wear properties to hyaline articular cartilage surfaces, SF also provides a pool of nutrients for surrounding

tissues and a medium of cellular communication with the semi-permeable synovial membrane allowing passive protein transfer and synoviocytes secreting regulatory cytokines and growth factors (Blewis *et al.*, 2007; Gibson and Rooney, 2007; Mahendran *et al.*, 2017; Tamer, 2013). Given this passive movement of proteins, below a certain size, across the synovial membrane, SF can be considered a dialysate of plasma (Sundblad, 1950). Due to the close relationship, both in terms of location and biological communication, that SF holds with surrounding tissues which are primarily altered during orthopaedic pathologies, SF provides a unique source of chemical information and holds great promise for biomarker discovery (Anderson, Phelan, *et al.*, 2018; Mateos *et al.*, 2012). SF can also be sampled from conscious horses with relative ease, meaning that SF analysis has the potential to translate to a clinical setting as a diagnostic aid.

1.1.2. Osteoarthritis (OA)

OA is an age-related degenerative musculoskeletal disease characterised by a loss of articular cartilage, abnormal bone proliferation, synovial membrane dysfunction, subchondral bone sclerosis and altered biochemical and biomechanical properties (Figure 1) (Kramer, Tsang, *et al.*, 2014; Truong *et al.*, 2006). Despite a high prevalence within humans and numerous mammal species, OA aetiology and pathophysiology remains poorly understood with an inability to achieve early diagnosis. A clinical human study of OA has identified distinct patterns of protein expression suggesting separate subgroups of disease which are independent of the duration of OA, highlighting the complexity of this condition (Gobezie *et al.*, 2007).

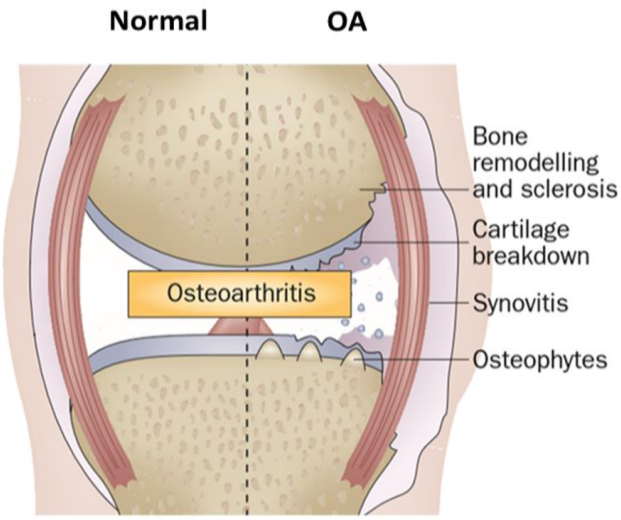

Figure 1. Characteristic gross pathologic joint changes associated with osteoarthritis (OA). Adapted from Wluka *et al.*, 2013.

For horses in the UK, OA is one of the leading welfare issues, resulting in substantial morbidity and mortality (Ireland *et al.*, 2011, 2012). Although recent advances in diagnostic imaging have improved identification of the condition, the slow onset of OA often leads to substantial pathology of the joint and articular cartilage prior to diagnosis (Brommer *et al.*, 2003). There is therefore a need to develop diagnostic tests which are sensitive and specific to the early stages of OA, with the ability to achieve a diagnosis, which are repeatable and reproducible, as well as enabling a greater understanding of the underlying pathogenesis (Hunter *et al.*, 2014; McIlwraith *et al.*, 2018). Although non-steroidal anti-inflammatory drugs and corticosteroids are often utilised to reduce inflammation and pain associated with OA, these pharmaceutical agents are limited as to the extent they can slow OA progression (Caron and Genovese, 2003; Kramer, Tsang, *et al.*, 2014). Thus, current management of OA is entirely symptomatic, with no treatments able to prevent or reverse the condition; in order to manage this debilitating condition more effectively it is hoped that ongoing interrogation of OA tissues at a molecular level will identify pathways and molecules which are altered during OA pathogenesis and thus develop novel therapeutic targets.

1.1.2.1. Osteoarthritis Pathogenesis

OA pathology has previously been considered as resultant from repetitive joint overloading, leading to an excessive biomechanical joint stress (Silawal *et al.*, 2018). Additionally, several risk factors have been identified including joint malalignment, ageing, genetic predisposition and obesity, although the underlying pathogenesis of OA remains largely unknown (Xia *et al.*, 2014). Whilst obesity leads to increased joint loading, OA has also been identified within non-weight bearing joints in obese individuals, suggesting complex metabolic interactions are involved within the underlying disease pathogenesis (Griffin and Guilak, 2008; Oliveria *et al.*, 1999; Pottie *et al.*, 2006).

1.1.2.1.1. Articular Cartilage

Articular cartilage is a porous, highly hydrated connective tissue which lacks vascular, nervous and lymphatic structures (Bonassar *et al.*, 1995). The extracellular matrix (ECM) consists of 15-20% (wet weight) collagen type II, 4-7% proteoglycans and < 5% collagen types V, VI, IX, X, XI, XII and XIV, perlecan, lumican, biglycan, epiphycan, fibromodulin and decorin (Xia *et al.*, 2014). The ECM provides the unique mechanical properties of articular cartilage, generating elasticity and high tensile strength, enabling normal function (Buckwalter *et al.*, 2005). Chondrocytes are the only cell type present within articular cartilage and are responsible for both the generation and maintenance of cartilaginous ECM (Heijink *et al.*, 2012). Although repeated mechanical loading is essential for chondrocyte regulation of metabolic activity, excessive loading results in cartilage inflammation and degradation facilitated via the release of inflammatory and ECM-degrading factors including tumour necrosis factor-α (TNF-α), interleukin-1β (IL-1β) and matrix metalloproteinases (MMPs) (Silawal *et al.*, 2018). In particular, MMP-13 preferentially cleaves collagen type II, although it also degrades other ECM proteins including collagen types IV and IX, aggrecan and perlecan (Xia *et al.*, 2014). As well as joint instability and overloading, the above mentioned OA risk factors disrupt whole joint homeostasis leading to the release of various catabolic and

inflammatory factors, in which cytokines TNF-α and IL-1β hold a central role, inducing a low grade inflammation and MMP activation (Silawal *et al.*, 2018).

1.1.2.2. Human Osteoarthritis Biomarkers

Biomarkers associated with the musculoskeletal system are usually normal products or by-products of metabolic processes which can be used to assess abnormal turnover of skeletal tissue (Billinghurst, 2002; McIlwraith, 2005). Various markers of OA have been described in humans, identified in urine, serum and SF, including collagen type II, cartilage oligomeric matrix protein (COMP), tissue inhibitors of metalloproteinases (TIMPs) and MMPs (Rousseau and Delmas, 2007). However, to date few have been approved by regulatory authorities for OA diagnosis, prognosis or monitoring (Bay-Jensen *et al.*, 2016).

1.1.2.3. Equine Synovial Fluid Osteoarthritis Biomarkers

Various studies have investigated potential OA biomarkers in SF, utilising both clinical samples and experimental OA models and identifying numerous potential equine OA markers (Table 1). These markers of interest include several proteins. Similarly to human OA studies, MMP activity/abundance within SF has shown diagnostic potential for equine OA (Ariza-Suárez *et al.*, 2017; Brama *et al.*, 1998, 2004; Clegg *et al.*, 1997; Fietz *et al.*, 2008; Jouglin *et al.*, 2000; Ma *et al.*, 2017; Misumi *et al.*, 2001; Zrimsek *et al.*, 2007). However, studies investigating COMP levels have revealed conflicting results with SF COMP abundance unable to stage equine OA (Arai *et al.*, 2005; Bertuglia *et al.*, 2016; Clegg *et al.*, 1997; Misumi *et al.*, 2001; Skiöldebrand *et al.*, 2001; Taylor *et al.*, 2006; Yamanokuchi *et al.*, 2009; Zrimsek *et al.*, 2007). Elevated levels of the neuropeptide substance P have been identified within OA SF and have been associated with joint pain (de Grauw, van de Lest, *et al.*, 2006; de Grauw *et al.*, 2009; Kirker-Head *et al.*, 2000). Additionally, non-protein molecules have been reported as potential OA biomarkers. Elevated SF levels of keratan sulphate, chondroitin sulphate and prostaglandin E_2 have been associated with OA pathology (Alwan *et al.*, 1990; Baccarin *et al.*, 2014; Bertone *et al.*, 2001; Frisbie *et al.*, 2003, 2008; Gibson *et al.*, 1996; de Grauw *et al.*, 2009; Kirker-Head *et al.*, 2000). However Brown *et al.* identified that SF chondroitin

sulphate levels were not indicative to that of cartilage (Brown *et al.*, 1998). Results regarding glycosaminoglycan levels (GAG) have been contradictory, with both elevated and decreased levels identified within equine OA SF depending on the study (Alwan *et al.*, 1991; van den Boom *et al.*, 2005; Frisbie *et al.*, 2003; Palmer *et al.*, 1995).

These markers are generated following significant joint pathology, including substantial articular cartilage degradation, and thus there is a need to identify markers at an earlier disease stage, when intervention would provide the most benefit. Presently, no biomarkers which are specific to equine OA have been identified and none used to aid earlier clinical diagnosis (Anderson, Phelan, *et al.*, 2018). There is therefore a need to identify markers and develop diagnostic tests which are sensitive and specific to the early stages of OA, which are repeatable and reproducible, as well as gaining a greater understanding of the underlying pathogenesis (Hunter *et al.*, 2014; McIlwraith *et al.*, 2018).

Table 1. Potential equine osteoarthritis biomarkers identified within studies investigating synovial fluid.

Authors	Clinical or Experimental OA	Tissue Type	Main Techniques	Increased in OA	Decreased in OA
Alwan *et al.*, 1990	Clinical	SF and Serum	ELISA	SF: KS, Serum: KS	
Alwan *et al.*, 1991	Clinical	SF, Serum and Urine	DMMB	SF, Serum and Urine: GAG	
Arai *et al.*, 2005	Clinical	SF	ELISA, Western Blotting	COMP, COMP fragmentation	
Arai *et al.*, 2008	Clinical	SF, Serum and Urine	Western Blotting, ELISA	Urine: COMP/creatinine ratio	
Ariza-Suárez *et al.*, 2017	Clinical	SF	ELISA	MMP-3	
Baccarin *et al.*, 2014	Clinical	SF	Gel Electrophoresis	Chondroitin Sulphate (articular cartilage damage)	
Bertone *et al.*, 2001	Clinical	SF	ELISA	IL-6 and PGE_2	
Bertuglia *et al.*, 2016	Clinical	SF and Serum	ELISA	SF: IL-1β, IL-6, TNF-α, CTX-II, COMP, TNF-α, Serum: CTX-II, COMP, TNF-α	
Brama *et al.*, 1998	Clinical	SF	Fluorometric MMP activity assay	MMP activity	
Brama *et al.*, 2004	Clinical	SF	Fluorometric MMP activity assay	MMP-1 activity	
Brown *et al.*, 1998	Clinical	SF and Cartilage	Capillary zone electrophoresis	SF: CS not indicative of cartilage CS, Cartilage: Percentage of delta Di0S	Cartilage: 6-sulfation of CS terminal residues
Chiaradia *et al.*, 2012	Clinical	SF	2D-gel electrophoresis, MALDI-TOF-MS, nano LC-ESI-LIT-MS/MS	Complement component C4A, Carboxylesterase D1, α-2-Macroglobulin, Ceruloplasmin, Inter-α-trypsin inhibitor heavy chain H1-like, Serotransferrin, Vitamin D binding protein, Antithrombin III, Serum albumin, Haptoglobin, Apoliprotein A-I	Plasminogen, Serum albumin, Afamin, α-1B-glycoprotein, Ig γ 5 heavy chain constant region, Haptoglobin, Transthyretin
Cleary *et al.*, 2010	Experimental	SF and Serum	ELISA	SF: CTX-II	Serum: CTX-II
Clegg *et al.*, 1997	Clinical	SF	Gelatin zymography	MMP-2, MMP-9 activity	
Dagleish *et al.*, 2003	Clinical	SF	ELISA, Western Blotting	ENE2A (Inflammation)	
de Grauw, van de Lest, *et al.*, 2006	Clinical	SF	Immunoassay	Substance P (clinical joint pain)	
de Grauw *et al.*, 2009	Experimental (Inflammation)	SF	ELISA, fluorimetric assay, 1,9-dimethylmethyleneblue assay	PGE_2, substance P, bradykinin and MMP activity, GAG, CS846 epitope, C2C, CPII, collagen II markers	
Fietz *et al.*, 2008	Clinical	SF	Gelatin zymography and immunocapture activity assays	MMP-2, MMP-9 activity	
Frisbie *et al.*, 1999	Clinical	SF and Serum	UNKNOWN	SF: epitope 846 and total protein concentrations, linearly related to osteochondral fragmentation grade, Serum: epitope 846 and CPII concentrations	
Frisbie *et al.*, 2002	Experimental	SF and Serum	UNKNOWN	Serum: CS846, CPII, sGAG and CTXI. Serum osteocalcin and CS846 best predictors of pain	

Frisbie *et al.*, 2003	Experimental	SF	UNKNOWN	CS-846, PGE_2, sGAG, CPII, COL2–3/4C_{short}, osteocalcin	
Frisbie *et al.*, 2008	Experimental	SF and Serum	ELISA	SF: CS846, CPII, Col CEQ, C1,2C, osteocalcin, Col I and PGE_2, Serum: CS846, CPII, GAG and C1,2C	
Fuller *et al.*, 2001	Clinical	SF	ELISA, dimethylmethylene blue assay	Bone specific alkaline phosphatase	Hyaluronan, 5D4 epitope of keratan sulphate, KS:GAG ratio
Gibson *et al.*, 1996	Clinical	SF	ELISA, radioimunoassay	PGE_2	
Jouglin *et al.*, 2000	Clinical	SF	Gelatin zymography	MMP-9 monomer and dimer	
Kamm *et al.*, 2013	Experimental	SF, cartilage, synovial membrane, WBCs, Serum	Microarray, PCR, ELISA	WBCs: hUNC-93A mRNA	WBCs: ADAMDEC1 mRNA, RRM2 mRNA
Kawcak *et al.*, 2008	Experimental	SF	ELISA	Type I and Type II collagen	
Kirker-Head *et al.*, 2000	Clinical	SF	Radioimmunoassay	Substance P and prostaglandin E_2	
Ley *et al.*, 2007	Clinical	SF	Bioassay using proliferation of IL-6-dependent murine B9 hybridoma cells	IL-6 (Osteochondral fragmentation)	
Ma *et al.*, 2017	Experimental	SF	ELISA	Before OA Symptoms: IL-1, IL-6, MMP-9, MMP-13, ADAMTS-5, CS846, GAG, HA, CTX-II and COMP, After OA Symptoms: TNF-α, MMP-2 and MMP-3	
Misumi *et al.*, 2001	Clinical	SF	ELISA, Western Blotting	COMP fragments, MMP gelatinolytic activity	COMP
Misumi *et al.*, 2002	Clinical	SF and Serum	ELISA		Serum: COMP, KS
Nicholson *et al.*, 2010	Clinical	SF and Serum	ELISA	SF: CPII, CTX-II, C1,2C, C2C, Serum: C1,2C	SF: Serum: CTX-II, C2C
Palmer *et al.*, 1995	Clinical	SF and Serum	DMMB, colorimetric assay	SF: GAG, CS, KS	
Peffers *et al.*, 2015	Clinical	SF	LC-MS/MS	S100-A10, CD109 antigen, Phospholipid transfer protein isoform 1, Complement component C8 gamma chain	Collagen alpha-1(I) chain, Calsyntenin-1, Integral membrane protein 2B, Mannan-binding lectin serine protease 2, Keratin, type II cytoskeletal 7, Cyclin D binding myb-like transcription factor 1 isoform 1
Reesink *et al.*, 2017	Experimental & Clinical	SF, synovial membrane and cartilage	ELISA, PCR	SF: Lubricin, Synovial membrane: Proteoglycan 4	Cartilage: Proteoglycan 4
Ribera *et al.*, 2013	Clinical	SF	Quantitative immunoturbidimetric latex agglutination assay	D-dimer (not statistically different)	
Skiöldebrand *et al.*, 2001	Clinical	SF and Serum	ELISA	Serum: COMP (Swedish Warmblood riding horses)	SF: COMP, Aggrecan, Serum: COMP (Standardbred trotters)

Skiöldebrand *et al.*, 2005	Clinical	SF	ELISA	Fragmented COMP	
Skiöldebrand *et al.*, 2017	Clinical	SF	LC-MS/MS, Neopeptide ELISA	COMP neopeptide (SGPTHEGVC)	
Svala *et al.*, 2017	Clinical	SF	Cartilage explants, ELISA, Western blotting, LC-MS/MS	Monosialylated Core 1 *O*-glycans	Disialylated Core 1 *O*-glycan
Taylor *et al.*, 2006	Clinical	SF	ELISA		COMP
Trumble *et al.*, 2008	Clinical	SF and Serum	ELISA	SF: BAP (Concentrations of BAP in the serum (< 30 U/L), SF (> 22 U/L) and a 0.5 ratio of SF to serum were predictive of OC injury)	Serum: BAP
Trumble *et al.*, 2009	Clinical	SF	ELISA	Type II collagen degradation product (collagenase cleavage neoepitope commercially known as C2C)	
van den Boom *et al.*, 2004	Adult Horses - Clinical (Abattoir samples)	SF	HPLC, Hydroxyproline assay	Hydroxyproline positively correlated with cartilage degeneration index and general MMP activity	
van den Boom *et al.*, 2005	Clinical	SF	(HPLC) analysis following derivatisation with a fluorescent label of secondary amino acids, 1,9-dimethylmethylene blue assay (DMMB), modified fluorometric assay	Positive correlation between MMP activity and hydroxyproline	GAG
Yamanokuchi *et al.*, 2009	Clinical	SF and Serum	ELISA	SF: COMP, Serum: COMP	
Zrimsek *et al.*, 2007	Clinical	SF	Gelatin zymography	MMP-2 and MMP-9 activity	

Abbreviations: ADAMDEC1 = a metalloproteinase domain-like protein decysin-1, ADAMTS-5 = a disintegrin and metalloproteinase with thrombospondin motifs-5, BAP = bone alkaline phosphatase, C1, 2C = collagen type I and II cleavage, C2C = collagen type II cleavage, Col CEQ = collagen CEQ epitope, Col I = collagen type 1, COMP = cartilage oligomeric matrix protein, CPII = C-propeptide of type II collagen, CS = chondroitin sulphate, CS846 = chondroitin sulphate epitope 846, CTXI = C-terminal telopeptide of type 1 collagen, CTX-II = C-telopeptide fragments of type II collagen, delta Di0S = delta-disaccharide 0S, DMMB = dimethylmethylene blue, ELISA = enzyme-linked immunosorbent assay, ENE2A = equine neutrophil elastase 2A, ESI-LIT = electrospray ionisation-linear ion trap, GAG = glycosaminoglycan, HA = hyaluronic acid, HPLC = high performance liquid chromatography, hUNC-93A = Unc-93 homolog A, IL = interleukin, KS = keratan sulphate, LC-MS/MS = liquid chromatography-tandem mass spectrometry, MALDI-TOF-MS = matrix-assisted laser desorption/ionization-time of flight-mass spectrometry, MMP = matrix metalloproteinase protein, mRNA = messenger ribonucleic acid, OA = osteoarthritis, PCR = polymerase chain reaction, PGE_2 = prostaglandin E_2, RRM2 = ribonucleotide reductase M2 polypeptide, SF = synovial fluid, sGAG = sulphated glycosaminoglycans, TNF-α = tumour necrosis factor-α.

1.1.2.4. TNF-α/IL-1ß Osteoarthritis Model

TNF-α and IL-1β are both pro-inflammatory cytokines which are central to OA pathogenesis (Wojdasiewicz *et al.*, 2014). TNF-α and IL-1β, secreted by mononuclear cells, synoviocytes and articular cartilage, upregulate gene expression of MMPs, ADAMTS-4 and ADAMTS-5, leading to significant ECM degradation (Fernandes *et al.*, 2002; Goldring and Goldring, 2004; Wang *et al.*, 2011). Elevations in TNF-α and IL-1β are regularly identified within OA SF, including that of horses (Bertuglia *et al.*, 2016; Ma *et al.*, 2017; Westacott *et al.*, 1990). TNF-α and IL-1β have therefore become established experimental treatments for modelling OA pathology within *in vitro* and *ex-vivo* studies (Williams, 2014). These two cytokines have been utilised in combination, and separately, to model OA using both chondrocyte cultures as well as cartilage explants (De Ceuninck *et al.*, 2004; Pretzel *et al.*, 2009; Stevens *et al.*, 2008, 2009; Williams, 2014).

1.1.2.5. Osteoarthritis Stratification

The heterogeneous nature of OA suggests varying underlying aetiologies, with studies identifying different molecular subgroups which are independent of OA duration/severity (Gobezie *et al.*, 2007; Soul *et al.*, 2018). When grouping OA, current literature has applied the term 'stratification' to refer both to these subgroups, which are distinct from OA severity, as well as to groups which are able to stage OA according to severity (Berger *et al.*, 2012; Schiphof *et al.*, 2013; Soul *et al.*, 2018; Turmezei *et al.*, 2014). Within this thesis, the term 'stratification' has been used in reference to the identification of molecular profiles/markers which are able to grade OA severity.

1.1.3. Osteochondrosis (OC)

OC commonly affects growth cartilage of both humans and domesticated animals; including rats, cats, dogs, pigs, cows and horses (Ytrehus *et al.*, 2007). Currently, the underlying aetiology and pathogenesis of OC is not fully understood (McCoy *et al.*, 2013). OC involves a focal disturbance of endochondral ossification within the epiphyseal-articular cartilage complex during bone growth (de Grauw *et al.*, 2011;

Rejnö and Strömberg, 1978). An interrupted blood supply to epiphyseal cartilage channels leads to focal regions of chondronecrosis, resulting in clefts which extend through the articular cartilage and into subchondral bone (McCoy *et al.*, 2013). In horses, OC is the most common developmental joint disorder, presenting clinically with lameness, joint distension, postural abnormalities, reduced activity levels, stiffness and a reluctance to get up (de Grauw *et al.*, 2011; Wright and Minshall, 2005). In equine OC, elevated levels of a C-propeptide of cartilage type II procollagen, osteocalcin, prostaglandin E_2 and leukotriene B4 have shown potential as a diagnostic aid (Billinghurst *et al.*, 2004; Donabedian *et al.*, 2008; de Grauw, Brama, *et al.*, 2006; Laverty *et al.*, 2000). However, these markers have not translated to clinical practice.

1.1.4. Synovial Sepsis

In horses, synovial sepsis is most commonly caused by injuries penetrating synovial structures leading to bacterial contamination and subsequent infection (Haltmayer *et al.*, 2017; Robinson *et al.*, 2017). Although life threatening, early diagnosis and timely treatment intervention results in improved survival (Robinson *et al.*, 2017). However, to date, no validated markers which are both sensitive and specific to synovial sepsis have been identified within veterinary medicine, making early diagnosis a challenge.

1.1.4.1. Synovial Sepsis Diagnosis

Together with clinical examination, synovial sepsis diagnosis is based on SF culture and intracellular bacteria identification (both low sensitivity) as well as total protein, total nucleated cell count and percentage of neutrophils whose results are open to interpretation and are affected by standard treatment protocols (Robinson *et al.*, 2017; Sanchez-Teran, Bracamonte, Hendrick, Burguess, *et al.*, 2016; Sanchez-Teran, Bracamonte, Hendrick, Riddell, *et al.*, 2016; Sanchez Teran *et al.*, 2012). Reduced levels of glucose in human and equine SF, due to an increase in synovial and neutrophil cell glycolytic activity in severe inflammation or infection, have previously been identified, with a serum-synovial glucose difference of > 2.2 mmol/L considered supportive of a diagnosis of synovial sepsis (Krey and Bailen,

1979; Roberts *et al.*, 1967). However, this parameter is non-specific and can be influenced by multiple variables, including synovial necrosis, diet, pain and white blood cell count. Elevations in lactate during the acute infection phase have previously been identified in SF of septic human, canine and equine joints, due to an increase in the consumption of glucose and subsequent production of lactate within an anaerobic environment (Gobelet and Gerster, 1984; Proot *et al.*, 2015; Tulamo *et al.*, 1989). However, other studies have not been able to differentiate septic and non-septic arthropathies based on lactate levels alone (Arthur *et al.*, 1983; Washington, 1980). Synovial D-lactate (produced via bacterial fermentation and a stereoisomer of mammalian L-lactate) was recently found not to aid diagnosis of equine synovial sepsis (Robinson *et al.*, 2017).

1.1.5. Rheumatoid Arthritis (RA)

Although not a condition diagnosed or considered to occur in horses, after OA, RA is the second most common form of arthritis in people and the most common autoimmune arthritis (American College of Rheumatology; Arthritis Research UK, 2018). Despite both these chronic conditions being typically age-related with insidious onset, their underlying aetiologies are markedly different (Brouwers *et al.*, 2015; Majithia and Geraci, 2007). RA is a systemic, inflammatory autoimmune disease that primarily affects the synovium of joints, presenting as a symmetric polyarthritis (Bartok and Firestein, 2010; Davis and Matteson, 2012; Scott *et al.*, 2010). RA joints are marked by inflammation of the synovium and destruction of articular cartilage and underlying bone. The RA synovium becomes hyperplastic with infiltration by a variety of immunocompetent cells (activated neutrophils in particular) (Wright *et al.*, 2014). RA SF is enriched with cytokines, inflammatory mediators such as leukotrienes, and proteases that degrade the ECM and hyaluronic acid (Wright *et al.*, 2012, 2014).

1.2. Metabolomics

Metabolomics encompasses the comprehensive profiling of metabolic changes, including the study of metabolic pathways and quantification of unique biochemical molecules, within living systems (Wang, Zhang, *et al.*, 2012). Small molecule

metabolites include metabolic intermediates, secondary metabolites, hormones and other signalling molecules (Jukarainen, 2009). Metabolomics studies are mainly carried out via two separate platforms, mass spectrometry (MS) or nuclear magnetic resonance (NMR) spectroscopy (Beltran *et al.*, 2012). The major advantage of NMR spectroscopy is the analysis of native samples with a minimal level of sample preparation using a non-invasive and non-destructive method, subsequently producing results which are more reproducible and robust in comparison to those produced through alternative techniques (Keun and Athersuch, 2011). Additionally, unambiguous identification of metabolites compensates for its relatively low sensitivity (Nagana Gowda and Raftery, 2017). However, due to the separate physiochemical properties demonstrated by these different techniques, they can both be applied to the same sample to expand the coverage of identified metabolites and thus provide a wider metabolome interrogation (Beltran *et al.*, 2012; Mickiewicz, Kelly, *et al.*, 2015).

1.2.1. NMR Spectroscopy

NMR spectroscopy utilises magnetic moments of atomic nuclei to inform on molecular structure and dynamics (Blaum, 2010). Angular momentum nuclear spin is dependent upon the interactions between protons and neutrons within the nucleus (Figure 2) (Becker, 2000). With an odd total number of protons and neutrons, ^{1}H nuclei exhibit a spin of ½. These nuclei can adopt two different orientations of equal energy. However, following the application of an external magnetic field (B_0), these energy levels split into higher and lower energy planes (-½ and ½), denoted by a magnetic quantum number (m), whereby ½ is the most stable (Nuclear Magnetic Resonance Spectroscopy, Sheffield Hallam University). This change in energy state (ΔE) can be calculated using the following equation (Escalona, 2015):

$\Delta E = \gamma h B_0 / 2\pi$

ΔE = Change in energy state

γ = Gyromagnetic ratio

h = Planck's constant

B_0 = External magnetic field

Due to a difference between the nuclei populations within each energy state, a small net nuclear magnetisation is generated in the z plane (M_z) in which B_0 is situated. The application of a short, intense pulse of radiofrequency radiation subsequently induces the movement of the nuclear magnetisation away from the z plane, rotating in the xy plane (M_{xy}), and termed precession. A wire coil detects this varying field, generating a current within the coil, oscillating at the frequency of M_{xy}. Following pulse removal and relaxation, this oscillation will decay to zero, termed the free induction decay (FID). Finally, a Fourier Transform is applied to the FID signal to produce an NMR spectrum, with signal intensities proportional to the number of nuclei (Escalona, 2015; Rattle, 1995).

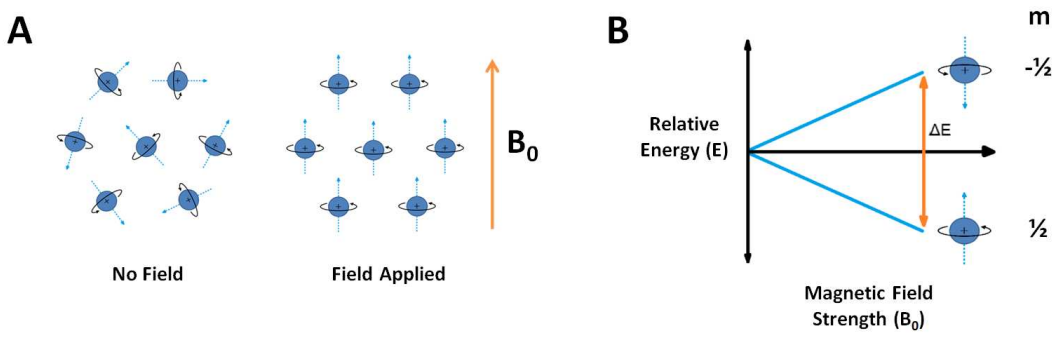

Figure 2. Theory of nuclear magnetic resonance (NMR) spectroscopy. (A) Alignment of ^1H nuclear spins following the application of an external magnetic field (B_0). (B) Transition between energy states following external magnetic field application. m = magnetic quantum number. Adapted from Hunt, University of Calgary.

1.2.1.1. Chemical Shift

The magnetic field applied to the nucleus is partially shielded by the surrounding electron cloud which subsequently results in small differences in the magnetic field experienced by the nucleus compared to the applied B_0 (Brink *et al.*, 1988). On a final NMR spectrum, separate peaks are generated for each ^1H chemical environment within a sample (Rattle, 1995). The chemical shift is usually expressed by the dimensionless parameter parts per million (ppm) from a reference standard, meaning that spectra can be compared irrespective of the field strength in which the spectra was acquired (Escalona, 2015).

1.2.1.2. Spin-Spin Coupling Multiplicity

NMR active nuclei, which are in close proximity, interact with each other via their associated orbiting electrons (Escalona, 2015; Rattle, 1995). Within a molecule consisting of two atoms, the orientation of the nuclear spin of the first nucleus will cause an alteration to the local magnetic environment experienced by the second via these electrons (Rattle, 1995). These spin-spin couplings, also known as J-couplings, result in a splitting of the NMR signal into various groups, generating multiplicity. The number of peaks within these multiplets are dependent on the number of interacting adjacent nuclei, with relative peak intensities following a Pascal's triangle distribution (Escalona, 2015).

1.2.2. Metabolomic Studies of Synovial Fluid Investigating Osteoarthritis

Various studies have used a metabolomics approach to investigate OA through SF analysis, using both MS and NMR platforms (Table 2). Although these studies have generally concentrated on clinical human SF (Hugle *et al.*, 2012; Kang *et al.*, 2015; Kim *et al.*, 2017; Mickiewicz, Kelly, *et al.*, 2015; Zheng *et al.*, 2017), clinical equine SF (Lacitignola *et al.*, 2008), experimental canine SF (Damyanovich *et al.*, 1999) and experimental ovine SF (Mickiewicz, Heard, *et al.*, 2015) have also been studied. Elevated levels of alanine have been identified within OA SF of both dogs and horses (Damyanovich *et al.*, 1999; Lacitignola *et al.*, 2008). As alanine is one of the main amino acid residues which constitutes collagen, it is likely that increased alanine abundance identified within OA SF is resultant of degradation of the

cartilage collagen framework, subsequently releasing alanine into the surrounding SF (Huster *et al.*, 2004; Shet *et al.*, 2012). Identified glucose abundances within OA SF have been contradictory, with two studies describing an elevation in OA (Lacitignola *et al.*, 2008; Mickiewicz, Heard, *et al.*, 2015) whilst another found decreased levels (Damyanovich *et al.*, 1999). Kim *et al.* have previously undertaken an MS-led metabolomics approach to stratify OA in human SF, identifying 90 metabolites differentially abundant between early- and late-OA (Kim *et al.*, 2017). However, to date no studies have undertaken stratification of OA SF using NMR or equine OA SF samples.

Table 2. Metabolomic studies undertaken on synovial fluid which include investigation of osteoarthritis.

Authors	Clinical or Experimental OA	Species	Study Groups	Technique	Total Number of Metabolites Identified	Differentially Abundant Metabolites
Damyanovich *et al.*, 1999	Experimental	Canine	OA & Normal	NMR	Not Stated	**Increased in OA:** acetamide, acetate, alanine, glycerol, hydroxybutyrate, hydroxyisobutyrate, isoleucine, lactate, lipoprotein-associated fatty acids, N-acetylglycoprotcins, pyruvate; **Decreased in OA:** glucose
Hügle *et al.*, 2012	Clinical	Human	OA, RA, gout, calcium pyrophosphate disease, spondylarthritis & septic arthritis	NMR	35	None Stated
Kang *et al.*, 2015	Clinical	Human	OA & RA	UPLC-QTOF-MS	81	**Increased in OA:** 11b-hydroxy-3,20-dioxopregn- 4-en-21-oic acid, 12,20-dioxoleukotriene B4, 3-hydroxymandelic acid, indoleacetaldehyde, indolelactic acid, kynurenine, L-carnitine, lysoPC(18:1), N'-formylkynurenine, N6,N6,N6-trimethyl-L-lysine, phenylactic acid, trihydroxyeicosatrienoic acid/13,14-dihydrolipoxin A4; **Decreased in OA:** (S)-ureidoglycolic acid, 5-L-glutamyltaurine, CE[24:1(15Z)], docosapentaenoic acid, galactosylceramide, methylguanine, taurine, trimethyltridecanoic acid
Kim *et al.*, 2017	Clinical	Human	Early OA & Late OA	GC/TOF MS	114	**Increased in Late Stage OA:** 86 metabolites, including malate, ethanolamine, glycerol, myristic acid, and oleic acid; **Decreased in Late Stage OA:** urate, arabitol, cysteine, and threitol
Lacitignola *et al.*, 2008	Clinical	Equine	OA & Normal	NMR	Not Stated	**Increased in OA:** acetate, alanine, citrate, N-acetylglucosamine, creatine/creatinine, glycerol, HDL-choline, lactate, pyruvate, α-glucose
Mickiewicz, Heard, *et al.*, 2015	Experimental	Ovine	ACL reconstruction (early OA) & Sham-surgical Control	NMR	65	**Increased in early OA:** isobutyrate, glucose; **Decreased in early OA:** uridine, serine, asparagine, hydroxyproline
Mickiewicz, Kelly, *et al.*, 2015	Clinical	Human	OA & Normal	NMR & GC-MS	90	**Increased in OA:** citrate, fructose; **Decreased in OA:** malate, methionine, N-phenylacetylglycine, O-acetylcarnitine, hexanoylcarnitine, creatine, ethanol, athanolamine, 3-Hydroxybutyrate
Zheng *et al.*, 2017	Clinical	Human	OA, RA & Normal	GC-TOF/MS & LC-MS/MS	81	**Increased in OA compared to normal:** threonine, 1,5-anhydroglucitol & gluconic lactone; **Decreased in OA compared to normal:** tyramine, 8-aminocaprylic acid & glutamine; **Decreased in RA compared to normal:** tyramine, 8-aminocaprylic acid & gluconic lactone; **Increased in OA compared to RA:** threonine, 1,5-anhydroglucitol & gluconic lactone; **Decreased in OA compared to RA:** glutamine

Abbreviations: Groups, OA = osteoarthritis, RA = rheumatoid arthritis; Techniques, GC-MS = gas chromatography-mass spectrometry, GC/TOF MS = gas chromatography/time-of-flight mass spectrometry, LC-MS/MS = liquid chromatography-tandem mass spectrometry, NMR = nuclear magnetic resonance, UPLC-QTOF-MS = ultra-high performance liquid chromatography-quadrupole time-of-flight mass spectrometry.

1.3. Proteomics

The term 'proteome' can be defined as the complete complement of proteins and peptides, including modifications, expressed by an organism or cell. The proteome will vary over time and under the influence or various stresses, different conditions and disease states (Christians *et al.*, 2017). Proteomics, first coined by Wilkins (1996), is the umbrella term for proteome study, obtaining information on protein quantities, structure, function, modifications and variations as well as associated/interacting proteins to improve understanding of cellular processes and networks (Wilkins *et al.*, 1996). Clinical proteomics is a subgroup of proteomics, applying these same techniques to clinical specimens in order to discover biomarkers and biosignatures of disease that may be used to aid in diagnosis, prognosis and/or prediction of response to treatment (National Cancer Institute, 2016).

1.3.1. Mass Spectrometry

Mass spectrometry (MS) is a sensitive platform, identifying as little as 10^{-15} moles of a 1 kDa compound, thus allowing compound identification within complex mixtures. MS ionises samples, producing a beam of gaseous ions which are separated according to their mass-to-charge ratio (*m/z*) and their abundances recorded (Kang, 2012). Electrospray ionisation (ESI) and matrix-assisted laser desorption/ionization (MALDI) are the most common methods for ionisation of peptides/proteins prior to MS analysis, involving the addition or removal of a proton (Fenn *et al.*, 1989; Karas and Hillenkamp, 1988). Coupling of ESI to liquid based separation tools allows for the analysis of complex biological samples, ionising the analyte out of solution, when integrated with liquid chromatography (LC) and LC-MS based systems (Peffers, 2013). Ions of a certain *m/z* are then usually isolated from the complex mixture as a preliminary step prior to ion fragmentation with greater characterisation via tandem MS (MS/MS) (Savaryn *et al.*, 2016).

1.3.1.1. Clinical Proteomics

Within the field of clinical proteomics, the discovery of protein biomarkers of disease is presently achieved through a 'bottom-up' approach, utilising MS-based systems which are coupled to either LC or gel electrophoresis methods (Fernandez-Costa *et al.*, 2012). Shotgun proteomics uses this 'bottom-up' approach whereby proteins are denatured, digested into constituent peptides, separated via LC and analysed using MS/MS (Figure 3). Peptide identification can then be inferred by matching the fragmentation spectra generated by MS/MS to theoretical peptide sequence spectra from a protein database and thus use peptides as a surrogate for protein quantification/identification (Klammer and MacCoss, 2006).

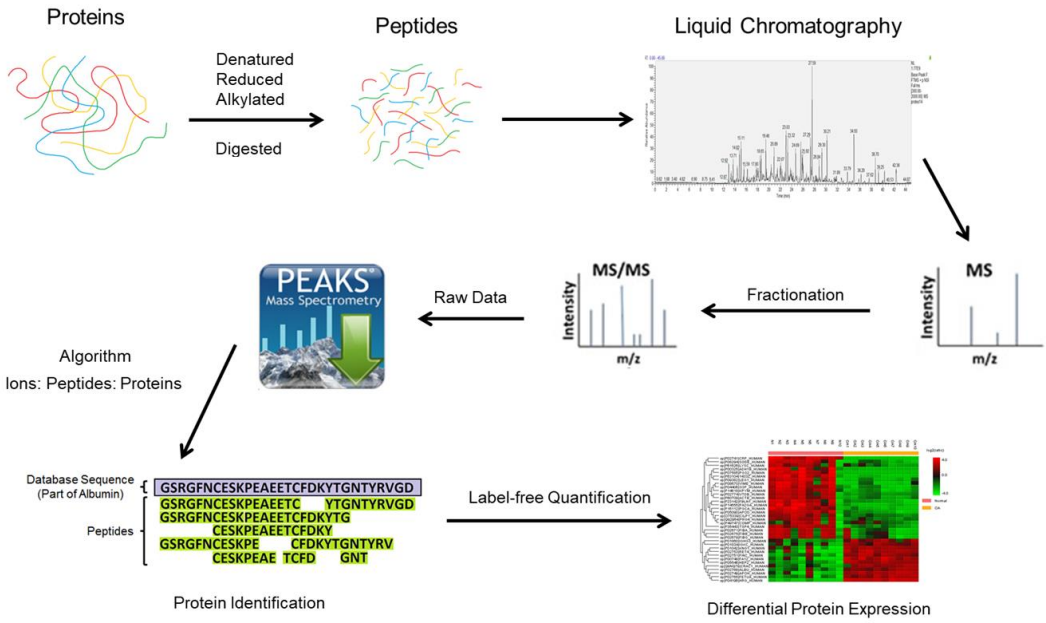

Figure 3. Workflow for label free quantification of protein abundances using a liquid chromatography-tandem mass spectrometry platform.

1.3.1.2. Q Exactive™ Hybrid Quadrupole-Orbitrap™ Mass Spectrometer

The Q Exactive™ is a high performance benchtop quadrupole-orbitrap mass spectrometer which can be employed to analyse complex biological samples

(Michalski *et al.*, 2011). Prior to Q Exactive™ MS analysis, peptides are usually separated via reverse phase C18 high-performance liquid chromatography (HPLC) (Fanigliulo *et al.*, 2011). The Q Exactive™ consists of an atmospheric pressure ion source (API), a stacked-ring ion guide (S-lens), quadrupole mass filter, C-trap, higher-energy collisional dissociation (HCD) cell and an orbitrap mass analyser (Figure 4) (Michalski *et al.*, 2011).

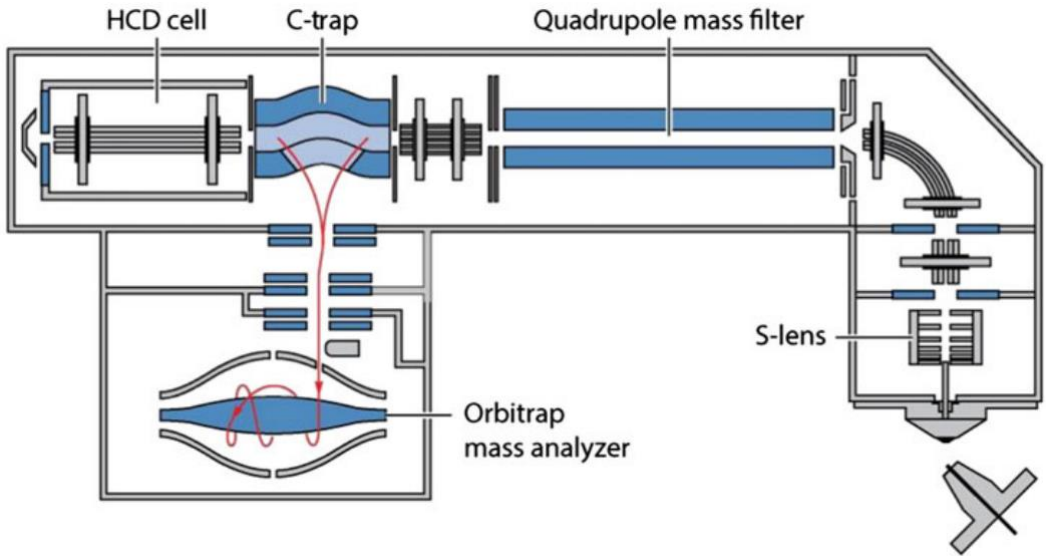

Figure 4. Schematic of the Q Exactive™, a hybrid quadrupole-orbitrap mass spectrometer. Taken from Li *et al.*, 2017.

The S-lens comprises of a series of flat ring electrodes to which radio frequency voltages are applied, focusing the ions into a tight beam, within the central axis where the field is weakest, propelling the ions forward without the need for a direct current gradient (Guan and Marshall, 1996; ThermoFisher, n.d.). The quadrupole mass filter consists of four rods applied with alternate and direct current voltages which alter the transmission of ions, selecting a narrow *m/z* range, due to stabilities within the x-z and y-z planes, thus acting as a band-pass mass filter (Figure 5) (Savaryn *et al.*, 2016). Ions are subsequently cooled and accumulate within a radio frequency only storage C-trap prior to injection via converging lines into an orbitrap for single Fourier transform acquisition (Makarov, 2012; Rosen *et al.*, 2015). Coupling of the C-trap to an HCD cell enables fragmentation of ions, improving fragmentation in the low mass region when compared to traditional collision-

induced dissociation (CID) (Demarque *et al.*, 2016). Finally, within the orbitrap, ions oscillate both around a central spindle-like electrode as well as oscillating in the axial dimension (Figure 5). Electrodes detect this axial oscillation producing an ion oscillation frequency which is unique for each *m/z*. Ion oscillation frequencies are subsequently converted via Fourier transformation into the mass spectrum. Within the orbitrap, all *m/z* values are simultaneously detected (Savaryn *et al.*, 2016).

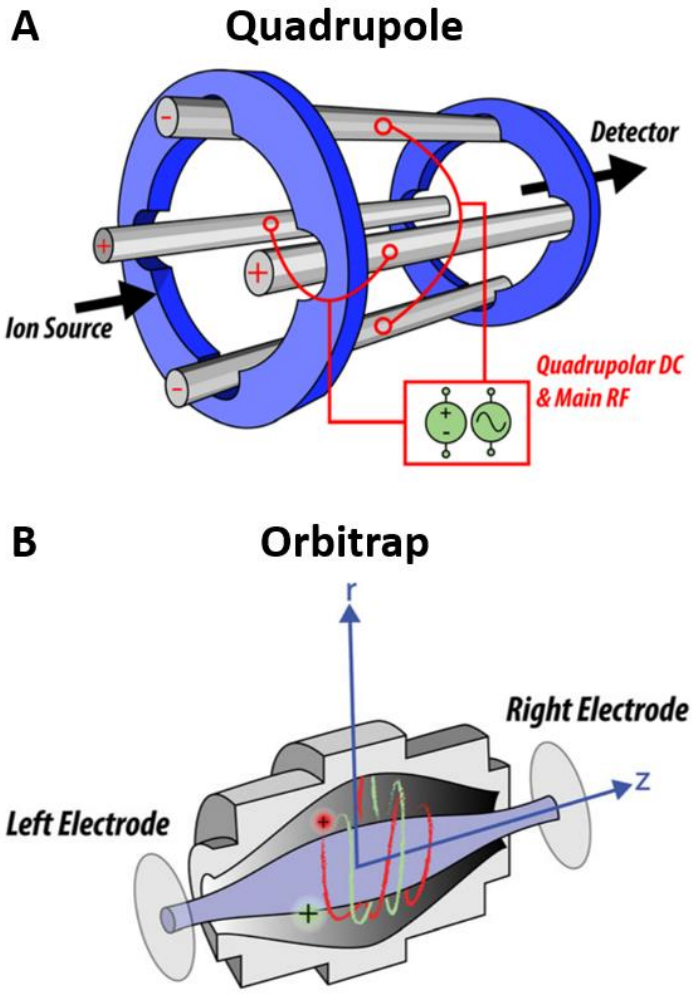

Figure 5. Schematics of the (A) quadrupole and (B) orbitrap chamber components present within specific mass spectrometers. DC = direct current, RF = radiofrequency. Adapted from Savaryn *et al.*, 2016.

1.3.2.1. Biofluid Protein Complexity

The development of liquid chromatography tandem mass spectrometry (LC-MS/MS) has provided a fast and sensitive methodology to identify and quantify proteins within complex biological samples (Hsueh *et al.*, 2014; Mahendran *et al.*, 2017; Peffers *et al.*, 2019). However, the complexity and variability of intensity of proteins within biofluids can lead to many challenges associated with proteome analysis (Puangpila *et al.*, 2015). Similarly to serum, the SF proteome is dominated by highly abundant proteins, with an estimated substantial differential expression of 10x compared to the least abundant proteins, with 95% of the serum proteome consisting of approximately only 20 proteins, although representing just 0.1% of the total number of proteins (Anderson and Anderson, 2002; Fernandez-Costa *et al.*, 2012; Peffers, McDermott, *et al.*, 2015; Roche *et al.*, 2006; Seligner and Kellner, 2006). These high abundant proteins can therefore mask and interfere with the detection of low abundant proteins, thus compromising potential biomarker discovery and understanding of pathogenesis pathways (Shen *et al.*, 2004). This sub-optimal identification of low abundant proteins is essentially due to a limited ion capacity restricting the isolation, fragmentation and detection of the least abundant peptide ions within ion trap mass spectrometers. Thus, until improvements within MS technology allow for increased coverage of the native biofluid proteome, at present, focusing on modifying the concentration dynamic range of biofluids to within the mass spectrometer's detectable dynamic range is the preferred method to quantify low abundant protein biomarkers (Fonslow *et al.*, 2011). However, within the field at this time there is no agreed method to achieve this compression of the protein concentration dynamic range (Fernandez-Costa *et al.*, 2012). Numerous techniques have been applied including the use of immuno-affinity depletion through high performance liquid chromatography columns comprising antibodies to highly abundant proteins (Balakrishnan *et al.*, 2014; Fernandez-Costa *et al.*, 2012; Garner *et al.*, 2013). However a fundamental flaw to this methodology is the resultant loss of low molecular weight proteins of interest that are closely associated with albumin and other highly abundant proteins (Peffers, McDermott, *et al.*, 2015; Zhou *et al.*, 2004).

1.3.2.2. ProteoMiner™ Protein Enrichment Columns

An alternative approach to compress the protein concentration dynamic range involves the use of combinational ligand libraries to achieve peptide-based depletion but allowing preservation of the whole proteome (Furka *et al.*, 1991; Lam *et al.*, 1991). This methodology has recently been used in the development of ProteoMiner™ protein enrichment columns (Bio-Rad Laboratories Ltd., Hemel Hempstead, UK). This technique was found to generate the largest increase in protein identifications compared to other protein depletion methods when applied to serum (Pisanu *et al.*, 2018). The columns consist of an assortment of porous beads which are bound to combinations of randomised hexapeptides (oligopeptides containing six amino acids) generating 64 million combinations from 20 amino acids to which proteins can selectively bind (Figure 6) (Righetti and Boschetti, 2008). Following the introduction and overloading of a complex protein biofluid, ligands selecting for highly abundant proteins will become saturated with excess protein lost in the flow through from the column. Alternatively low abundant proteins will be completely bound to the column, with binding increasing proportionally to protein content of the biofluid introduced (Hartwig *et al.*, 2009; Righetti and Boschetti, 2008). Thus this peptide-based approach produces a compressed protein concentration dynamic range, depleting highly abundant proteins and enriching those less abundant (Fonslow *et al.*, 2011). This technique for quantifying low abundant proteins within a complex biofluid has previously been validated by Hartwig *et al.* (2009) in which human serum was supplemented with *Escherichia coli* lysate. However, the elution solution present within the kit is not compatible with LC-MS/MS analysis, due to the presence of 3-((3-cholamidopropyl) dimethylammonio)-1-propanesulfonate (CHAPS) (Williams, 2014). Although 'clean-up' and alternative elution protocols are available, these introduce a further process in sample preparation and subsequently a source of variation. Peffers *et al.* have previously developed an on-bead trypsin digestion protocol for analysis of ProteoMiner™ processed SF (Davidson *et al.*, 2017; Hulme *et al.*, 2017; Peffers, McDermott, *et al.*, 2015). However, although the reproducibility of ProteoMiner™

beads when used in conjunction with serum has been examined, reproducibility with SF or on-bead digestions have yet to be investigated (Li *et al.*, 2009).

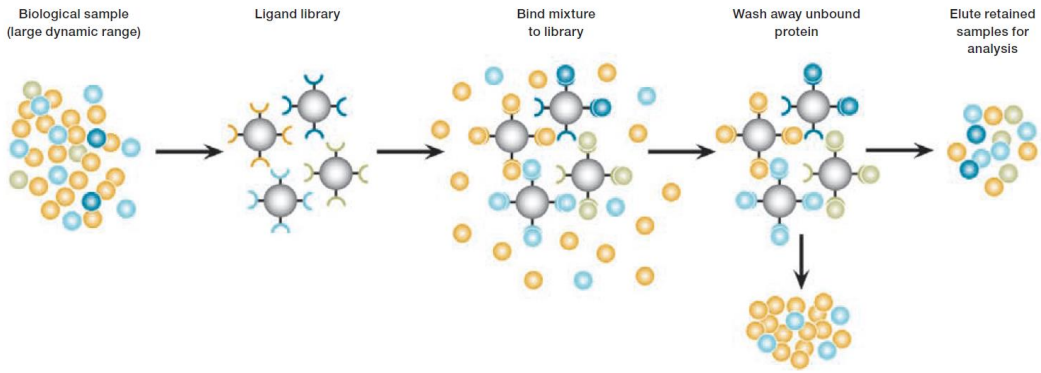

Figure 6. ProteoMiner™ Protein Enrichment Columns. Hexapeptide ligands specifically bind to proteins until saturation, enabling depletion of high abundant proteins and enrichment of low abundant proteins, compressing the protein concentration dynamic range. Taken from Freeby *et al.*, 2010.

1.3.1.2. Semi-Tryptic Peptides and Neopeptides

Increased activity of MMP, ADAMTS, cathepsin and serine protease enzymes during OA leads to cartilage breakdown and the generation of OA-specific peptide degradation products (neopeptides) (Ben-Aderet *et al.*, 2015; Peffers *et al.*, 2016; Polur *et al.*, 2010). During tryptic digestion of biological proteins for MS analysis, arginine and lysine are cleaved on the carboxyl side, unless followed directly by proline (Siepen *et al.*, 2007). Thus non-tryptic peptide degradation sites may be resultant of this increased enzymatic activity during OA, with peptides with one tryptic and one non-tryptic cleavage site referred to as 'semi-tryptic' peptides (Peffers *et al.*, 2016). Using MS, these neopeptides can be identified, quantified and thus utilised as potential molecular biomarkers of early OA. Additionally, a recent mouse study identified that a 32 amino acid peptide fragment, generated through degradation of aggrecan via increased ADAMTS-4/5 and MMP activity, drives OA pain through Toll-like receptor 2 (Miller *et al.*, 2018). Thus, targeting neopeptides may provide analgesia and reduce significant pain associated with joint degeneration. Various studies have identified potential neopeptides associated with

OA in equine cartilage and SF (Peffers *et al.*, 2014; Peffers, McDermott, *et al.*, 2015; Peffers *et al.*, 2016; Skiöldebrand *et al.*, 2017). Subsequent development of neopeptide antibodies would allow for the detection and monitoring of cartilage degeneration as well as assessing response to therapeutics, in both laboratory and clinical settings (Peffers *et al.*, 2017). In addition, identification of OA specific neopeptides may provide novel therapeutic targets.

1.4. Multi 'Omics' Integration

In recent years there has been a huge increase in the number of publications which are reporting results using 'omics' techniques, most highly represented by transcriptomics, genomics, metabolomics and proteomics (Cavill *et al.*, 2016). Computational integration of these separate datasets can work synergistically, greatly enhancing the information that can be obtained opposed to analysing these datasets separately. In light of this, various software programs are now available which undertake pathway analysis and multi 'omics' data visualisation, generating joint pathway p- values (Eichner *et al.*, 2014; García-Alcalde *et al.*, 2011; van Iersel *et al.*, 2008; Xia *et al.*, 2013). In most cases, an optimal experimental design involves the splitting of samples which are subsequently used for appropriate 'omics' studies, termed a 'split sample study' design (Cavill *et al.*, 2016).

Recently, a study has used a multi 'omics' integration approach, utilising genomics, proteomics and miRNomics of human plasma for biomarker discovery in the study of the inherited cardiac disorder Brugada syndrome, providing further information on disease pathogenesis (Scumaci *et al.*, 2018). Within musculoskeletal biology, Ritter *et al.* carried out MS proteomic analysis of early and late stage human OA SF and combined these results with transcriptomic results of articular tissues to inform on the source of differentially abundant synovial proteins (Ritter *et al.*, 2013). Thus, a multi 'omics' approach can still yield more information and further support/validate a study even if the complementary 'omics' approaches are not performed on the same source material or data is drawn from publicly available data repositories. However, despite the growing field of multi 'omics' approaches, to date no studies have combined NMR metabolomics and MS proteomic datasets.

1.5. Hypothesis and Aims

It is hypothesised that the synovial fluid metabolome and proteome can discriminate different articular pathologies and can stratify equine osteoarthritis according to severity.

To answer this hypothesis, the aims and objectives of this study were to:

1. Optimise collection and processing of synovial fluid for NMR metabolomic and LC-MS/MS proteomic analysis (Chapter 2).
2. Compare the metabolite and protein profiles of equine synovial fluid associated with differing severities of osteoarthritis (Chapter 3).
3. Undertake metabolomic and proteomic longitudinal analysis of an *ex-vivo* equine cartilage explant osteoarthritis model (Chapter 4).
4. Compare the human synovial fluid metabolite profiles of osteoarthritis and rheumatoid arthritis (Chapter 5).
5. Undertake metabolomic and proteomic analysis of equine synovial fluid diagnosed with septic and nonseptic articular pathologies (Chapters 6 and 7).

2. Manuscript 1

Optimisation of Synovial Fluid Collection and Processing for NMR Metabolomics and LC-MS/MS Proteomics

James R Anderson[1], Marie M Phelan[2,3], Luis M Rubio-Martinez[1,4], Peter D Clegg[1] and Mandy J Peffers[1]

[1]Institute of Ageing and Chronic Disease, University of Liverpool, Liverpool, UK
[2]Institute of Integrative Biology, University of Liverpool, Liverpool, UK
[3]HLS Technology Directorate, University of Liverpool, Liverpool, UK
[4]Institute of Veterinary Science, University of Liverpool, Leahurst Campus, Neston, UK

Keywords

Synovial Fluid, Metabolomics, Nuclear Magnetic Resonance, Proteomics, Mass Spectrometry, Lys-C Endopeptidase

Declaration of Author Contributions

Dr Marie Phelan provided training in NMR spectral acquisition and training in NMR spectral analysis. Dr Luis Rubio-Martinez, Professor Peter Clegg and Professor Mandy Peffers supervised this study. All experimental work was conducted by Mr James Anderson.

2.1. Abstract

Synovial fluid (SF) is of great interest for the investigation of orthopaedic pathologies as it is in close proximity to various tissues which are primarily altered during these disease processes and can be collected using minimally invasive protocols. Therefore, SF has substantial potential for improved understanding of underlying disease pathogenesis and biomarker discovery. Nuclear magnetic resonance (NMR) metabolomics is a rapidly expanding field, providing comprehensive metabolite profiling of complex biological samples with high levels of technical reproducibility. However, currently there are no agreed standard protocols which are published for SF collection and processing for use with NMR metabolomic analysis. The development of liquid chromatography tandem mass spectrometry (LC-MS/MS) has provided a fast and sensitive methodology to identify and quantify proteins within complex biological samples. However, the large protein concentration dynamic range present within SF can mask the detection of low abundant proteins. Combinational ligand libraries (ProteoMiner™ columns) have been developed to reduce this dynamic range, achieving peptide-based depletion whilst allowing preservation of the whole proteome. However, the reproducibility of ProteoMiner™ columns when used in conjunction with SF or on-bead protein digestion protocol reproducibility have yet to be investigated. During this study, protocols have been optimised for the collection, processing and storage of SF for NMR metabolite analysis. We have also optimised protocols for analysis of the SF proteome using LC-MS/MS, with the inclusion of a Lys-C endopeptidase digestion step prior to tryptic digestion found to increase the number of protein identifications and improve the reproducibility of on-bead ProteoMiner™ digestions.

2.2. Introduction

Synovial fluid (SF) primarily acts as a biological lubricant, reducing friction between synovial joint articular cartilage surfaces, but also functions as a pool of nutrients for surrounding tissues and allows movement of regulatory cytokines (Blewis *et al.*, 2007; Tamer, 2013). SF is of great interest for the investigation of orthopaedic pathologies, including osteoarthritis (OA), osteochondrosis, rheumatoid arthritis and synovial sepsis, as it is in close proximity to various tissues which are primarily altered during these disease processes, with minimally invasive collection protocols (Anderson, Phelan, *et al.*, 2018; Mateos *et al.*, 2012). Therefore, SF has the potential for improved understanding of underlying disease pathogenesis and biomarker discovery.

Nuclear magnetic resonance (NMR) metabolomics is a rapidly expanding field, providing comprehensive metabolite profiling of complex biological samples with high levels of technical reproducibility (Beckonert *et al.*, 2007; Beltran *et al.*, 2012). Numerous studies have utilised NMR to investigate the SF metabolome of orthopaedic diseases in various species, including humans, dogs, pigs and horses (Anderson, Phelan, *et al.*, 2018; Damyanovich *et al.*, 1999; Duffy *et al.*, 1993; Hugle *et al.*, 2012; Lacitignola *et al.*, 2008; Meshitsuka *et al.*, 1999; Mickiewicz, Heard, *et al.*, 2015; Mickiewicz, Kelly, *et al.*, 2015). Although the effect of freeze thaw cycles and long term low temperature storage have been investigated, no studies to date have investigated the impact of different freezing methods on NMR metabolite analysis (Damyanovich *et al.*, 2000). Currently, there are no agreed standard protocols which are published for SF collection and processing for use with NMR metabolomic analysis.

Various studies have used mass spectrometry (MS) based proteomics approaches to analyse SF, with the development of liquid chromatography tandem mass spectrometry (LC-MS/MS) providing a fast and sensitive methodology to identify and quantify proteins within complex biological samples (Hsueh *et al.*, 2014; Mahendran *et al.*, 2017). However, due to the multivariate nature of sample analysis, a large number of biological replicates are required in order to achieve an adequately powered study, which for LC-MS/MS, may be cost prohibitive.

Additionally, the large protein concentration dynamic range present within SF leads to various challenges associated with proteome analysis (Puangpila *et al.*, 2015). A small number of highly abundant proteins, including albumin, can mask the detection of low abundant proteins, thus compromising potential biomarker discovery (Roche *et al.*, 2006). Combinational ligand libraries have been developed to reduce this dynamic range, achieving peptide-based depletion whilst allowing preservation of the whole proteome (Furka *et al.*, 1991; Lam *et al.*, 1991). This methodology has recently been used in the development of ProteoMiner™ protein enrichment columns (Bio-Rad Laboratories Ltd., Hemel Hempstead, UK), depleting highly abundant proteins and enriching those less abundant (Fonslow *et al.*, 2011). This technique was found to generate the largest increase in protein identifications compared to other protein depletion methods when applied to serum (Pisanu *et al.*, 2018). However, the elution solution present within the kit is not compatible with LC-MS/MS analysis, due to the presence of 3-((3-cholamidopropyl) dimethylammonio)-1-propanesulfonate (CHAPS) (Williams, 2014). Although 'clean-up' and alternative elution protocols are available, these introduce a further process in sample preparation and subsequently a source of variation. Peffers *et al.* have previously developed an on-bead trypsin digestion protocol for analysis of ProteoMiner™ processed SF (Davidson *et al.*, 2017; Hulme *et al.*, 2017; Peffers, McDermott, *et al.*, 2015). However, although the reproducibility of ProteoMiner™ beads when used in conjunction with serum has been examined, reproducibility with SF or on-bead digestions have yet to be investigated (Li *et al.*, 2009).

Lys-C serine endopeptidase is the second most common enzyme used within bottom-up proteomics studies following trypsin, efficiently hydrolysing the peptide bond of lysine residues on the carboxyl side (Jekel *et al.*, 1983; Wu *et al.*, 2018). Whilst trypsin digests peptides at Arg-C or Lys-C residues, unless followed directly by proline, cleavage at the Lys-C site is comparatively poor when compared to Lys-C endopeptidase activity (Siepen *et al.*, 2007; Wu *et al.*, 2018). Thus, a combined digestion protocol can produce an overall improved digestion efficiency. When used within an in-solution protein digestion protocol, a Lys-C/trypsin protocol was found to produce significantly less missed cleavages and a more efficient digestion than a

tryptic digestion alone (Glatter *et al.*, 2012). However, on-bead ProteoMiner™ digestion protocols to date have used trypsin alone, with the potential improved digestion of the addition of Lys-C endopeptidase into this protocol yet to be investigated.

Cartilage breakdown products are generated during orthopaedic pathology, i.e. OA, due to elevations in enzymatic activity within synovial joints (Peffers *et al.*, 2016). These products may be recognised via MS as semi-tryptic peptides. Identification and quantification of these semi-tryptic peptides within pathological groups has potential as an early OA biomarker as well as enabling disease stratification. However, the reproducibility of semi-tryptic peptide quantification is yet to be investigated following ProteoMiner™ processing.

We hypothesise that refining SF collection and processing protocols for NMR metabolomic and LC-MS/MS proteomic analysis will maximise the number of molecule identifications as well as optimise technical reproducibility.

2.3. Methods

2.3.1. Study Overview

Table 1 below summarises the main NMR and LC-MS/MS protocols investigated during this study for metabolite, protein and peptide identification and quantification.

Table 1. Nuclear magnetic resonance and liquid chromatography-tandem mass spectrometry protocols investigated during this study for metabolite, protein and peptide identification and quantification.

METABOLITES	PROTEINS/PEPTIDES
Nuclear Magnetic Resonance (NMR)	**Liquid Chromatography-Tandem Mass Spectrometry (LC-MS/MS)**
Spun vs Unspun	Hyaluronidase Treatment Protocol Optimisation
Different Freezing Protocols	ProteoMiner™ Bead Protein Loading
Reproducibility of Separate Synovial Fluid Donors	Gradient Length and Blank Acquisition
	Protein Digestion Optimisation
	Tryptic Peptide Reproducibility
	Semi-Tryptic Peptide Reproducibility

2.3.2. Equine Synovial Fluid Collection

All equine SF was collected post mortem from an abattoir within 8 hrs of euthanasia. Metacarpophalangeal (MCP) joints were opened aseptically and SF collected on ice using a 10 ml syringe. For NMR metabolomics analysis, SF was pooled from four MCP joints from four separate donors and vortexed for 1 min. SF was also collected from an additional three equine MCP joints from three donors and processed separately. For proteomic analysis SF was pooled from five MCP joints from five separate donors, pooled and vortexed for 1 min. All joints used for this study were considered to be macroscopically normal and were assigned a score of 0 according to the equine OARSI histopathology initiative scoring system (McIlwraith *et al.*, 2010).

2.3.3. Human Synovial Fluid Collection

SF was collected, with ethical approval, from the acetabulofemoral joint of nine patients diagnosed with OA undergoing total hip replacement surgery at The Queen Elizabeth Hospital Birmingham and stored at -80°C. Further information on collection protocols is unavailable.

2.3.4. NMR Metabolomics

2.3.4.1. Sample Preparation - Spun vs Unspun

150 µl of equine SF was aliquoted into nine eppendorfs which did not undergo centrifugation prior to freezing (unspun) and nine eppendorfs which were centrifuged (spun). In the spun group, SF was centrifuged at 2,540*g* and 4°C for 5 min and the supernatant transferred to a new eppendorf. All samples were subsequently snap frozen in liquid nitrogen and stored at -80°C.

2.3.4.2. Sample Preparation - Different Freezing Protocols

150 µl of equine SF was aliquoted into 32 eppendorfs which were subsequently centrifuged at 2,540*g* and 4°C for 5 min and the supernatant removed. The samples were then divided into four separate groups (eight in each) and frozen either at

-20°C, -80°C, placed onto dry ice or snap frozen in liquid nitrogen. Following freezing, all samples were stored at -80°C.

2.3.4.3. Sample Preparation - Reproducibility of Separate Synovial Fluid Donors

Following collection, equine SF was separated into three separate 150 µl aliquots for each of the three separate donors, nine aliquots in total. SF was then centrifuged at 2,540*g* and 4°C for 5 min, supernatant removed, snap frozen in liquid nitrogen and stored at -80°C.

2.3.4.4. Sample Preparation for NMR Spectrometry

150 µl of each thawed SF sample was diluted to a final volume containing 50% (v/v) SF, 40% (v/v) dd $^{1}H_2O$ (18.2 MΩ), 10% (v/v) 1 M PO_4^{3-} pH 7.4 buffer (Na_2HPO_4, VWR International Ltd., Radnor, Pennsylvania, USA and NaH_2PO_4, Sigma-Aldrich, Gillingham, UK) in deuterium oxide ($^{2}H_2O$, Sigma-Aldrich) and 0.0025% (v/v) sodium azide (NaN_3, Sigma-Aldrich). Samples were vortexed for 1 min, centrifuged at 13,000*g* and 4˚C for 2 min and 200 µl transferred (taking care not to disturb any pelleted material) into 3 mm outer diameter NMR tubes using a glass pipette.

2.3.4.5. NMR Spectral Acquisition

All SF samples were individually analysed. 1D ^{1}H NMR spectra were acquired using a 700 MHz NMR Bruker Avance III HD spectrometer with associated TCI cryoprobe and chilled Sample-Jet autosampler. A Carr-Purcell-Meiboom-Gill (CPMG) filter was used to attenuate macromolecule signals using a standard cpmgpr1d vendor pulse sequence. All CPMG spectra were acquired at 37˚C with a 15 ppm spectral width, a 4 s interscan delay and 32 transients. Spectral acquisition and processing was carried out using Topsin 3.1 (Bruker Corporation, Billerica, Massachusetts, USA) and IconNMR 4.6.7 (Bruker).

2.3.4.6. Spectral Bucketing

All spectra were aligned to a single formate peak at 8.46 ppm. All peaks within each spectrum were then placed into ‘buckets’, excluding the peak generated by water,

with each bucket intensity divided by the width in order to negate intensity variance.

2.3.5. LC-MS/MS Proteomics

2.3.5.1. Hyaluronidase Treatment Protocol Optimisation

750 µl aliquots of equine SF were supplemented with hyaluronidase (from bovine testes, Sigma-Aldrich) at a final concentration of 0, 0.05, 0.10, 0.25, 0.50, 0.75, 1.00, 1.50 or 2.00 µg/ml and vortexed for 30 s. All samples (bar two 0 µg/ml treated samples) were then incubated at 37°C for 1 hr and rotated. All samples (bar two 0 µg/ml and one 1.00 µg/ml treated samples) were then passed through polypropylene microcentrifuge tube filters with 0.22 µm pore cellulose acetate membranes (Costar Spin-X, Corning, Tokyo, Japan) for 15 min at 5,000*g*. 1 µl of each sample was analysed by one dimensional sodium dodecyl sulphate polyacrylamide gel electrophoresis (1D SDS PAGE) and stained with Coomassie Blue (Bio-Rad).

2.3.5.2. Standard Trypsin Protein Digestion Protocol

During this study, previously developed standard trypsin digestion protocols were used for native SF protein digestion and on-bead ProteoMiner™ protein digestion, or a variation of this protocol as stated (Peffers, McDermott, *et al.*, 2015) (Figure 1). 160 µl of 25 mM ammonium bicarbonate (Fluka Chemicals Ltd., Gillingham, UK) containing 0.05% (w/v) RapiGest (Waters, Elstree, Hertfordshire, UK) was added to ProteoMiner™ columns. For native SF and ProteoMiner™ column flow-through, the appropriate volume containing 100 µg of protein was diluted to a final volume of 160 µl 25 mM ammonium bicarbonate (Fluka) containing 0.05% (w/v) RapiGest. Samples were heated for 10 min at 80°C, 3 mM final concentration DL-Dithiothreitol (Sigma-Aldrich) added, heated at 60°C for 10 min and 9 mM final concentration iodoacetamide (Sigma-Aldrich) added and incubated at room temperature for 30 min in the dark. Protein digestion was carried out through the addition of 2 µg of proteomics grade trypsin (Sigma-Aldrich), rotation at 37°C for 16 hrs with repeated trypsin supplementation for 2 hrs, again rotating at 37°C. Columns were centrifuged at 1,000*g* for 1 min, 0.5% (v/v) final concentration trifluoroacetic acid (TFA, Sigma-

Aldrich) added, rotated at 37°C for 30 min, centrifuged at 13,000*g* and 4°C for 15 min and the supernatant removed.

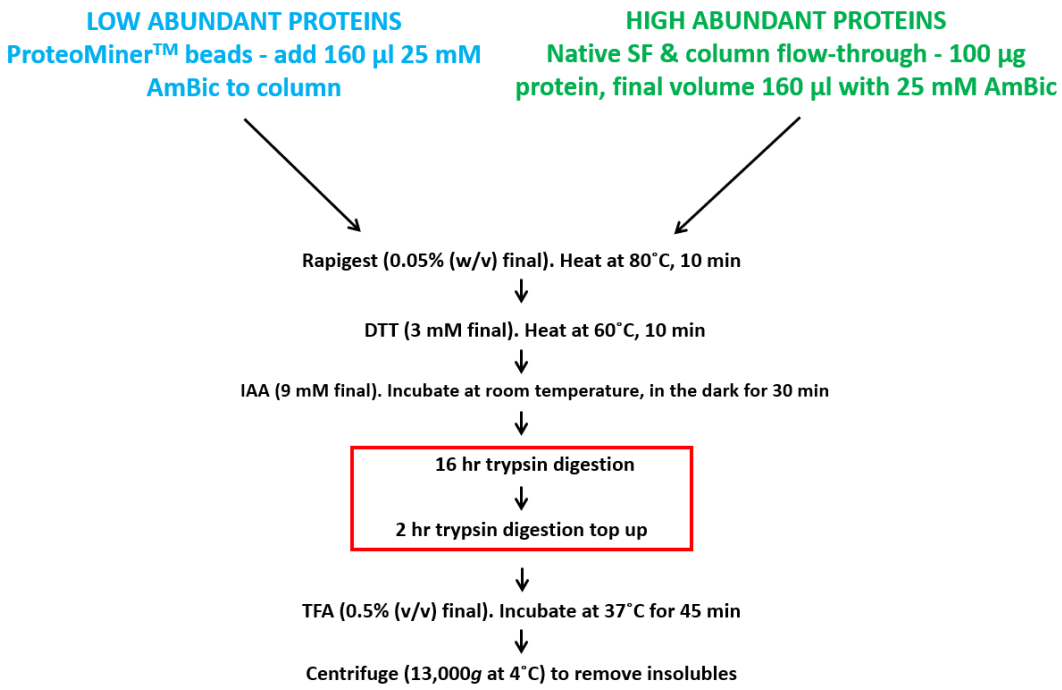

Figure 1. Standard trypsin digestion protocol for on-bead ProteoMiner™ protein digestion, native synovial fluid (SF) and ProteoMiner™ column flow-through protein digestion. Red box indicates enzymatic protein digestion steps. AmBic = Ammonium Bicarbonate, DTT = DL-Dithiothreitol, IAA = Iodoacetamide, TFA = Trifluoroacetic acid.

2.3.5.3. ProteoMiner™ Bead Protein Fractions

Pooled equine SF was treated using the standard protocol of adding 1 µg/ml hyaluronidase, heating at 37°C for 1 hr, centrifuging at 1,000*g* for 5 min, removing the supernatant and passing through a 0.22 µm cellulose acetate filter at 5,000*g* for 15 min. A ProteoMiner™ Small Capacity bead column (Bio-Rad) was loaded with 3.5 mg of protein and processed according to manufacturer instructions. The sample was rotated at room temperature for 2 hrs, centrifuged at 1,000*g* for 1 min (flow-through also collected), the beads washed in 200 µl phosphate buffered saline (PBS), rotated for 5 min and centrifuged for 1 min at 1,000*g* with the wash flow-

through collected. The wash step was completed three further times with the final being completed using deionised water. 20 µl of elution buffer (8 M urea, 5% acetic acid and 2% CHAPS) was added to the column, vortexed several times over 15 min, centrifuged at 1,000*g* for 15 min and the elution collected. The elution step was repeated two further times. All fractions collected during the protocol were analysed to assess the protein profiles/abundant protein depletion and protein content via 1D SDS PAGE and stained with Coomassie Blue and a Pierce® 660 nm protein assay (Thermo Scientific, Waltham, Massachusetts, USA) respectively.

2.3.5.4. ProteoMiner™ Bead Protein Loading

Following the standard hyaluronidase treatment protocol, 1.0 mg, 2.5 mg and 5.0 mg of a pooled SF sample and 5.0 mg and 10.0 mg of a separate pooled SF sample were loaded onto separate ProteoMiner™ columns. Sample incubation and wash steps were completed according to manufacturer instructions. However, instead of protein elution, a standard on-bead digestion protocol was undertaken as previously stated. 100 µg of native SF protein and 100 µg of protein column flow-through were also digested using the same reduction, alkylation and digestion steps. Protein profiles were assessed using 1D SDS PAGE and stained with Coomassie Blue. Digests were individually analysed via LC-MS/MS with 120 min LC gradients.

2.3.5.5. Gradient Length and Blank Acquisition

SF protein digests used to assess ProteoMiner™ bead protein loading (100 µg native SF and 2.5 mg column loading) were both analysed using LC-MS/MS with 60, 90 and 120 min LC gradients and the number of proteins and peptides identified for each protocol recorded. To assess peptide carry-over between successive samples, after each sample a 'blank' sample (containing only sample buffer (97% (v/v) high performance liquid chromatography (HPLC) grade H_20 (VWR International), 2.9% acetonitrile (Thermo Scientific) and 0.1% TFA was run on a 30 min LC gradient and the spectra acquired. Following one SF sample a series of five successive blank samples were also run and again the spectra acquired. The abundance of each peptide identified within the blank sample was calculated as a percentage of the

abundance within the previous SF sample and the median of peptide percentage carry-overs recorded.

2.3.5.6. Synovial Fluid Protein Digestion Profiles: Coomassie Brilliant Blue vs Silver Stain

100 µg of protein of native human SF and 3 mg loaded ProteoMiner™ columns for the same nine separate human donors underwent a standard 16hr + 2hr trypsin digestion protocol. Digestion profiles were then analysed via 1D SDS PAGE and stained using both Coomassie Brilliant Blue and silver staining.

2.3.5.7. Protein Digestion Optimisation

Variations of the previously stated standard digestion protocols were used for 100 µg and 2.5 mg loaded ProteoMiner™ columns using the 16hr + 2hr trypsin digestion method (Table 2). Native and ProteoMiner™ processed SF was digested using 4hr, 16hr and 16hr + 2hr trypsin protocols. Additionally, for ProteoMiner™ processed SF, a 16hr + 16hr trypsin on-bead digestion protocol was also investigated as well as 16hr trypsin digests centrifuged at 1,000*g* for 1 min and the second stage protein digestion (2hr or 16hr trypsin digestion) carried out on the resulting supernatant. Each of these ProteoMiner™ protocols was also analysed using a pre-digest step of Lys-C endopeptidase (FUJIFILM Wako Pure Chemical, Osaka, Japan). Prior to trypsin digestion, 2 µg of Lys-C (10 µg/ml final digest concentration) was added to the column and incubated at 37˚C for 4 hr. A longer 16hr Lys-C pre-digest was also investigated for the standard 16hr + 2hr trypsin digestion protocol. Different ProteoMiner™ column loading methods were also investigated. After an initial 2hr on-bead sample incubation and centrifugation, a second SF load of equal protein was added to the column and a second 2 hr incubation undertaken. Additionally to this, following a 2 hr on-bead sample incubation and centrifugation, the resultant flow-through was reloaded onto the column and a second 2 hr incubation carried out. As well as on-bead digestion protocols, one column did not undergo protein digestion with the intact proteins eluted using the manufacturer's instructions and elution buffer, as previously described, to compare the protein bound protein profile to that of the digested protein profiles. Following processing, samples, and

ProteoMiner™ beads, were analysed by 1D SDS PAGE and silver staining. LC-MS/MS was undertaken with a 1hr LC gradient.

Table 2. Different digestion protocols of native and ProteoMiner™ processed equine synovial fluid.

		Lys-C	16hr Trypsin	Spin Down	2nd 16hr Trypsin	2hr Trypsin
ProteoMiner™	1		✓			✓
	2	✓ (4 hrs)	✓			✓
	3	✓ (16 hrs)	✓			✓
	4		✓		✓	
	5	✓ (4 hrs)	✓		✓	
	6		✓	✓		✓
	7	✓ (4 hrs)	✓	✓		✓
	8		✓	✓	✓	
	9	✓ (4 hrs)	✓	✓	✓	

		4 hr Trypsin	16 hr Trypsin	2hr Trypsin	
ProteoMiner™	10	✓			
	11		✓		
	12		✓	✓	Reloaded Native SF onto Column
	13		✓	✓	Reloaded Flow-Through onto Column
	14	Eluted off beads with elution buffer			

		4 hr Trypsin	16 hr Trypsin	2hr Trypsin
Native	15	✓		
	16		✓	
	17		✓	✓

2.3.5.8. Tryptic Peptide Reproducibility

Using the same pooled equine SF, following hyaluronidase treatment and CoStar processing, 100 µg of protein and 2.5 mg loaded ProteoMiner™ columns (including ProteoMiner™ flow-throughs) underwent a standard 16hr + 2hr trypsin digestion protocol with three technical replicates of each. All samples were analysed using LC-MS/MS with a 2 hr LC gradient. Additionally, for each sample type, the same vial was also analysed three times to investigate the reproducibility of LC-MS/MS alone. ProteoMiner™ columns loaded with 2.5 mg of pooled SF which underwent a 4hr Lys-C + 16hr + 2hr trypsin protocol were also analysed, although flow-through and repeated vial analysis was not undertaken.

2.3.5.9. Semi-Tryptic Peptide Reproducibility

100 µg protein of native SF underwent 4hr trypsin and 16hr + 2hr trypsin protocols in technical triplicates. 2.5 mg loaded ProteoMiner™ columns underwent 4hr trypsin, 16hr + 2hr trypsin, 4hr Lys-C + 4hr trypsin and 4hr Lys-C + 16hr + 2hr trypsin digestion protocols, also in technical triplicate. All digests were analysed by LC-MS/MS with using 1hr and 2hr LC gradients.

2.3.5.10. 1D SDS PAGE

1 µl of native SF, 5 µl of digested SF or 8 µl of ProteoMiner™ beads were used for 1D SDS PAGE for optimal optimisation of protein bands. Samples were added to Laemmli loading buffer Novex™ (Thermo Scientific) with a final concentration of 15% glycerine, 2.5% SDS, 2.5% Tris (hydroxymethyl) aminomethane, 2.5% HCL and 4% β-mercaptoethanol at pH 6.8 and heated for 5 min at 95˚C. Samples were loaded onto a 4-12% Bis-Tris polyacrylamide electrophoresis gel (NuPAGE™ Novex™, Thermo Scientific) with protein separation undertaken at 200V for 30 min at room temperature.

2.3.5.11. Coomassie Brilliant Blue Staining (Sensitivity = 100 ng of Protein)

Following 1D SDS PAGE, gels were washed three times in ddH_2O for 5 min, stained with Coomassie Brilliant Blue stain (R-250, Bio-Rad) for 1 hr, Coomassie stain removed and de-stained with Coomassie Brilliant Blue de-staining solution (R-250, Bio-Rad) for 16 hr.

2.3.5.12. Silver Staining (Sensitivity = 1 ng of Protein)

Following 1D SDS PAGE, gels were silver stained according to manufacturer instructions (Thermo Scientific). Gels were washed twice in ddH_2O for 5 min, fixed in 30% (v/v) ethanol (Sigma-Aldrich): 10% (v/v) acetic acid (Sigma-Aldrich): 60% (v/v) ddH_20 for 15 min and the fixing step repeated. Gels were washed twice in 10% (v/v) ethanol: 90% (v/v) ddH_20 for 5 min, twice in 100% ddH_2O for 5 min, incubated in a sensitizer working solution for 1 min and washed twice in 100% ddH_2O for 1 min. The gel was then incubated in a stain working solution for 30 min, washed twice in ddH_2O for 20 s, incubated in developer working solution for 2-3 min until bands

appeared and finally 5% (v/v) acetic acid: 95% (v/v) ddH_2O added and incubated for 10 min.

2.3.5.13. LC-MS/MS Spectral Acquisition

All digests were individually analysed via LC-MS/MS on an UltiMate 3000 Nano LC System (Dionex/Thermo Scientific) coupled to a Q Exactive™ Quadrupole-Orbitrap instrument (Thermo Scientific). Full LC-MS/MS instrument methods are described in chapter 7. Tryptic peptides (equivalent to 200 ng of protein) were loaded onto the column and run over a 30 min, 60 min, 90 min or 120 min LC gradient as stated.

2.3.5.14. PEAKS® Search Parameters

For peptide/protein database searches using PEAKS® Studio 8.5 (Bioinformatics Solutions Inc., Waterloo, Canada) the *Equus caballus* database was used with search parameters including: precursor mass error tolerance, 10.0 ppm; fragment mass error tolerance, 0.01 Da; precursor mass search type, monoisotopic; enzyme, trypsin; maximum missed cleavages, 1; non-specific cleavage, none; fixed modifications, carbamidomethylation; variable modifications, oxidation or hydroxylation and oxidation (methionine). A 1% false discovery rate (FDR) was set and a minimum of 2 unique peptides required for protein identification. No normalisation was undertaken. PEAKS® searches were used for all peptide and protein identifications except for protein digestion optimisation and semi-tryptic peptide analysis.

2.3.5.15. Mascot Search Parameters

For peptide/protein database searches using an in-house Mascot server Version 2.6.2 (Perkins *et al.*, 1999) the *Equus caballus* database was used with search parameters including: peptide mass tolerance, 10.0 ppm; fragment mass tolerance, 0.01 Da; enzyme, trypsin; missed cleavages allowed, one; fixed modifications, carbamidomethylation (cysteine) and variable modifications; oxidation (methionine), oxidation (proline) and oxidation (lysine). Mascot database searches were used for protein digestion optimisation and semi-tryptic peptide analysis.

2.3.5.16. Semi-Tryptic Peptide Identification and Quantification

Raw spectral files underwent spectral alignment, peak picking and peptide quantification in Progenesis™ QI 2.0 (Nonlinear Dynamics, Waters). No normalisation was undertaken. Peptide identifications were carried out for the top ten spectra of each feature with Mascot, using the same *Equus caballus* search parameters as for tryptic peptides, except a 'semi-tryptic' search was conducted opposed to 'tryptic'. Peptides, with a 1% FDR correction, were exported from Progenesis™ and technical replicates of semi-tryptic peptide abundances compared using the online neopeptide tool (Peffers *et al.*, 2017).

2.3.6. Statistical Analysis

Principal component analysis (PCA) plots were conducted using MetaboAnalyst 4.0 (Chong *et al.*, 2018). T tests were conducted in the software package R (https://cran.r-project.org/), box plots constructed using SPSS 24 and histograms drawn using Excel 2013. Peptide reproducibility was analysed using the coefficient of variation (CV) statistic on raw, non-normalised abundance values.

2.4. Results

2.4.1. NMR Metabolomics

2.4.1.1. Spun vs Unspun

Including a centrifugation step prior to freezing identified clear separation on a PCA plot (Figure 2a). Two distinct metabolomes can be discerned with separation determined by PC2.

2.4.1.2. Different Freezing Protocols

Unlike the centrifugation protocols, PCA of different SF freezing protocols did not generate separate metabolomic profiles with no distinct groupings identified according to the freezing method used (Figure 2b). However, the SF samples frozen by snap freezing in liquid nitrogen displayed the least variance between technical replicates and this protocol was therefore the most reproducible of those studied.

2.4.1.3. Reproducibility of Separate Synovial Fluid Donors

The collection and processing protocol was identified to be reproducible with three technical replicates of three macroscopically normal MCP joints from three horses clustering separately on a PCA plot (Figure 2c).

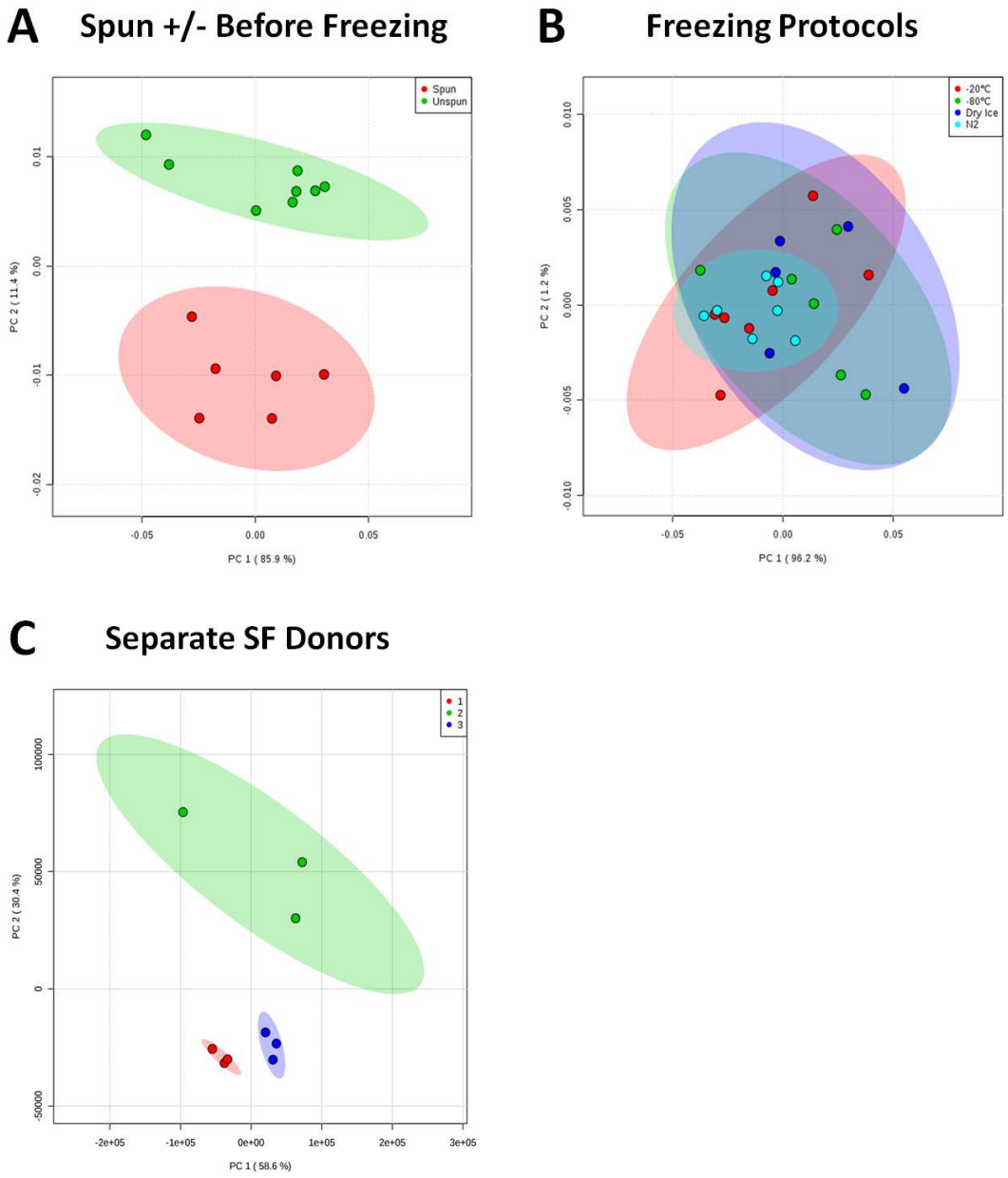

Figure 2. Optimisation of equine synovial fluid processing for 1D ^{1}H NMR metabolome analysis. The reproducibility of the metabolome for different processing protocols for equine synovial fluid (SF) was assessed using principal component analysis (PCA). These protocols included (A) with (n=6) and without (n=8) a centrifugation step (2,540*g* and 4°C for 5 min) prior to freezing and (B) the use of different freezing methods (-20˚C (n=7), -80˚C (n=6), dry ice (n=5) and liquid nitrogen (n=7)). (C) PCA showing reproducibility of the finalised SF processing method (including centrifugation and liquid nitrogen snap freezing) using three separate equine donors with three technical replicates for each donor. PCA shaded regions depict 95% confidence regions.

2.4.2. LC-MS/MS Proteomics

2.4.2.1. Hyaluronidase Treatment Protocol Optimisation

SF treated with hyaluraonidase at final concentrations of 0 - 0.50 µg/ml did not fully pass through cellulose acetate membrane filters due to incomplete hyaluraonidase degradation of hyaluronic acid, producing < 200 µl of flow-through (Figure 3a). Concentrations of 0.75 - 2.00 µg/ml however all yielded the same greater volume of flow-through (> 550 µl). No differences were identified between the global proteome profiles between the different hyaluraonidase treatment protocols (Figure 3b).

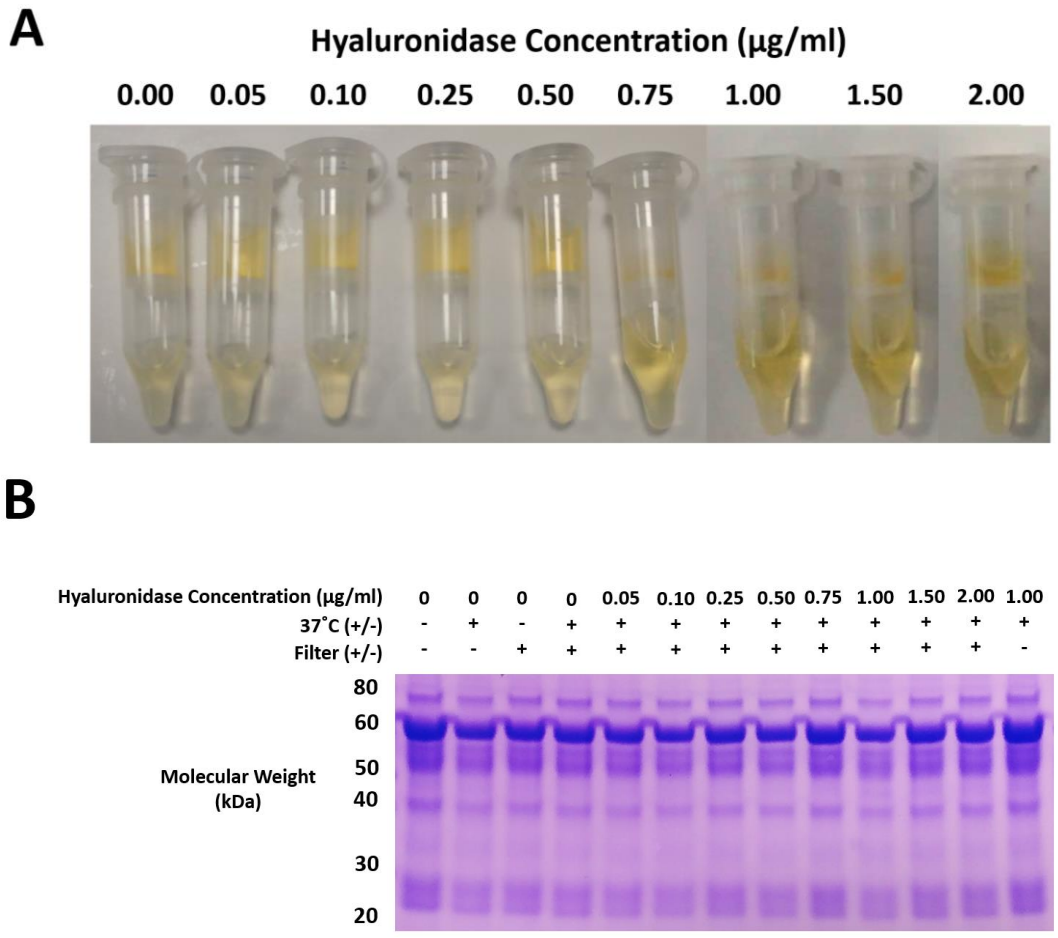

Figure 3. Synovial fluid hyaluronidase treatment optimisation. (A) Synovial fluid flow-through via cellulose acetate membrane filters following heating at 37°C, for 0-2 µg/ml hyaluronidase treatments and (B) 1D SDS PAGE of protein profiles using different hyaluronidase protocols.

2.4.2.2. ProteoMiner™ Bead Protein Fractions

ProteoMiner™ columns were found to be effective in equalling the protein concentration dynamic range (Figure 4a). Most of the protein was removed within the initial flow-through with 0.9% attaching to the beads for further analysis of low abundant proteins (Figure 4b).

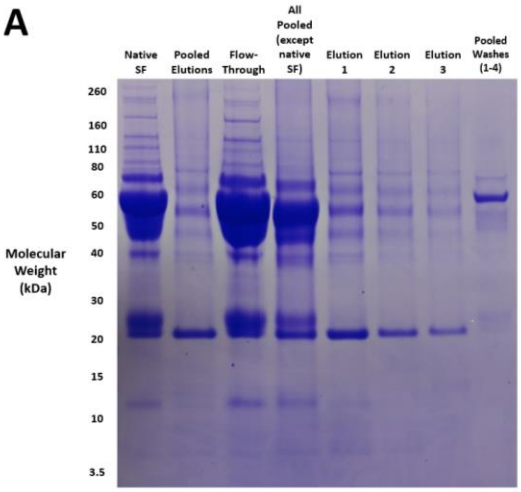

B

	Total Protein (mg)	Percentage of Original Load (%)
Native SF loaded	3.500	100.0
Flow-Through	3.159	90.3
Wash 1	0.093	2.7
Wash 2	0.081	2.3
Wash 3	0.075	2.1
Wash 4	0.051	1.5
Elution 1	0.018	0.5
Elution 2	0.009	0.3
Elution 3	0.004	0.1
TOTAL Protein Recovered	**3.456**	**98.7**
TOTAL Protein Eluted	**0.031**	**0.9**
TOTAL Protein in Washes	**0.300**	**8.6**

Figure 4. Synovial Fluid Protein Fractions during ProteoMiner™ Column Processing. (A) 1D SDS PAGE of protein profiles at each stage of the low abundant protein enrichment process and (B) total protein within each fraction.

2.4.2.3. ProteoMiner™ Bead Protein Loading

ProteoMiner™ columns were found to increase the number of identified proteins within equine SF compared to native SF analysis, with 1 mg, 2.5 mg and 5 mg column loadings increasing protein identifications by 112%, 161% and 201% respectively (Figure 5b). Proteomic analysis of flow-through following 5 mg protein loading identified a similar number of proteins compared to native SF. For a separate pooled equine SF sample set, increasing the protein loading from 5 mg to 10 mg only resulted in a small increase in protein identifications (21 proteins, 6%) (Figure 5c). At the level of Coomassie staining, tryptic digestion was sufficient for LC-MS/MS analysis for all protein loadings analysed (1-5 mg) (Figure 5a). Intensity of the highly abundant protein bands, 40-80 kDa, increased with increased protein

load. SF was loaded at equal concentration, thus indicating a higher proportion of these proteins within the flow-through with increasing protein load.

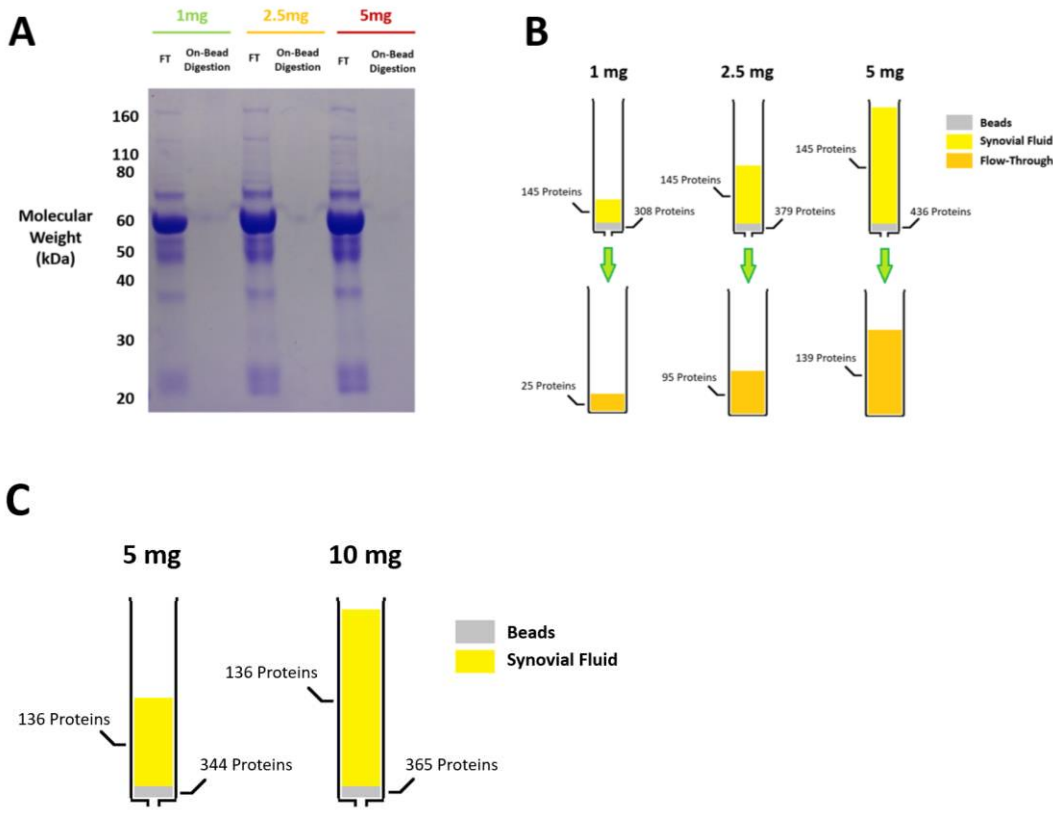

Figure 5. ProteoMiner™ Column Loading of Synovial Fluid. (A) Protein profiles of on-bead digests and flow-through (FT) following 1 mg, 2.5 mg and 5 mg protein loading. (B) Number of proteins identified via LC-MS/MS following bead enrichment of depleted proteins and column flow-through for 1 mg, 2.5 mg and 5 mg protein loadings and (C) 5 mg and 10 mg protein loadings for another set of pooled synovial fluid.

2.4.2.4. Gradient Length and Blank Acquisition

For both native and ProteoMiner™ processed SF, longer LC gradient lengths resulted in increased numbers of identified proteins, with a higher number of proteins identified following ProteoMiner™ processing (Figure 6). All of the acquired blank samples, bar one, had a low carry-over of peptides from the previous test sample, all with a median percentage carry-over of less than 1 for

peptides identified within the blanks. Running a series of consecutive blanks did reduce the number of peptides identified and their peptide abundance carry-over percentage, although this effect was regarded as minimal.

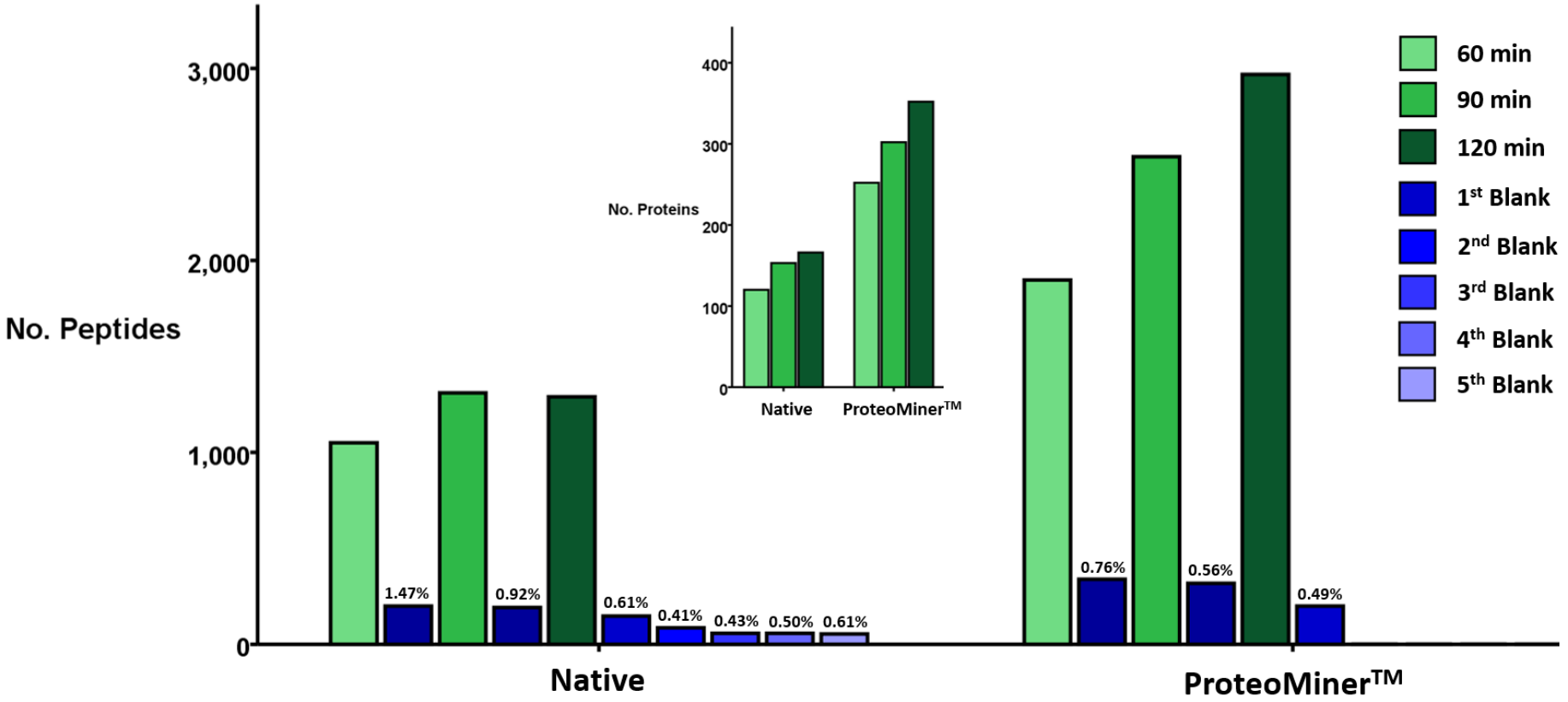

Figure 6. Number of peptides identified within native and ProteoMiner™ processed equine synovial fluid using LC-MS/MS for 60 min, 90 min and 120 min LC gradients. The number of peptides identified within blank samples run after synovial fluid samples were also recorded, with the median percentage carry of peptides identified within the blank compared to the previous synovial fluid sample stated above the relevant bar. Inset: Number of proteins identified for the same samples for 60 min, 90 min and 120 min LC gradients.

2.4.2.5. Synovial Fluid Protein Digestion Profiles: Coomassie Brilliant Blue vs Silver Stain

At the level of protein sensitivity of Coomassie Brilliant Blue staining, the 16hr + 2hr trypsin digestion protocol indicated complete digestion of both native and ProteoMiner™ processed SF (Figure 7). However, the increased sensitivity of silver staining revealed that whilst native SF digestion was confirmed as complete, incomplete digestion was present on the ProteoMiner™ column. Additionally, the level of incomplete digestion was not uniform across different donors.

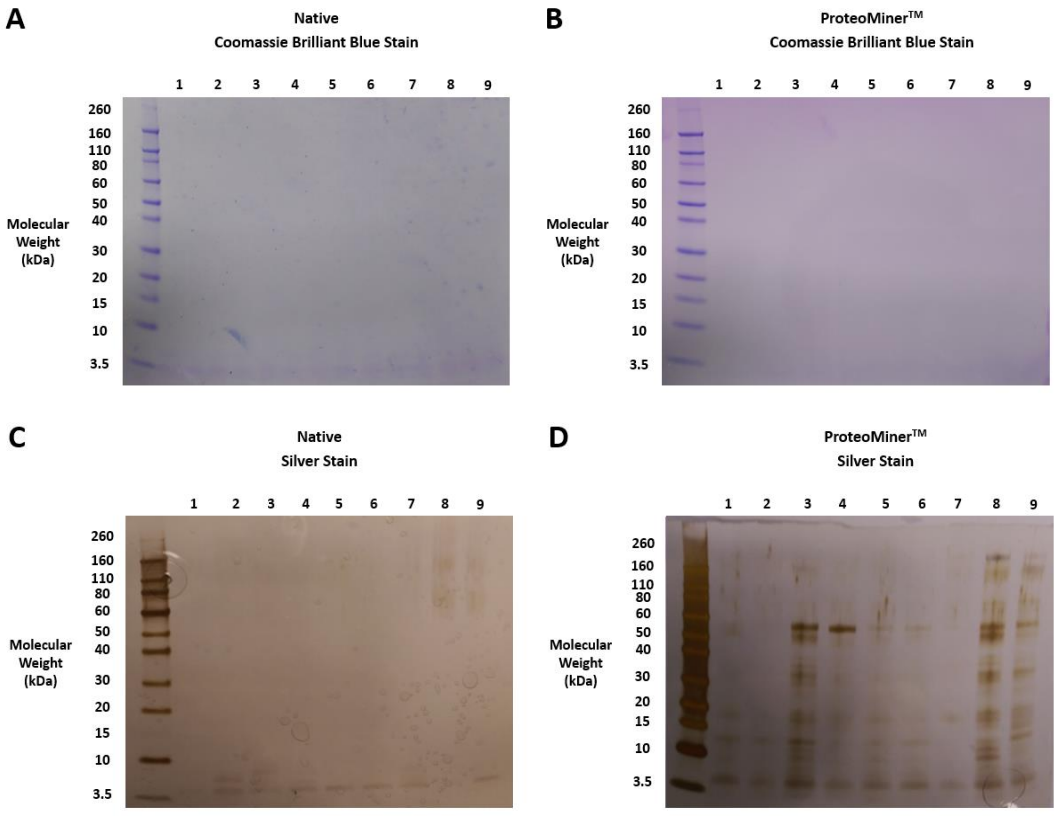

Figure 7. Protein profiles of (A and C) native and (B and D) ProteoMiner™ processed human synovial fluid following trypsin digestion and (A and B) Coomassie Brilliant Blue or (C and D) silver staining.

2.4.2.6. Protein Digestion Optimisation

Neither increased length of trypsin digestion nor an additional trypsin supplementation appeared to alter the protein profile of Native SF following digestion (Figure 8b). However, for on-bead ProteoMiner™ digestion, increased length of trypsin exposure and supplementation improved digestion efficiency, with clear protein bands present at 50-60 kDa and 260 kDa after 4hr trypsin digestion and near complete digestion following a 16hr + 2hr trypsin digestion protocol. Of the different on-bead tryptic digestion protocols investigated, protein profiles of the digested solutions of equine SF did not reveal as many undigested protein bands as identified previously for human SF (Figure 8a). However, a separate ProteoMiner™ 16hr + 2hr tryptic digestion of equine SF has also previously led to a series of undigested protein bands, detected at the sensitivity of Coomassie Blue (Supplementary Figure 1). However, an undigested protein band was detected at > 260 kDa for equine SF digests, which was not present for all protocols including the 4hr Lys-C pre-digest.

For protein profile analysis of the ProteoMiner™ beads, 4hr and 16hr trypsin digestions revealed significant levels of proteins were retained on the beads > 50 kDa, indicating significant incomplete digestion (Figure 8c). A 16hr + 2hr tryptic digestion protocol revealed significant retention of undigested proteins bound to the beads, with molecular weights in the range of 3.5-20 kDa. However, the intensity of these bands was significantly reduced with the introduction of the 4hr Lys-C pre-digestion, and to a lesser extent a 16hr Lys-C pre-digestion step. The intensity of these same bands were less for a 16hr + 16hr trypsin digestion compared to the standard protocol, and were again reduced by the 4hr Lys-C pre-digestion. Protocols in which the second trypsin digestion was completed in-solution, following an on-bead 16hr trypsin digestion, revealed significant levels of

undigested proteins remaining on the beads. However, the 4hr Lys-C pre-digestion step resulted in complete digestion of these proteins.

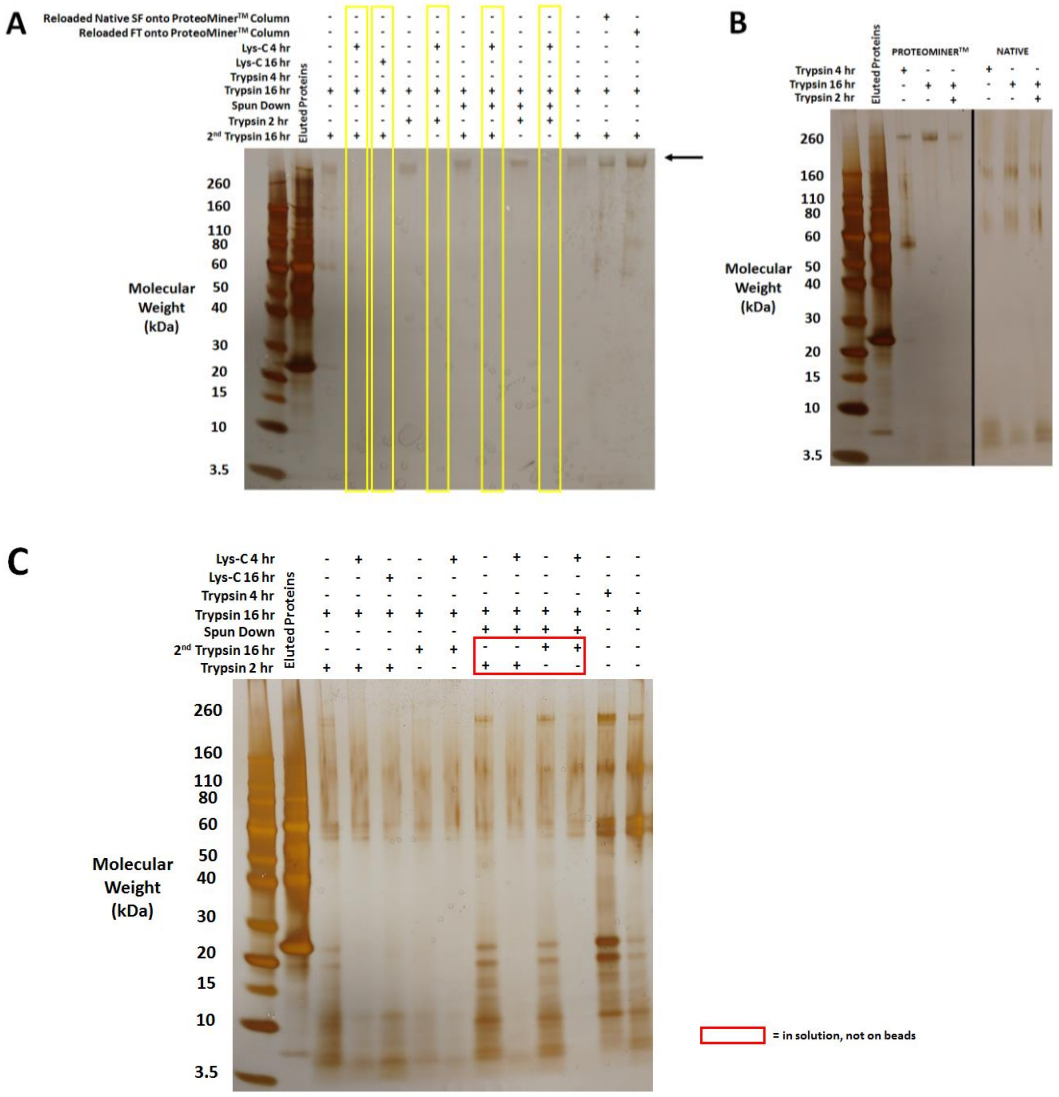

Figure 8. Protein profiles of native and ProteoMiner™ processed equine synovial fluid following protein digestion. (A) Different ProteoMiner™ loading and digestion protocols ± Lys-C endopeptidase pre-digestion (yellow boxes indicate profiles including Lys-C pre-digestion, arrow indicates a protein band not present following Lys-C pre-digestion protocols). (B) Trypsin digestion protocols for native and ProteoMiner™ processed synovial fluid. (C) ProteoMiner™ bead protein profiles following digestion protocols (red box indicates last stages of digestion were carried out in-solution, not on the beads).

Increased trypsin exposure time did not significantly increase the number of proteins identified for native SF (Figure 9). All Proteominer™ processed SF protocols resulted in an increased number of protein identifications compared to unprocessed native SF. Increased length in time of trypsin exposure increased the number of protein identifications for 4hr to 16hr + 2hr trypsin protocols, however a reduced number of proteins were identified following a 16hr + 16hr trypsin protocol. Neither repeated loading of native SF onto the column or reloading of flow-through increased the number of protein identifications, with both methods in fact leading to a reduction in the number of identifications. All trypsin digestion protocols in which Lys-C pre-digestion was included resulted in an increased number of protein identifications compared to the same protocol without a Lys-C pre-digest. Of all protocols examined, the 16hr Lys-C + 16hr + 2hr trypsin protocol resulted in the highest number of protein identifications.

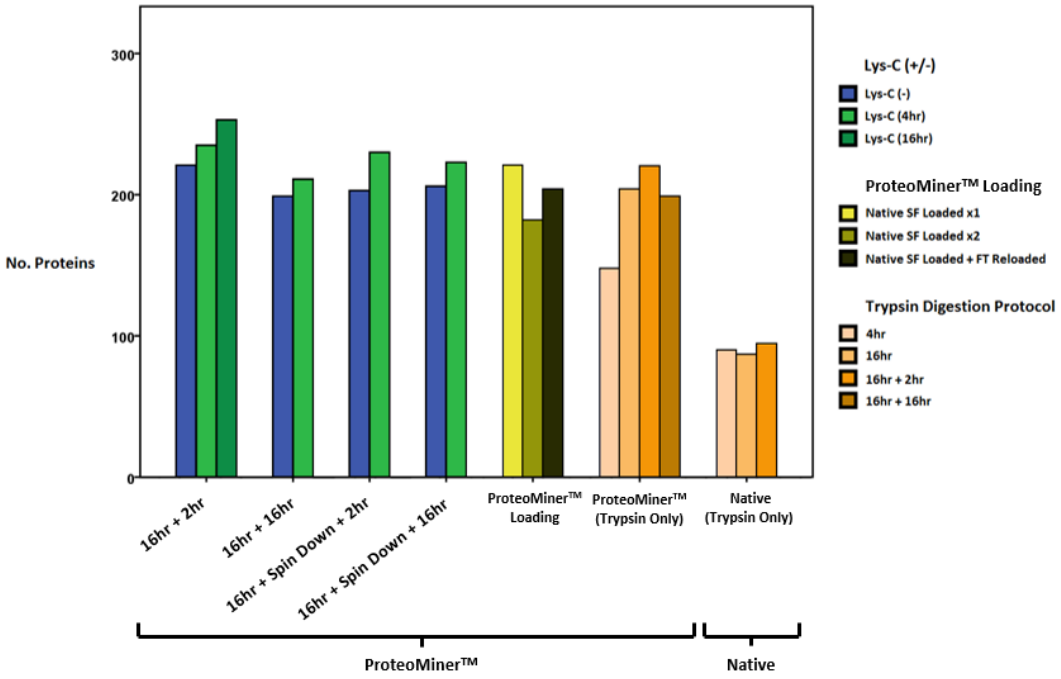

Figure 9. Number of Mascot protein identifications for native and ProteoMiner™ processed equine synovial fluid following different loading and protein digestion protocols involving trypsin ± Lys-C endopeptidase pre-digestion. Pilot study, n=1/digestion protocol.

2.4.2.7. Tryptic Peptide Reproducibility

When the same trypsin digested sample vial was analysed via LC-MS/MS three times, reproducibility was high for all sample types, with 67-87% of identified peptides having a CV value of < 10% (Figure 10). Triplicate repeats of native SF digests provided a good level of reproducibility, with 78% of identified peptides having a CV value of < 20%. Following ProteoMiner™ processing and an on-bead digestion protocol, reproducibility was reduced to 57% of identified peptides having a CV value of < 20%. Analysis of flow-through tryptic peptides provided a reproducibility level between that of native SF and ProteoMiner™ processing and an on-bead digestion, with 61% of identified peptides having a CV value of < 20%.

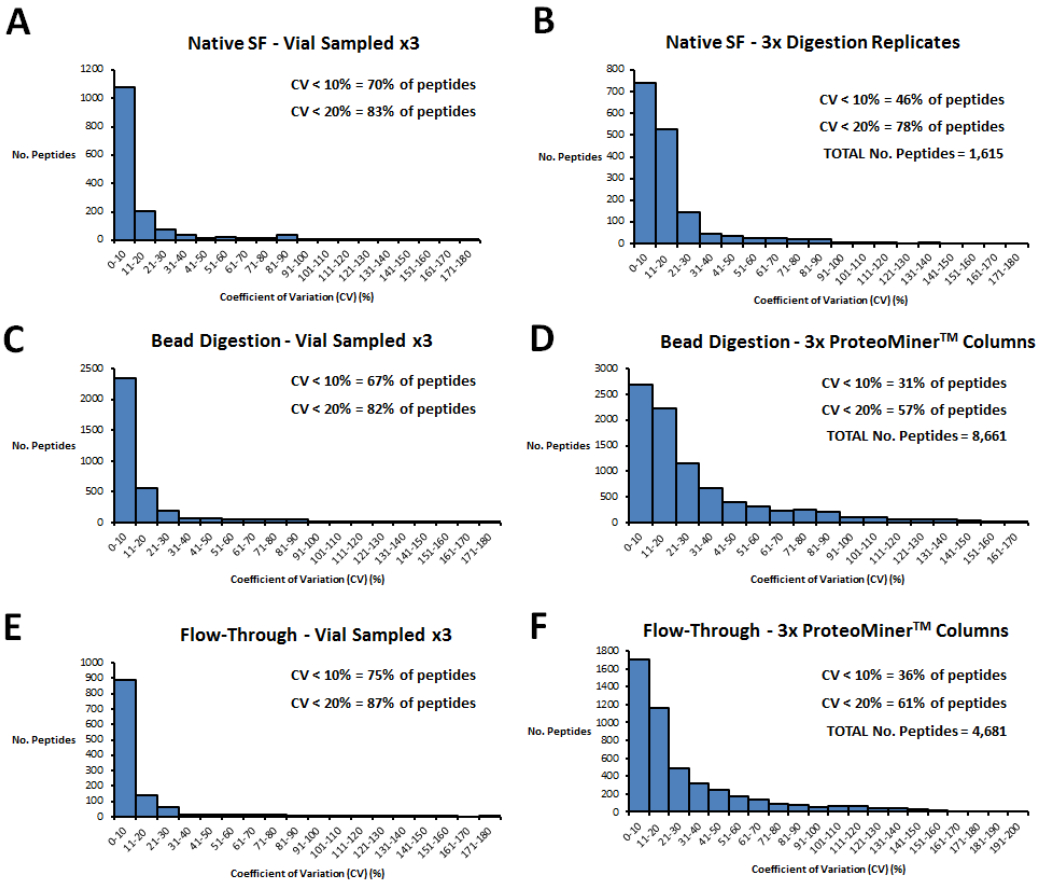

Figure 10. (A) Technical reproducibility of tryptic peptide abundances following a 16hr + 2hr trypsin digestion protocol of native equine SF with the same digested sample analysed three times and (B) digestion triplicates, (C) 2.5 mg protein loaded ProteoMiner™ columns with the same digested sample analysed three times and (D) digestion triplicates and (E) their subsequent flow-through, with the same digested sample analysed three times and (F) digestion triplicates. Peptide abundances were analysed via LC-MS/MS with a 2hr LC gradient and reproducibility calculated using peptide coefficient of variation (CV) values.

A 4hr Lys-C pre-digestion prior to the standard on-bead 16hr + 2hr trypsin digestion protocol did not increase reproducibility in terms of CV values (Figure 11). However, Lys-C pre-digestion significantly reduced the average number of missed cleavages/peptide during the digestion protocol, with less variation in the number of missed cleavages per sample. Additionally, analysis using a non-supervised PCA approach, when applying a Lys-C pre-digestion step, reduced the variability between tryptic digestion protocols, providing a more consistent digestion.

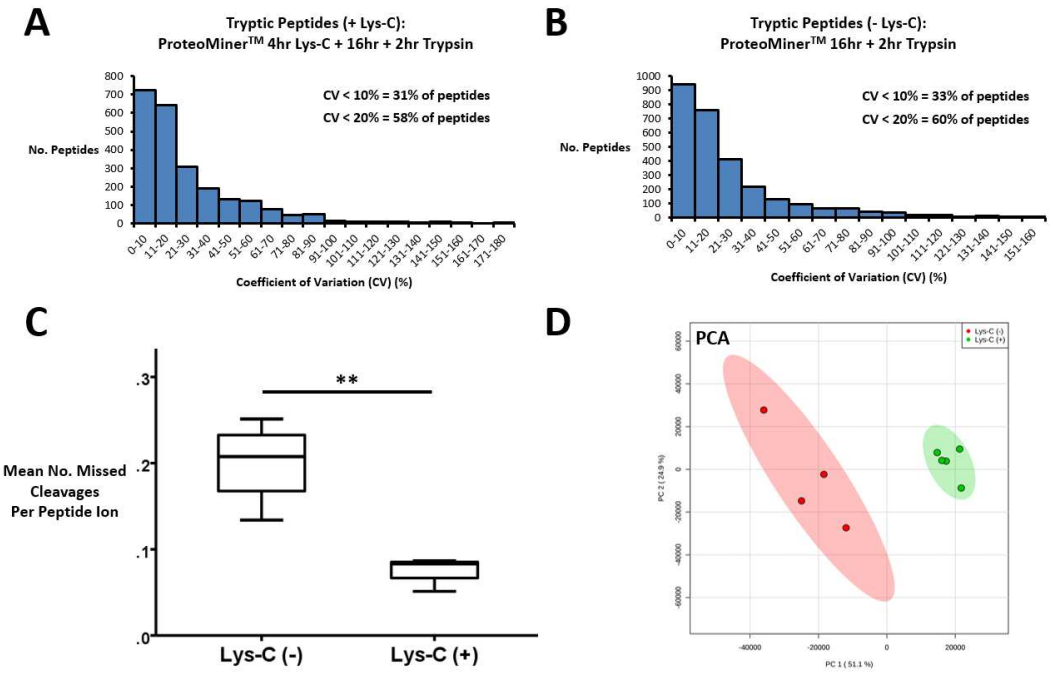

Figure 11. Reproducibility of ProteoMiner™ processed synovial fluid protein digests with and without Lys-C endopeptidase pre-digestion. Tryptic peptide reproducibility of three technical replicates (A) with and (B) without a 4hr Lys-C pre-digestion prior to 16hr + 2hr on-bead trypsin digestion. (C) Average number of missed cleavages per peptide and (D) principal component analysis (PCA) of tryptic peptide profiles with (green) and without (red) Lys-C pre-digestion for a series of trypsin digestion protocols. Peptide abundances were analysed via LC-MS/MS with a 1hr LC gradient. CV = coefficient of variation. ** = $p < 0.01$.

2.4.2.8. Semi-Tryptic Peptide Reproducibility

For semi-tryptic peptide quantification, when using variations of a 4hr trypsin digestion protocol with a 1hr LC gradient, a 4hr on-bead trypsin digestion was by far the most reproducible, with 71% of peptides having a CV value of < 20% (Figure 12). A 4hr Lys-C pre-digestion substantially increased the number of identified peptides (38 to 265) although this was accompanied by a significant reduction in reproducibility, with only 29% of peptides having a CV value of < 20%. For 16hr + 2hr trypsin digestion protocols with a 2hr gradient, digestion of native SF was the most reproducible, with 74% of peptides having a CV value of < 20%. Although ProteoMiner™ column processing increased the number of identified semi-tryptic peptides, both with and without a 4hr Lys-C pre-digestion step, reproducibility

dropped significantly, with 33% and 36% of peptides having a CV value of < 20% respectively.

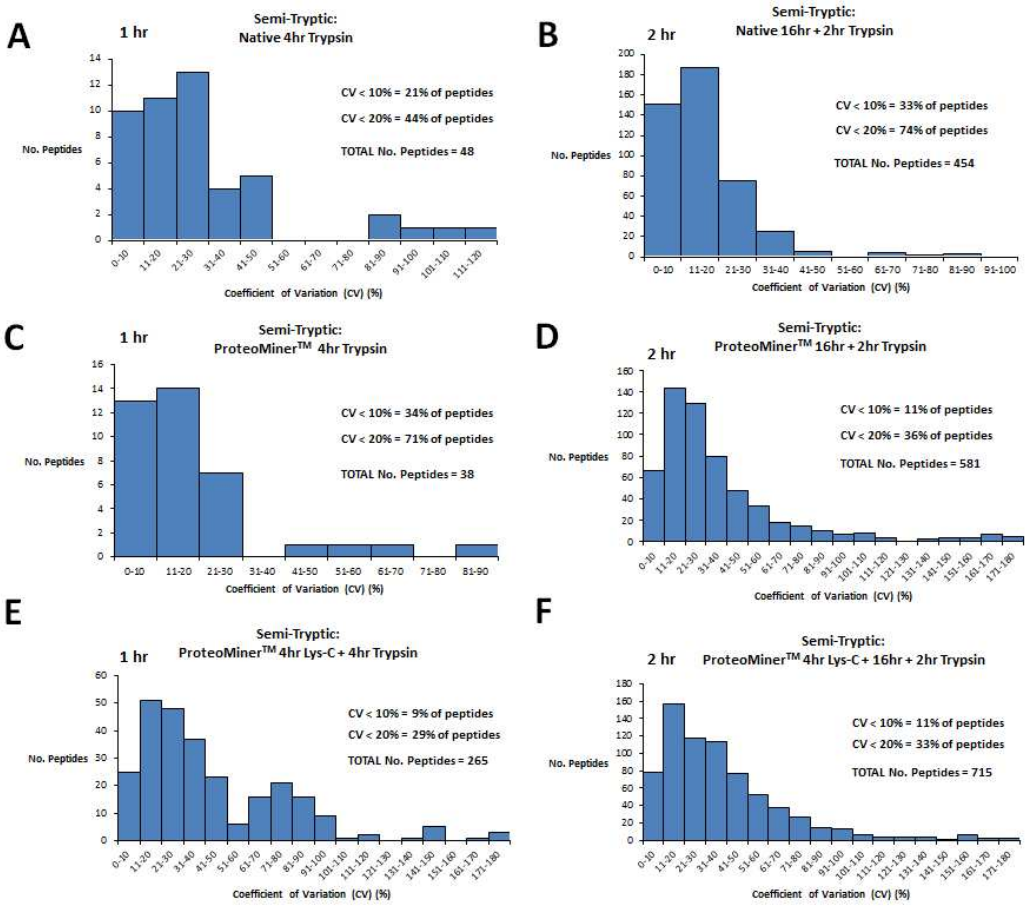

Figure 12. Reproducibility of semi-tryptic peptide abundances within equine synovial fluid analysed by technical triplicates. (A) Native synovial fluid, 4hr trypsin digestion, (B) Native synovial fluid, 16hr + 2hr trypsin digestion, (C) ProteoMiner™ processed synovial fluid, 4hr trypsin digestion, (D) ProteoMiner™ processed synovial fluid, 16hr + 2hr trypsin digestion, (E) ProteoMiner™ processed synovial fluid, 4hr Lys-C + 4hr trypsin digestion, (F) ProteoMiner™ processed synovial fluid, 4hr Lys-C + 16hr + 2hr trypsin digestion. Native synovial fluid digestions were undertaken on 100 µg of protein and ProteoMiner™ columns were loaded with 2.5 mg of protein. Protocols with a 4hr trypsin digestion component were analysed using a 1 hr liquid chromatography gradient whilst those containing a 16hr + 2hr trypsin digestion component were analysed via a 2 hr liquid chromatography gradient prior to tandem mass spectrometry analysis. CV = coefficient of variation.

2.5. Discussion

In this study, protocols were optimised for collection and processing of SF for NMR metabolomic and LC-MS/MS proteomic analysis. Optimal NMR metabolome analysis required SF centrifugation followed by snap freezing in liquid nitrogen. Optimisation of LC-MS/MS proteomic analysis entailed treatment of SF with 1 µg/ml hyaluronidase and rotational incubation at 37°C for 1 hr with Lys-C endopeptidase pre-digestion greatly improving on-bead tryptic protein digestion when used in conjunction with small-capacity ProteoMiner™ column kits. For semi-tryptic peptide identification, a 16hr + 2hr tryptic digestion of native SF and a 4hr on-bead tryptic digestion were identified as the most reproducible protocols.

SF is an important biofluid to further understand the pathogenesis of articular diseases, and identify specific biomarkers, as it is situated in close proximity to various tissues which are primarily altered by these pathologies (Anderson, Phelan, *et al.*, 2018; Mateos *et al.*, 2012). The use of global metabolite and protein profiling using systematic approaches, including NMR and LC-MS/MS, are becoming increasingly popular. However, to date, there are no agreed standardised published protocols available for collection and processing of SF for these platforms with reproducibility of on-bead digestions of ProteoMiner™ columns, used for peptide-based depletion, yet to be investigated.

Centrifugation of SF prior to freezing, removing cells and cellular debris, resulted in a distinct metabolome compared to SF which did not go through this processing step. It would therefore be recommended to undertake NMR metabolomic analysis on cellular-free SF, avoiding the variation and distinct changes that cell lysis and analysis of cellular contents that may incur on the SF metabolome. This current protocol is however unlikely to remove microvesicles, with a longer and faster centrifugation stage required to achieve this. Further work is required to investigate how the inclusion/exclusion of microvesicles would subsequently affect the SF metabolome. Different freezing method protocols did not result in distinct metabolic profiles, however snap freezing with liquid nitrogen was found to be the most consistent. Snap freezing with liquid nitrogen would therefore be the recommended gold standard freezing method for future studies. However, if SF has

been frozen using a different method, it may be acceptable to be included within the same study, provided that cellular material was removed prior to freezing. It should though be noted that freezing methods not involving liquid nitrogen will result in greater variation which may affect study results. It has also been found that storage of SF at low temperature for prolonged periods can alter the biochemical profile (Damyanovich *et al.*, 2000). Therefore, to optimise study design when freezing is required, analysed SF should be stored for similar periods of time prior to analysis, with this time period kept to a minimum. Using the centrifugation and liquid nitrogen freezing protocol described in this study, we have also demonstrated this method to be reproducible in identifying consistent separate SF metabolite profiles for individual equine donors.

Hyaluronidase breaks down hyaluronic acid and chondroitin sulphate through the cleavage of β-N-acetylhexosamine-(1,4)-glycosidic bonds, causing extracellular matrix breakdown and reduced SF viscosity, resulting in an increased number of protein identifications during LC-MS/MS analysis (Catterall *et al.*, 2006; Stern and Jedrzejas, 2006). During this study, treatment with 0.75 μg/ml hyaluronidase resulted in sufficient digestion of hyaluronic acid, enabling efficient centrifugation through a 0.22 μm pore cellulose acetate membrane. In order to ensure complete digestion however, a treatment protocol of 1 μg/ml hyaluronidase would be recommended. However, during this study the effect on the number of proteins identified for each hyaluronidase concentration was not investigated. This therefore may be a relevant area for future study.

Small-capacity ProteoMiner^{TM} column kits recommend a minimum protein loading of 10 mg. However, with a maximum loading capacity of 1 ml, as SF protein concentrations are often less than 10 mg/ml (particularly for post mortem samples) this threshold for protein loading can often not be met (Yahia and El-Hakiem, 2014). Neither initial loading of 5 mg of protein followed by a repeated 5 mg protein load nor reloading of the resultant column flow-through led to an elevation in the number of identified proteins. However, reduced protein loads of 1 mg, 2.5 mg and 5 mg were all found to significantly increase the number of proteins identified, with a 2.5 mg load also shown to be of acceptable reproducibility when undergoing an

on-bead protein digestion protocol. Thus, the small-capacity ProteoMiner™ column kit is still compatible with SF to achieve protein concentration dynamic range reductions, despite there being sub-optimal protein loading.

As expected, for both native and ProteoMiner™ processed SF, longer LC gradients resulted in an increased number of protein identifications (Hsieh *et al.*, 2013). For native SF a 120 min LC gradient resulted in only a small increase in the number of proteins identified compared to a 90 min LC gradient, 166 compared to 153 proteins. As this small increase in protein identifications is likely to include less abundant proteins, which will also be identified within the ProteoMiner™ processed samples, if native and ProteoMiner™ processed SF are to be analysed within the same study, a 90 min LC gradient is sufficient for native SF analysis. For ProteoMiner™ processed SF however, a 120 min gradient identified substantially more proteins than a 90 min gradient and thus this would be a recommended gradient length for this sample type.

Quantitative proteomic study approaches have become an important methodology for biomarker discovery within complex biological samples (Li *et al.*, 2017). However, due to the multivariate nature of sample analysis, a large number of biological replicates are required in order to achieve an adequately powered study. Thus, when undertaking LC-MS/MS, analysing sufficient samples to achieve adequate study power can be cost prohibitive. Within this study, peptide carry-over onto the following sample run was found to be minimal and resultant sample contamination can therefore be considered insignificant. Inclusion of a 'blank' sample prior to the following run did result in a reduced number of peptides carried over and a reduced carry-over percentage of those identified, although these decreases were minimal. Thus, a gold standard approach would be to include a 'blank' sample in between acquired sample spectra. However, excluding inter-sample blanks will have a minimal impact on experimental analysis and may allow for an increased n number within experimental groups and subsequently a higher powered study and more robust statistical analysis.

For all parameters investigated during this study, pre-digestion with Lys-C prior to tryptic digestion resulted in improved on-bead digestion, irrelevant of the tryptic

digestion protocol involved. Lys-C digestion resulted in a reduction of undigested proteins bound to ProteoMiner™ beads, a reduction in the number of peptide missed cleavages, improved reproducibility of tryptic peptide quantification and an increased number of protein identifications. Any of the protocols investigated during this study which included a Lys-C pre-digestion step would be acceptable for SF proteome analysis. Although a 16hr Lys-C + 16hr + 2hr trypsin protocol produced the highest number of protein identifications, despite a longer Lys-C incubation time, undigested bound proteins remained bound to the beads which may introduce variability. Although the reason for increased binding of undigested proteins following a 16hr Lys-C digestion compared to 4hr is unknown. 4hr Lys-C + 16hr trypsin on-bead digestion protocols followed by 2hr trypsin digestion (on-bead and in solution) or 16hr trypsin in solution digestion all resulted in minimal levels of undigested proteins remaining bound to the beads. A second 16hr in-solution digestion did not result in an overall increase in the number of identified proteins. Therefore, our recommended on-bead digestion protocol would be a 4hr Lys-C pre-digestion + 16hr tryptic digestion followed by a 2hr trypsin supplementation, either on-bead or in-solution.

Reproducibility of quantifying tryptic peptides following protein concentration dynamic range compression of SF via ProteoMiner™ on-bead digestion has not previously been investigated. Although reproducibility decreased compared to native SF, as expected given the additional selective processing stage, reproducibility was still sufficient to retain confidence in this processing step and is certainly advantageous for biomarker discovery given the increased number of peptides identified. As LC-MS/MS analysis of SF is primarily used for discovery investigations, validation of native SF using orthologous methodologies, including Western blotting and enzyme-linked immunosorbent assays, would also provide greater confidence in the results.

Semi-tryptic peptides are of interest within SF as increased enzymatic activity and cartilage breakdown during arthropathies, such as OA, lead to peptide degradation products which have potential as a diagnostic aid and disease stratification tool (Lotz *et al.*, 2013). Of the protocols investigated, a 16hr + 2hr tryptic digestion of

native SF and a 4hr on-bead tryptic digestion were found to be the most reproducible for semi-tryptic peptide quantification. Although these protocols resulted in the fewest semi-tryptic peptide identifications, increased confidence in the semi-tryptic peptides identified is more advantageous, particularly given the time, cost and technical difficulty involved in the development of monoclonal antibodies which might lead on from potential neopeptide discovery (Caterson *et al.*, 1985). Of these two protocols, a shorter, 4hr trypsin protocol would be recommended as longer trypsin incubations can lead to a greater number of non-specific cleavages which may potentially generate false positive biological semi-tryptic peptide identifications (Loziuk *et al.*, 2013). Further validation of semi-tryptic peptides of interest would always be recommended, using a multiple reaction monitoring targeted MS/MS approach or carrying out digestion protocols in $H_2{}^{18}O$ water to separate biological semi-tryptic peptides from those generated via miscleavages during tryptic digestion (Havliš and Shevchenko, 2004; Mirgorodskaya *et al.*, 2000; Parker and Borchers, 2014).

2.5.1. Conclusion

During this study we have optimised collection and processing protocols for NMR metabolomic and LC-MS/MS proteomic analysis of SF. For optimal metabolomic NMR analysis reproducibility, SF should first be centrifuged then frozen via snap freezing in liquid nitrogen. For proteomic analysis, treatment of SF with 1 µg/ml hyaluronidase and rotational incubation at 37^{o}C for 1 hr provided sufficient enzymatic activity to enable efficient centrifugation through a 0.22 µm pore cellulose acetate membrane. Lys-C endopeptidase pre-digestion was identified to greatly improve on-bead tryptic protein digestion when used in conjunction with small-capacity ProteoMiner^{TM} column kits, resulting in a reduction of undigested proteins bound to ProteoMiner^{TM} beads, a reduction in the number of peptide missed cleavages, improved reproducibility of tryptic peptide quantification and an increased number of protein identifications. To maximise protein identifications using ProteoMiner^{TM} columns, a 4hr Lys-C pre-digestion + 16hr tryptic digestion followed by a 2hr trypsin supplementation would be recommended. For semi-

tryptic peptide identification, a 16hr + 2hr tryptic digestion of native SF and a 4hr on-bead tryptic digestion were found to be the most reproducible.

2.6. Ethics

Equine SF samples were collected as a by-product of the agricultural industry. The Animals (Scientific Procedures) Act 1986, Schedule 2, does not define collection from these sources as scientific procedures and ethical approval was therefore not required. Human SF collection was authorised by the ethics committee at the University of Birmingham via a material transfer agreement and also underwent NHS research ethics service approval.

2.7. Funding

Mr James Anderson is funded through a Horse Trust PhD studentship (G1015) and Professor Mandy Peffers through a Wellcome Trust Intermediate Clinical Fellowship (107471/Z/15/Z). Software licences for data analysis used in the Shared Research Facility for NMR metabolomics were funded by the MRC Clinical Research Capabilities and Technologies Initiative (MR/M009114/1).

2.8. Acknowledgements

The authors would like to thank staff at F Drury and Sons abattoir, Swindon, Dr Simon Jones, MRC-ARUK Centre for Musculoskeletal Ageing, University of Birmingham, staff and patients at The Queen Elizabeth Hospital Birmingham and members of the Centre for Protein Research, University of Liverpool including Professor Rob Beynon, Dr Philip Brownridge and Ms Lynn McLean.

2.9. Supplementary Information

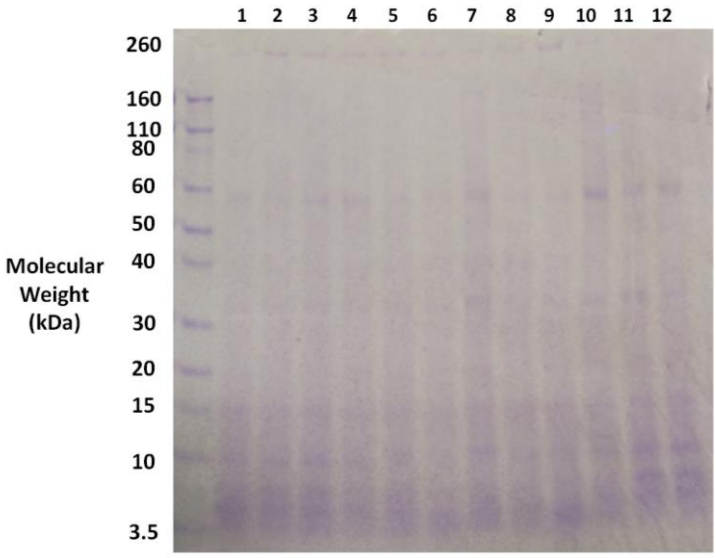

Supplementary Figure 1. Undigested proteins within twelve equine synovial fluid samples following a 16hr + 2hr on-bead tryptic digestion protocol using ProteoMiner^{TM} beads. Protein gel stained using Coomassie Brilliant Blue.

3. Manuscript 2

Metabolomic and Proteomic Stratification of Equine Osteoarthritis

James R Anderson[1], Marie M Phelan[2,3], Eva Caamaño-Gutiérrez[2], Peter D Clegg[1], Luis M Rubio-Martinez[1,4], Christopher M Riggs[5] and Mandy J Peffers[1]

[1]Institute of Ageing and Chronic Disease, University of Liverpool, Liverpool, UK
[2]Institute of Integrative Biology, University of Liverpool, Liverpool, UK
[3]HLS Technology Directorate, University of Liverpool, Liverpool, UK
[4]Institute of Veterinary Science, University of Liverpool, Leahurst Campus, Neston, UK
[5]Hong Kong Jockey Club, Equine Hospital, Sha Tin Racecourse, New Territories, Hong Kong

Keywords

Osteoarthritis, Equine, Synovial Fluid, Metabolomics, Nuclear Magnetic Resonance, Proteomics, Mass Spectrometry

Declaration of Author Contributions

Dr Marie Phelan provided training in NMR spectral acquisition and training in NMR spectral analysis. Collection and delivery of equine samples from the Hong Kong Jockey Club was organised by Professor Christopher Riggs. Dr Luis Rubio-Martinez collected clinical synovial fluid samples from the The Philip Leverhulme Equine Hospital, University of Liverpool. Dr Eva Caamaño-Gutiérrez conducted computational analysis integrating metabolomic and proteomic datasets. Professor Peter Clegg and Professor Mandy Peffers supervised this study and advised on experimental design. All other experimental work was conducted by Mr James Anderson.

3.1. Abstract

Osteoarthritis (OA) is characterised by loss of articular cartilage, synovial membrane dysfunction and subchondral sclerosis. Few studies have used a global approach to stratify equine synovial fluid (SF) molecular profiles according to OA severity. SF was collected from 58 metacarpophalangeal (MCP) and metatarsophalangeal joints of racing Thoroughbred horses (Hong Kong Jockey Club; HKJC) and 83 MCP joints of mixed breed horses from an abattoir (biobank). Joints were histologically and macroscopically assessed for OA severity. For proteomics, native SF and SF loaded onto ProteoMiner™ equalisation columns, to deplete high abundant proteins, were analysed using liquid chromatography-tandem mass spectrometry (LC-MS/MS) and label-free quantification. ELISA validation of selected differentially expressed proteins was undertaken with clinical SF collected during diagnostic investigation. Native SF metabolites were analysed using 1D ^{1}H Nuclear Magnetic Resonance (NMR). 1, 834 proteins and 40 metabolites were identified in equine SF. Afamin levels decreased with synovitis severity and four uncharacterised proteins decreased with OA severity. Gelsolin and lipoprotein binding protein decreased with OA severity and apolipoprotein A1 levels increased for mild and moderate OA. Within the biobank, glutamate levels decreased with OA severity and for the HKJC, 2-aminobutyrate, alanine and creatine increased with severity. Proteomic and metabolomic integration was undertaken using linear regression via Lasso penalisation modelling, incorporating 29 variables (R^2 = 0.82) with PC2 able to discriminate advanced OA from earlier stages, predominantly driven by H9GZQ9, F6ZR63 and alanine. Combining biobank and HKJC datasets, DAPC model prediction was good for mild OA (90%). This study has stratified equine OA using both metabolomic and proteomic SF profiles and identified a panel of markers of interest which may be applicable to grading OA severity. This is also the first study to undertake computational integration of NMR metabolomic and LC-MS/MS proteomic datasets of any biological system.

3.2. Introduction

The age-related degenerative musculoskeletal condition osteoarthritis (OA) is mainly characterised by articular cartilage degradation, synovitis, subchondral bone sclerosis and abnormal bone proliferation (Kramer, Tsang, *et al.*, 2014; Truong *et al.*, 2006). OA is an important welfare issue for equids, with up to 60% of lameness cases attributed to OA, leading to substantial morbidity and mortality (Caron and Genovese, 2003; Ireland *et al.*, 2011, 2012). Although it is known that degradation of the extracellular matrix (ECM) is driven by increased enzymatic activity of multiple matrix metalloproteinases (MMPs) and a disintegrin and metalloproteinases with thrombospondin motifs (ADAMTSs), the underlying pathogenesis of OA is yet to be fully understood (Li *et al.*, 2007; Marhardt and Muurahainen, 2015; Struglics *et al.*, 2006). Currently, equine OA is predominantly diagnosed through radiography, however due to the slow onset of the condition this often leads to substantial pathology of the joint and articular cartilage degradation prior to diagnosis (Brommer *et al.*, 2003). There is therefore a need to develop accurate biomarkers of early OA which can be applied to a clinical setting and allow for timely intervention, as well as improving our understanding of OA pathogenesis and identifying potentially novel therapeutic targets.

Currently, no equine OA-specific biomarkers have been identified to aid an early clinical diagnosis (Anderson, Phelan, *et al.*, 2018). For human OA diagnosis, increased synovial fluid (SF) abundances of both matrix metalloproteinases (MMPs) and cartilage oligomeric matrix protein (COMP) have been identified as markers of interest (Balakrishnan *et al.*, 2014). For horses, MMP activity has also shown OA diagnostic potential, however studies investigating COMP levels have shown conflicting results with SF COMP abundance unable to stage equine OA (Arai *et al.*, 2005; Bertuglia *et al.*, 2016; Clegg *et al.*, 1997; Misumi *et al.*, 2001; Skiöldebrand *et al.*, 2001; Taylor *et al.*, 2006; Yamanokuchi *et al.*, 2009; Zrimsek *et al.*, 2007). However, these markers are generated following significant joint pathology, including substantial articular cartilage degradation, and thus there is a need to identify markers at an earlier disease stage, where intervention would provide the most benefit.

Palmar/plantar osteochondral disease (POD), located at the distal condyles of metacarpal III and metatarsal III, is a highly prevalent pathology of racehorses, resultant of repetitive joint overload during cyclic locomotion at high-speed (Barr *et al.*, 2009; Kawcak *et al.*, 2000; Pinchbeck *et al.*, 2013). POD lesions range in severity, from mild to end-stage disease, and as the disease originates within the subchondral bone, provides an effective model to investigate subchondral bone mediated OA (Barr, 2010).

The inner layer of the joint capsule consists of a one-cell thick lining of synoviocytes within a hyaluronic acid and collagen matrix, called the synovial membrane, which produces SF (Gibson and Rooney, 2007; Mahendran *et al.*, 2017). SF primarily acts as a lubricant within the joint, protecting hyaline articular cartilage surfaces (Hui *et al.*, 2012). However, SF also provides a pool of nutrients for surrounding tissues and a medium of cellular communication with the semi-permeable synovial membrane allowing passive protein transfer and synoviocytes secreting regulatory cytokines and growth factors (Blewis *et al.*, 2007; Gibson and Rooney, 2007; Hui *et al.*, 2012; Mahendran *et al.*, 2017; Tamer, 2013). Due to the close relationship, both in terms of location and biological communication that SF holds with surrounding tissues which are primarily altered during OA, and its accessibility, SF can provide a unique source of chemical information and holds great promise for biomarker discovery (Anderson, Phelan, *et al.*, 2018; Mateos *et al.*, 2012).

Various studies have utilised ^{1}H nuclear magnetic resonance (NMR) to investigate metabolite markers associated with OA in various species, including pigs, dogs, humans and horses (Anderson, Phelan, *et al.*, 2018; Damyanovich *et al.*, 1999; Hugle *et al.*, 2012; Lacitignola *et al.*, 2008; Mickiewicz, Heard, *et al.*, 2015; Mickiewicz, Kelly, *et al.*, 2015). Lacitignola *et al.* identified a panel of ten metabolites which were elevated in equine OA SF compared to a normal control group. This panel included alanine, acetate, N-acetyl glucosamine, pyruvate, citrate, creatine/creatinine, choline, glycerol, lactate and α-glucose. However, no studies to date have used ^{1}H NMR to stratify OA to identify changes to the metabolite profile at different stages of OA severity.

Several studies have used mass spectrometry (MS) based methodologies to investigate equine OA SF (Chiaradia *et al.*, 2012; Peffers, McDermott, *et al.*, 2015; Skiöldebrand *et al.*, 2017; Svala *et al.*, 2017). The relatively recent development of liquid chromatography tandem mass spectrometry (LC-MS/MS) has enabled a method which can quickly, with high sensitivity, quantify proteins present within biological fluids of high complexity (Mahendran *et al.*, 2017). Protein biomarker discovery is however hindered by the large protein concentration dynamic range exhibited by SF, meaning that highly abundant proteins can mask those of less abundance (Puangpila *et al.*, 2015; Roche *et al.*, 2006). ProteoMiner^{TM} protein enrichment columns (Bio-Rad Laboratories Ltd., Hemel Hempstead, UK) have however been developed which utilise combinational ligand library technology, depleting highly abundant proteins and subsequently enriching low abundance proteins to reduce this dynamic range (Fonslow *et al.*, 2011; Furka *et al.*, 1991; Lam *et al.*, 1991). This methodology has successfully been used to investigate OA in equine SF (Peffers, McDermott, *et al.*, 2015). However, this technique has not yet been utilised with SF to enable OA stratification, analysing SF at different OA severities.

Increased activity of MMPs, ADAMTSs, cathepsins and serine proteases during OA leads to cartilage breakdown and the generation of OA-specific peptide degradation products (neopeptides) (Ben-Aderet *et al.*, 2015; Peffers *et al.*, 2016; Polur *et al.*, 2010). Numerous studies investigating equine tissue have identified potential OA neopeptides of interest using *ex-vivo* cartilage and SF (Peffers *et al.*, 2014; Peffers, McDermott, *et al.*, 2015; Peffers *et al.*, 2016; Skiöldebrand *et al.*, 2017). As OA neopeptides have also been shown to be a driver of OA pain, identification and quantification of neopeptides has the potential to stratify OA, providing markers of early OA pathology and providing potential novel OA therapeutic and analgesic targets (Miller *et al.*, 2018).

Within this study we have interrogated equine SF from horses with naturally occurring OA and those exhibiting POD pathology, as a subchondral bone mediated OA model using both ^{1}H NMR metabolomics and LC-MS/MS proteomics to stratify

equine OA. This is the first study to use both techniques on the same samples and the first to statistically integrate NMR-led metabolomics with MS-based proteomics.

3.3. Methods

3.3.1. Sample Collection and Processing

Equine post mortem samples were collected from both a commercial abattoir and The Hong Kong Jockey Club (HKJC) Equine Hospital in Hong Kong. Abattoir samples were collected from horses of mixed breed and sex and represented naturally occurring OA disease. HKJC samples were exclusively from Thoroughbred racehorses (aged 3-10 years old) with a high prevalence of POD, providing a model for subchondral bone mediated OA.

3.3.2. Biobank - University of Liverpool

Following euthanasia at the abattoir (F Drury & Sons, Swindon, UK) distal equine forelimbs were transported to the University of Liverpool. Within 8 hr of euthanasia the metacarpophalangeal (MCP) joint was opened aseptically and the distal metacarpal III photographed. SF was removed using a 10 ml syringe, transferred to a plain eppendorf, centrifuged at 2,540*g* and 4˚C for 5 min, supernatant removed, snap frozen in liquid nitrogen and stored at -80˚C (Figure 1). SF was separated into separate 1 ml eppendorfs prior to snap freezing to optimise study design prior to multi 'omics' analysis and integration (Cavill *et al.*, 2016). Wedge sections of articular cartilage/subchondral bone (measuring 4 cm x 1.5 cm x 0.5 cm) were also sampled from the distal condylar region of metacarpal III, lateral to the sagittal ridge, and placed into 4% paraformaldehyde (PFA, Sigma-Aldrich, Gillingham, UK) in phosphate buffered saline (PBS, Sigma-Aldrich) (Supplementary Figure 1). Following decalcification in ethylenediaminetetraacetic acid (EDTA, Sigma-Aldrich), these were then sectioned and stained with Haematoxylin and eosin (H & E) (TCS Biosciences Ltd, Buckingham, UK) and Safranin O (BDH Chemicals, Poole, UK). Decalcification, sectioning and staining were undertaken by Ms Valerie Tilston.

As biobank samples were obtained from a commercial abattoir, horses sampled were of mixed breed and sex and represented naturally occurring OA disease.

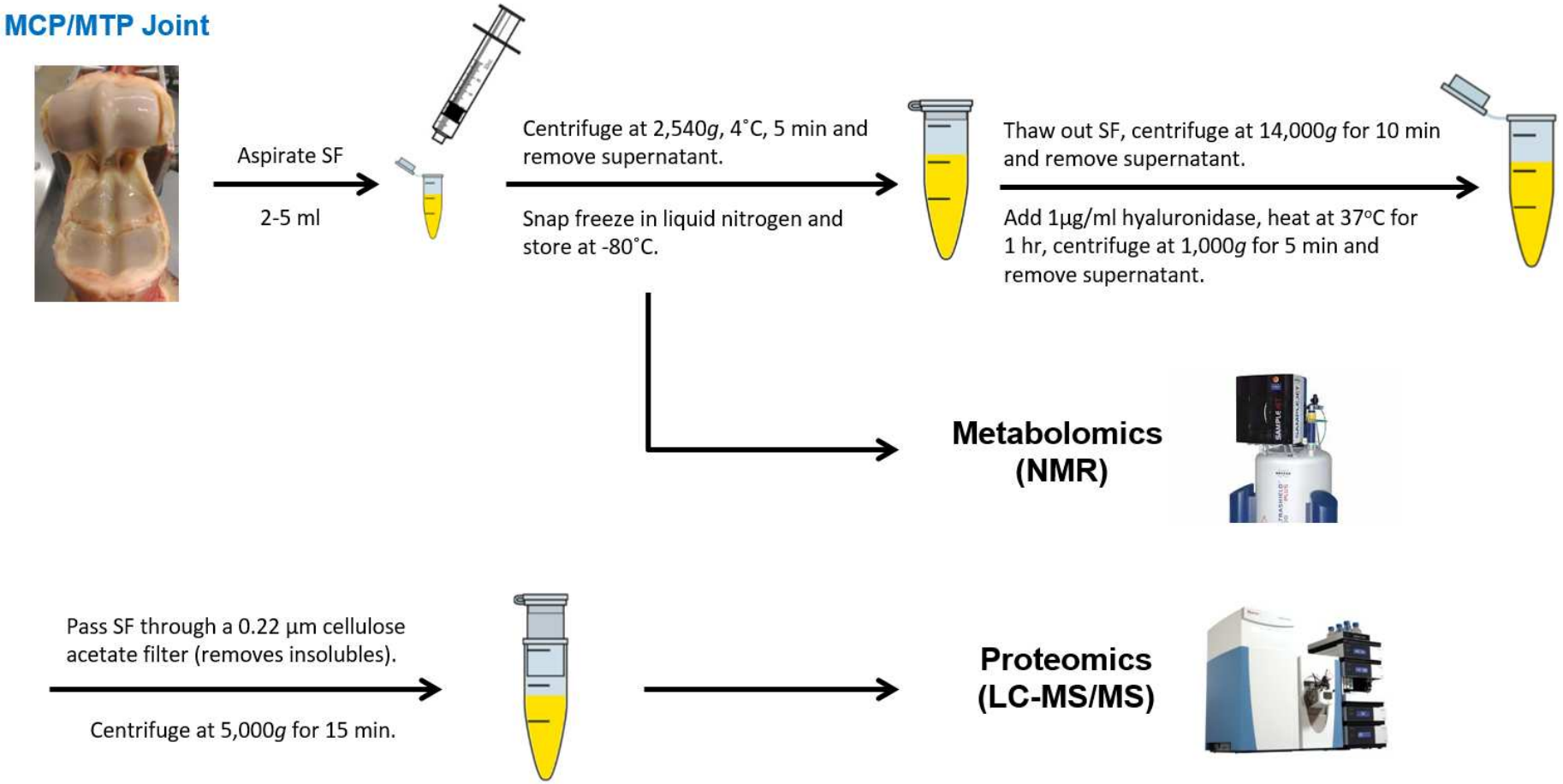

Figure 1. Protocol for synovial fluid (SF) collection and processing prior to NMR metabolomic and LC-MS/MS proteomic analysis. MCP = metacarpophalangeal, MTP = metatarsophalangeal.

3.3.4. Hong Kong Jockey Club

HKJC samples were collected using the same collection protocols as used for the University of Liverpool equine biobank. In addition, synovial membranes were also dissected, fixed in 4% PFA and processed to prepare H & E stained histology slides. For HKJC samples, both MCP and metatarsophalangeal (MTP) joints were sampled. Following snap freezing with liquid nitrogen, frozen SF samples were shipped to Liverpool on dry ice.

3.3.5. Clinical Synovial Fluid Collection for ELISA

During clinical diagnostic investigations of horses presenting to The Philip Leverhulme Equine Hospital, University of Liverpool between 2014 and 2017, excess aspirated SF was collected and subsequently processed using the same processing steps as used for biobank and HKJC SF samples. Clinical OA was diagnosed via clinical examination, radiography and/or arthroscopy. Healthy/control SF samples were collected during clinical examinations, including diagnostic analgesia, whereby the joint involved was not identified as the cause of the current lameness. However, underlying joint pathology, not leading to a clinical manifestation, could not be ruled out. These clinical SF samples were used for enzyme-linked immunosorbent assay (ELISA) validations of protein abundances.

3.3.6. Osteoarthritis Pathology: Macroscopic and Microscopic Scoring

Biobank distal metacarpal III articular surfaces were assessed for macroscopic OA pathology using the equine OARSI scoring scale by two independent scorers (McIlwraith *et al.*, 2010). Histological sections were also assessed for microscopic OA related pathology using the microscopic aspect of the equine OARSI scoring scale by two independent scorers. Within the HKJC group, distal metacarpal III samples were assessed macroscopically and microscopically for OA related and POD pathology using separate published scoring scales (Barr *et al.*, 2009; Little *et al.*, 2010). Marginal remodelling and dorsal impact injury categories were excluded from the macroscopic scoring scale as these could not be scored using the joint photographs which were provided. Synovial membrane histological sections were

also scored according to synovitis severity (Krenn *et al.*, 2006). Macroscopic scoring was carried out by two independent scorers whilst microscopic OA and synovitis grading was carried out by one scorer only as scoring was conducted historically and histological sections were unavailable for repeated assessment. For synovitis scoring, three separate regions of each slide were scored and then averaged.

3.3.7. Metabolomics

3.3.7.1. Sample Preparation - NMR

SF was thawed out over ice and centrifuged for 15 min at 13,000*g* and 4°C. 150 µl of supernatant was then diluted to produce a final volume containing 50% (v/v) SF, 40% (v/v) dd $^{1}H_2O$, 10% (v/v) 1M PO_4^{3-} pH 7.4 buffer (Na_2HPO_4, VWR International Ltd., Radnor, Pennsylvania, USA and NaH_2PO_4, Sigma-Aldrich) in deuterium oxide ($^{2}H_2O$, Sigma-Aldrich) and 0.0025% (v/v) sodium azide (NaN_3, Sigma-Aldrich). Prepared samples were then vortexed for 1 min, centrifuged for 2 min at 13,000*g* and 4˚C and, using a glass pipette, 195 µl transferred into 3 mm outer diameter NMR tubes.

3.3.7.2. NMR Acquisition

All SF samples were individually analysed. A 700 MHz NMR Bruker Avance III HD spectrometer with associated TCI cryoprobe and chilled Sample-Jet autosampler was used to acquire all spectra. 1D ^{1}H NMR spectra, using a Carr-Purcell-Meiboom-Gill (CPMG) filter to attenuate macromolecule (e.g. protein) signals, were acquired using a standard cpmgpr1d vendor pulse sequence. Spectral acquisition was carried out at 37˚C with a 4 s interscan delay, 32 transients and a 15 ppm spectral width. Software programmes Topsin 3.1 and IconNMR 4.6.7 were used for acquisition and processing, carrying out automated phasing, baseline correction and a standard vendor processing routine (exponential window function with 0.3 Hz line broadening).

3.3.7.3. Metabolite Annotation and Identification

All 1D ^{1}H NMR spectra were scrutinised to make sure that the minimum reporting standards were met, as outlined by the Metabolomics Society (Sumner *et al.*, 2007). Spectra were aligned to a single formate peak at 8.46 ppm. Chenomx NMR Suite 8.2 (330-mammalian metabolite library) software was used to carry out metabolite annotations and relative abundances. Metabolite identifications were confirmed where possible using in-house 1D ^{1}H NMR metabolite spectral library standards.

3.3.8. Proteomics

3.3.8.1. Synovial Fluid Processing and Protein Assay

SF was thawed on ice and centrifuged at 4°C at 14,000*g* for 10 min. The supernatant was treated with 1µg/ml of hyaluronidase (bovine origin, Sigma-Aldrich) at 37˚C for 1 hr, centrifuged at 1,000*g* for 5 min, supernatant removed and 1 ml centrifuged through a polypropylene microcentrifuge tube filter with 0.22 µm pore cellulose acetate membrane (Costar Spin-X, Corning, Tokyo, Japan) at 5000*g* for 15 min to remove remaining insoluble particulates (Mateos *et al.*, 2012). A Pierce® 660 nm protein assay (Thermo Scientific, Waltham, Massachusetts, USA) was used to determine SF protein concentrations.

3.3.8.2. ProteoMiner™ Column Processing

2 mg of protein was loaded onto ProteoMiner™ Small Capacity bead columns (Bio-Rad Laboratories Ltd., Hemel Hempstead, UK) to achieve peptide-based depletion of the most abundant proteins. SF samples were rotated for 2 hr at room temperature and centrifuged at 1,000*g* for 60 s. ProteoMiner™ beads were then washed in PBS, rotated for 5 min and centrifuged at 1,000*g* for 60 s. The wash step was repeated two further times.

3.3.8.3. Protein Digestion

To assess both high and low abundance synovial proteins, both native and ProteoMiner™ processed SF were analysed. For native SF, 100 µg of protein was used for each protein trypsin digestion. 25 mM ammonium bicarbonate (Fluka

Chemicals Ltd., Gillingham, UK) containing 0.05% (w/v) RapiGest (Waters, Elstree, Hertfordshire, UK) was added to both native SF and peptide bound ProteoMiner™ beads to produce a final volume of 160 µl and heated at 80°C for 10 min. DL-Dithiothreitol (Sigma-Aldrich) was added (3 mM final concentration) and incubated at 60°C for 10 min. Iodoacetamide (Sigma-Aldrich) was added (9 mM final concentration) and incubated at room temperature for 30 min in the dark. ProteoMiner™ processed samples then underwent an additional step which entailed the addition of 2 µg of Lys-C endopeptidase (FUJIFILM Wako Pure Chemical, Osaka, Japan) and incubation at 37˚C for 4 hr (Chapter 1). 2 µg of proteomics grade trypsin (Sigma-Aldrich) was added to all samples and rotated for 16 hr at 37°C, followed by a second trypsin supplementation for 2 hr incubation. Digests were centrifuged at 1,000*g* for 1 min, supernatant removed, trifluoroacetic acid (TFA, Sigma-Aldrich) added (0.5% (v/v) final concentration) and rotated for 30 min at 37°C. Digests were then centrifuged at 13,000*g* for 15 min at 4°C and the supernatant removed and stored at -80°C. To ensure complete protein digestion, 5 µl of each digest was analysed by 1D SDS PAGE and stained with either Coomassie Blue (Bio-Rad) or silver stain (Thermo Scientific) following manufacturer instructions (data not shown).

3.3.8.4. Sample Processing for Neopeptide Analysis

After 4 hr of the 16 hr tryptic digestion of ProteoMiner™ processed samples, 10 µl was removed and supplemented with TFA and stored at -80°C using the same protocol as mentioned above.

3.3.8.5. Label Free LC-MS/MS

All SF digest samples underwent randomisation and were individually analysed using LC-MS/MS on an UltiMate 3000 Nano LC System (Dionex/Thermo Scientific) coupled to a Q Exactive™ Quadrupole-Orbitrap instrument (Thermo Scientific). Full LC-MS/MS instrument methods are described in chapter 7. Tryptic peptides, which were equivalent to 200 ng of protein, were loaded onto the column and run over 60 min, 90 min and 120 min LC gradients for 4 hr Lys-C + 4 hr tryptic digest ProteoMiner™ samples, native SF and 4 hr Lys-C + 16 hr + 2 hr tryptic digest

ProteoMiner™ processed samples respectively. Representative ion chromatograms are shown in Supplementary Figure 2.

3.3.8.6. LC-MS/MS Spectra Processing and Protein Identification

Progenesis™ QI 2.0 (Nonlinear Dynamics, Waters) software was used to process raw spectral files and undertake spectral alignment, peak picking, total protein abundance normalisation and peptide/protein quantification. The top ten spectra for each feature were then exported with peptide and protein identifications carried out with PEAKS® Studio 8.5 (Bioinformatics Solutions Inc., Waterloo, Ontario, Canada) using the reviewed *Equus caballus* database. Search parameters included: precursor mass error tolerance, 10.0 ppm; fragment mass error tolerance, 0.01 Da; precursor mass search type, monoisotopic; enzyme, trypsin; maximum missed cleavages, 1; non-specific cleavage, none; fixed modifications, carbamidomethylation; variable modifications, oxidation or hydroxylation and oxidation (methionine). The false discovery rate (FDR) was set to 1% with only proteins identified with > 2 unique peptides used for quantitation.

3.3.8.7. Semi-Tryptic Peptide Identification

A 'semi-tryptic' search was undertaken to identify potential synovial neopeptides. PEAKS® search parameters were kept the same as those used for protein identifications, apart from 'Non-specific Cleavage' which was changed from 'none' to 'one'. The exported 'peptide ion measurements' file from Progenesis™ was then analysed using an online neopeptide analyser software tool to identify only semi-tryptic peptides and perform normalisation (Peffers *et al.*, 2017).

3.3.9. Batch Corrections

ProteoMiner™ processed samples for both the biobank and HKJC cohorts were run in three separate batches on the Q Exactive™ for protein analysis. To eliminate batch effects on the final analysis, a COMBAT batch correction was applied (Supplementary Figure 3) (Johnson *et al.*, 2007). Metabolomic spectra were also acquired over 3 batches for both biobank and HKJC cohorts and data also underwent COMBAT batch correction.

3.3.10. ELISA Protein Validations

Differentially expressed proteins apolipoprotein A1 (ApoA1), gelsolin and lipopolysaccharide binding protein (LBP) were selected for ELISA as commercially available kits were compatible with equine samples. Equine ApoA1 (MBS034194, MyBioSource Inc., San Diego, California, USA) and equine LBP (MBS062216, MyBioSource) utilised sandwich ELISA technology using undiluted SF whilst equine gelsolin (CSB-EL009965HO, Cusabio Technology LLC, Houston, Texas, USA) was a competitive inhibition assay with SF diluted 1:1250. 3-6 dependent (and independent where stated) SF samples were analysed per group. Aliquots of 100 µl were analysed in duplicate for each sample with absorbance measured at 450 nm and protein concentrations calculated from assay standard curves. Protein concentrations were normalised to total protein.

3.3.11. Separate Dataset Statistical Analysis

SF metabolite abundances underwent median normalisation and protein abundances were normalised to the total ion current (TIC). Before multivariate analysis, both metabolite and protein datasets underwent Pareto scaling (Worley and Powers, 2013). All principal component analysis (PCA), ANOVA and t-tests of metabolite, protein and neopeptide abundances were conducted using MetaboAnalyst 4.0 (http://www.metaboanalyst.ca). ELISA t-tests and ANOVAs were performed using Minitab version 17. For protein analysis an additional filter of > 2 fold abundance was implemented. A p value of < 0.05 was considered statistically significant following correction for multiple testing using the Benjamini-Hochberg false discovery rate method (Benjamini and Hochberg, 1995). All box plots were produced using SPSS 24.

3.3.12. NMR metabolomics and LC-MS/MS Proteomics Integration

Metabolomic and proteomic data integration was conducted by Dr Eva Caamaño-Gutiérrez at the Computational Biology Facility, University of Liverpool. Only datasets for horses which had both metabolite and protein abundance values were used for integration. Proteomics datasets were again normalised to the TIC whilst NMR datasets were normalised via probabilistic quotient normalisation (PQN) (Kohl

et al., 2012). When combining ProteoMiner™ processed SF and native SF protein abundances for the same SF sample, in which the same protein had been identified in both datasets, the higher abundance was included for analysis. The Mahalanobis distance on principal components was calculated and Chi-squared testing undertaken to identify potential outliers. When combining metabolite and protein variables, categorisation was carried out in accordance to macroscopic OA scoring. A linear regression, using Lasso (least absolute shrinkage and selection operator) penalisation to select the most important variables, was applied to combined datasets for both the biobank and HKJC sample groups. Additionally, correlations of all variables (proteins and metabolites) with macroscopic OA score were calculated, with significant variables ($p < 0.05$) included for further analysis. Significant variables across all analyses were then applied to a collective dataset, combing both biobank and HKJC results. This dataset was stratified into healthy, mild OA and severe OA and a discriminant analysis of principal components (DAPC) applied. All integration analyses were undertaken using standard analytical routines within the software package R (https://cran.r-project.org/).

3.3.13. Uncharacterised Proteins

Within this study, proteins which were considered uncharacterised were also analysed using BLAST (Basic local alignment search tool) to assess similarity of their amino acid sequence to characterised proteins within the *Equus caballus* database as well as other species (Altschul *et al.*, 1990). Search parameters included: Matrix, blosum62; threshold, 0.1 E; filtering, none; gapped, true.

3.3.14. Pathway Analysis

Pathway analysis was conducted on proteins and metabolites which were considered significant variables for DAPC when carrying out NMR metabolomic and LC-MS/MS proteomic dataset integration. Metabolite pathway analysis was conducted using the online tool KEGG for *Equus caballus* with protein pathways also analysed using KEGG, via the STRING database (Ogata *et al.*, 1999; Szklarczyk *et al.*, 2015). A filter of a minimum of two metabolites or proteins was set for inclusion of the relevant biological pathway.

3.4. Results

3.4.1. Stratification Groups

Interrater reliability score assessment for microscopic and macroscopic OA pathology scores of biobank samples and macroscopic OA pathology scores of HKJC samples identified good agreement with Cohen's kappa coefficient scores of 0.78, 0.70 and 0.69 respectively (McHugh, 2012). HKJC microscopic OARSI and synovitis scores were unable to be assessed as these were only scored once as slides were unavailable for second scoring. Histological microscopic OA scores vs macroscopic scores for biobank and HKJC samples both showed a weak positive correlation with R^2 coefficient values of 0.12 and 0.17 respectively (Supplementary Figure 4). Where grading was carried out by two scorers, if the grading scores differed by more than 1, a third scorer was used. For final grade scores an average of both scores was taken and grouped according to microscopic OA pathology, macroscopic OA pathology and synovitis scores (Table 1). Examples of gross and histological scores are shown in Figures 2 and 3. Although scored using different scoring systems, overall the HKJC samples exhibited a more severe OA phenotype. Macroscopically, scores were on average 30% of the highest possible score, compared to 14% within the biobank and microscopic scores 31% compared to 15% within the biobank. All scoring is shown in Supplementary Tables 3-7. Overall, the HKJC dataset was a younger cohort than the biobank cohort, with average ages of 6.6 ± 1.9 years and 14.3 ± 7.6 years respectively (Supplementary Table 2).

Table 1. Stratification groups according to microscopic osteoarthritis, macroscopic osteoarthritis and synovitis pathology used for synovial fluid LC-MS/MS proteomic and NMR metabolomic analysis.

Biobank

Metabolomics	OARSI Microscopic OA Group			OARSI Macroscopic OA Group			
	0	1	2	0	1	2	3
Number of Donors	8	34	28	14	27	21	14
Joint	8 x MCP	34 x MCP	28 x MCP	14 x MCP	27 x MCP	21 x MCP	14 x MCP
Mean Age (years)	8	15	17	9	15	16	19
Sex (M/F)	1 F, 7 Unknown	6 M, 10 F, 18 Unknown	12 M, 10 F, 6 Unknown	2 M, 5 F, 7 Unknown	7 M, 12 F, 8 Unknown	9 M, 5 F, 7 Unknown	6 M, 3 F, 5 Unknown

Proteomics	OARSI Microscopic OA Group			OARSI Macroscopic OA Group			
	0	1	2	0	1	2	3
Number of Donors	8	34	28	11	25	18	12
Joint	8 x MCP	34 x MCP	28 x MCP	11 x MCP	25 x MCP	18 x MCP	12 x MCP
Mean Age (years)	8	15	17	9	15	16	20
Sex (M/F)	1 F, 7 Unknown	6 M, 10 F, 18 Unknown	12 M, 10 F, 6 Unknown	1 M, 3 F, 7 Unknown	6 M, 11 F, 8 Unknown	6 M, 5 F, 7 Unknown	5 M, 2 F, 5 Unknown
Mean Protein Concentration (mg/ml)	5	5	4	5	4	5	6

Hong Kong Jockey Club

Metabolomics	Microscopic OA Group			Macroscopic OA Group			Synovitis Group		
	0	1	2	0	1	2	0	1	2
Number of Donors	17	20	13	13	25	12	1	38	17
Joint	10 x MCP, 7 x MTP	8 x MCP, 12 x MTP	9 x MCP, 4 x MTP	5 x MCP, 8 x MTP	13 x MCP, 12 x MTP	11 x MCP, 11 x MTP	1 x MTP	22 x MCP, 16 x MTP	10 x MCP, 7 x MTP
Mean Age (years)	6	7	7	5	7	7	6	7	7
Sex (M/F)	UNKNOWN			UNKNOWN			UNKNOWN		

Proteomics	Microscopic OA Group			Macroscopic OA Group			Synovitis Group		
	0	1	2	0	1	2	0	1	2
Number of Donors	16	20	13	13	24	12	1	34	19
Joint	9 x MCP, 7 x MTP	8 x MCP, 12 x MTP	9 x MCP, 4 x MTP	5 x MCP, 8 x MTP	12 x MCP, 12 x MTP	11 x MCP, 11 x MTP	1 x MTP	18 x MCP, 16 x MTP	10 x MCP, 9 x MTP
Mean Age (years)	6	7	7	5	7	7	6	7	7
Sex (M/F)	UNKNOWN			UNKNOWN			UNKNOWN		
Mean Protein Concentration (mg/ml)	10	9	13	7	9	17	16	9	12

Abbreviations: OA = Osteoarthritis; Joints, MCP = Metacarpophalangeal joint, MTP = Metatarsophalangeal joint; Sex, M = male, F = Female.

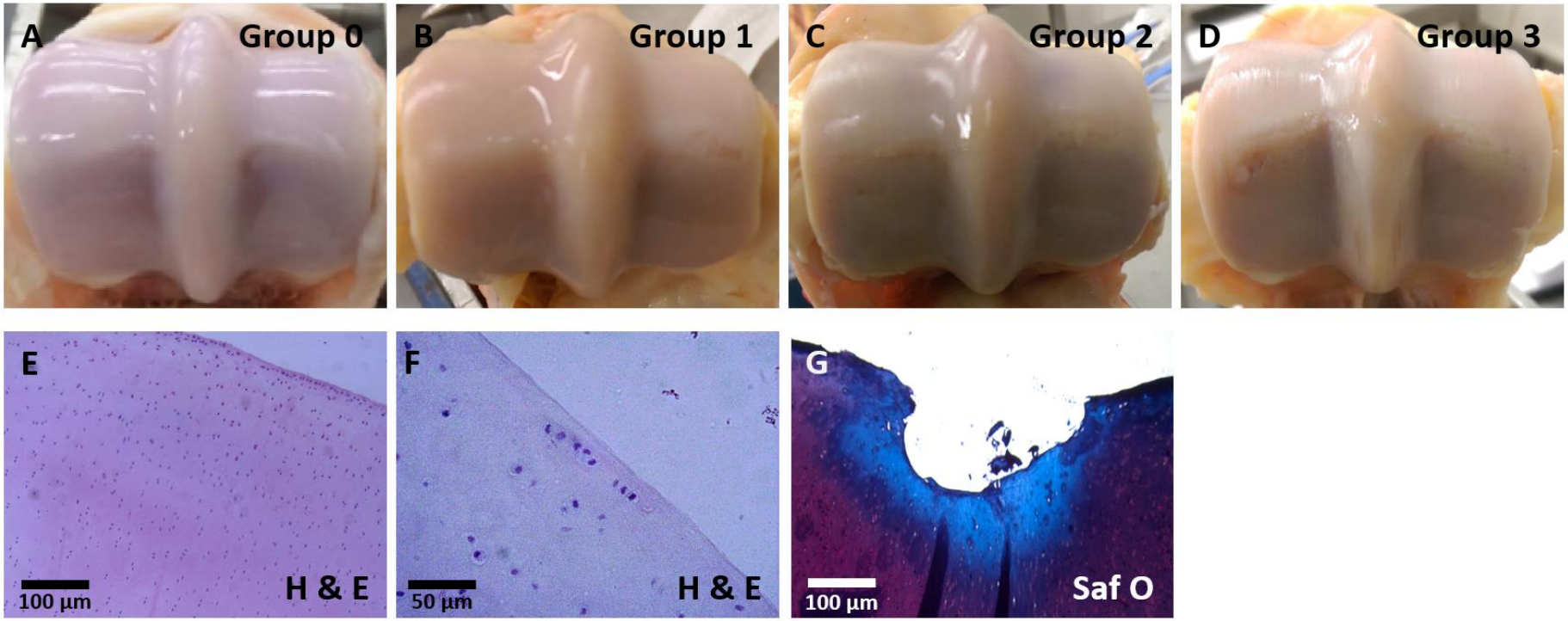

Figure 2. Examples of macroscopic and microscopic osteoarthritis related pathology scoring for the biobank group using the equine OARSI scoring scale (McIlwraith *et al.*, 2010). Macroscopic scoring was conducted on the distal metacarpal III articular surface. (A) Group 0, normal; (B) Group 1, grade 1 erosions; (C) Group 2, grade 1 erosions, grade 1 wear lines; (D) Group 3, grade 1 erosions, grade 2 wear lines, grade 2 palmar arthrosis. Microscopic scoring was conducted on wedge sections of articular cartilage/subchondral bone stained with haematoxylin and eosin (H & E) or Safranin O (Saf O). (E) grade 0 fissuring, grade 0 focal cell loss, grade 0 chondrone formation; (F) grade 0 fissuring, grade 1 focal cell loss, grade 2 chondrone formation; (G) grade 4 fissuring, grade 4 Saf O uptake.

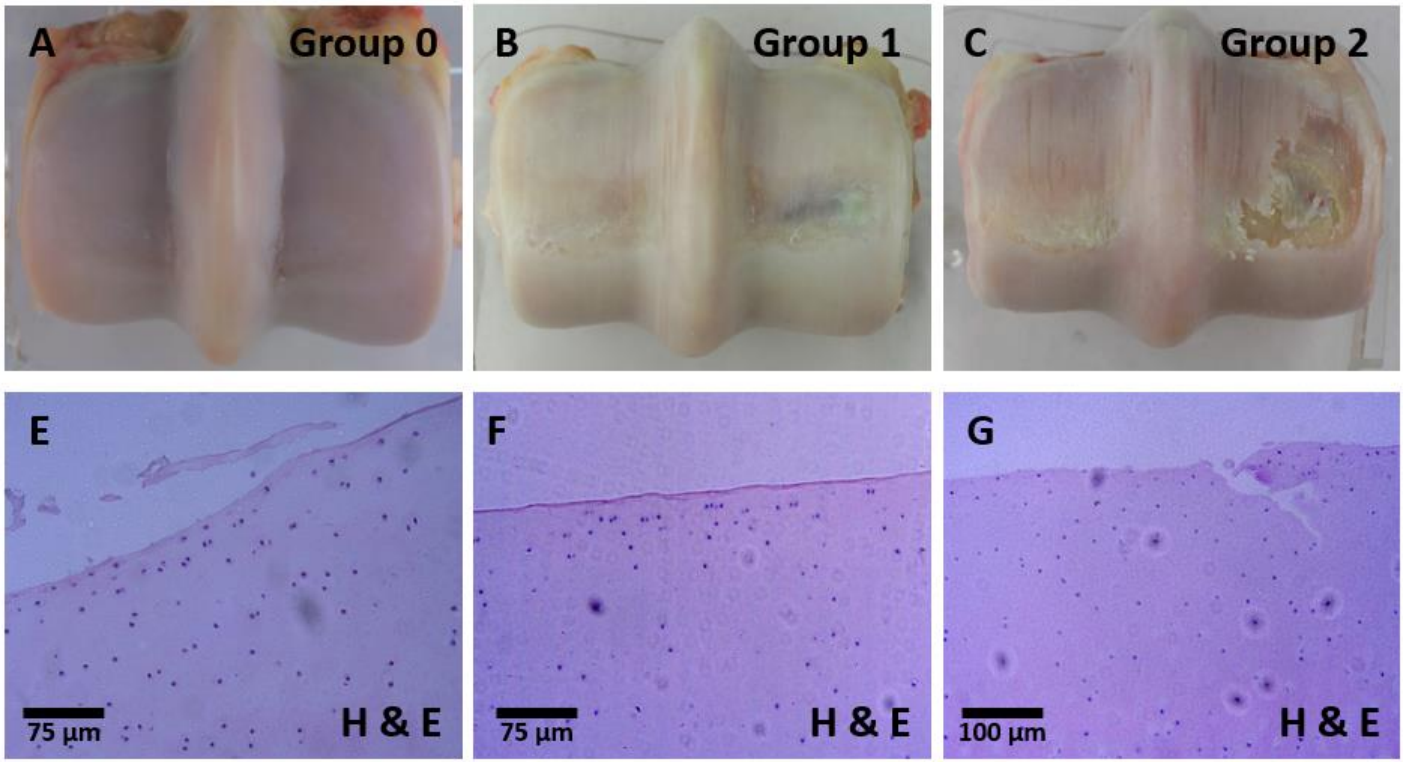

Figure 3. Examples of macroscopic and microscopic osteoarthritis pathology scoring for the Hong Kong Jockey Club group using osteoarthritis related and palmar/plantar osteochondral disease (POD) pathology using published scoring scales (Barr *et al.*, 2009; Little *et al.*, 2010). Macroscopic scoring was conducted on the distal metacarpal III and metatarsal III articular surfaces. (A) Group 0, normal; (B) Group 1, grade 1 POD, grade 2 wear lines, grade 1 cartilage loss; (C) Group 2, grade 3 POD, grade 2 wear lines, grade 3 cartilage loss. Microscopic scoring was conducted on wedge sections of articular cartilage/subchondral bone stained with haematoxylin and eosin (H & E). (E) grade 3 structure, grade 0 chondrocyte density, grade 2 cell cloning; (F) grade 0 structure, grade 2 chondrocyte density, grade 2 cell cloning; (G) grade 4 structure, grade 1 chondrocyte density, grade 0 cell cloning.

3.4.2. NMR Metabolomics

Overall, both the biobank and HKJC SF 1D ^{1}H NMR spectra produced similar profiles, although quantile plots revealed the biobank group exhibited more variation between samples (Supplementary Figure 5). In total, 40 metabolites were identified within equine SF (Table 2). For the biobank cohort, unsupervised multivariate PCA did not identify separation between OA grades based on microscopic or macroscopic scoring (Figure 2). However, when stratified according to macroscopic grade, glutamate levels were found to be differentially abundant, with lower levels identified at grades 2 and 3 compared to 1. PCA also did not identify clear separation between severity grades of OA or synovitis for HKJC SF samples (Figure 3). When stratified according to macroscopic OA pathology, three metabolites were found to be differentially abundant. 2-aminobutyrate levels were increased at grades 1 and 2 compared to 0 and alanine and creatine levels were increased with OA severity.

Table 2. Synovial fluid metabolites identified using Chenomx software. Metabolites which had also undergone identification using a 1D ^{1}H NMR in-house spectral library were assigned to Metabolomics Standards Initiative (MSI) level 1 (Salek *et al.*, 2013).

Database Identifier	Metabolite Identification	Reliability
HMDB00650	2-Aminobutyrate	MS Level 2
HMDB00357	3-Hydroxybutyrate	MS Level 2
HMDB00754	3-Hydroxyisovalerate	MS Level 2
HMDB01149	5-Aminolevulinate	MS Level 2
HMDB00042	Acetate	MS Level 1
HMDB00194	Anserine	MS Level 2
HMDB00043	Betaine	MS Level 1
HMDB00097	Choline	MS Level 1
HMDB00094	Citrate	MS Level 1
HMDB00064	Creatine	MS Level 1
HMDB01511	Creatine phosphate	MS Level 2
HMDB00562	Creatinine	MS Level 1
HMDB00122	D-Glucose	MS Level 1

HMDB04983	Dimethyl sulfone	MS Level 2
HMDB00142	Formate	MS Level 2
HMDB00123	Glycine	MS Level 1
HMDB00128	Guanidoacetate	MS Level 2
HMDB00172	Isoleucine	MS Level 1
HMDB00190	Lactate	MS Level 1
HMDB00161	L-Alanine	MS Level 1
HMDB00062	L-Carnitine	MS Level 2
HMDB00174	L-Fucose	MS Level 2
HMDB00148	L-Glutamate	MS Level 1
HMDB00641	L-Glutamine	MS Level 1
HMDB00177	L-Histidine	MS Level 1
HMDB00687	L-Leucine	MS Level 1
HMDB00159	L-Phenylalanine	MS Level 1
HMDB00158	L-Tyrosine	MS Level 1
HMDB00883	L-Valine	MS Level 1
HMDB00691	Malonate	MS Level 2
HMDB01844	Methylsuccinate	MS Level 2
HMDB31419	N-Nitrosodimethylamine	MS Level 2
HMDB00895	O-Acetylcholine	MS Level 2
HMDB00243	Pyruvate	MS Level 1
HMDB00254	Succinate	MS Level 1
HMDB00294	Urea	MS Level 1
HMDB00296	Uridine	MS Level 1
HMDB00292	Xanthine	MS Level 2
HMDB00001	π-Methylhistidine	MS Level 2
HMDB00001	τ-Methylhistidine	MS Level 2

Metabolomics Standards Initiative definitions: MS Level 1 = Identified metabolite using two or more orthogonal properties of an authentic chemical standard analysed in the researcher's laboratory. MS Level 2 = Putatively annotated metabolite which does not require matching to data for authentic chemical standards acquired within the same laboratory.

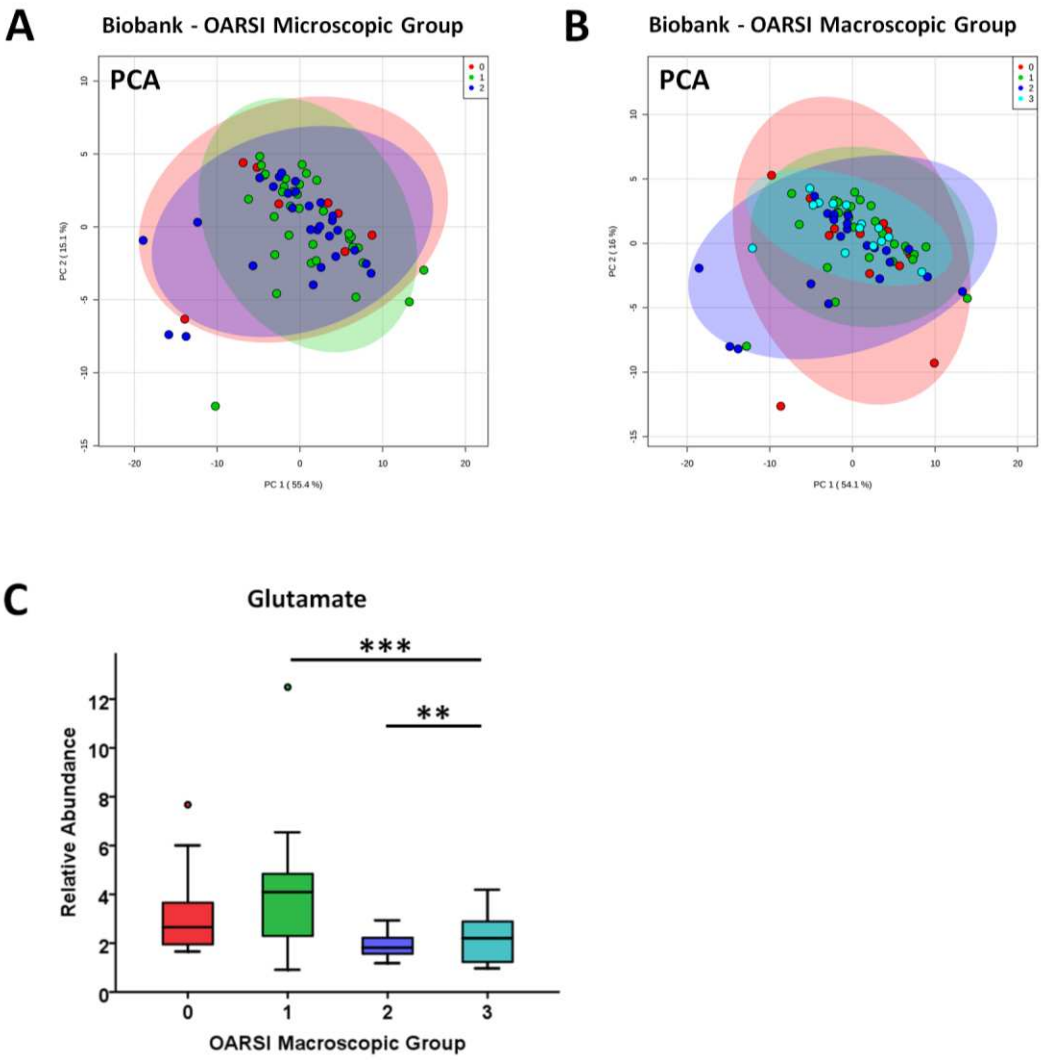

Figure 2. Principal component analysis (PCA) of metabolite profiles of equine biobank synovial fluid grouped according to (A) OARSI microscopic (n=70) and (B) OARSI macroscopic (n=76) grading. (C) Glutamate abundances according to macroscopic osteoarthritis grading. ANOVA: ** = $p < 0.01$ and *** = $p < 0.001$.

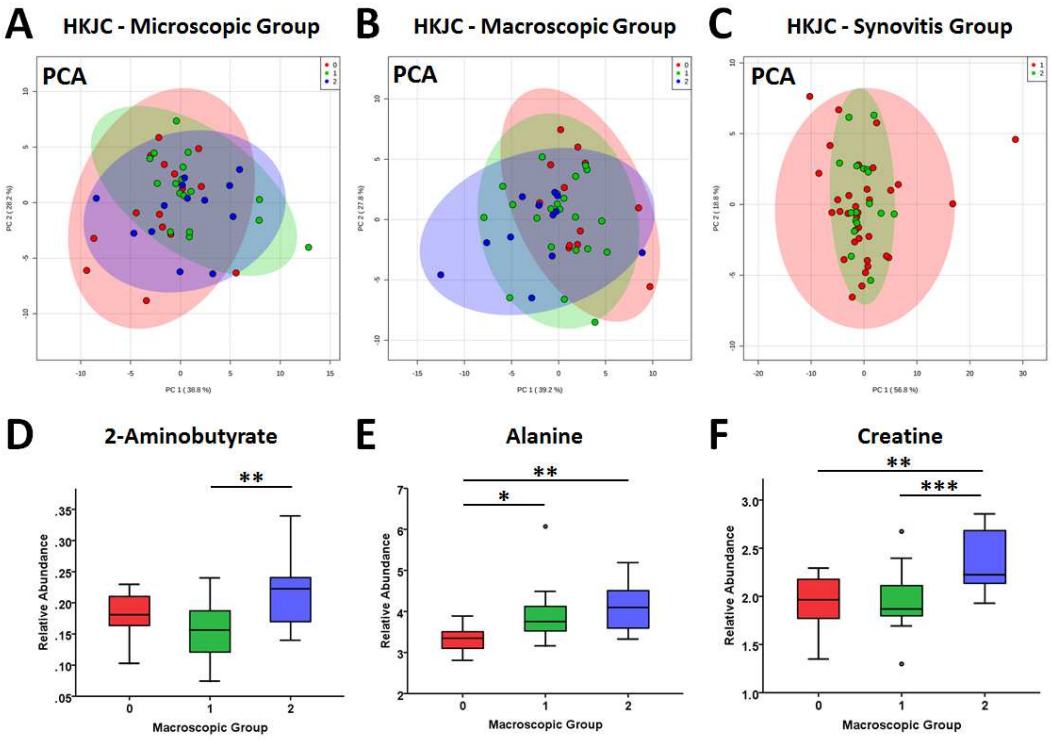

Figure 3. Principal component analysis (PCA) of metabolite profiles of equine Hong Kong Jockey Club (HKJC) synovial fluid (SF) grouped according to (A) OARSI microscopic (n=50), (B) OARSI macroscopic (n=50) and (C) synovitis (n=56) grading. For OARSI macroscopic grading, (D) 2-aminobutyrate, (E) alanine and (F) creatine were identified as being differentially abundant between osteoarthritis severity grades. ANOVA: * = $p < 0.05$, ** = $p < 0.01$ and *** = $p < 0.001$.

3.4.3. LC-MS/MS Proteomics

Within the biobank cohort, 74 native SF samples were analysed with 68 of these additionally processed using ProteoMiner™ columns. For the HKJC group, 56 native SF samples were analysed with 55 of these additionally having also undergone ProteoMiner™ processing. In total, across all samples 1, 834 proteins were identified (Figure 4). A combination of an increase in LC gradient length and ProteoMiner™ processing resulted in a 168% increase in the overall number of identified proteins compared to native SF analysis.

	NATIVE	PROTEOMINER™
No. Samples	130	124
LC gradient length (mins)	90	120
Total no. proteins identified	621	1,666
Mean no. proteins identified/sample	182	357
Median no. proteins identified/sample	165	294
Lowest no. proteins identified in a sample	115	124
Highest no. proteins identified in a sample	407	870

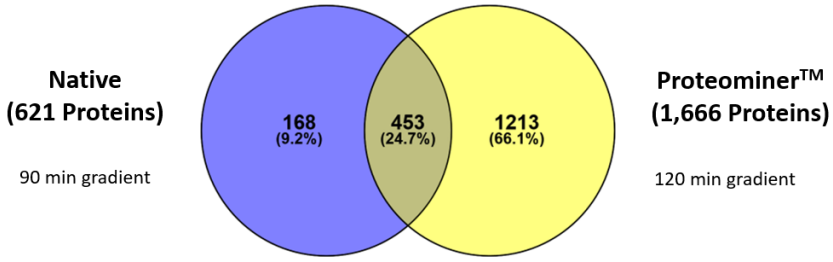

Figure 4. Number of proteins identified within native and ProteoMiner™ processed equine synovial fluid using liquid chromatography-tandem mass spectrometry. Search criteria included > 2 unique peptides with an FDR of 1%. LC = liquid chromatography.

For biobank and HKJC groups, when categorised according to macroscopic OA severity, PCA identified that increased OA severity resulted in less variation between samples (Figure 5). However, this was not evident when categorised according to microscopic OA grading. For native SF biobank samples categorised according to macroscopic grading, the abundance of three uncharacterised proteins and immunoglobulin kappa constant decreased with increasing OA severity. An uncharacterised protein (a member of the superfamily containing a leucine-rich repeat) and ApoA1 abundances both increased initially with OA pathology but then returned towards baseline with greater OA severity. Microscopic OA categorisation for native SF biobank as well as macroscopic and microscopic OA categorisation of native SF HKJC samples did not identify any differentially abundant proteins. The proteomes of native SF HKJC samples, categorised according to synovitis grade, were not separated via PCA (Figure 6). However, the abundance of afamin was identified as differentially abundant between low and high grade synovitis, decreasing with synovitis severity. ProteoMiner™ processing of both biobank and HKJC SF did not identify any differentially abundant proteins or distinct proteome

clusters (PCA) for any OA or synovitis categorisations (Supplementary Figures 6 and 7). However, LC-MS/MS analysis of ProteoMiner™ processed biobank SF identified trends in gelsolin and LBP abundance, decreasing with increasing OA severity (Figure 7). ELISA analysis of gelsolin using the same SF samples that were analysed by LC-MS/MS corroborated this finding and was additionally supported by an independent clinical cohort, with gelsolin abundance lower in clinical OA cases compared to controls. LBP ELISA analysis of both dependent and independent SF samples also supported the trend identified via LC-MS/MS, although statistical significance was not reached. For biobank native and ProteoMiner™ processed SF we identified a trend that ApoA1 increased initially with OA severity and subsequently decreased. This trend was supported by ApoA1 ELISA analysis using dependent SF samples; however statistical significance was not reached.

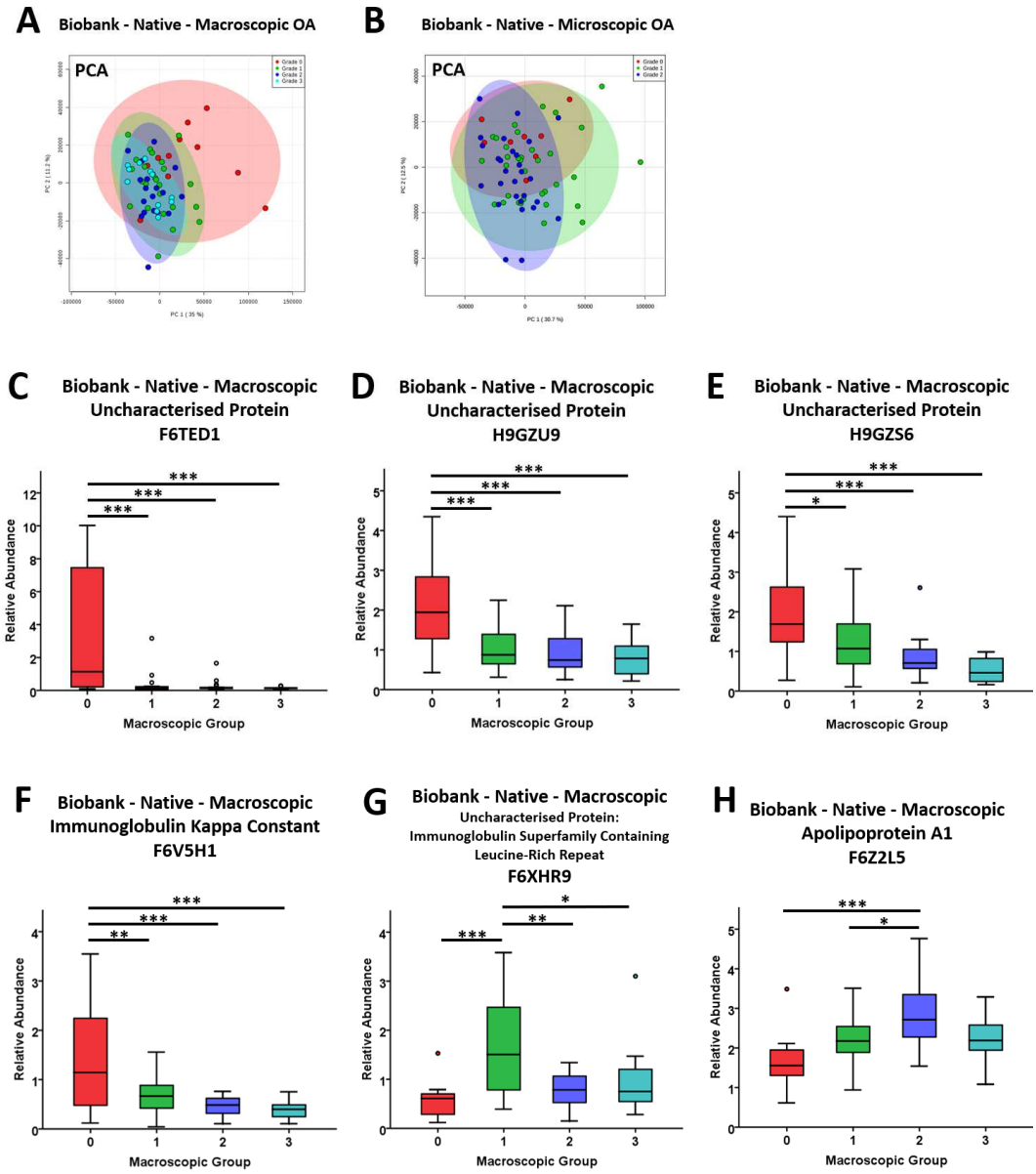

Figure 5. Principal component analysis (PCA) of the biobank native synovial fluid proteome categorised by (A) macroscopic osteoarthritis (OA) grade and (B) microscopic OA grade using LC-MS/MS. (C-H) Differentially expressed proteins when categorised according to macroscopic OA grade. ANOVA: * = $p < 0.05$, ** = $p < 0.01$, *** = $p < 0.001$. Macroscopic OA, n=66, Microscopic OA, n=70.

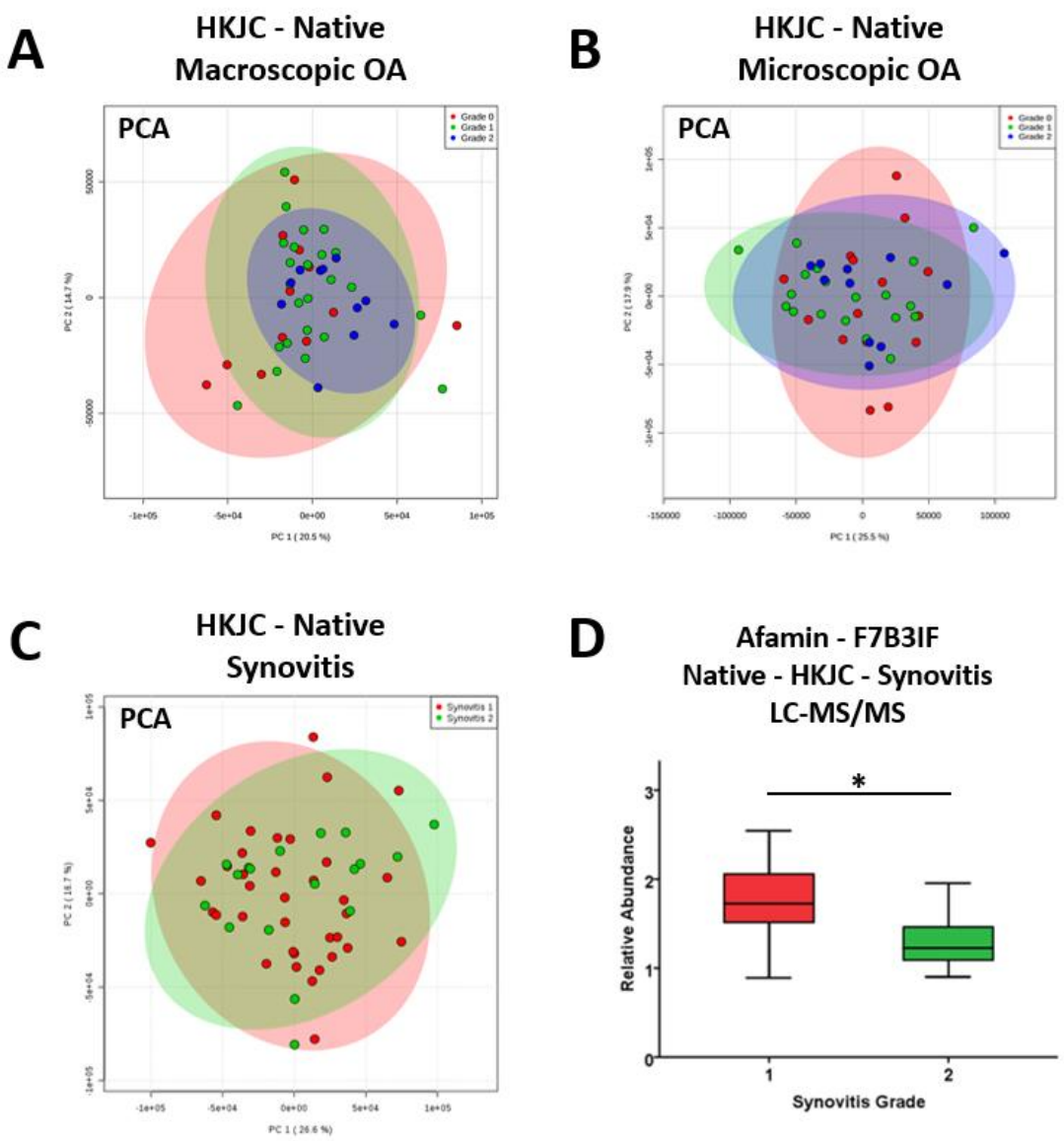

Figure 6. Principal component analysis (PCA) of the Hong Kong Jockey Club (HKJC) native synovial fluid proteome profile categorised by (A) macroscopic osteoarthritis (OA) grade (n=49), (B) microscopic OA grade (n=49) and (C) synovitis grade (n=53) using LC-MS/MS. (D) Differential expression of afamin identified between synovitis grade 1 and 2. t-test: * = $p < 0.05$.

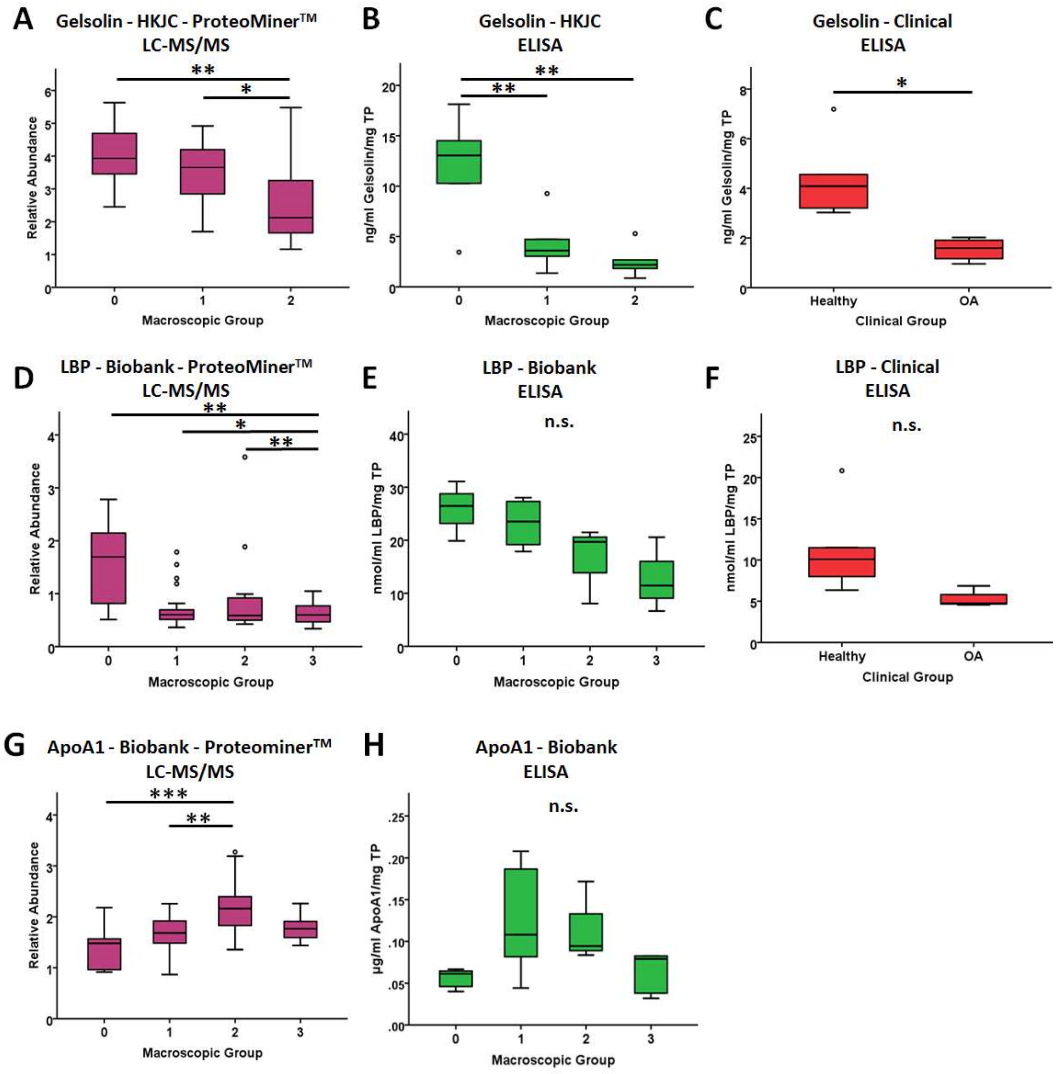

Figure 7. Abundances of gelsolin, lipopolysaccharide binding protein (LBP) and apolipoprotein A1 (ApoA1) within equine synovial fluid via LC-MS/MS (A, D & G) and ELISA validation using dependent (B, E & H) and independent (C & F) synovial fluid samples according to osteoarthritis (OA) grade. LC-MS/MS; HKJC, n=47; Biobank, n=60; ELISA, n=3-6/group. ANOVA and t-tests: * = $p < 0.05$, ** = $p < 0.01$, *** = $p < 0.001$. LC-MS/MS p values corrected for multiple testing within sample, but not for entire dataset.

3.4.3.1. Semi-Tryptic Peptide Profiles

No semi-tryptic peptides arising from ECM proteins were identified which were more highly abundant at more severe OA levels and thus no potential neopeptide biomarkers were identified. Neither for the biobank or HKJC groups were distinct profiles identified between severities of OA (Figure 8). For the HKJC group there was less intra-group variation identified with increased levels of OA and synovitis pathology. However, conversely for the biobank group, samples with no OA pathology showed the least variation.

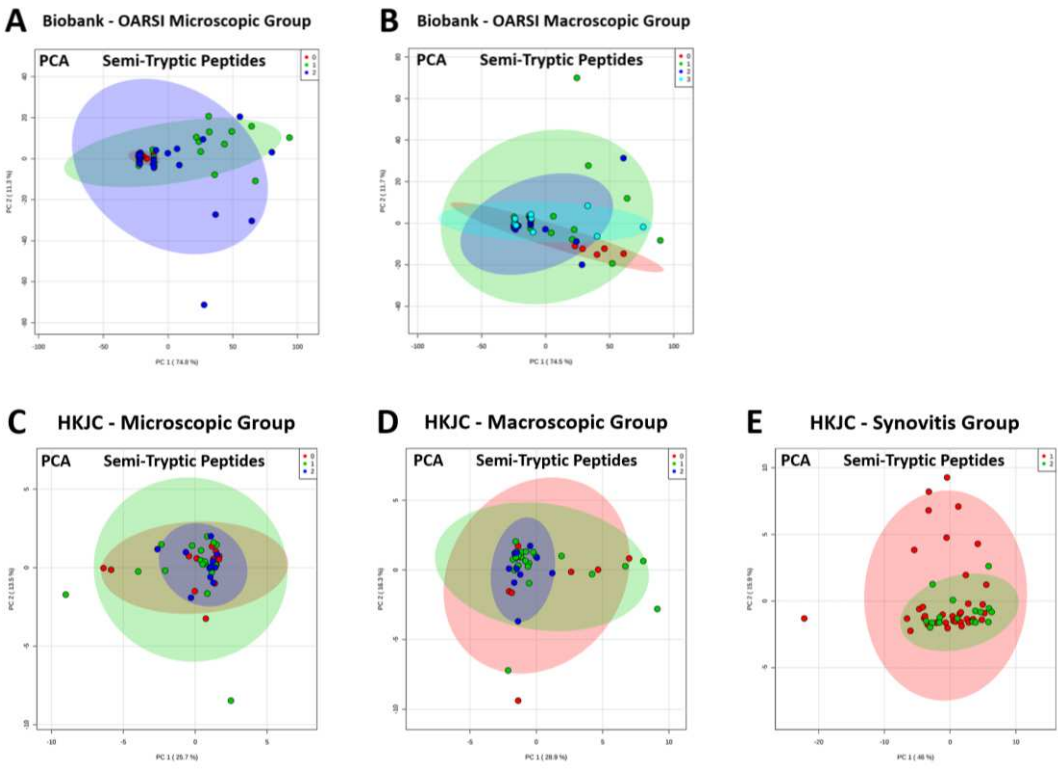

Figure 8. Principal component analysis (PCA) of equine synovial fluid semi-tryptic peptide profiles grouped according to (A) microscopic osteoarthritis (n=62) and (B) macroscopic osteoarthritis (n=59) severity for the biobank cohort and (C) microscopic osteoarthritis (n=46), (D) macroscopic osteoarthritis (n=46) and (E) synovitis (n=53) severity for the Hong Kong Jockey Club (HKJC).

3.4.4. NMR metabolomics and LC-MS/MS Proteomics Integration

For the HKJC dataset, linear regression using Lasso penalisation modelling was unable to select a suitable number of parameters without overfitting the model. However, correlation analysis of all variables (proteins and metabolites) identified 58 significant variables, with a range in correlation from -0.48 to 0.42 (Table 3). Using these selected variables, PCA identified less variation between samples with more severe macroscopic OA scores, although their grouping could not clearly be distinguished from lower scoring samples (Figure 9).

Table 3. Correlation of each variable (proteins and metabolites) to macroscopic OA score for the Hong Kong Jockey Club synovial fluid integrated dataset. $p < 0.05$.

Variable	Correlation	Permutation p value	Characterisation
P60708	-0.44	0	Actin, cytoplasmic 1
HMDB00001	0.37	0	τ-Methylhistidine
F6UL68	-0.45	0	Transthyretin
F6VCB4	-0.36	0	Histone H3
F6VS95	-0.48	0	Protein disulfide isomerase family A member 6
F6W3T1	-0.38	0	L-lactate dehydrogenase
F6YNM7	-0.36	0	Prolyl endopeptidase
F6YRC5	-0.39	0	IQ motif containing GTPase activating protein 1
F6YRE0	-0.36	0	Tubulin alpha chain
F6ZMJ5	-0.40	0	ATPase H^+ transporting V1 subunit E2
F7ABC9	-0.38	0	Fibulin-1
F7D8W6	-0.43	0	Guanylate binding protein 2
F7DNT0	-0.42	0	Tubulin alpha chain
F7DYV0	-0.43	0	Galectin
A2Q0Z0	-0.28	0.01	Elongation factor 1-alpha 1
Q28372	-0.35	0.01	Gelsolin
F6T0P6	-0.36	0.01	GC, vitamin D binding protein
F6UZI2	-0.35	0.01	Coagulation factor XIII A chain
F6V6L8	-0.36	0.01	IQ motif containing GTPase activating protein 2
F6YIU8	-0.39	0.01	Methylenetetrahydrofolate dehydrogenase, cyclohydrolase and formyltetrahydrofolate synthetase 1
F6YXS1	0.37	0.01	Receptor protein-tyrosine kinase
F6ZFH9	-0.39	0.01	Tyrosine 3-monooxygenase/tryptophan 5-monooxygenase activation protein gamma

F7AYC1	-0.31	0.01	Secreted phosphoprotein 1
F7BNQ2	-0.36	0.01	Complement component 4 binding protein alpha
F7BQD6	0.35	0.01	Complement C1s
F7CYG2	-0.38	0.01	Tyrosine 3-monooxygenase/tryptophan 5-monooxygenase activation protein eta
HMDB00062	0.35	0.02	Carnitine
HMDB00190	-0.33	0.02	Lactate
F6QXN5	-0.34	0.02	Transgelin
F6S0P5	-0.34	0.02	ADP ribosylation factor 4
F6S2C3	-0.33	0.02	Cathepsin Z
F6UN85	-0.40	0.02	Carboxylic ester hydrolase
F6Y0G5	0.42	0.02	Periostin
F6Y4J0	-0.31	0.02	ATPase H^+ transporting V1 subunit B2
F6Z8W0	-0.36	0.02	WD repeat domain 1
F7APS1	-0.27	0.02	Uncharacterised
F7BM69	-0.31	0.02	Uncharacterised
F7BTK9	-0.36	0.02	Family with sequence similarity 129 member A
F7DA17	-0.39	0.02	Transglutaminase 2
F7DEW5	-0.31	0.02	Coronin
F7DXM5	0.32	0.02	Uncharacterised
HMDB00161	0.29	0.03	L-Alanine
F6PKE1	-0.33	0.03	Uncharacterised
F6QKR7	-0.38	0.03	Myocilin
F6RCA8	-0.34	0.03	Peroxiredoxin 5
F6YV40	-0.31	0.03	Glyceraldehyde-3-phosphate dehydrogenase
F6YV53	-0.31	0.03	Actinin alpha 4
HMDB00122	0.30	0.04	D-Glucose
Q95182	-0.34	0.04	Major allergen Equ c 1
F6RMN2	-0.34	0.04	Drebrin like
F6SN52	-0.34	0.04	Eukaryotic translation initiation factor 5A
F6SP02	-0.33	0.04	Tyrosine 3-monooxygenase/tryptophan 5-monooxygenase activation protein theta
F6T201	-0.29	0.04	Chondroitin sulfate proteoglycan 4
F6UF75	-0.33	0.04	Protein S100
F6WWW7	-0.32	0.04	Capping actin protein of muscle Z-line alpha subunit 1
F6XEB4	-0.36	0.04	Tyrosine 3-monooxygenase/tryptophan 5-monooxygenase activation protein zeta
F7B320	-0.32	0.04	Dihydropyrimidinase like 2
H9GZU9	-0.30	0.04	Uncharacterised

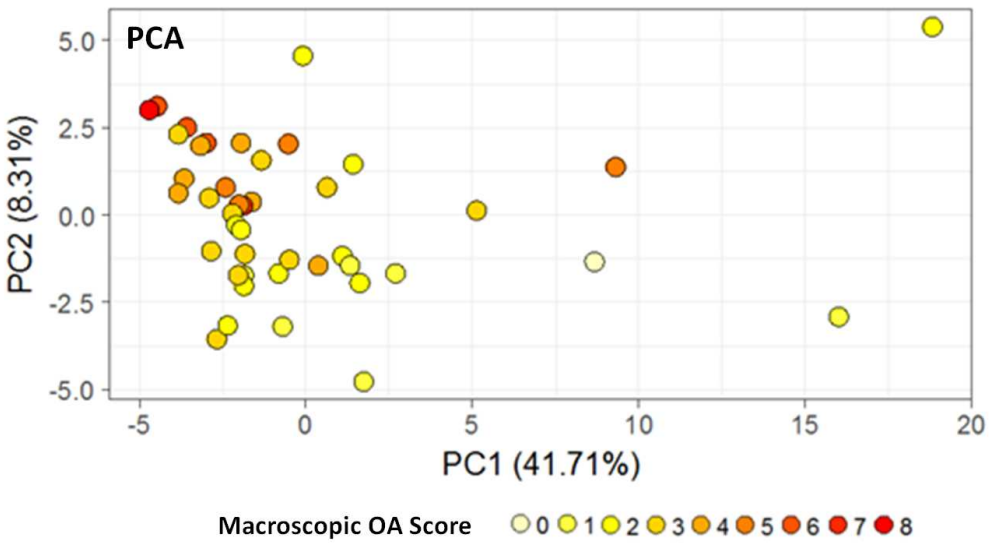

Figure 9. Principal component analysis (PCA) using 58 selected variables (proteins and metabolites) for the Hong Kong Jockey Club synovial fluid combined datasets (n=43) following batch correction, grouped according to macroscopic osteoarthritis score. OA = osteoarthritis.

For the biobank dataset, Lasso penalisation produced a model incorporating 29 variables (Supplementary Table 1). This produced a good model (R^2 = 0.82) with PC2 able to discriminate more advanced stages of OA from the earlier stages (Figure 10). This model was predominantly driven by two uncharacterised proteins (H9GZQ9 and F6ZR63) and alanine. Correlation analysis of all variables (proteins and metabolites) identified 32 significant variables, with a range in correlation from -0.44 to 0.49 (Table 4).

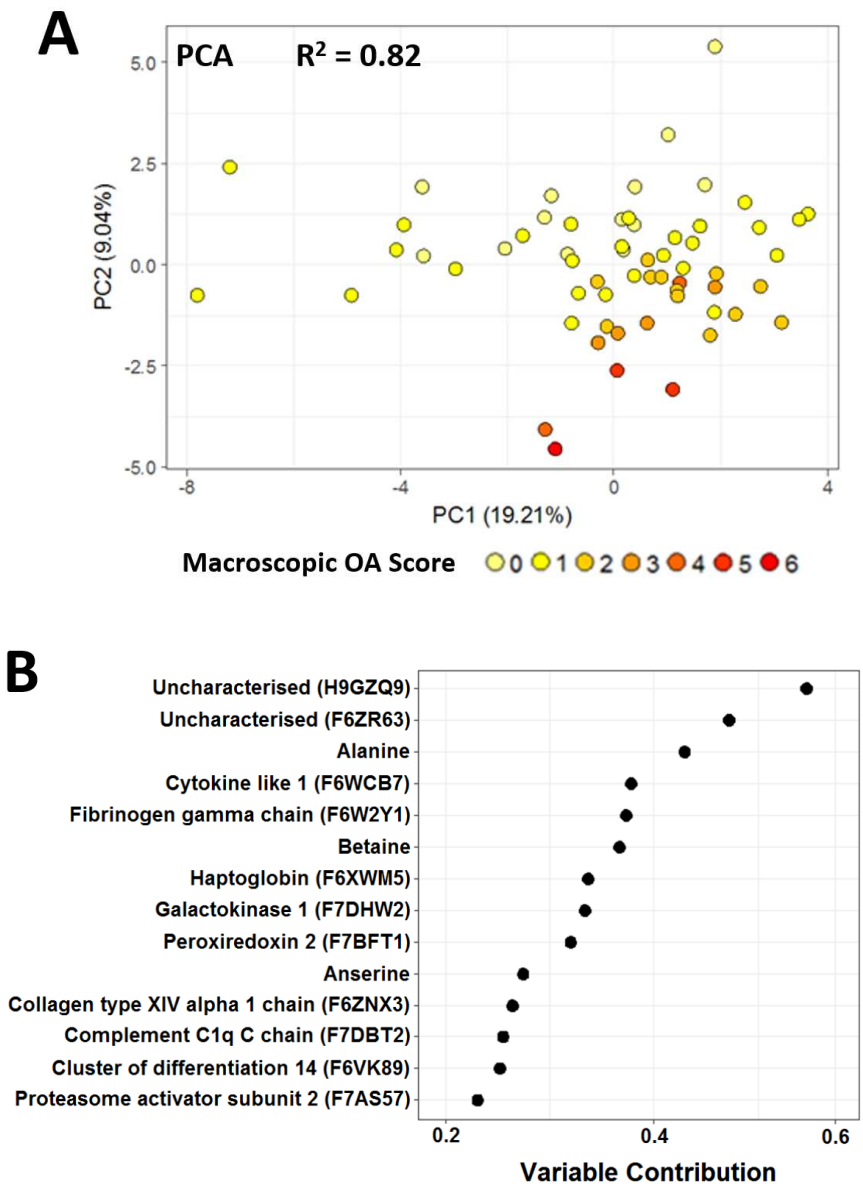

Figure 10. (A) Principal component analysis (PCA) following Lasso model selection using the top 29 variables of influence for biobank synovial fluid, integrating metabolite and protein abundances and grouped according to macroscopic osteoarthritis scoring. (B) Top 14 variables of influence contributing to the model. n=60.

Table 4. Correlation of each variable (proteins and metabolites) to macroscopic OA score for the biobank synovial fluid integrated dataset. $p < 0.05$.

Variable	Correlation	Permutation p value	Characterisation
H9GZS6	-0.44	0	Uncharacterised
F7BFT1	-0.43	0	Peroxiredoxin 2
F6Q4N3	-0.41	0	Neural EGFL like 2
F6WCB7	-0.40	0	Cytokine like 1
F6ZR63	-0.38	0	Uncharacterised
H9GZU9	-0.37	0	Uncharacterised
F6RRV1	-0.35	0	Fetuin B
P35747	0.33	0	Serum albumin
Q28369	0.34	0	Retinol-binding protein 4
F6X667	0.34	0	Vitamin K-dependent protein C
F7A1W7	0.49	0	Apolipoprotein C2
H9GZV0	-0.34	0.01	Uncharacterised
F6SP11	-0.32	0.01	Uncharacterised
F6ZRF6	-0.31	0.01	Serpin family A member 7
F6QF58	-0.31	0.01	60S ribosomal protein L6
H9GZQ9	-0.29	0.01	Uncharacterised
F7ASE1	0.32	0.01	Interleukin 1 receptor accessory protein
F6RM73	0.36	0.01	Apolipoprotein A-II
F7DRS2	-0.33	0.02	Serpin family A member 6
F6WLX9	-0.29	0.02	tRNA-splicing ligase RtcB homolog
F6XPL9	-0.27	0.02	Obg-like ATPase 1
F6XI92	-0.27	0.02	Bridging integrator 2
F6YV40	0.21	0.02	Glyceraldehyde-3-phosphate dehydrogenase
F7DBT2	0.27	0.02	Complement C1q C chain
F6PRI5	0.28	0.02	Carboxylic ester hydrolase
F6T0P6	0.32	0.02	GC, vitamin D binding protein
F6UCZ2	-0.24	0.03	Translin
HMDB00562	0.30	0.03	Creatinine
F6XWJ6	-0.32	0.04	RUN and FYVE domain containing 1
F6V1V8	-0.27	0.04	Cluster of differentiation 109
F7BA94	-0.20	0.04	40S ribosomal protein S3
F7AS57	0.24	0.04	Proteasome activator subunit 2

Combining both the biobank and HKJC datasets, including significant protein and metabolite variables, DAPC analysis produced a model whereby OA severity prediction was good for mild OA (90%) although this was reduced significantly for healthy (57%) and severe OA (35%) classifications (Figure 11). Linear discriminant 1

was driven predominantly by neural EGFL like 2, serum albumin and alanine whilst linear discriminant 2 was driven by periostin, gelsolin and myocilin.

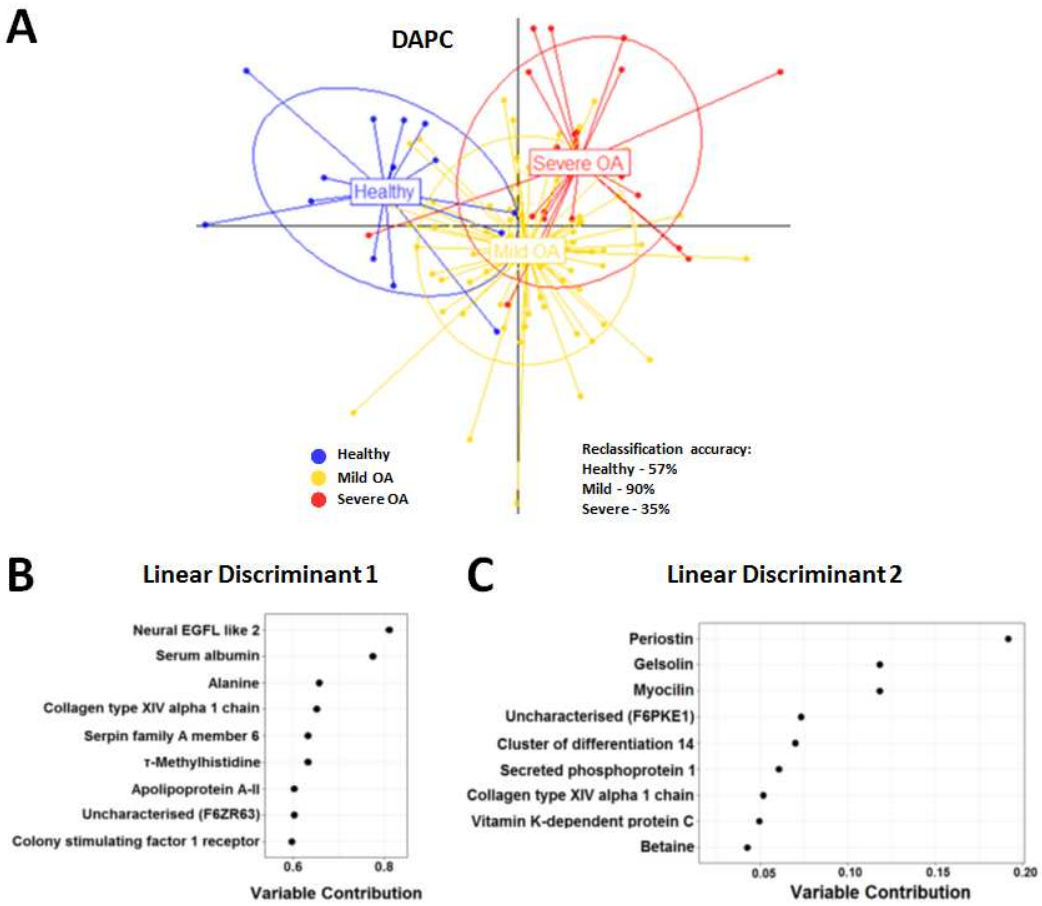

Figure 11. (A) Discriminant analysis of principal components (DAPC) of selected variables (proteins and metabolites) for a combined biobank and Hong Kong Jockey Club synovial fluid dataset (n=103), built using 20 principal components and two linear discriminants. (B) Top 25% of variables for the DAPC model contributing to linear discriminant 1 and (C) linear discriminant 2. Macroscopic osteoarthritis (OA) scoring; Healthy = 0, Mild OA = 1-3, Severe OA = 4-8.

3.4.5. Uncharacterised Proteins

BLAST analysis of amino acid sequences of 12 uncharacterised proteins included within this study identified various related characterised proteins. The characterised protein with the highest percentage amino acid sequence similarity for each uncharacterised protein is shown in Table 5.

Table 5. BLAST analysis of amino acid sequences of uncharacterised proteins included within this study, identifying the characterised protein with the highest percentage amino acid sequence similarity for each uncharacterised protein.

Accession Number of Uncharacterised Protein	Analysis Present In	Accession Number of Similar Protein	Similar Protein	Species	E-Value	Similarity (%)
F6PKE1	HKJC Macroscopic OA Correlation DAPC Linear Discriminant 2	A0A340XC13	Inhibitor of carbonic anhydrase-like isoform X1	*Lipotes vexillifer*	0	77.2
F6S2I3	Biobank Lasso Model	A0A1U7U041	Glutathione S-transferase	*Tarsius syrichta*	4.60 e^{-144}	88.5
F6SP11	Biobank Macroscopic OA Correlation	A0A0A1E4I0	Immunoglobulin lambda light chain variable region	*Equus caballus*	8.10 e^{-60}	100.0
F6TED1	Native (Macroscopic OA) Biobank Lasso Model	A0A091E338	Immunoglobulin kappa chain V-III region MOPC 63	*Fukomys damarensis*	2.20 e^{-44}	70.1
F6ZR63	Biobank Macroscopic OA Correlation DAPC Linear Discriminant 1 Biobank Lasso Model	A0A383YWT8	Complement factor H-like isoform X1	*Balaenoptera acutorostrata scammoni*	0	68.6
F7APS1	HKJC Macroscopic OA Correlation	Q862Z5	Cystatin-B	*Macaca fuscata fuscata*	2.30 e^{-57}	87.8
F7BM69	HKJC Macroscopic OA Correlation	A0A337SQC1	Immunoglobulin kappa variable 4-1	*Felis catus*	1.50 e^{-56}	77.4
F7DXM5	HKJC Macroscopic OA Correlation	B5BV10	Alpha-1-antitrypsin	*Equus caballus*	0	98.1
H9GZQ9	Biobank Macroscopic OA Correlation Biobank Lasso Model	Q95M34	Immunoglobulin gamma 1 heavy chain constant region	*Equus caballus*	0	99.7
H9GZS6	Native (Macroscopic OA) Biobank Macroscopic OA Correlation	Q95M34	Immunoglobulin gamma 1 heavy chain constant region	*Equus caballus*	7.40 e^{-173}	70.1
H9GZU9	Native (Macroscopic OA) HKJC Macroscopic OA Correlation Biobank Macroscopic OA Correlation	Q95M34	Immunoglobulin gamma 1 heavy chain constant region	*Equus caballus*	1.10 e^{-159}	67.9
H9GZV0	Biobank Macroscopic OA Correlation	L5JR68	Immunoglobulin epsilon chain C region	*Pteropus alecto*	0	65.0

Abbreviations: DAPC, Discriminant analysis of principal components; HKJC, Hong Kong Jockey Club; OA, Osteoarthritis

3.4.6. Pathway Analysis

Pathway analysis conducted on proteins and metabolites which were considered significant variables during DAPC modelling, when carrying out NMR metabolomic and LC-MS/MS proteomic dataset integration, identified the complement and coagulation cascades pathway and ABC transporters pathway to be the most represented (Tables 6 and 7). These pathways consisted of 7/96 proteins and 4/9 metabolites included within the pathway analysis respectively.

Table 6. Pathway analysis conducted on proteins which were considered significant variables during DAPC modelling, when carrying out NMR metabolomic and LC-MS/MS proteomic dataset integration.

Pathway ID	Pathway Description	Number of Proteins in Pathway	False Discovery Rate
4610	Complement and coagulation cascades	7	0.00000573
4145	Phagosome	6	0.00498
4390	Hippo signalling pathway	5	0.0188

Table 7. Pathway analysis conducted on metabolites which were considered significant variables during DAPC modelling, when carrying out NMR metabolomic and LC-MS/MS proteomic dataset integration.

Pathway ID	Pathway Description	Number of Metabolites in Pathway
2010	ABC transporters	4
4978	Mineral absorption	3
10	Glycolysis / Gluconeogenesis	2
4974	Protein digestion and absorption	2
340	Histidine metabolism	2
4066	HIF-1 signalling pathway	2
4976	Bile secretion	2
4922	Glucagon signalling pathway	2
970	Aminoacyl-tRNA biosynthesis	2
1230	Biosynthesis of amino acids	2

3.5. Discussion

Equine OA is currently predominantly diagnosed through radiography and clinical examination, however, due to the slow onset of the condition this often leads to substantial pathology of the joint and articular cartilage degradation prior to diagnosis (Brommer *et al.*, 2003). Presently, no equine OA-specific biomarkers have been identified which are able to accurately diagnose and stratify OA with none used to aid an earlier clinical diagnosis (Anderson, Phelan, *et al.*, 2018). Within this study we have investigated equine SF of varying severities of associated OA pathology using both NMR-led metabolomics and MS-based proteomics approaches.

Although both the biobank and HKJC datasets produced a degree of OA stratification, markers of interest were generally distinct. This may be reflective of the more severe OA phenotype demonstrated by the HKJC horses, whilst markers identified within the biobank represent a subtler grade of OA. Alternatively, the differences in markers identified may be due to the varying OA aetiologies, with the biobank representing a naturally occurring OA whilst the HKJC horses demonstrate a POD model for subchondral bone mediated OA, which is associated with trauma and overload (Barr, 2010). Additionally, the biobank cohort is on average an older donor group than the HKJC cohort which may also account for differences between the datasets. ^{1}H NMR SF spectra were more variable between biobank donors compared to the HKJC donors. This is likely because the biobank is a more heterogeneous population, including age, breed, work done and diet. The HKJC group is a much more controlled sample set, with all horses housed together, all Thoroughbred racehorses, generally fed and trained similarly and all of a similar age at euthanasia. These differentials may also reflect the different markers of interest identified between the biobank and HKJC groups.

Proteomic analysis of biobank samples identified several proteins which were able to discriminate a healthy phenotype from early OA changes. Although these proteins were largely uncharacterised, BLAST analysis of the amino acid sequences of three uncharacterised proteins, decreasing in abundance with OA severity,

identified high levels of similarity to immunoglobulin gamma 1 heavy chain constant region and immunoglobulin kappa chain V-III region MOPC 63 proteins. However, abundances of these uncharacterised proteins could not be validated using antibody methodologies. Recently, a study investigating the SF proteome of a surgery-induced OA model in rabbits identified reduced levels of immunoglobulin heavy chain protein compared to sham controls (Luo *et al.*, 2018). Immunoglobulins have previously been identified within superficial articular cartilage layers of a proportion of OA patients as well as elevated levels found within the synovial membrane of dogs diagnosed with cranial cruciate ligament rupture (Cooke *et al.*, 1975; Lawrence *et al.*, 1998). Thus, reduction of these immunoglobulins within the SF may be reflective of their translocation to surrounding articular tissues.

3.5.1. Glutamate

Glutamate is an excitatory amino acid neurotransmitter within the central nervous system, although evidence also suggests glutamate operates through intercellular signally cascades, as an autocrine/paracrine factor, in non-neuronal tissues (Wen *et al.*, 2015). A self-sufficient glutamate signalling machinery has been identified within chondrocytes with a peripheral NMDA receptor proposed to have a role within inflammation and cartilage degradation (Piepoli *et al.*, 2009). Within our study, the biobank group showed a reduction in synovial glutamate levels at higher OA severities. Previously, elevated levels of glutamate have been identified within OA SF of humans and within an OA rat models (Jean *et al.*, 2005; Lawand *et al.*, 2000; McNearney *et al.*, 2000). However, no increase in glutamate was identified with equine OA SF using ^{1}H NMR, although it is not clear whether glutamate was identified during this study (Lacitignola *et al.*, 2008). The disparity between the lower glutamate levels identified within the biobank group and elevated levels within the literature may be reflective of the subtler OA phenotype exhibited by the biobank samples, and they may be indicative of glutamate levels at an earlier OA severity. However, the HKJC dataset, reflective of a higher grade OA, did not identify differential abundance. Therefore, at this stage the relationship between synovial glutamate abundance and equine OA remains inconclusive.

3.5.2. Creatine

Creatine is a nonessential amino acid involved in cellular energy metabolism, maintaining cellular adenosine triphosphate (ATP) levels, in particular within the muscle and brain (da Silva *et al.*, 2014). Creatine SF levels increased with OA severity, which is supported by previous human and equine studies which also identified elevated SF creatine in OA SF (Ciurtin *et al.*, 2006; Lacitignola *et al.*, 2008). Approximately 95% of stored creatine is located within skeletal muscle (Snow and Murphy, 2001). Thus, given the association of muscle atrophy with OA, this elevation in synovial creatine may be reflective of an associated muscle mass loss (Porter, 2005).

3.5.3. Alanine

Within this study, alanine levels were identified to be increasing in SF in accordance with OA severity, which was also observed by Lacitignolia *et al.* (Lacitignola *et al.*, 2008). Previously, depleted alanine abundance has been identified within human OA cartilage using high resolution magic angle spinning NMR spectroscopy (Shet *et al.*, 2012). As alanine is one of the main amino acid residues which constitutes collagen, it may be that the reduction in alanine abundance identified with OA cartilage is resultant of degradation of the cartilage collagen framework, which are subsequently released into the SF resulting in the elevated synovial abundance within this study (Huster *et al.*, 2004; Shet *et al.*, 2012).

3.5.4. Gelsolin

Gelsolin (82-84 kDa) is a multifunctional, calcium ion-regulated actin filament severing, capping, and nucleating protein which is involved in the determination of cell shape, secretion and chemotaxis (Kaneva *et al.*, 2017; Yin *et al.*, 1984). Previous studies of gelsolin on different biological systems have identified gelsolin as a potential predictor of both inflammation and tissue injury (DiNubile *et al.*, 2002; Ito *et al.*, 1992; Piktel *et al.*, 2018). Within rheumatoid arthritis patients, reduced circulating levels of plasma gelsolin have been identified (Osborn *et al.*, 2008). The authors propose this may be due to gelsolin redistribution to the affected joint space, binding to a plasma factor, reduced production or increased degradation.

Within this study, SF gelsolin abundance was identified as decreasing with OA severity. Gelsolin was also identified as having a significant correlation with OA severity and was found to be a highly influential factor when a model combining both biobank and HKJC datasets was developed. These results are supported by a mouse model whereby gelsolin knockout mice resulted in arthritis exacerbation (Aidinis *et al.*, 2005). Additionally, within a mouse model of pain and acute inflammation, exogenous delivery of gelsolin was identified to have effective analgesic and anti-inflammatory properties (Gupta *et al.*, 2015). Exogenous gelsolin administration has also been shown to have chondroprotective properties, nullifying the effect of interleukin-1β and OA SF on anabolic gene expression and increased glycosaminoglycan deposition in chondrocytes and protection of the integrity of murine cartilage following intra-articular injection (Kaneva *et al.*, 2017). Therefore, gelsolin has potential as a biomarker of equine OA as well as an OA therapeutic target, and potential analgesic.

3.5.5. Lipopolysaccharide Binding Protein (LBP)

LBP is an endogenous protein which binds to lipopolysaccharides and catalytically delivers monomeric liposaccharides to cluster of differentiation 14 (CD14) protein (Citronberg *et al.*, 2016; Ranoa *et al.*, 2013). Previously, serum and synovial levels of LBP were not identified to be differentially expressed between human degenerative arthropathy patients and control samples (Heumann *et al.*, 1995). However, increased plasma LBP levels have recently been described to predict knee OA progression (Huang *et al.*, 2018). Within this current study, the trends identified suggest a decreasing SF abundance of LBP with increasing OA severity. It has previously been identified that mononuclear cell activation, induced by lipopolysaccharides, is enhanced by low LBP concentrations (Lamping *et al.*, 1998). Activation of monocytes and macrophages by lipopolysaccharides leads to the secretion of tumour necrosis factor alpha and interleukin-1 beta, two pro-inflammatory cytokines which are central to OA pathogenesis (Schumann *et al.*, 1994; Wojdasiewicz *et al.*, 2014). Thus, decreasing synovial LBP levels may have a role in OA development. With CD14 also identified as a key variable within the

biobank and HKJC combined model, this provides further support that this pathway is involved in equine OA pathogenesis.

3.5.6. Apolipoproteins

Elevations in synovial ApoA1 were identified in mild and moderate OA within the biobank group although abundance decreased for severe OA. Elevations in OA SF have previously been identified in horses and dogs (Chiaradia *et al.*, 2012; Shahid, 2018). ApoA1 is the primary protein component of high density lipoproteins (HDLs) and involved in HDL binding to ATP-binding cassette (ABC) transporters as well as being a lecithin cholesterol acyl transferase cofactor (Luc *et al.*, 1996; Rader, 2003; Ramella *et al.*, 2018; Silver *et al.*, 2001). ApoA1 has previously been found to induce the expression of interleukin-6, MMP-1 and MMP-3 in chondrocytes and synoviocytes through toll-like receptor 4 with the same study identifying a dissociation between the relationship of ApoA1 and HDLs in OA SF (de Seny *et al.*, 2015). When combining datasets within this study, apolipoprotein A-II (ApoA2) was also found to be an important variable. ApoA2 has previously been identified to be involved in the acute phase response which is associated with reactive amyloid A amyloidosis, via lipoprotein conformational changes, an associated complication of rheumatoid arthritis (Yang *et al.*, 2018). Thus, this study provides further evidence that OA is a metabolic syndrome with disruption of lipid homeostasis due to alterations to apolipoprotein activity (de Seny *et al.*, 2015).

3.5.7. Synovitis - Afamin

Synovitis has previously been identified as an important aspect of OA pathogenesis (Berenbaum, 2013; Mathiessen and Conaghan, 2017; Sellam and Berenbaum, 2010). This study identified reduced synovial abundance of afamin in high grade synovitis compared to low grade. Similarly, reduced afamin levels have been recorded in equine OA SF compared to healthy joints (Chiaradia *et al.*, 2012). In a previous study however, elevated levels of afamin were identified within human knee OA SF (Ritter *et al.*, 2014). Afamin is a vitamin E binding glycoprotein and a member of the albumin gene family (Dieplinger and Dieplinger, 2015). Afamin forms a 1:1 complex with various hydrophobic Wnt proteins, solubilising the proteins and

producing a biologically active complex (Mihara *et al.*, 2016). A growing body of evidence has identified that the Wnt/β-catenin signalling cascade is likely to have a central role within OA pathogenesis (Zhou *et al.*, 2017). Thus, a reduction in synovial abundance of afamin may be reflective of a translocation following Wnt solubilisation to surrounding articular tissues, i.e. the synovium. However, it should be noted that a differential abundance of afamin was not identified when categorised according to OA severity.

3.5.8. Semi-Tryptic Peptide Profiles

For the HKJC the semi-tryptic profile was most consistent between samples in the groups with the most severe OA and synovitis pathology. This suggests, as expected, the OA phenotype is driving the semi-tryptic peptide profile, most likely due to an increase in enzymatic activity leading to ECM degradation fragments (Lotz *et al.*, 2013). However, this was not evident within the biobank SF sample set. This may be because the OA pathology identified within this group was far subtler than that identified within the HKJC samples and thus the level of pathology present was not severe enough to drive a global change within the semi-tryptic peptide profile.

3.5.9. Metabolomic and Proteomic Integration

Computational integration of separate 'omics' datasets can work synergistically, greatly enhancing the information that can be obtained from separate analyses. However, this poses the challenge of developing multi 'omic' integration techniques. Previously, a study carried out MS proteomic analysis comparing early and late stage human OA SF and combined this with transcriptomics of articular tissues to identify the source of differentially abundant synovial proteins (Ritter *et al.*, 2013). However, no previous studies have combined NMR metabolomics and MS proteomic datasets.

Integrating the metabolomic and proteomic datasets separately for the biobank and HKJC both identified groupings associated with OA severity. Although correlation values of variables to OA severity were generally low for the HKJC samples, stratification was still evident. Modelling was most robust for the biobank dataset,

with the application of a Lasso model, with the model's strength being the separation of more severe OA grades. However, within this sample set there were relatively few samples which were assigned to the higher OA severity grades compared to lower and is therefore a limitation of the model. Combining all results from both the biobank and HKJC datasets produced a model which was found to be highly accurate in correctly assigning samples within the mild OA group based on their integrated metabolomic and proteomic profiles. This is promising as mild OA recognition is the current unmet clinical need, aiding in early diagnosis and allowing for timely OA interventional management. However, the model is dominated by predominantly mild OA graded samples, and thus this will inevitably introduce bias into the model and make a correct reclassification of mild OA more likely.

3.5.9.1. Periostin

Within the combined dataset DAPC model, periostin was the principal driver of linear discriminant 2. Periostin is a 90 kDa matricellular protein which has regulatory functions in cell differentiation, cell adhesion and ECM organisation (Kudo and Kii, 2018; Li *et al.*, 2015). In human medicine, a positive correlation has been identified between both plasma and SF periostin abundance and knee OA severity (Honsawek *et al.*, 2015). *In-vivo* results have identified that interleukin-13 may induce the production of periostin during OA, with periostin subsequently stimulating the production of MMPs within synoviocytes (Tajika *et al.*, 2017). In women, serum periostin levels were found to be associated with both prevalence and the risk of development/progression of knee OA (Rousseau *et al.*, 2015). Thus for equids, periostin may also provide a potential therapeutic target and prognostic indicator.

3.5.10. Pathway Analysis

Protein pathway analysis identified the 'complement and coagulation cascades' pathway to be altered during OA pathology. Additionally, the uncharacterised protein F6ZR63, the second most important variable of influence driving the biobank Lasso model, was found to have a high level of amino acid sequence similarity to complement factor H-like isoform X1. The complement system is an

important component of the innate immune response, encompassing various roles including opsonisation initiation, pathogen phagocytosis, the inflammatory response and terminating within cell lysis (Horwitz *et al.*, 2019; Silawal *et al.*, 2018). However, a growing body of evidence has identified a role of complement activation within OA pathogenesis, which is further supported by this study (Silawal *et al.*, 2018). Complement has been identified to have a role in the degradation of cartilage ECM, synovitis and osteophyte formation, with complement split fragment C3a found to upregulate gene expression of tumour necrosis factor-α and Interleukin-1β, pro-inflammatory cytokines central to OA pathogenesis (Silawal *et al.*, 2018; Wojdasiewicz *et al.*, 2014). Therefore, targeting the complement cascade may provide a novel therapeutic target for OA treatment.

Within experimental arthritis models, coagulation and fibrinolysis pathways are known to play a role within disease pathogenesis, with these cascades also found to be activated within both the joint and circulation of degenerative and inflammatory arthropathies (So *et al.*, 2003). Within the synovium of patients diagnosed with OA, the coagulation factor fibrinogen is present throughout the tissue with elevations in tissue factor, a coagulation initiator, identified near endothelial cells (Weinberg *et al.*, 1991). Previously, fibrinogen has been identified as a potential target for arthritis therapy, with removal of fibrinogen-leukocyte integrin receptor αMβ2 interactions limiting inflammatory processes whilst maintaining normal fibrinogen coagulation function (Raghu and Flick, 2011). Thus these pathways may also hold potential as a novel target for OA therapy.

Metabolite pathway analysis identified the 'ABC transporters' pathway to be altered during OA pathology. ABC transporters utilise ATP hydrolysis to import or export molecules across cell membranes (Rees *et al.*, 2009). ABC exporters have an important role in the export of cholesterol, fatty acid and lipids from cells, with dysregulation of this pathway underlying numerous diseases. The Wnt/β-catenin signalling cascade, with a proposed central role within OA pathogenesis, has previously been identified as a regulator of ABC transporters (Takamatsu *et al.*, 2014). Additionally, the ABC transporter MRP5 has been found to be the principal exporter of hyaluronan from its site of synthesis within the cell to the ECM (Schulz

et al., 2007). However, as only four key metabolites were identified within this pathway, caution should be applied when analysing these results to avoid over interpretation.

3.5.11. Further Work

Several proteins of interest identified within this study were uncharacterised. BLAST amino acid sequence analysis of similar proteins provided further information on their potential function, however this could be taken further by conducting 3D modelling of these proteins to help confirm function and potential interactions with other proteins/molecules. Additionally, developing monoclonal antibodies which are specific to these uncharacterised proteins would allow this methodology to provide an orthologous method to confirm protein abundances. Within the cohorts used in this study, there was an over-representation of mild OA diagnoses opposed to more severe phenotypes. Although this is advantageous in terms of identifying early OA markers, in order to fully stratify OA, the addition of a greater number of donors with higher grade OA would provide a more comprehensive synovial profile of the metabolite and protein profiles at differing OA grades and provide more robust models. As this study adopted a cross-sectional approach, further work of interest would be to conduct repeated measures within a longitudinal study to discover whether the identified markers of interest validate this study's findings. Also, given the differential abundance of ApoA1 and LBP identified within this study, it would be of interest to further interrogate SF, using both NMR and MS based approaches, to investigate the lipid profile and identify changes during OA progression.

3.5.12. Conclusions

In conclusion, this study has stratified equine OA using both metabolomic and proteomic SF profiles and identified a panel of markers of interest which may be applicable to grading OA severity. This is also the first study to undertake computational integration of NMR metabolomic and LC-MS/MS proteomic datasets of any biological system.

3.6. Ethics

Hong Kong Jockey Club samples were collected under the regulations of the Hong Kong Jockey Club with owner consent. Abattoir samples were collected as a by-product of the agricultural industry, and hence ethical approval was not required. Ethical collection of excess clinical equine synovial fluid was approved by University of Liverpool Ethics approval, ref: VREC175 and VREC561.

3.7. Funding

Mr James Anderson is funded through a Horse Trust PhD studentship (G1015) and Dr Mandy Peffers funded through a Wellcome Trust Intermediate Clinical Fellowship (107471/Z/15/Z). Software licenses for data analysis used in the Shared Research Facility for NMR metabolomics were funded by the MRC Clinical Research Capabilities and Technologies Initiative (MR/M009114/1). ELISA protein validation experiments were funded by the Institute of Veterinary Science, University of Liverpool.

3.8. Acknowledgements

The authors would like to thank staff at both the F Drury and Sons abattoir, Swindon and Hong Kong Jockey Club for assistance in sample collection and processing, Ms Valerie Tilston for preparation of histology slides and Dr Ben McDermott, Dr Elizabeth Barr, Ms Amy McDermott, Mr Aibek Smagul and Mr Colin Anderson for conducting pathology scoring.

3.9. Supplementary Information

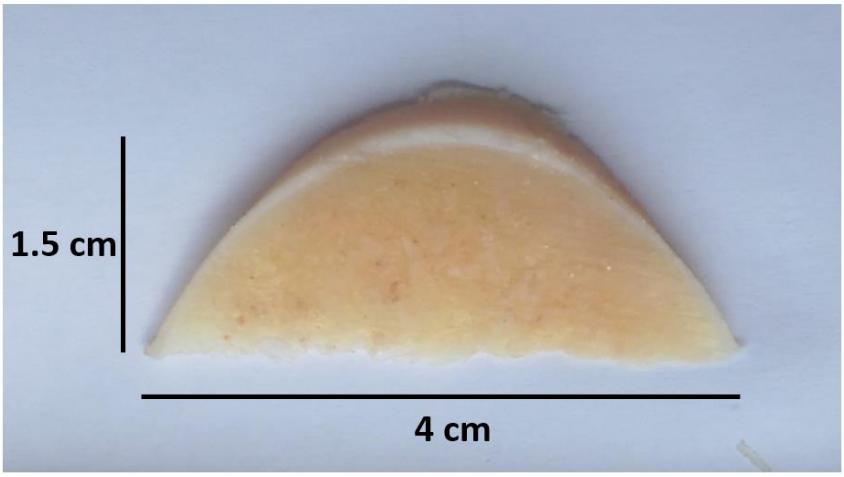

Supplementary Figure 1. Subchondral bone/cartilage wedge taken at post mortem from the distal articular condylar surface of metacarpal III, lateral to the sagittal ridge.

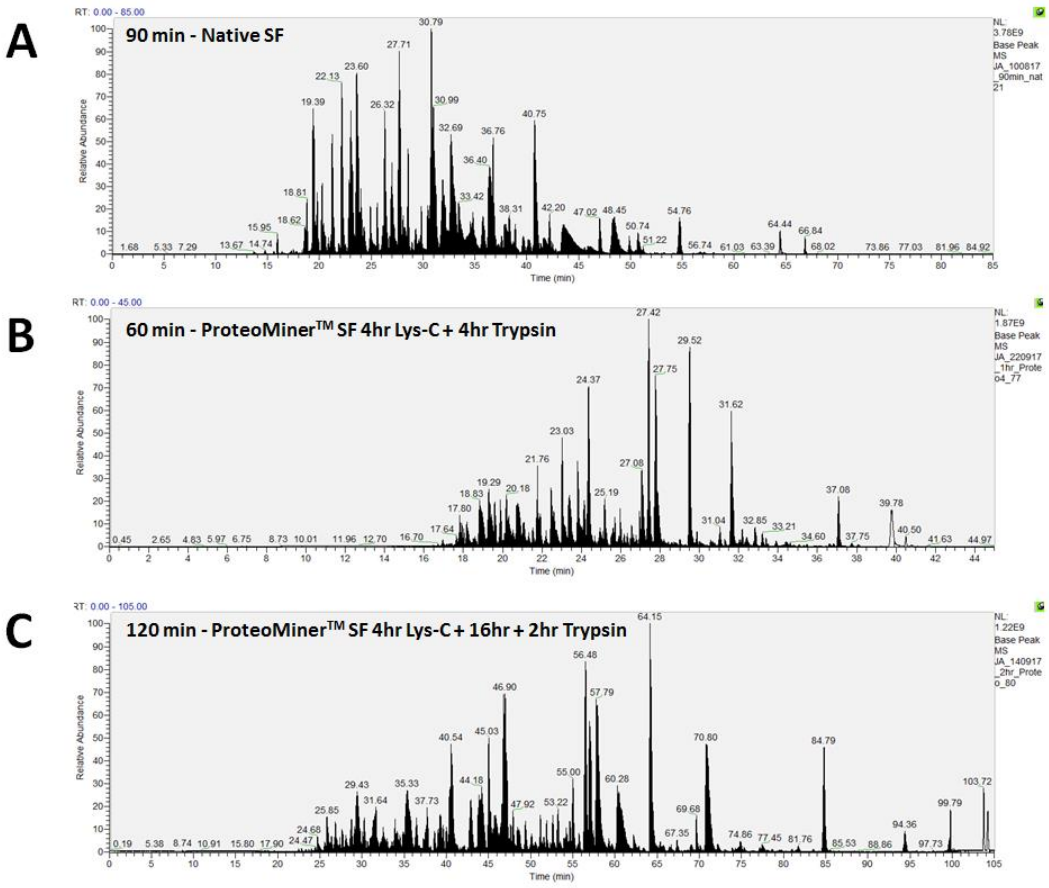

Supplementary Figure 2. Representative ion chromatograms for native synovial fluid (SF) using (A) a 90 min liquid chromatography (LC) gradient, (B) ProteoMiner™ processed SF following a 4hr Lys-C + 4hr trypsin digestion using a 60 min LC gradient and (C) ProteoMiner™ processed SF following a 4hr Lys-C + 16hr + 2hr trypsin digestion using a 120 min LC gradient.

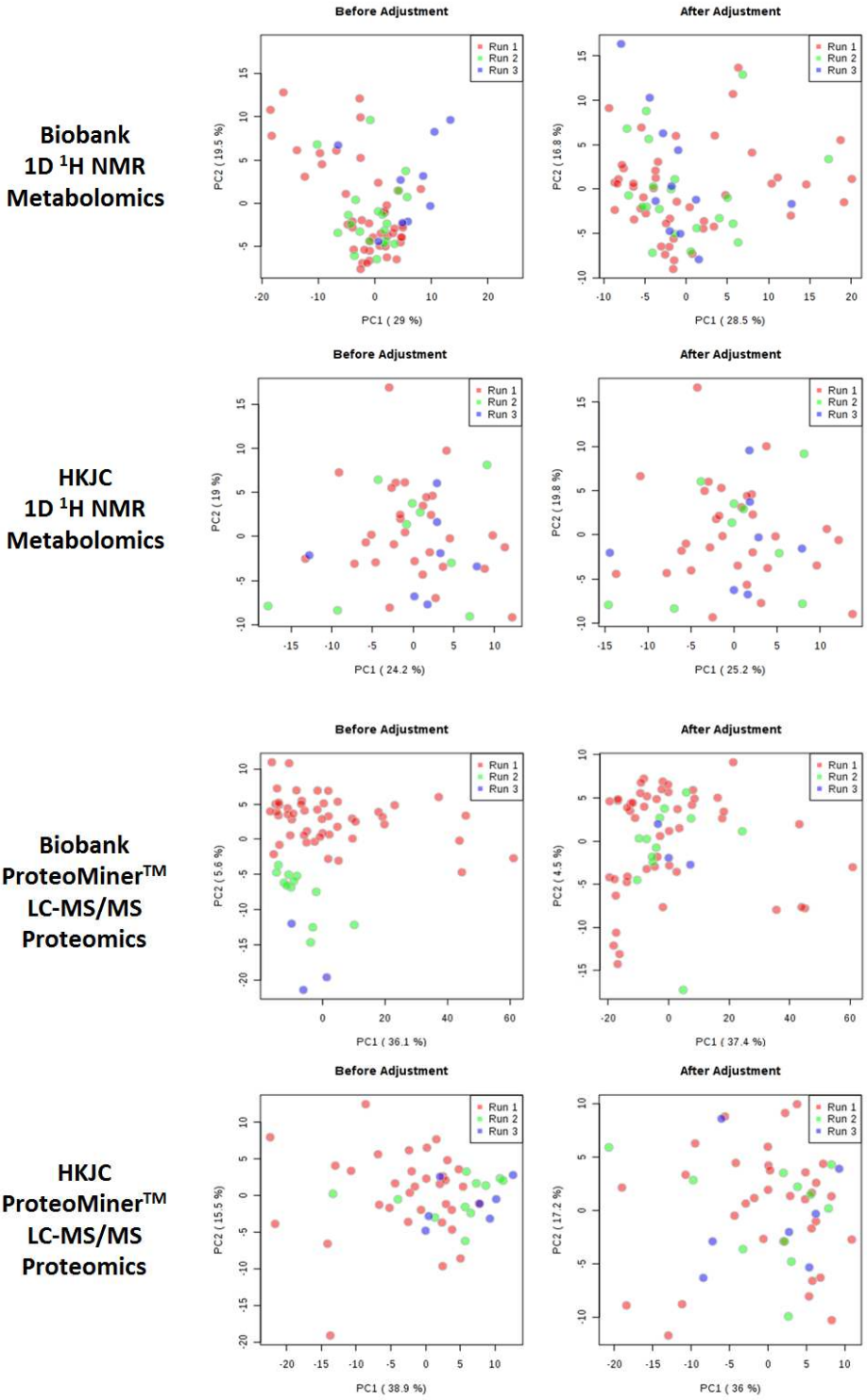

Supplementary Figure 3. Principal component analyses of biobank and Hong Kong Jockey Club (HKJC) equine synovial fluid NMR metabolomes and LC-MS/MS proteomes before and after application of a COMBAT batch correction. biobank; metabolomics, n=76, proteomics, n=70, HKJC; metabolomics, n=56, proteomics, n=53.

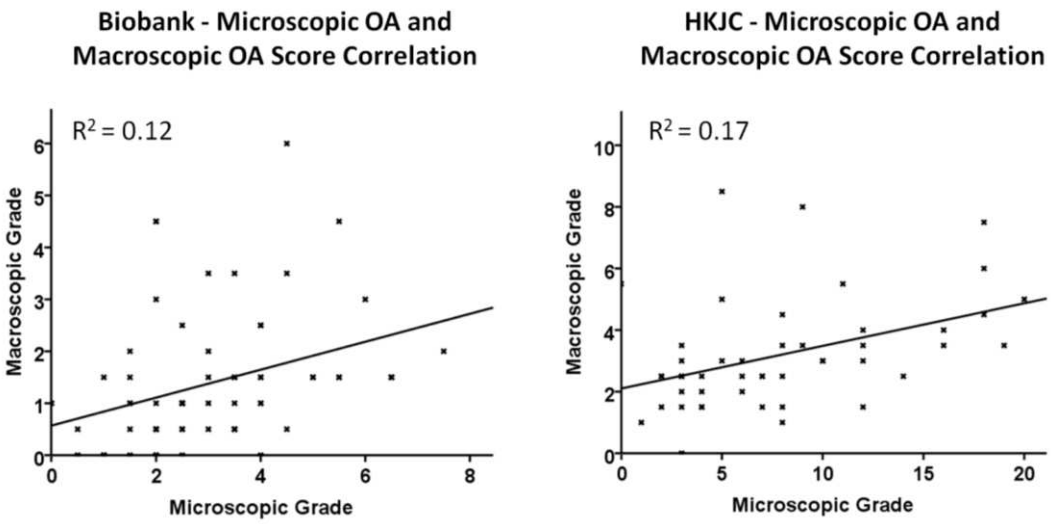

Supplementary Figure 4. Correlation between microscopic and macroscopic osteoarthritis (OA) grading scores for biobank (n=41) and Hong Kong Jockey Club (HKJC, n=41) cohorts.

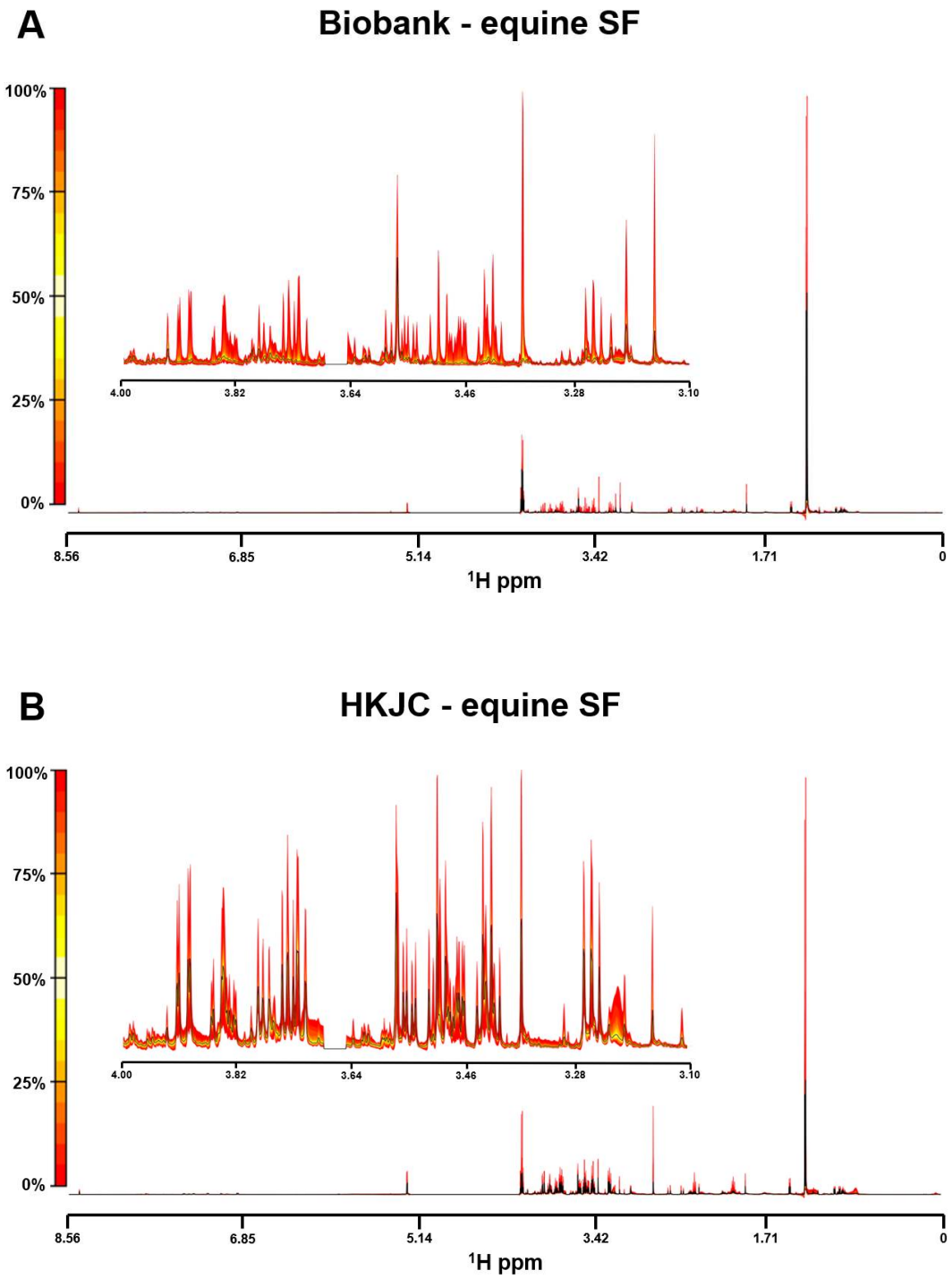

Supplementary Figure 5. Quantile plots of (A) biobank (n=83) and (B) Hong Kong Jockey Club (HKJC, n=52) synovial fluid (SF) NMR spectra. The median spectra are depicted by a black line, with variation from the median spectral plot depicted by a yellow to red scale. The full spectral range is shown (8.56-0 ppm) with a more detailed region inset (4-3.1 ppm). Spectral regions 3.681-3.643 ppm and 1.201-1.162 ppm have been removed due to ethanol contamination.

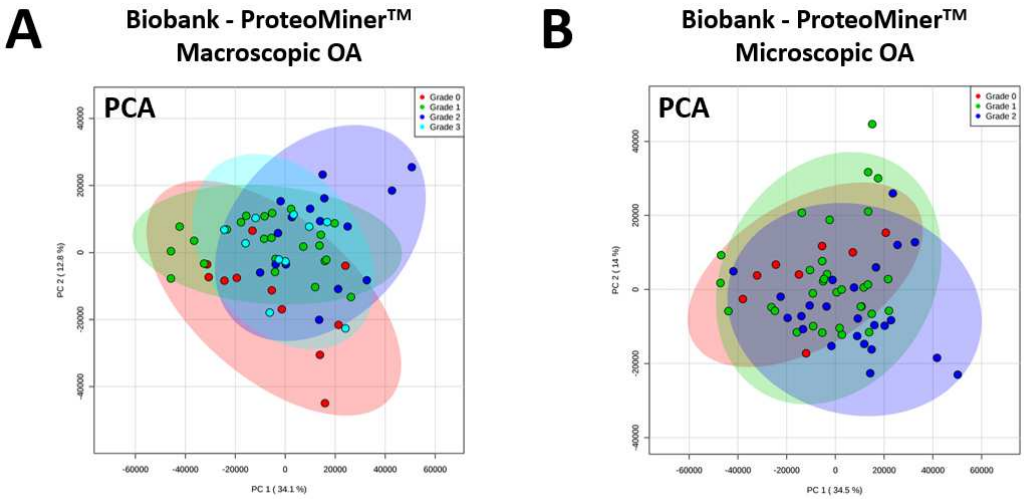

Supplementary Figure 6. Principal component analysis of biobank ProteoMiner™ processed (16hr + 2hr trypsin digestion) synovial fluid proteome categorised by (A) macroscopic OA grade (n=60) and (B) microscopic OA grade (n=64) using LC-MS/MS.

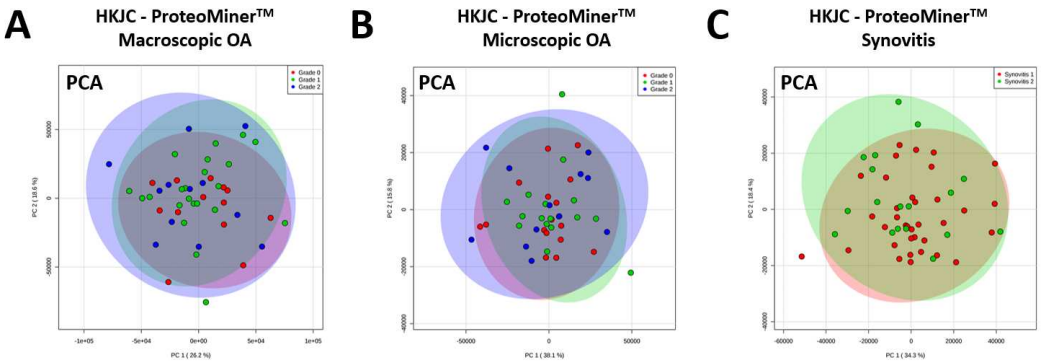

Supplementary Figure 7. Principal component analysis of the Hong Kong Jockey Club (HKJC) ProteoMiner™ processed (16hr + 2hr trypsin digestion) synovial fluid proteome categorised by (A) macroscopic OA grade (n=47), (B) microscopic OA grade (n=45) and (C) synovitis grade (n=53) using LC-MS/MS.

Supplementary Table 1. Selected variables (proteins and metabolites) used to produce Lasso model for biobank synovial fluid.

Variable	Description
HMDB00194	Anserine
F7A1W7	Apolipoprotein C2
F6XUJ2	ATP synthase subunit alpha
HMDB00043	Betaine
F6TK05	Chaperonin containing TCP1 subunit 2
F6VK89	Cluster of differentiation 14
F6ZNX3	Collagen type XIV alpha 1 chain
F7DBT2	Complement C1q C chain
F7BQD6	Complement C1s
F6WCB7	Cytokine like 1
F6W2Y1	Fibrinogen gamma chain
F7DHW2	Galactokinase 1
F7BKK5	Glutathione S-transferase
F6XWM5	Haptoglobin
HMDB00161	L-Alanine
HMDB00883	L-Valine
F6X485	Myosin heavy chain 9
F7BJV0	Myosin IC
F7BFT1	Peroxiredoxin 2
F7AS57	Proteasome activator subunit 2
F6XWJ6	RUN and FYVE domain containing 1
Q2QLB2	Testin
F7CS04	Tropomyosin 1
F6S2I3	Uncharacterised
F6TED1	Uncharacterised
F6ZR63	Uncharacterised
H9GZQ9	Uncharacterised
F6RYX0	Vacuolar protein sorting-associated protein 29
F6X667	Vitamin K-dependent protein C

Supplementary Table 2. Age comparison between the biobank and Hong Kong Jockey Club (HKJC) cohorts.

	Biobank	HKJC
Number of donors	83	58
Mean age (years)	14.3	6.6
Median age (years)	16	7
Standard deviation (years)	7.6	1.9
t-test (mean age)	$p = 6.22\ e^{-12}$	

Supplementary Table 3. Macroscopic osteoarthritis scoring of distal metacarpal III for the University of Liverpool equine biobank.

	Scorer 1				Scorer 2				Scorer 3					
Horse	**Wear Lines (0-3)**	**Erosions (0-3)**	**Palmar Arthrosis (0-3)**	**Total**	**Wear Lines (0-3)**	**Erosions (0-3)**	**Palmar Arthrosis (0-3)**	**Total**	**Wear Lines (0-3)**	**Erosions (0-3)**	**Palmar Arthrosis (0-3)**	**Total**	**Average TOTAL**	**Macroscopic OA Grade**
1	Not Scored				Not Scored									
2	0	2	0	**2**	1	2	0	**3**					3	3
3	0	0	0	**0**	0	0	0	**0**					0	0
4	Not Scored				Not Scored									
5	Not Scored				Not Scored									
6	Not Scored				Not Scored									
7	0	1	0	**1**	0	0	0	**0**					1	1
8	1	0	2	**3**	2	1	1	**4**					4	3
9	0	1	0	**1**	0	0	0	**0**					1	1
10	0	0	0	**0**	0	1	1	**2**	0	1	0	**1**	2	2
11	0	1	0	**1**	1	1	0	**2**					2	2
12	0	0	1	**1**	1	1	0	**2**					2	2
13	1	2	1	**4**	1	1	3	**5**					5	3
14	0	0	0	**0**	1	0	1	**2**	1	0	0	**1**	2	2
15	Not Scored				Not Scored									
16	0	0	1	**1**	1	0	2	**3**	1	0	0	**1**	1	1
17	Not Scored				Not Scored									
18	0	0	0	**0**	0	0	0	**0**					0	0
19	0	2	2	**4**	0	0	0	**0**	0	0	0	**0**	0	0
20	0	0	0	**0**	0	0	0	**0**					0	0
21	0	2	0	**2**	1	1	0	**2**					2	2
22	0	0	0	**0**	0	0	0	**0**					0	0
23	0	1	0	**1**	0	1	0	**1**					1	1
24	0	1	0	**1**	0	1	0	**1**					1	1
25	0	1	0	**1**	0	1	0	**1**					1	1
26	0	1	0	**1**	0	0	1	**1**					1	1

27	1	2	0	**3**	0	1	0	**1**	0	1	0	**1**	1	1
28	2	0	0	**2**	1	0	0	**1**					2	2
29	0	1	1	**2**	0	2	0	**2**					2	2
30	2	2	0	**4**	3	2	1	**6**	3	2	1	**6**	6	3
31	0	2	0	**2**	0	2	0	**2**					2	2
32	3	1	0	**4**	2	1	0	**3**					4	3
33	1	1	0	**2**	0	0	1	**1**					2	2
34	1	1	0	**2**	0	1	0	**1**					2	2
35	2	2	0	**4**	3	2	2	**7**	2	1	2	**5**	5	3
36	0	0	1	**1**	0	0	1	**1**					1	1
37	0	0	0	**0**	0	0	1	**1**					1	1
38	0	1	0	**1**	0	2	0	**2**					2	2
39	0	2	1	**3**	1	2	1	**4**					4	3
40	0	1	0	**1**	0	2	0	**2**					2	2
41	0	2	0	**2**	0	1	0	**1**					2	2
42	Not Scored				Not Scored									
43	0	1	0	**1**	0	0	1	**1**					1	1
44	0	0	0	**0**	0	1	0	**1**					1	1
45	1	0	0	**1**	0	0	0	**0**					1	1
46	0	0	0	**0**	0	0	0	**0**					0	0
47	0	0	1	**1**	1	2	0	**3**	0	0	1	**1**	1	1
48	2	2	0	**4**	2	3	0	**5**					5	3
49	1	2	0	**3**	0	2	0	**2**					3	3
50	0	0	0	**0**	0	1	0	**1**					1	1
51	1	2	0	**3**	0	2	0	**2**					3	3
52	0	0	0	**0**	0	0	0	**0**					0	0
53	0	2	0	**2**	0	1	0	**1**					2	2
54	0	0	0	**0**	0	0	0	**0**					0	0
55	0	0	0	**0**	0	1	0	**1**					1	1
56	1	0	0	**1**	0	1	0	**1**					1	1
57	0	0	0	**0**	0	0	0	**0**					0	0
58	0	0	1	**1**	0	2	0	**2**					2	2
59	0	0	0	**0**	0	1	0	**1**					1	1
60	0	1	0	**1**	0	1	0	**1**					1	1

61	0	0	0	**0**	0	1	0	**1**					1	1
62	0	0	0	**0**	0	1	0	**1**					1	1
63	0	0	0	**0**	0	0	0	**0**					0	0
64	0	0	0	**0**	0	1	0	**1**					1	1
65	0	2	0	**2**	0	1	0	**1**					2	2
66	0	1	0	**1**	0	1	0	**1**					1	1
67	0	0	0	**0**	0	0	0	**0**					0	0
68	1	2	0	**3**	1	1	1	**3**					3	3
69	1	0	0	**1**	0	1	0	**1**					1	1
70	0	1	0	**1**	0	2	0	**2**					2	2
71	3	0	0	**3**	3	0	0	**3**					3	3
72	0	0	2	**2**	1	1	2	**4**	0	0	2	**2**	2	2
73	0	0	0	**0**	0	1	0	**1**					1	1
132	0	0	2	**2**	0	0	0	**0**	0	0	0	**0**	0	0
133	0	0	0	**0**	0	0	0	**0**					0	0
134	0	2	0	**2**	0	1	0	**1**					2	2
135	0	2	1	**3**	0	1	0	**1**	0	1	0	**1**	1	1
136	1	0	1	**2**	1	1	0	**2**					2	2
137	0	0	1	**1**	1	2	1	**4**	1	2	0	**3**	4	3
138	0	0	0	**0**	0	0	0	**0**					0	0
139	3	0	1	**4**	3	0	0	**3**					4	3
140	1	1	0	**2**	0	1	0	**1**					2	2
141	0	0	1	**1**	0	0	0	**0**					1	1

Supplementary Table 4. Microscopic osteoarthritis scoring of distal metacarpal III for the University of Liverpool equine biobank.

	Scorer 1						Scorer 2						Scorer 3							
Horse	**Fissuring (0-4)**	**Focal Cell Loss (0-4)**	**Chond. Nec. (0-4)**	**Chon. Form. (0-4)**	**Saff O Stain (0-4)**	**Total**	**Fissuring (0-4)**	**Focal Cell Loss (0-4)**	**Chond. Nec. (0-4)**	**Chon. Form. (0-4)**	**Saff O Stain (0-4)**	**Total**	**Fissuring (0-4)**	**Focal Cell Loss (0-4)**	**Chond. Nec. (0-4)**	**Chon. Form. (0-4)**	**Saff O Stain (0-4)**	**Total**	**Average TOTAL**	**Microscopic OA Grade**
1	0	1	1	0	0	**2**	1	1	0	0	0	**2**							**2**	**1**
2	2	1	0	1	0	**4**	2	0	1	1	0	**4**							**4**	**2**
3	0	1	0	0	0	**1**	0	0	0	0	0	**0**							**1**	**0**
4	0	0	1	0	0	**1**	0	1	1	0	0	**2**							**2**	**1**
5	1	1	0	0	0	**2**	1	1	0	1	0	**3**							**3**	**1**
6	0	0	0	0	0	**0**	0	2	1	0	0	**3**	0	0	0	0	0	**0**	**0**	**0**
7	1	1	0	0	0	**2**	1	0	1	0	1	**3**							**3**	**1**
8	1	0	1	1	0	**3**	2	1	1	1	0	**5**	2	1	0	1	0	**4**	**5**	**2**
9	1	0	0	0	1	**2**	0	2	2	0	1	**5**	0	1	0	0	0	**1**	**2**	**1**
10	0	0	0	1	0	**1**	1	1	0	0	0	**2**							**2**	**1**
11	1	2	0	0	0	**3**	1	0	0	0	0	**1**	1	0	0	0	0	**1**	**1**	**0**
12	2	2	1	0	0	**5**	2	1	2	0	0	**5**							**5**	**2**
13	1	1	0	0	0	**2**	1	1	0	0	0	**2**							**2**	**1**
14	1	1	1	2	0	**5**	1	3	0	1	0	**5**							**5**	**2**
15	1	1	0	0	0	**2**	1	1	0	0	0	**2**							**2**	**1**
16	0	2	0	1	0	**3**	0	1	0	1	0	**2**							**3**	**1**
17	Not Scored						Not Scored													
18	0	0	0	0	0	**0**	0	1	0	0	0	**1**	0	1	0	0	0	**1**	**1**	**0**
19	1	2	0	1	0	**4**	0	1	0	0	0	**1**	1	0	0	0	0	**1**	**1**	**0**
20	0	2	0	0	0	**2**	0	2	0	0	0	**2**							**2**	**1**
21	2	0	1	2	1	**6**	3	1	1	1	2	**8**	1	3	0	1	2	**7**	**8**	**2**
22	0	1	0	0	0	**1**	0	0	1	0	0	**1**							**1**	**0**
23	1	0	2	0	0	**3**	0	0	0	0	0	**0**	2	1	0	0	0	**3**	**3**	**1**
24	0	0	0	1	0	**1**	1	0	0	1	0	**2**							**2**	**1**
25	0	1	1	0	0	**2**	0	1	1	1	0	**3**							**3**	**1**
26	0	1	0	0	0	**1**	0	1	1	0	0	**2**							**2**	**1**

27	0	0	0	0	0	**0**	0	0	0	0	0	**0**							**0**	**0**
28	1	0	0	1	0	**2**	1	3	0	0	0	**4**	1	2	1	0	0	**4**	**4**	**2**
29	1	1	0	0	0	**2**	0	0	0	1	0	**1**							**2**	**1**
30	2	1	1	1	0	**5**	1	0	0	2	0	**3**	0	1	0	3	0	**4**	**5**	**2**
31	2	1	1	1	4	**9**	1	0	1	1	0	**3**	1	2	0	0	0	**3**	**3**	**1**
32	0	1	1	1	0	**3**	1	0	0	2	0	**3**							**3**	**1**
33	2	2	1	1	1	**7**	2	1	1	1	0	**5**	2	1	2	1	0	**6**	**7**	**2**
34	0	1	2	1	0	**4**	0	2	1	1	0	**4**							**4**	**2**
35	1	0	1	2	1	**5**	1	1	1	2	1	**6**							**6**	**2**
36	1	1	0	1	0	**3**	1	0	0	0	1	**2**							**3**	**1**
37	0	1	1	1	1	**4**	0	2	1	0	0	**3**							**4**	**2**
38	1	0	1	1	0	**3**	1	1	2	1	0	**5**	2	1	2	1	0	**6**	**6**	**2**
39	0	1	0	1	2	**4**	0	0	1	0	1	**2**	0	1	0	0	2	**3**	**4**	**2**
40	1	0	1	2	2	**6**	1	0	0	1	1	**3**	2	0	1	2	2	**7**	**7**	**2**
41	2	1	1	2	0	**6**	1	2	2	3	0	**8**	2	2	0	1	0	**5**	**6**	**2**
42	0	2	1	0	1	**4**	0	1	1	0	0	**2**	0	2	0	1	1	**4**	**4**	**2**
43	1	0	1	1	0	**3**	1	0	1	0	0	**2**							**3**	**1**
44	0	1	1	2	1	**5**	1	0	1	1	1	**4**							**5**	**2**
45	0	1	1	0	0	**2**	0	1	1	0	0	**2**							**2**	**1**
46	0	0	0	1	0	**1**	0	1	1	0	0	**2**							**2**	**1**
47	0	1	0	1	1	**3**	1	0	0	0	1	**2**							**3**	**1**
48	0	1	1	0	0	**2**	0	1	1	2	0	**4**	1	1	0	0	0	**2**	**2**	**1**
49	1	1	0	1	1	**4**	0	0	0	1	0	**1**	0	1	1	1	1	**4**	**4**	**2**
50	1	1	2	0	0	**4**	2	0	1	0	0	**3**							**4**	**2**
51	0	1	1	0	1	**3**	1	0	1	2	1	**5**	0	0	0	2	0	**2**	**3**	**1**
52	Not Scored						Not Scored													
53	1	0	0	2	1	**4**	2	0	0	1	0	**3**							**4**	**2**
54	0	1	1	0	0	**2**	0	2	0	0	0	**2**							**2**	**1**
55	0	1	1	0	1	**3**	0	0	0	0	0	**0**	0	1	0	0	1	**2**	**3**	**1**
56	1	1	0	0	2	**4**	0	1	0	0	1	**2**	1	1	0	0	2	**4**	**4**	**2**
57	0	1	0	0	1	**2**	0	2	1	0	1	**4**	1	1	0	0	0	**2**	**2**	**1**
58	0	1	0	2	0	**3**	0	1	2	0	0	**3**							**3**	**1**
59	0	0	0	0	0	**0**	0	1	0	1	1	**3**	1	1	0	1	1	**4**	**4**	**2**
60	1	0	0	1	0	**2**	2	0	0	2	0	**4**	0	2	0	2	0	**4**	**4**	**2**

61	0	1	1	1	0	**3**	0	0	1	0	2	**3**							**3**	**1**
62	0	1	0	0	1	**2**	1	1	1	0	1	**4**	0	1	0	1	0	**2**	**2**	**1**
63	0	2	1	1	0	**4**	0	1	1	0	2	**4**							**4**	**2**
64	1	1	0	2	1	**5**	0	1	0	1	0	**2**	1	1	0	0	0	**2**	**2**	**1**
65	1	2	0	1	0	**4**	0	1	0	1	0	**2**	0	1	0	2	0	**3**	**4**	**2**
66	1	2	1	0	1	**5**	1	0	0	1	0	**2**	0	2	0	0	0	**2**	**2**	**1**
67	0	1	1	1	0	**3**	0	0	0	1	1	**2**							**3**	**1**
68	1	1	0	0	0	**2**	2	0	0	0	0	**2**							**2**	**1**
69	2	0	1	1	0	**4**	1	0	1	1	0	**3**							**4**	**2**
70	3	1	1	1	2	**8**	2	0	1	1	2	**6**	3	2	0	0	2	**7**	**8**	**2**
71	2	2	1	1	0	**6**	1	1	0	1	0	**3**	1	2	0	3	0	**6**	**6**	**2**
72	Not Scored						Not Scored													
73	2	1	1	0	0	**4**	0	0	0	0	0	**0**	1	0	0	0	0	**1**	**1**	**0**
132	Not Scored						Not Scored													
133	Not Scored						Not Scored													
134	Not Scored						Not Scored													
135	Not Scored						Not Scored													
136	Not Scored						Not Scored													
137	Not Scored						Not Scored													
138	Not Scored						Not Scored													
139	Not Scored						Not Scored													
140	Not Scored						Not Scored													
141	Not Scored						Not Scored													

Supplementary Table 5. Macroscopic osteoarthritis scoring of distal metacarpal III or metatarsal III for the Hong Kong Jockey Club sample set.

		Scorer 1					Scorer 2					Scorer 3						
Horse	Joint	POD (0-3)	Wear lines (0-2)	Cart. loss (0-3)	Linear fissures (0-3)	TOTAL	POD (0-3)	Wear lines (0-2)	Cart. loss (0-3)	Linear fissures (0-3)	TOTAL	POD (0-3)	Wear lines (0-2)	Cart. loss (0-3)	Linear fissures (0-3)	TOTAL	Average TOTAL	Macroscopic OA Grade
74	MCP	Not Scored					Not Scored											
75	MCP	2	0	3	0	5	1	0	1	0	2	2	0	2	0	4	5	2
76	MCP	0	2	2	1	5	2	2	1	0	5						5	2
77	MCP	3	2	3	1	9	3	2	3	0	8						9	2
78	MCP	0	2	0	2	4	0	1	0	0	1	0	1	0	1	2	2	0
79	MCP	0	1	0	2	3	0	1	1	0	2						3	1
80	MCP	3	2	1	0	6	3	2	1	0	6						6	2
81	MCP	Not Scored					Not Scored											
82	MCP	2	1	0	0	3	2	1	1	0	4						4	1
83	MCP	1	2	1	0	4	1	2	1	0	4						4	1
84	MCP	0	0	3	1	4	0	0	1	1	2	0	1	1	1	3	4	1
85	MCP	0	2	3	0	5	0	2	1	0	3	0	2	1	0	3	3	1
86	MCP	2	2	3	0	7	2	1	1	0	4	1	1	1	0	3	4	1
87	MCP	3	2	3	0	8	3	2	1	0	6	2	1	2	0	5	6	2
88	MCP	1	0	0	0	1	1	0	0	2	3	1	1	0	1	3	3	1
89	MCP	3	2	3	0	8	3	2	1	0	6	3	2	3	0	8	8	2
90	MCP	1	0	3	0	4	1	0	1	0	2	1	1	1	0	3	4	1
91	MCP	1	1	2	0	4	1	1	1	0	3						4	1
92	MCP	3	2	3	0	8	1	1	1	0	3						6	2
93	MCP	2	0	3	0	5	2	0	2	1	5						5	2
94	MCP	0	0	2	0	2	1	1	1	0	3						3	1
95	MCP	2	1	3	3	9	1	1	1	3	6	2	1	2	1	6	6	2
96	MCP	2	0	3	0	5	2	0	1	1	4						5	2
97	MCP	2	2	1	0	5	2	1	0	0	3	1	2	1	0	4	5	2
98	MCP	0	0	0	1	1	0	0	0	1	1						1	0
99	MCP	0	0	0	0	0	0	1	0	1	2	0	0	0	0	0	0	0

100	MCP	0	1	0	2	3	1	1	0	1	3						3	1
101	MCP	1	0	0	0	1	0	0	1	1	2						2	0
102	MCP	1	1	2	0	4	1	1	2	1	5						5	2
103	MCP	0	0	0	1	1	0	0	1	1	2						2	0
104	MCP	Not Scored					Not Scored											
105	MTP	Not Scored					Not Scored											
106	MTP	0	0	2	2	4	0	0	1	1	2	0	0	0	1	1	2	0
107	MTP	Not Scored					Not Scored											
108	MTP	0	0	1	2	3	1	0	1	1	3						3	1
109	MTP	2	0	1	2	5	2	0	1	2	5						5	2
110	MTP	3	2	3	0	8	0	0	0	1	1	0	1	1	0	2	2	0
111	MTP	0	2	2	0	4	1	1	0	1	3						4	1
112	MTP	Not Scored					Not Scored											
113	MTP	0	1	3	1	5	1	1	0	1	3	0	1	0	2	3	3	1
114	MTP	1	0	1	0	2	1	0	1	1	3						3	1
115	MTP	0	1	0	3	4	1	1	0	2	4						4	1
116	MTP	0	0	0	3	3	0	0	0	2	2						3	1
117	MTP	0	0	0	3	3	0	1	0	1	2						3	1
118	MTP	0	0	0	2	2	1	0	0	2	3						3	1
119	MTP	0	0	1	2	3	0	0	0	2	2						3	1
120	MTP	1	1	0	0	2	0	1	0	2	3						3	1
121	MTP	0	0	0	1	1	0	0	0	1	1						1	0
122	MTP	0	0	0	3	3	0	0	0	1	1						2	0
123	MTP	1	1	0	0	2	1	0	0	2	3						3	1
124	MTP	Not Scored					Not Scored											
125	MTP	2	0	0	2	4	1	0	0	1	2						3	1
126	MTP	Not Scored					Not Scored											
127	MTP	0	0	0	1	1	0	0	0	2	2						2	0
128	MTP	0	0	0	2	2	0	0	0	2	2						2	0
129	MTP	1	0	0	1	2	1	0	0	2	3						3	1
130	MTP	0	0	0	2	2	0	0	0	1	1						2	0
131	MCP	0	1	3	1	5	1	1	1	0	3						4	1

Supplementary Table 6. Microscopic osteoarthritis scoring of distal metacarpal III or metatarsal III for the Hong Kong Jockey Club sample set.

Horse	Joint	Structure (0-10)	Cell Density (0-4)	Cell Cloning (0-4)	Staining (0-4)	Tidemark (0-3)	TOTAL	Microscopic OA Grade
74	MCP	Not Scored						
75	MCP	1	0	2	2	3	8	**1**
76	MCP	8	1	4	4	3	20	**2**
77	MCP	1	0	1	1	2	5	**1**
78	MCP	2	0	0	1	1	4	**0**
79	MCP	1	1	1	0	0	3	**0**
80	MCP	Not Scored						
81	MCP	Not Scored						
82	MCP	8	4	4	2	1	19	**2**
83	MCP	6	2	3	4	1	16	**2**
84	MCP	0	1	1	0	0	2	**0**
85	MCP	1	1	1	2	1	6	**1**
86	MCP	1	2	2	1	2	8	**1**
87	MCP	0	0	0	0	0	0	**0**
88	MCP	3	0	2	2	3	10	**1**
89	MCP	2	1	1	3	2	9	**1**
90	MCP	7	1	0	3	3	14	**2**
91	MCP	7	1	1	4	3	16	**2**
92	MCP	10	1	0	4	3	18	**2**
93	MCP	4	2	0	2	3	11	**2**
94	MCP	2	1	2	1	3	9	**1**
95	MCP	10	1	2	2	3	18	**2**
96	MCP	Not Scored						
97	MCP	1	0	1	0	1	3	**0**
98	MCP	0	0	1	0	0	1	**0**
99	MCP	2	1	0	0	0	3	**0**
100	MCP	Not Scored						
101	MCP	3	0	0	2	2	7	**1**
102	MCP	10	2	0	3	3	18	**2**
103	MCP	1	0	0	1	2	4	**0**
104	MCP	2	0	2	0	0	4	**0**
105	MTP	Not Scored						
106	MTP	1	0	0	1	0	2	**0**
107	MTP	2	0	1	2	2	7	**1**
108	MTP	5	0	0	2	3	10	**1**
109	MTP	2	1	1	1	0	5	**1**
110	MTP	4	2	0	4	2	12	**2**
111	MTP	5	1	1	3	2	12	**2**
112	MTP	Not Scored						
113	MTP	2	0	1	1	1	5	**1**
114	MTP	2	1	3	4	2	12	**2**
115	MTP	3	3	4	1	1	12	**2**
116	MTP	2	0	1	0	0	3	**0**
117	MTP	1	1	1	2	2	7	**1**
118	MTP	3	0	1	3	1	8	**1**
119	MTP	1	0	0	1	0	2	**0**
120	MTP	1	0	1	1	0	3	**0**

121	MTP	1	1	1	2	3	8	**1**
122	MTP	1	1	1	0	0	3	**0**
123	MTP	1	0	0	3	3	7	**1**
124	MTP	Not Scored						
125	MTP	2	1	1	2	0	6	**1**
126	MTP	2	0	0	1	2	5	**1**
127	MTP	2	1	1	2	2	8	**1**
128	MTP	1	0	1	1	3	6	**1**
129	MTP	1	0	0	1	2	4	**0**
130	MTP	1	1	1	1	0	4	**0**
131	MCP	0	1	1	1	0	3	**0**

Supplementary Table 7. Synovitis scoring of distal metacarpal III or metatarsal III for the Hong Kong Jockey Club sample set.

		Lining Cell Layer (0-3)				**Resident Cells (0-3)**				**Inflammatory infiltrate (0-3)**					
Horse	**Joint**	**1**	**2**	**3**	**Average**	**1**	**2**	**3**	**Average**	**1**	**2**	**3**	**Average**	**Total**	**Synovitis Grade**
74	MCP	1	1	0	**0.7**	2	2	0	**1.3**	2	2	1	**1.7**	**4**	**1**
75	MCP	1	1	1	**1.0**	1	2	1	**1.3**	0	0	1	**0.3**	**3**	**1**
76	MCP	2	2	1	**1.7**	1	1	1	**1.0**	1	2	1	**1.3**	**4**	**1**
77	MCP	2	1	3	**2.0**	2	2	1	**1.7**	1	1	1	**1.0**	**5**	**2**
78	MCP	2	1	1	**1.3**	1	1	1	**1.0**	1	1	1	**1.0**	**3**	**1**
79	MCP	1	2	2	**1.7**	1	1	1	**1.0**	1	1	1	**1.0**	**4**	**1**
80	MCP	1	2	2	**1.7**	1	1	1	**1.0**	1	1	1	**1.0**	**4**	**1**
81	MCP	0	1	1	**0.7**	1	2	2	**1.7**	0	3	3	**2.0**	**4**	**1**
82	MCP	1	1	3	**1.7**	1	2	2	**1.7**	2	2	3	**2.3**	**6**	**2**
83	MCP	2	1	2	**1.7**	1	1	1	**1.0**	1	1	1	**1.0**	**4**	**1**
84	MCP	1	1	2	**1.3**	1	1	1	**1.0**	1	1	1	**1.0**	**3**	**1**
85	MCP	2	2	2	**2.0**	2	1	1	**1.3**	1	1	1	**1.0**	**4**	**1**
86	MCP	2	2	1	**1.7**	1	1	1	**1.0**	1	1	1	**1.0**	**4**	**1**
87	MCP	2	3	1	**2.0**	3	2	3	**2.7**	0	1	0	**0.3**	**5**	**2**
88	MCP	2	2	2	**2.0**	1	1	1	**1.0**	2	1	1	**1.3**	**4**	**1**
89	MCP	2	3	2	**2.3**	2	2	2	**2.0**	2	2	2	**2.0**	**6**	**2**
90	MCP	3	2	3	**2.7**	3	3	3	**3.0**	2	2	2	**2.0**	**8**	**2**
91	MCP	1	2	2	**1.7**	1	2	1	**1.3**	1	1	2	**1.3**	**4**	**1**
92	MCP	2	3	3	**2.7**	1	1	2	**1.3**	1	1	2	**1.3**	**5**	**2**
93	MCP	3	2	2	**2.3**	2	1	3	**2.0**	1	2	1	**1.3**	**6**	**2**
94	MCP	0	1	1	**0.7**	1	2	1	**1.3**	1	1	2	**1.3**	**3**	**1**
95	MCP	2	2	3	**2.3**	3	2	3	**2.7**	2	2	2	**2.0**	**7**	**2**
96	MCP	1	1	3	**1.7**	2	2	2	**2.0**	1	1	1	**1.0**	**5**	**2**
97	MCP	1	2	3	**2.0**	1	1	1	**1.0**	1	1	1	**1.0**	**4**	**1**
98	MCP	2	1	1	**1.3**	1	1	1	**1.0**	1	1	1	**1.0**	**3**	**1**
99	MCP	1	1	1	**1.0**	1	1	1	**1.0**	1	1	1	**1.0**	**3**	**1**
100	MCP	0	1	1	**0.7**	1	1	1	**1.0**	0	1	1	**0.7**	**2**	**1**
101	MCP	0	0	0	**0.0**	1	1	1	**1.0**	1	1	1	**1.0**	**2**	**1**
102	MCP	3	3	3	**3.0**	2	2	3	**2.3**	2	2	1	**1.7**	**7**	**2**
103	MCP	1	0	2	**1.0**	1	1	1	**1.0**	2	2	1	**1.7**	**4**	**1**
104	MCP	0	1	2	**1.0**	0	1	1	**0.7**	1	1	1	**1.0**	**3**	**1**

105	MTP	1	2	2	**1.7**	1	3	3	**2.3**	2	2	2	**2.0**	**6**	**2**
106	MTP	2	1	2	**1.7**	1	1	1	**1.0**	1	1	1	**1.0**	**4**	**1**
107	MTP	1	2	1	**1.3**	1	1	1	**1.0**	1	1	1	**1.0**	**3**	**1**
108	MTP	1	1	0	**0.7**	0	1	0	**0.3**	1	1	1	**1.0**	**2**	**1**
109	MTP	2	2	3	**2.3**	1	1	1	**1.0**	1	1	1	**1.0**	**4**	**1**
110	MTP	3	1	0	**1.3**	1	1	0	**0.7**	1	2	1	**1.3**	**3**	**1**
111	MTP	2	2	0	**1.3**	1	1	1	**1.0**	1	1	1	**1.0**	**3**	**1**
112	MTP	2	2	1	**1.7**	1	1	1	**1.0**	2	1	2	**1.7**	**4**	**1**
113	MTP	2	3	1	**2.0**	1	2	0	**1.0**	1	3	0	**1.3**	**4**	**1**
114	MTP	1	1	1	**1.0**	1	1	1	**1.0**	1	1	1	**1.0**	**3**	**1**
115	MTP	0	0	1	**0.3**	0	0	0	**0.0**	1	1	1	**1.0**	**1**	**0**
116	MTP	2	3	3	**2.7**	1	1	1	**1.0**	1	1	1	**1.0**	**5**	**2**
117	MTP	1	1	2	**1.3**	0	1	1	**0.7**	1	1	1	**1.0**	**3**	**1**
118	MTP	3	2	2	**2.3**	2	1	2	**1.7**	1	1	1	**1.0**	**5**	**2**
119	MTP	2	2	2	**2.0**	2	3	1	**2.0**	2	2	2	**2.0**	**6**	**2**
120	MTP	1	1	1	**1.0**	1	1	1	**1.0**	1	1	1	**1.0**	**3**	**1**
121	MTP	0	2	2	**1.3**	1	1	3	**1.7**	2	2	3	**2.3**	**5**	**2**
122	MTP	2	1	3	**2.0**	1	1	1	**1.0**	1	1	2	**1.3**	**4**	**1**
123	MTP	2	2	1	**1.7**	1	1	1	**1.0**	2	1	1	**1.3**	**4**	**1**
124	MTP	2	2	2	**2.0**	1	2	1	**1.3**	1	1	1	**1.0**	**4**	**1**
125	MTP	2	2	2	**2.0**	1	1	0	**0.7**	1	1	1	**1.0**	**4**	**1**
126	MTP	1	2	1	**1.3**	1	1	1	**1.0**	1	1	1	**1.0**	**3**	**1**
127	MTP	0	2	2	**1.3**	1	2	2	**1.7**	1	2	2	**1.7**	**5**	**2**
128	MTP	1	3	3	**2.3**	1	1	2	**1.3**	1	3	3	**2.3**	**6**	**2**
129	MTP	2	2	1	**1.7**	2	2	1	**1.7**	1	2	1	**1.3**	**5**	**2**
130	MTP	3	3	2	**2.7**	1	1	1	**1.0**	1	1	1	**1.0**	**5**	**2**
131	MCP	1	3	2	**2.0**	1	1	1	**1.0**	1	1	1	**1.0**	**4**	**1**

A.3.10. Appendix to Manuscript 2

Synovial Fluid Osmolality and Serum Metabolomic Analysis in Equine Osteoarthritis

A.3.10.1. Introduction

Presently, no equine osteoarthritis (OA)-specific biomarkers have been identified which are able to accurately diagnose and stratify OA with none in current clinical use to aid an earlier diagnosis (Anderson, Phelan, *et al.*, 2018). A previous study in human synovial fluid (SF) identified that OA SF has a reduced osmolality compared to healthy samples (Shanfield *et al.*, 1988). However, no studies have investigated equine OA SF osmolality. Previous studies have identified various molecules of interest which were found to be differentially abundant in OA equine serum compared to normal, including keratan sulphate (Alwan *et al.*, 1990), glycosaminoglycan (Alwan *et al.*, 1991), C-telopeptide fragments of type II collagen (Cleary *et al.*, 2010), cartilage oligomeric matrix protein, tumour necrosis factor-α (Bertuglia *et al.*, 2016) and bone alkaline phosphatase (Trumble *et al.*, 2008). However, although nuclear magnetic resonance (NMR) spectroscopy has previously been used to investigate equine serum to study osteochondrosis, synovitis and an acute fracture, NMR has not been utilised to study serum of horses diagnosed with OA (Ralston *et al.*, 2011; Turlo *et al.*, 2018).

Within this study we have investigated equine SF osmolality and the equine serum metabolome, using ^{1}H NMR, to identify potential OA markers.

A.3.10.2. Methods

A.3.10.2.1. Sample Collection

A.3.10.2.1.1. Equine Synovial Fluid Collection

SF was collected from 86 horses within the Biobank and 36 horses at the Hong Jong Jockey Club at post mortem from the metacarpophalangeal, metatarsophalangeal and carpal joints. For collection protocols see manuscript 2.

A.3.10.2.1.2. Equine Serum Collection

Equine serum was collected from 34 horses at the Hong Kong Jockey Club (HKJC) via venepuncture following euthanasia and stored at -80°C. Further information on serum collection is unavailable.

A.3.10.2.2. Osteoarthritis Grading/Diagnosis

3.10.2.2.1. Osteoarthritis and Synovitis Grading - Synovial Fluid Samples

Macroscopic and microscopic OA grading was conducted on articular cartilage/subchondral bone wedge sections and microscopic synovitis scoring on synovial membrane collected at post mortem. For further details see manuscript 2.

A.3.10.2.2.2. Clinical Osteoarthritis diagnosis - Serum

Horses were assigned into their appropriate group according to their veterinary clinical records. Horses with a clear clinical diagnosis of OA were assigned into the OA group, with OA identified in one or more of the metacarpophalangeal, metatarsophalangeal or carpal joints. Where no clinical OA had been diagnosed, these horses were assigned to the healthy group. Samples from OA donors were all Thoroughbred racehorses.

A.3.10.2.3. Measurement of Synovial Fluid Osmolality

SF osmolality was measured with 100 µl of SF via freezing point depression, using an osmometer (MOD200Plus, Löser Messtechnik, Berlin, Germany).

A.3.10.2.4. NMR

A.3.10.2.4.1. NMR Sample Preparation

See manuscript 2.

A.3.10.2.4.2. NMR Acquisition

See manuscript 2.

A.3.10.2.4.3. Metabolite Annotation and Identification

See manuscript 2.

A.3.10.2.5. Statistical Analysis

Serum metabolite peak abundances underwent median normalisation and Pareto scaling prior to multivariate analysis (Worley and Powers, 2013). All principal component analysis (PCA) and t-tests of metabolite abundances were conducted using MetaboAnalyst 4.0 (http://www.metaboanalyst.ca). SF osmolality t-tests and ANOVAs were performed using Minitab version 17. All box plots were produced using SPSS 24.

A.3.10.3. Results

A.3.10.3.1. Synovial Fluid Osmolality

No difference in SF osmolality was identified within either the Biobank or HKJC groups when stratified according to microscopic OA pathology, macroscopic OA pathology or synovitis grade (Figure A1).

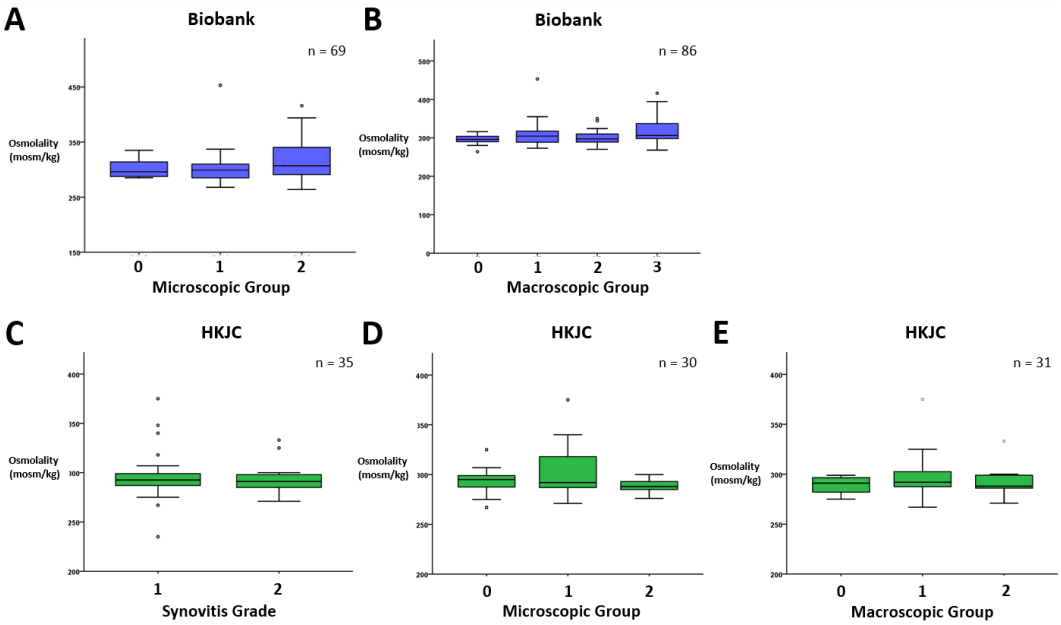

Figure A1. Equine synovial fluid osmolalities for the Biobank, stratified according to (A) cartilage microscopic osteoarthritis pathology and (B) cartilage macroscopic osteoarthritis pathology and the Hong Kong Jockey Club, stratified according to (C) synovitis grade, (D) cartilage microscopic osteoarthritis pathology and (E) cartilage macroscopic osteoarthritis pathology. HKJC = Hong Kong Jockey Club.

A.3.10.3.2. Equine Serum Metabolomics

PCA was unable to discriminate between the healthy and clinical OA groups with no differentially abundant metabolites identified (Figure A2). Additionally, no differences were observed between the global 1D ^{1}H NMR spectra of the two groups (Figure A3).

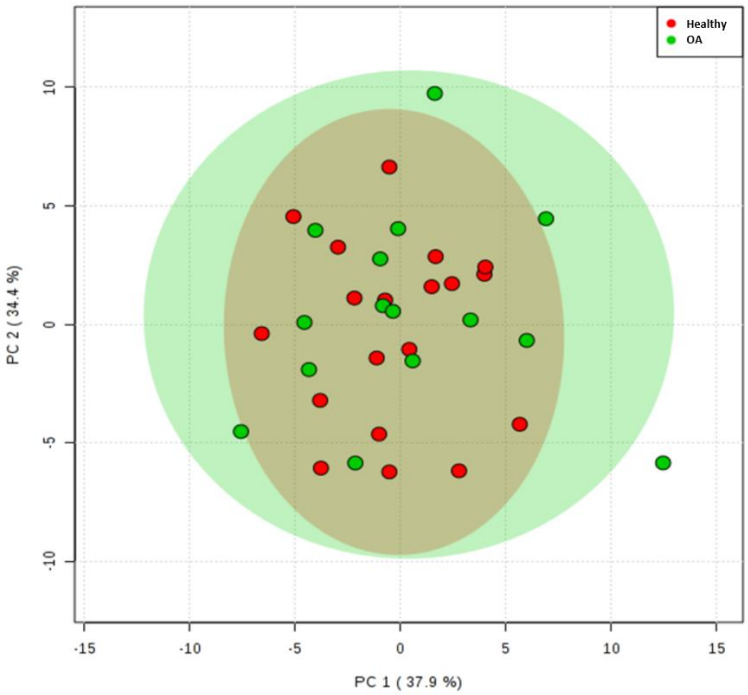

Figure A2. Principal component analysis of metabolite peaks identified within equine serum collected from the Hong Jong Jockey Club, categorised as healthy or clinically diagnosed with osteoarthritis (OA), using 1D ^{1}H NMR. Healthy; n=19, OA; n=15.

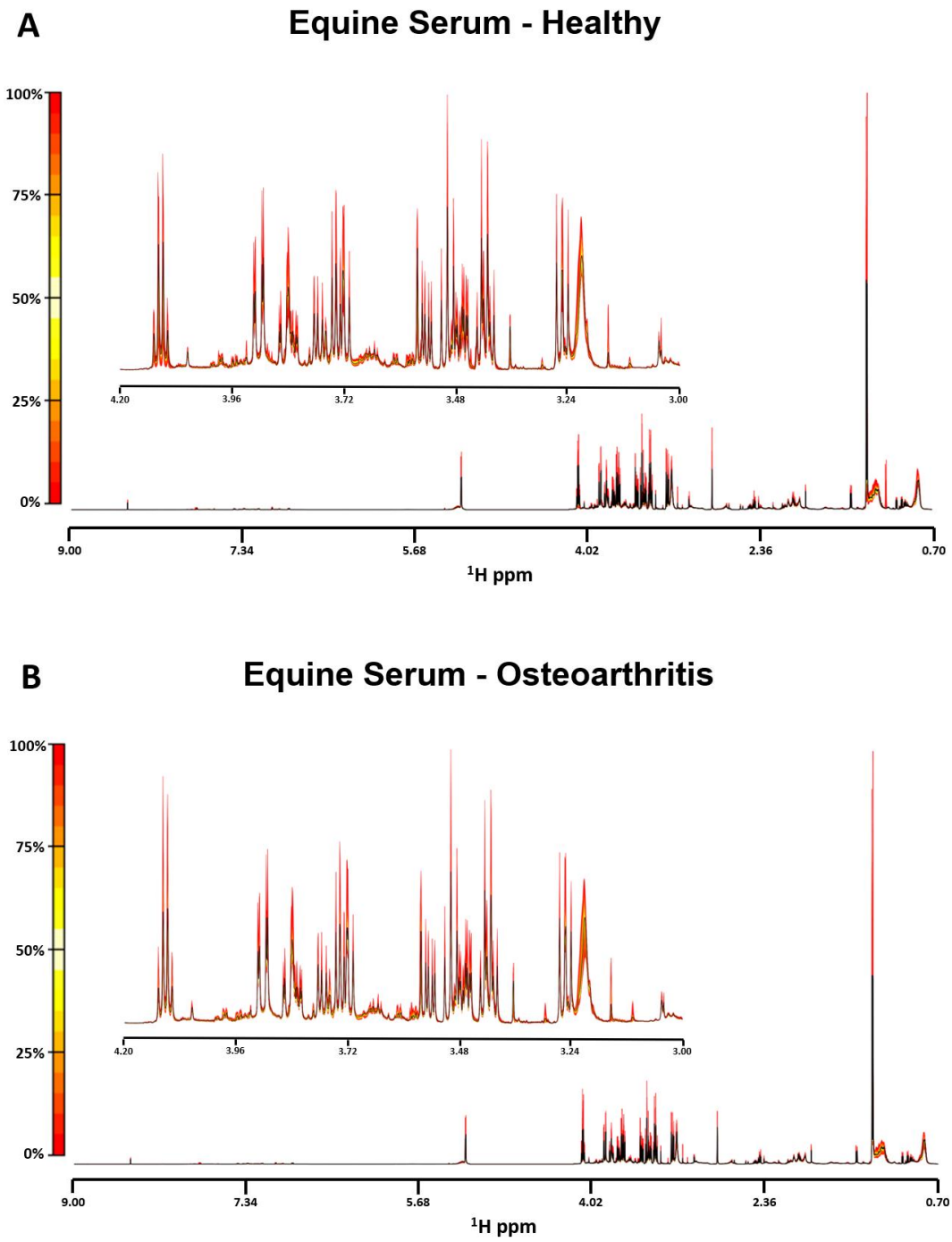

Figure A3. Quantile plots of serum collected from (A) healthy horses (n=21) and (B) horses diagnosed with osteoarthritis (n=15) from the Hong Kong Jockey Club. The median spectra are depicted by a black line, with variation from the median spectral plot depicted by a yellow to red scale. The full spectral range is shown (9.0-0.7 ppm) with a more detailed region inset (4.2-3.0 ppm).

A.3.10.4. Discussion

Presently, no equine OA-specific biomarkers have been identified which are able to accurately diagnose and stratify OA with none used to aid an earlier clinical diagnosis (Anderson, Phelan, *et al.*, 2018). Within this study we have investigated equine SF osmolality and the equine serum metabolome, using ^{1}H NMR, to identify potential OA markers. However, equine SF osmolality was unable to discriminate different grades of equine OA or synovitis. ^{1}H NMR metabolomics of equine serum was unable to discriminate healthy horses from those clinically diagnosed with OA.

A.3.10.4.1. Study Limitations

SF which was analysed during this study had previously undergone numerous freeze-thaw cycles prior to osmolality analysis. Previously, a study identified that osmolality values of human plasma following freeze-thawing produced significantly less reliable results than fresh samples analysed within 30 min of collection (Bohnen *et al.*, 1992). The study also identified differences in osmolality between plasma samples stored at 4°C or ambient temperature (21-24°C) prior to analysis. Therefore, given the susceptibility of biofluid osmolality to temperature changes, this may have affected the final osmolality readings collected and thus reduced experimental result reliability. Additionally, despite hyaluronidase treatment of SF, SF samples were more viscous than osmolality standards used for osmometer calibration, which might mean absolute osmolality values may be inaccurate. However, this should not have affected relative osmolality comparisons between samples.

Study constraints did not allow for collection of serum as advised by the Metabolomics Society (glucose fasted with a restricted diet) as all samples obtained were collected at euthanasia and not from an experimental study designed for this purpose. Therefore, influences from variations within these factors may have affected the metabolite analysis.

A.3.10.4.2. Conclusion

Equine SF osmolality was unable to discriminate different grades of equine OA or synovitis. ^{1}H NMR metabolomics of equine serum was unable to discriminate healthy horses from those clinically diagnosed with OA. However, limitations to the experimental methods led to a reduced reliability in the results and thus further experimentation with improved protocols is required to confirm these findings.

4. Manuscript 3

Ex-Vivo Equine Cartilage Explant Osteoarthritis Model - A Metabolomics and Proteomics Study

James R Anderson[1], Marie M Phelan[2,3], Laura Foddy[1], Peter D Clegg[1] and Mandy J Peffers[1]

[1]Institute of Ageing and Chronic Disease, University of Liverpool, Liverpool, UK
[2]Institute of Integrative Biology, University of Liverpool, Liverpool, UK
[3]HLS Technology Directorate, University of Liverpool, Liverpool, UK

Keywords

Osteoarthritis, Cartilage, Metabolomics, Proteomics, Nuclear Magnetic Resonance, Mass Spectrometry

Declaration of Author Contributions

Dr Marie Phelan provided training in NMR spectral acquisition, training in NMR spectral analysis and training in cartilage metabolite extraction. Ms Laura Foddy assisted with cartilage metabolite extraction and assisted with NMR cartilage metabolite spectral analysis. Professor Peter Clegg and Professor Mandy Peffers supervised this study and advised on experimental design. All other experimental work was conducted by Mr James Anderson.

4.1. Abstract

Osteoarthritis (OA) is an age-related degenerative musculoskeletal disease characterised by loss of articular cartilage, abnormal bone proliferation and subchondral bone sclerosis. The underlying pathogenesis of OA is yet to be fully elucidated with no OA specific biomarkers identified. Nuclear magnetic resonance (NMR) spectroscopy and mass spectrometry (MS) allow analysis of the global metabolome and proteome respectively. During this study, *ex-vivo* equine cartilage explants (n=5) were incubated in TNF-α/IL-1β supplemented culture media for 8 days, with media removed and replaced at 2, 5 and 8 days. Acetonitrile metabolite extractions of 8 day cartilage explants and media samples at all time points underwent ^{1}H NMR metabolic analysis with media samples also undergoing MS proteomic analysis. Within the cartilage, metabolites glucose and lysine levels were elevated following TNF-α/IL-1β treatment whilst adenosine, alanine, betaine, creatine, myo-inositol and uridine levels decreased. Within the culture media, four, four and six metabolites were identified as being differentially abundant between control and treatment groups for 1-2 day, 3-5 day and 6-8 day time points respectively. Culture media proteomics identified 154, 138 and 72 proteins were differentially abundant, with > 2 fold change, between control and treatment groups for 1-2 day, 3-5 day and 6-8 day time points respectively. Nine potential novel OA neopeptides were elevated in treated media. This is the first study to use a multi 'omics' approach to simultaneously investigate the metabolomic profile of *ex-vivo* cartilage and metabolomic/proteomic profiles of culture media using the TNF-α/IL-1β *ex-vivo* OA cartilage model. This study has identified a panel of metabolites, proteins and extracellular matrix derived neopeptides which are differentially abundant within an early phase of the OA model which may provide further information on underlying disease pathogenesis, allow potential translation for clinical markers and possible novel therapeutic targets.

4.2. Introduction

Osteoarthritis (OA) is an age-related degenerative musculoskeletal disease characterised by loss of articular cartilage, synovial membrane dysfunction, abnormal bone proliferation, subchondral bone sclerosis and altered biochemical and biomechanical properties (Kramer, Tsang, *et al.*, 2014; Truong *et al.*, 2006). For horses in the UK, OA is one of the leading welfare issues, resulting in substantial morbidity and mortality (Ireland *et al.*, 2011, 2012). It is estimated that OA accounts for 60% of lameness seen in horses (Caron and Genovese, 2003). Within OA, extracellular matrix (ECM) degradation is driven by multiple matrix metalloproteinases (MMPs) and a disintegrin and metalloproteinases with thrombospondin motifs (ADAMTSs) (Struglics *et al.*, 2006). However, the underlying pathogenesis of OA is yet to be fully elucidated with no licensed disease-modifying treatments currently available (Li *et al.*, 2007; Marhardt and Muurahainen, 2015). No OA specific biomarkers have been identified for OA in the horse with none currently used within clinical practice (Anderson, Phelan, *et al.*, 2018). Presently, equine OA is predominantly diagnosed through diagnostic imaging and clinical examination. However, due to the slow onset of the condition, this often leads to substantial pathology of the joint, particularly to articular cartilage prior to diagnosis (Brommer *et al.*, 2003). There is therefore a need to develop diagnostic tests which are sensitive and specific to the early stages of OA, which are repeatable and reproducible, as well as gaining a greater understanding of the underlying pathogenesis (Hunter *et al.*, 2014; McIlwraith *et al.*, 2018). Early detection of OA could allow for timely management interventions which could potentially slow the progression of the disease.

Tumour necrosis factor-α (TNF-α) and interleukin-1β (IL-1β) are both pro-inflammatory cytokines which are central in OA pathogenesis (Wojdasiewicz *et al.*, 2014). TNF-α and IL-1β are secreted by mononuclear cells, synoviocytes and articular cartilage and upregulate gene expression of MMPs, ADAMTS-4 and ADAMTS-5, leading to significant ECM degradation (Fernandes *et al.*, 2002; Goldring and Goldring, 2004; Wang *et al.*, 2011). Elevations in TNF-α and IL-1β are regularly identified within OA synovial fluid, including that of horses (Bertuglia *et al.*, 2016;

Ma *et al.*, 2017; Westacott *et al.*, 1990). TNF-α and IL-1β have therefore become established experimental treatments for modelling OA pathology within *in vitro* and *ex-vivo* studies, having been used both independently and as a combined treatment (Barksby *et al.*, 2006; De Ceuninck *et al.*, 2004; Cillero-Pastor *et al.*, 2010; Pretzel *et al.*, 2009; Stevens *et al.*, 2008, 2009; Williams, 2014).

Proteomics is the systematic, large scale study of proteins within biological systems to assess quantities, isoforms, modifications, structure and function (de Hoog and Mann, 2004). Previous studies have undertaken mass spectrometry (MS) based proteomics using TNF-α and IL-1β OA models for secretome analysis of chondrocytes *in vitro* and *ex-vivo* cartilage explants (Cillero-Pastor *et al.*, 2010; Stevens *et al.*, 2008, 2009; Williams, 2014). Results from these studies included increased media levels of MMPs, cartilage oligomeric matrix protein (COMP), aggrecan and collagen VI.

During OA pathology, disease-associated peptide fragments (neopeptides) are generated from cartilage breakdown due to increased enzymatic activity/abundance of MMPs, ADAMTSs, cathepsins and serine proteases (Ben-Aderet *et al.*, 2015; Peffers *et al.*, 2016; Polur *et al.*, 2010). Using MS, neopeptides can be identified and quantified and thus utilised as potential molecular biomarkers of early OA. Additionally, a recent mouse study identified that a 32 amino acid peptide fragment, generated through degradation of aggrecan via increased ADAMTS-4/5 and MMP activity, drives OA pain through Toll-like receptor 2 (Miller *et al.*, 2018). Thus, targeting neopeptides may provide analgesia and reduce significant pain associated with joint degeneration. Various studies have identified potential neopeptides associated with OA in equine cartilage and synovial fluid (SF) (Peffers *et al.*, 2014; Peffers, McDermott, *et al.*, 2015; Peffers *et al.*, 2016; Skiöldebrand *et al.*, 2017). Subsequent development of neopeptide antibodies would allow for the detection and monitoring of cartilage degeneration as well as assessing response to therapeutics, in both laboratory and clinical settings (Peffers *et al.*, 2017). In addition, identification of OA specific neopeptides may provide novel therapeutic targets.

Metabolomics uses a systematic methodology to comprehensively identify and quantify the metabolic profiles of biological samples (Beckonert *et al.*, 2007). ^{1}H Nuclear magnetic resonance (NMR) metabolomics analysis provides a high level of technical reproducibility with a minimal level of sample preparation (Beltran *et al.*, 2012). ^{1}H NMR analysis has previously been used to investigate OA in the SF of humans, horses, pigs and dogs (Anderson, Chokesuwattanaskul, *et al.*, 2018; Anderson, Phelan, *et al.*, 2018; Damyanovich *et al.*, 1999; Hugle *et al.*, 2012; Lacitignola *et al.*, 2008; Mickiewicz, Heard, *et al.*, 2015; Mickiewicz, Kelly, *et al.*, 2015). Synovial metabolites alanine, choline, creatine and glucose have been identified as differentially abundant in OA across multiple studies (Anderson, Chokesuwattanaskul, *et al.*, 2018; Anderson, Phelan, *et al.*, 2018; Damyanovich *et al.*, 1999; Lacitignola *et al.*, 2008; Mickiewicz, Heard, *et al.*, 2015; Mickiewicz, Kelly, *et al.*, 2015). NMR techniques have also previously been used to characterise cartilage with high resolution magical angle spinning (HRMAS) NMR utilised to assess enzymatic degradation of bovine cartilage (Ling *et al.*, 2008; Schiller *et al.*, 2001, 2004). A guinea pig OA model using HRMAS NMR identified elevations in methylene resonances associated with chondrocyte membrane lipids and an increase in mobile methyl groups of collagen (Borel *et al.*, 2009). Another HRMAS NMR study of human OA cartilage identified a reduction in alanine, choline, glycine, lactate methyne and N-acetyl compared to healthy control cartilage (Shet *et al.*, 2012). However, no NMR studies to date have investigated the metabolic profile of culture media following the incubation of *ex-vivo* cartilage within an OA model.

This is the first study to carry out ^{1}H NMR metabolomic analysis of extracted cartilage metabolites and the first to undertake ^{1}H NMR analysis of culture media using the TNF-α/IL-1β *ex-vivo* OA cartilage model. Additionally, this is also the first study to use a multi 'omics' approach to simultaneously investigate the metabolomic profile of *ex-vivo* cartilage and metabolomic/proteomic profiles of culture media using this OA model. It was hypothesised that following TNF-α/IL-1β treatment of *ex vivo* equine cartilage, ^{1}H NMR metabolomic and MS proteomic platforms would identify a panel of cartilage metabolites which were able to differentiate control from treated cartilage and a panel of metabolites, proteins and

neopeptides within the associated culture media which were differentially abundant at each tested time point of the OA model.

4.3. Methods

4.3.1 Equine *Ex-Vivo* Cartilage Collection

Full thickness cartilage was removed from all articular surfaces within five separate metacarpophalangeal joints of five nine-year-old mares of unknown breed within 24 hr of slaughter (F Drury and Sons, Swindon, UK). Cartilage collected from all joints was considered macroscopically normal with a score of 0 according to the OARSI histopathology initiative scoring system for horses (McIlwraith *et al.*, 2010) (Supplementary Figure 1). Cartilage was washed in complete media containing Dulbecco's modified Eagle's medium (DMEM, 31885-023, Life Technologies, Paisley, UK) supplemented with 10% (v/v) foetal calf serum (FCS, Life Technologies), 5 μg/ml Amphotericin B (Life Technologies), 100 U/ml Streptomycin and 100 U/ml Penicillin (Sigma-Aldrich, Gillingham, UK) (Figure 1).

Cartilage was dissected into 3 mm^2 sections and divided into two for each donor (control and treatment wells) on a twelve well plate (Greiner Bio-One Ltd., Stonehouse, UK). Explants were incubated for 24 hr in complete media within a humidified atmosphere of 5% (v/v) CO_2 at 37°C. Culture media was removed, explants washed in phosphate buffered saline (PBS, Sigma-Aldrich) and replaced with serum free media (control) or serum free media supplemented with 10 ng/ml TNF-α (PeproTech EC Ltd., London, UK) and 10 ng/ml IL-1β (R&D Systems Inc., Minneapolis, Minnesota, USA) (treatment). After 48 hr, media was removed, centrifuged at 13,000*g*, 4°C for 10 min, supernatant removed and ethylenediaminetetraacetic acid (EDTA)-free protease inhibitor cocktail (Roche, Lewes, UK) added to cell-free media. Supernatant was then snap frozen in liquid nitrogen and stored at -80°C. Cartilage was washed in PBS and control/treatment culture media replaced as appropriate. Media collection was repeated at five and eight days. After day eight, cartilage was washed in PBS, weighed, snap frozen in liquid nitrogen and stored at -80°C.

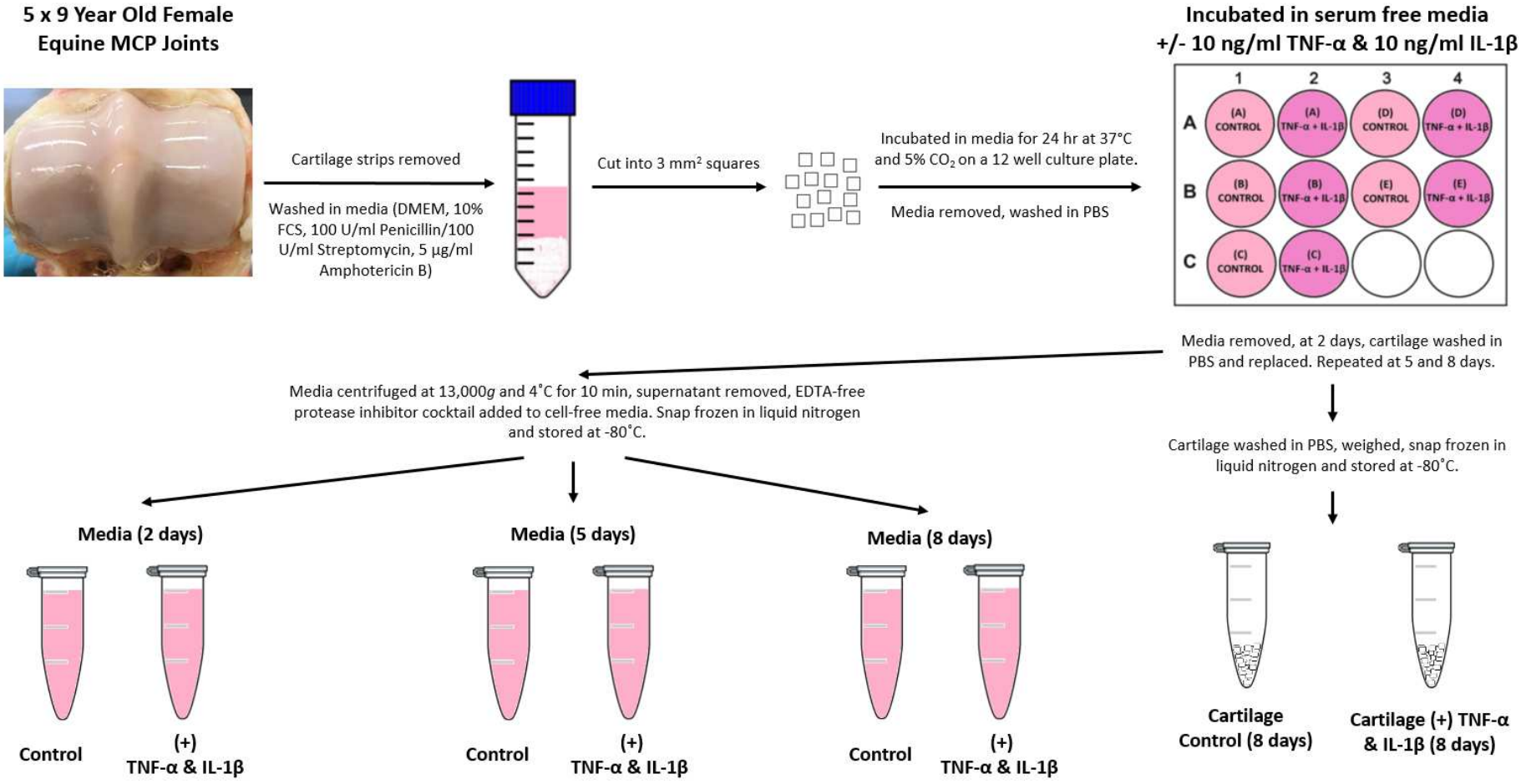

Figure 1. Experimental design for *ex-vivo* equine cartilage culture +/- TNF-α/IL-1β treatment. MCP = metacarpophalangeal.

4.3.2. NMR Metabolomics

4.3.2.1. Cartilage - Metabolite Extraction

Equal masses of cultured cartilage explants (in addition to three macroscopically normal equine cartilage samples, each divided into three to assess metabolite extraction reproducibility) were thawed out over ice and added to 500 µl of 50:50 (v/v) ice cold acetonitrile (ThermoFisher Scientific, Massachusetts, USA):dd $^{1}H_2O$ and incubated on ice for 10 min (Figure 2). Samples were then sonicated for three 30 s periods, interspersed with 30 s rests, vortexed for 1 min, centrifuged at 12,000*g* for 10 min at 4°C, supernatant removed, snap frozen in liquid nitrogen, lyophilised and stored at -80°C (Beckonert *et al.*, 2007).

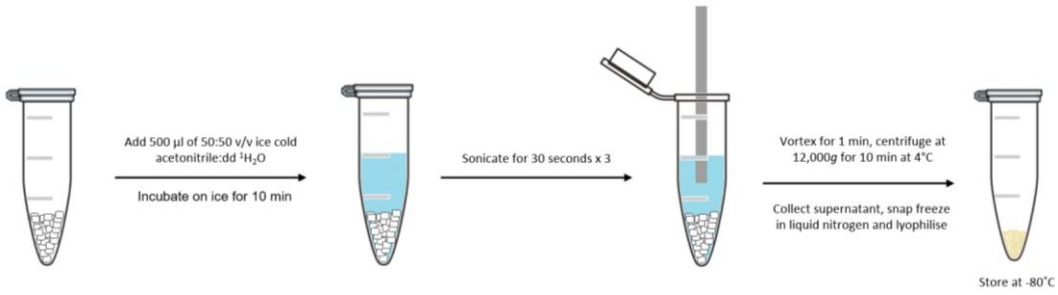

Figure 2. Protocol for cartilage metabolite extraction.

4.3.2.2. Cartilage - NMR Sample Preparation

Each lyophilised sample was dissolved through the addition of 178 µl of 100% deuterium oxide ($^{2}H_2O$, Sigma-Aldrich), 20 µl of 1M PO_4^{3-} pH 7.4 buffer (Na_2HPO_4, VWR International Ltd., Radnor, Pennsylvania, USA and NaH_2PO_4, Sigma-Aldrich), 0.2 µl of 100 mM d4 trimethylsilyl propionate (TSP, Sigma-Aldrich) and 0.2 µl of 1.2 mM sodium azide (NaN_3, Sigma-Aldrich). Samples were vortexed for 1 min, centrifuged at 12,000*g* for 2 min, 190 µl of supernatant removed and transferred into 3 mm outer diameter NMR tubes using a glass pipette.

4.3.2.3. Culture Media - NMR Sample Preparation

Culture media was thawed over ice and centrifuged for 5 min at 21,000*g* and 4°C. 150 µl of thawed culture media was diluted to a final volume containing 50% (v/v) culture media, 40% (v/v) dd $^{1}H_2O$, 10% $^{2}H_2O$ and 0.0025% (v/v) NaN_3, within an overall concentration of 500 mM PO_4^{3-} pH 7.4 buffer. Samples were vortexed for 1 min, centrifuged at 13,000*g* for 2 min at 4°C, 250 µl supernatant removed and transferred to 3 mm outer diameter NMR tubes using a glass pipette.

4.3.2.4. NMR Acquisition

For each individual sample, 1D ^{1}H NMR spectra, with the application of a Carr-Purcell-Meiboom-Gill (CPMG) filter to attenuate macromolecule (e.g. proteins) signals, were acquired using the standard vendor pulse sequence cpmgpr1d on a 700 MHz NMR Bruker Avance III HD spectrometer with associated TCI cryoprobe and chilled Sample-Jet autosampler. All spectra were acquired at 25°C, with a 4 s interscan delay, 256 transients for cartilage spectra and 128 transients for media spectra, with a spectral width of 15 ppm. Topsin 3.1 and IconNMR 4.6.7 software programmes were used for acquisition and processing undertaking automated phasing, baseline correction and a standard vendor processing routine (exponential window function with 0.3 Hz line broadening). In addition to all cartilage extract and culture media samples, protease inhibitor cocktail and treatment cytokines TNF-α and IL-1β were also analysed separately to evaluate their metabolite profiles.

4.3.2.5. Metabolite Annotation and Identification

All acquired spectra were assessed to determine whether they met minimum reporting standards (as outlined by the Metabolomics Society) prior to inclusion for statistical analysis (Sumner *et al.*, 2007). These included appropriate water suppression, flat spectral baseline and consistent linewidths. Metabolite annotations and relative abundances were carried out using Chenomx NMR Suite 8.2 (330-mammalian metabolite library). Where possible, metabolite identifications were confirmed using 1D ^{1}H NMR in-house spectral libraries of metabolite

standards. Quantile plots of 1D ^{1}H NMR spectra are shown in Supplementary Figure 2.

4.3.3. Culture Media Proteomics

4.3.3.1. Protein Assay and StrataClean™ Resin Processing

Culture media was thawed over ice and centrifuged for 5 min at 21,000*g* and 4°C. Media sample concentrations were determined using a Pierce® 660 nm protein assay (Thermo Scientific, Waltham, Massachusetts, USA). 50 µg of protein for each sample was diluted with dd H_2O, producing a final volume of 1 ml. 10 µl of StrataClean™ resin (Agilent, Santa Clara, California, USA) was added to each sample, rotated for 15 min, centrifuged at 400*g* for 1 min and the supernatant removed and discarded. Samples were then washed through the addition of 1 ml of ddH_2O, vortexed for 1 min, centrifuged at 400*g* for 1 min and the supernatant removed and discarded. The wash step was repeated two further times.

4.3.3.2. Protein Digestion

160 µl of 25 mM ammonium bicarbonate (Fluka Chemicals Ltd., Gillingham, UK) containing 0.05% (w/v) RapiGest (Waters, Elstree, Hertfordshire, UK) was added to each sample and heated at 80°C for 10 min. DL-Dithiothreitol (Sigma-Aldrich) was added to produce a final concentration of 3 mM, incubated at 60°C for 10 min then iodoacetamide (Sigma-Aldrich) added (9 mM final concentration) and incubated at room temperature in the dark for 30 min. 2 µg of proteomics grade trypsin (Sigma-Aldrich) was added to each sample, rotated at 37°C for 16 hr and trypsin treatment then repeated for a 2 hr incubation. Samples were centrifuged at 1,000*g* for 1 min, digest removed, trifluoroacetic acid (TFA, Sigma-Aldrich) added (0.5% (v/v) final concentration) and rotated at 37°C for 30 min. Finally, digests were centrifuged at 13,000*g* and 4°C for 15 min and the supernatant removed and stored at 4°C.

4.3.3.3. Label Free LC-MS/MS

All media digests were randomised and individually analysed using LC-MS/MS on an UltiMate 3000 Nano LC System (Dionex/Thermo Scientific) coupled to a Q

Exactive™ Quadrupole-Orbitrap instrument (Thermo Scientific). Full LC-MS/MS instrument methods are described in chapter 7. Tryptic peptides, equivalent to 250 ng of protein, were loaded onto the column and run over a 1 hr gradient, interspersed with 30 min blanks (97% (v/v) high performance liquid chromatography grade H_20 (VWR International), 2.9% acetonitrile (Thermo Scientific) and 0.1% TFA. In addition to Individual time points, pooled samples for control and treatment groups were also analysed to investigate differences in the overall secretome. Representative ion chromatograms are shown in Supplementary Figure 3.

4.3.3.4. LC-MS/MS spectra processing and protein identification

Spectral alignment, peak picking, total protein abundance normalisation and peptide/protein quantification were undertaken using Progenesis™ QI 2.0 (Nonlinear Dynamics, Waters). The exported top ten spectra for each feature were then searched against the *Equus caballus* database for peptide and protein identification using PEAKS® Studio 8.5 (Bioinformatics Solutions Inc., Waterloo, Ontario, Canada) software. Search parameters were: precursor mass error tolerance, 10.0 ppm; fragment mass error tolerance, 0.01 Da; precursor mass search type, monoisotopic; enzyme, trypsin; maximum missed cleavages, 1; non-specific cleavage, none; fixed modifications, carbamidomethylation; variable modifications, oxidation or hydroxylation and oxidation (methionine). A filter of a minimum of 2 unique peptides was set for protein identification and quantitation with a false discovery rate (FDR) of 1%.

4.3.3.5. 1D SDS PAGE

Media samples for each donor were combined for all time points and analysed via one dimensional sodium dodecyl sulphate polyacrylamide gel electrophoresis (1D SDS PAGE). 1 µg of each sample was added to Laemmli loading buffer Novex™ (Thermo Scientific) producing a final concentration of 15% glycerine, 2.5% SDS, 2.5% Tris (hydroxymethyl) aminomethane, 2.5% HCL and 4% β-mercaptoethanol at pH 6.8 and heated at 95°C for 5 min. Samples were loaded onto a 4-12% Bis-Tris polyacrylamide electrophoresis gel (NuPAGE™ Novex™, Thermo Scientific) and

protein separation carried out at 200 V for 30 min at room temperature. Protein bands were visualised via silver staining (Thermo Scientific) following manufacturer instructions. Gel images were converted to 8 bit grey scale and protein band intensities analysed using densitometry with the software Image J (NIH, Bethesda, Maryland).

4.3.3.6. Semi-Tryptic Peptide Identification

To identify potential neopeptides a 'semi-tryptic' search was carried out. The same PEAKS® search parameters were used as for protein identification, with the exception that 'non-specific cleavage' was altered from 'none' to 'one'. The 'peptide ion measurements' file was then exported and analysed using the online neopeptide analyser software tool (Peffers *et al.*, 2017).

4.3.4. Statistical Analysis

Cartilage metabolite profiles were normalised using probabilistic quotient normalisation (PQN) (Dieterle *et al.*, 2006). Media metabolites were normalised to TSP concentration and protein profiles normalised to total ion current (TIC). Prior to multivariate analysis, metabolite and protein profiles were Pareto scaled (Worley and Powers, 2013). MetaboAnalyst 3.5 (http://www.metaboanalyst.ca) was used to produce principal component analysis (PCA) and partial-least-squares discriminant analysis (PLS-DA) plots. t-tests were carried out using MetaboAnalyst 3.5 (protein and metabolite abundances) and the neopeptide analyser (neopeptides) with $p < 0.05$ (and a fold change of > 2 for proteins) considered statistically significant. The Benjamini-Hochberg false discovery rate method was applied for correction of multiple testing (Benjamini and Hochberg, 1995). The SPSS 24 software package was used to produce all box plots.

4.3.5. Pathway Analysis

Pathway analysis was conducted for differentially abundant metabolites using the online tool KEGG for *Equus caballus* (Ogata *et al.*, 1999). Differentially abundant proteins (> 2 fold change) were also analysed using KEGG via the STRING database

(Szklarczyk *et al.*, 2015). A filter of a minimum of two metabolites/proteins was set for each sample set for inclusion of the relevant biological pathway.

4.4. Results

4.4.1. NMR Metabolomics

4.4.1.1. Protease inhibitor cocktail, TNF-α and IL-1ß metabolite profiles

Protease inhibitor cocktail was found to have high levels of mannitol and thus this metabolite was removed from all analyses. Within the spectral profiles of TNF-α and IL-1β acquired separately, the metabolites acetate, acetone, ethanol, formate, lactate, methanol and succinate were identified. These metabolites were therefore also removed from further analyses.

4.4.1.2 Cartilage - Metabolites

Acetonitrile metabolite extraction was identified to be highly reproducible with technical replicates clustering within a PCA plot for three separate macroscopically normal cartilage samples (Figure 3). In total 35 metabolites were identified within equine cartilage (Table 1). Of these, following the removal of metabolites previously mentioned, eight were identified as being differentially abundant between control and treatment groups (Figure 4). Glucose and lysine levels were elevated following TNF-α/IL-1β treatment whilst adenosine, alanine, betaine, creatine, myo-inositol and uridine levels decreased. PCA identified that metabolite profiles separated into two distinct clusters, separating control and treatment groups (Figure 4a). PLS-DA (supervised multivariate discriminant analysis) produced a model comprising one component with a good predictive power (R^2 = 0.89, Q^2 = 0.82) (Figure 5b). Of the top 25 variables of influence (VIP), myo-inositol was found to be the most influential cartilage metabolite in separating control and treated samples, followed by glucose, betaine and alanine (Figure 5c).

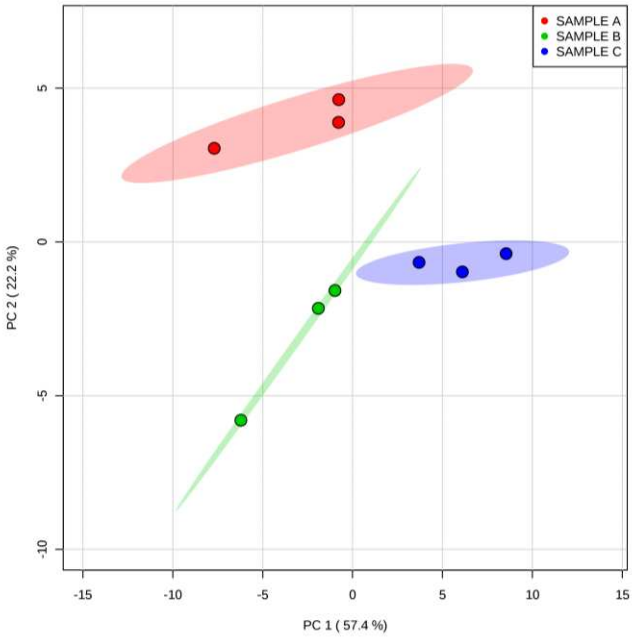

Figure 3. Principal component analysis scores plot identifying high reproducibility of acetonitrile cartilage metabolite extraction (three separate equine donors, technical triplicate for each donor) using 1D ^{1}H NMR metabolome analysis. Shaded regions depict 95% confidence regions.

Table 1. Metabolites annotated within cartilage and culture media using Chenomx. Metabolites additionally identified using a 1D ^{1}H NMR in-house library have been assigned to Metabolomics Standards Initiative (MSI) level 1 (Salek *et al.*, 2013).

Database Identifier	Metabolite Identification	Cartilage	Cartilage Reliability	Media	Media Reliability
HMDB00695	2-Oxoisocaproate			Y	MS Level 2
HMDB00491	3-Methyl-2-oxovalerate			Y	MS Level 2
HMDB31645	Acetamide	Y	MS Level 2		
HMDB00042	Acetate *	Y	MS Level 1	Y	MS Level 1
HMDB01659	Acetone *			Y	MS Level 2
HMDB00050	Adenosine	Y	MS Level 2		
HMDB00517	Arginine			Y	MS Level 2
HMDB00191	Aspartate	Y	MS Level 1		
HMDB00043	Betaine	Y	MS Level 1		
HMDB00097	Choline			Y	MS Level 1
HMDB00094	Citrate	Y	MS Level 1	Y	MS Level 1
HMDB00064	Creatine	Y	MS Level 1		
HMDB00562	Creatinine	Y	MS Level 1	Y	MS Level 1

HMDB00192	Cystine			Y	MS Level 2
HMDB00122	D-Glucose	Y	MS Level 1		
HMDB04983	Dimethyl sulfone	Y	MS Level 2		
HMDB00108	Ethanol *			Y	MS Level 1
HMDB00142	Formate *	Y	MS Level 2	Y	MS Level 2
HMDB00123	Glycine	Y	MS Level 1	Y	MS Level 1
HMDB00870	Histamine			Y	MS Level 2
HMDB00172	Isoleucine	Y	MS Level 1	Y	MS Level 1
HMDB00863	Isopropanol *			Y	MS Level 2
HMDB00190	Lactate *	Y	MS Level 1	Y	MS Level 1
HMDB00161	L-Alanine	Y	MS Level 1	Y	MS Level 1
HMDB00062	L-Carnitine			Y	MS Level 2
HMDB00148	L-Glutamate	Y	MS Level 1	Y	MS Level 1
HMDB00641	L-Glutamine	Y	MS Level 1	Y	MS Level 1
HMDB00177	L-Histidine			Y	MS Level 1
HMDB00687	L-Leucine	Y	MS Level 1	Y	MS Level 1
HMDB00159	L-Phenylalanine	Y	MS Level 1		
HMDB00167	L-Threonine	Y	MS Level 2	Y	MS Level 2
HMDB00158	L-Tyrosine	Y	MS Level 1	Y	MS Level 1
HMDB00883	L-Valine	Y	MS Level 1	Y	MS Level 1
HMDB00182	Lysine	Y	MS Level 1	Y	MS Level 1
HMDB00765	Mannitol *			Y	MS Level 1
HMDB01875	Methanol *			Y	MS Level 2
HMDB00696	Methionine	Y	MS Level 1	Y	MS Level 1
HMDB01844	Methylsuccinate	Y	MS Level 2		
HMDB00211	myo-Inositol	Y	MS Level 1		
HMDB03269	Nicotinurate	Y	MS Level 2	Y	MS Level 2
HMDB00895	O-Acetylcholine	Y	MS Level 2		
HMDB00210	Pantothenate	Y	MS Level 2	Y	MS Level 2
HMDB00267	Pyroglutamate			Y	MS Level 2
HMDB00243	Pyruvate	Y	MS Level 1		
HMDB00086	sn-Glycero-3-phosphocholine	Y	MS Level 2		
HMDB00254	Succinate *	Y	MS Level 1	Y	MS Level 1
HMDB00929	Tryptophan			Y	MS Level 1
HMDB00300	Uracil	Y	MS Level 2		
HMDB00296	Uridine	Y	MS Level 1		
HMDB00001	τ-Methylhistidine	Y	MS Level 2		

*Y = Yes; * = Metabolite removed from subsequent analyses*

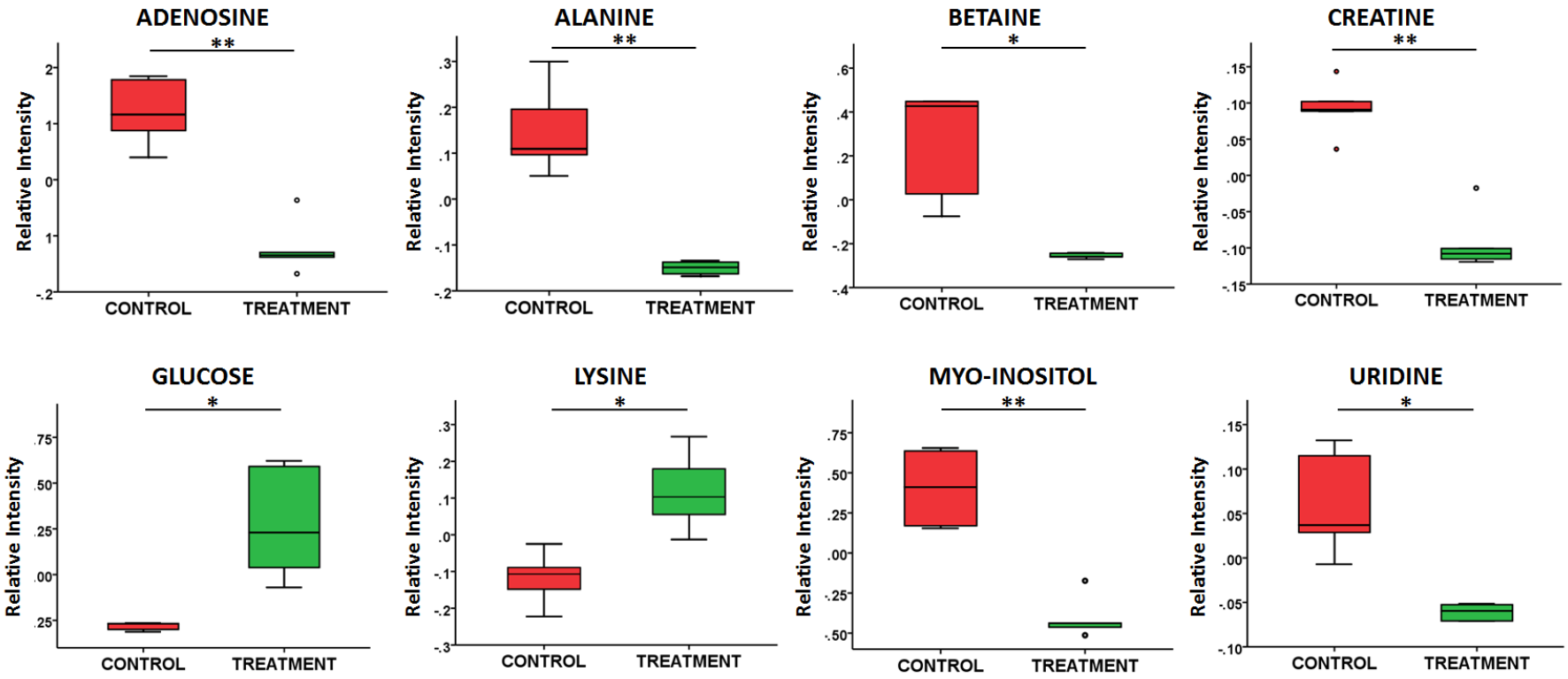

Figure 4. Boxplots of differentially abundant extracted *ex-vivo* equine cartilage metabolites for control (n=5) and following TNF-α/IL-1β treatment (n=5), shown as relative intensities. t-test: * = $p < 0.05$ and ** = $p < 0.01$.

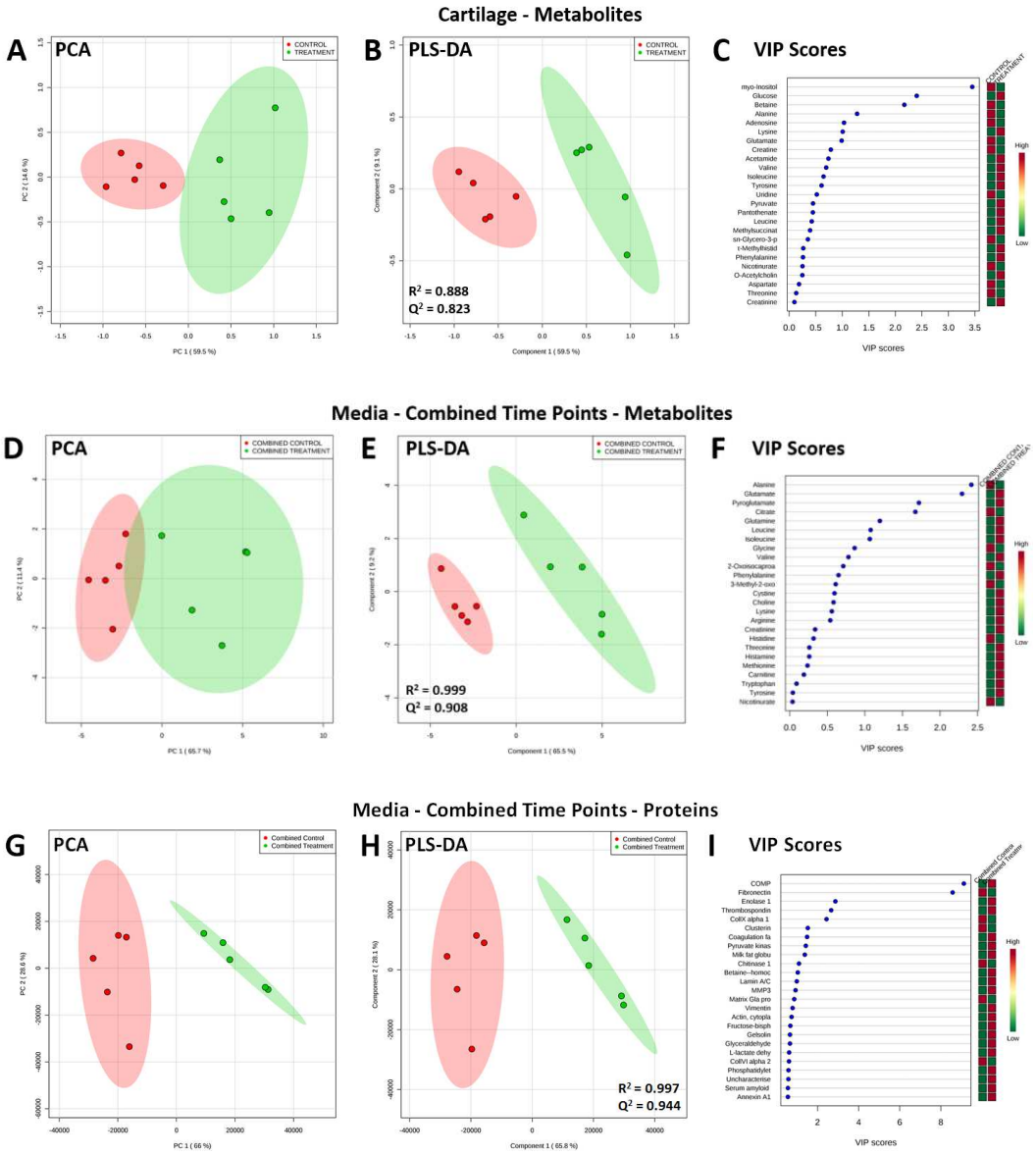

Figure 5. PCA (A, D and G), PLS-DA (B, E and H) plots and VIP scores (C, F and I) for the 25 most influential metabolites and proteins present in *ex-vivo* equine cartilage and culture media for combined time points over 8 days, comparing controls (red, n=5) to TNF-α/IL-1β treatment (green, n=5). It should be noted that 1, 5 and 4 components were used to fit PLS-DA models in B, E and H respectively.

4.4.1.3. Media - Metabolites

Phosphate salt precipitated out of solution for three samples (a 0-2 day treated sample, a control sample and a treated 3-5 time point sample) producing poor quality spectra which were therefore removed from further analyses. Isopropanol was identified within all media samples. As this was considered a likely contaminant

during cartilage culture, together with metabolites previously mentioned, isopropanol was also removed from all analyses. In total, 34 metabolites were identified within the culture media (Table 1). Time points were analysed separately with four, four and six metabolites identified as being differentially abundant between control and treatment groups for 1-2 day, 3-5 day and 6-8 day time points respectively (Figure 6). Choline levels were increased in treated samples compared to controls for all three time points whilst alanine and citrate levels decreased. At 3-5 days glutamate levels were reduced following treatment. At 6-8 days, following treatment, arginine and isoleucine levels were elevated whilst 2-oxoisocaproate and 3-methyl-2-oxovalerate levels were found to decrease. PCA of combined and separated time points identified clear separation between the metabolite profiles of control and treated media samples (Figure 5d and Figure 7a, b and c). PLS-DA of combined samples produced an excellent predictive model (R^2 = 0.999, Q^2 = 0.908) with separation driven primarily by alanine and glutamate (Figure 5e and f).

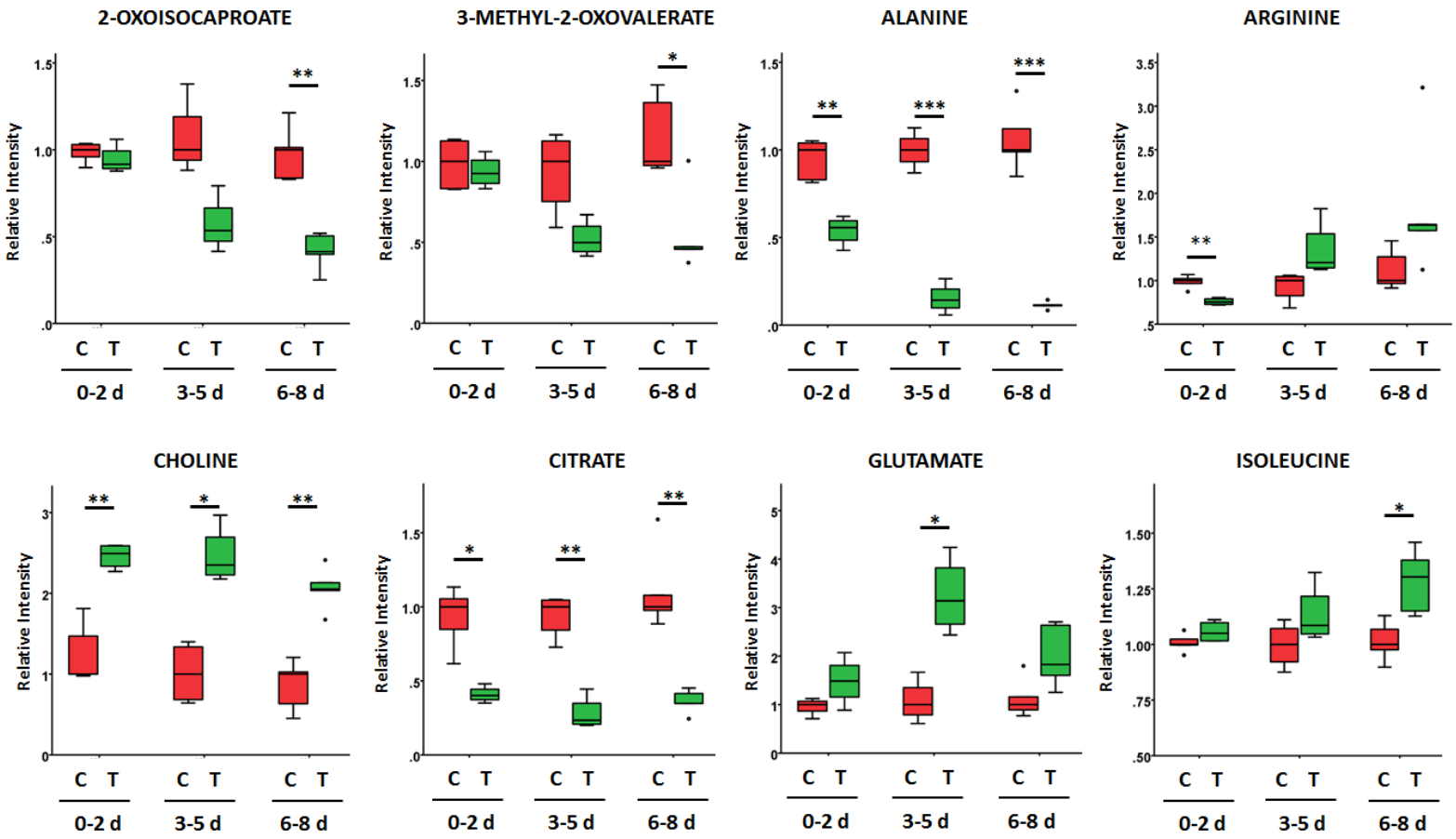

Figure 6. Boxplots of differentially abundant metabolites within the culture media following incubation of *ex-vivo* equine cartilage for control samples (C, red) and following TNF-α/IL-1β treatment (T, green), at 0-2, 3-5 and 6-8 days (d). Metabolite abundances shown as relative intensities. t-test: * = $p < 0.05$, ** = $p < 0.01$ and *** = $p < 0.001$. Control (n=5) and TNF-α/IL-1β treatment (n=5) for each separate time point.

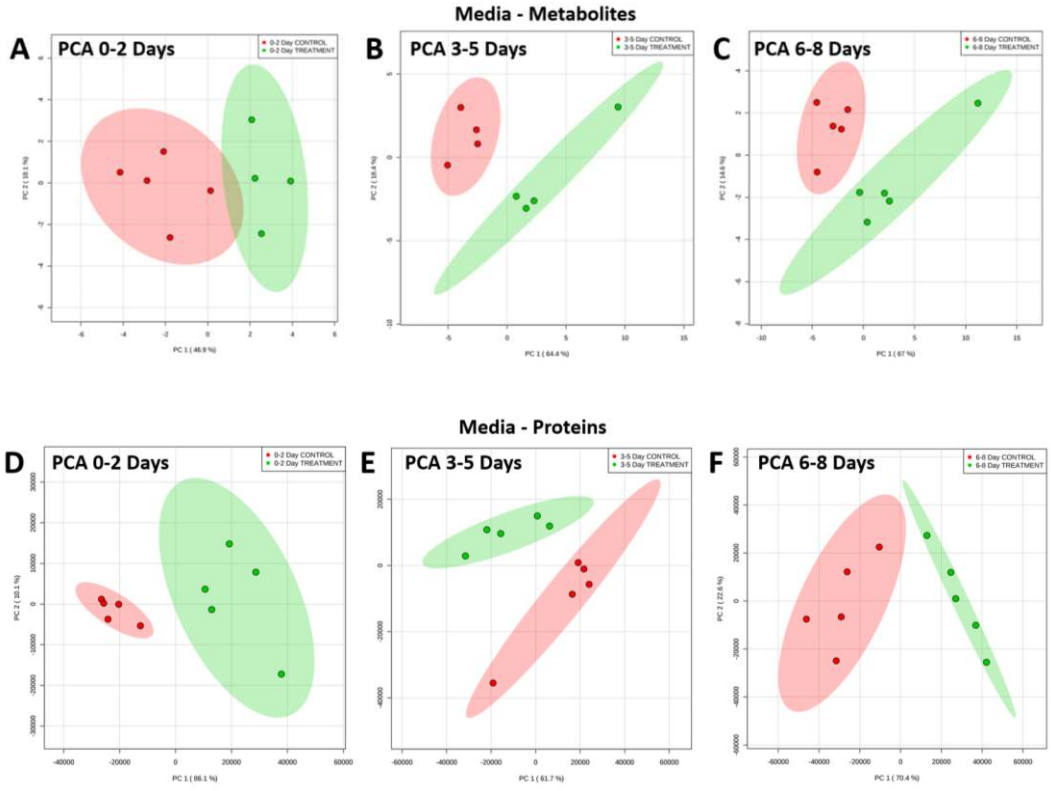

Figure 7. Principal component analysis (PCA) plots of media metabolite (A-C) and protein (D-F) profiles at 0-2, 3-5 and 6-8 days for controls (green, n=5) and TNF-α/IL-1β treatment (red, n=5) of *ex-vivo* equine cartilage.

4.4.2. LC-MS/MS Proteomics

4.4.2.1. Media - Proteomics

In total, 352 proteins were identified within analysed culture media samples with an elevated number of identified proteins within treated compared to control samples (Figure 8 and Supplementary Table 1). Of all identified proteins, 131 were identified within TNF-α/IL-1β treated media samples only. When time points were analysed separately, 154, 138 and 72 proteins were identified as being differentially abundant, with > 2 fold change, between control and treatment groups for 1-2 day, 3-5 day and 6-8 day time points respectively. Supervised PLS-DA analysis of combined protein profiles produced an excellent predictive model (R^2 = 0.997, Q^2 = 0.944) with separation primarily driven through elevated COMP and decreased fibronectin following treatment (Figure 5h and 5i). Unsupervised PCA multivariate analysis identified clear discrimination between control and treatment groups at all three time points (Figure 7). At each separated time point the top 25 VIP scoring proteins were identified (Supplementary Figure 4). Box plots in Figure 9 represent proteins which were found to be represented within the top 25 most influential proteins at all three time points (coagulation factor XIII A chain, COMP, enolase 1, Lamin A/C and MMP-3) and extracellular matrix related proteins of interest represented at 2/3 time points (collagen type VI α 2 chain, collagen type X α 1 chain, fibromodulin, fibronectin, matrix Gla protein, MMP1 and vimentin). Coagulation factor XIII A chain, enolase 1 and lamin A/C were elevated at all three time points following treatment. MMP-1 and MMP-3 levels were found to be statistically elevated at 0-2 days only. Fibromodulin and vimentin levels were increased following treatment at both 0-2 days and 3-5 day time points whilst COMP levels increased at 0-2 days and 6-8 days. Collagen type VI α 2 chain and matrix Gla protein levels decreased following treatment at 3-5 days and 6-8 days whilst collagen type X α 1 chain and fibronectin levels statistically decreased at 6-8 days alone.

Silver stain analysis of the media profiles for combined time points identified two protein bands which were decreased in abundance following TNF-α/IL-1β treatment, with molecular weights of 160-260 kDa and 260 kDa (Figure 10).

A

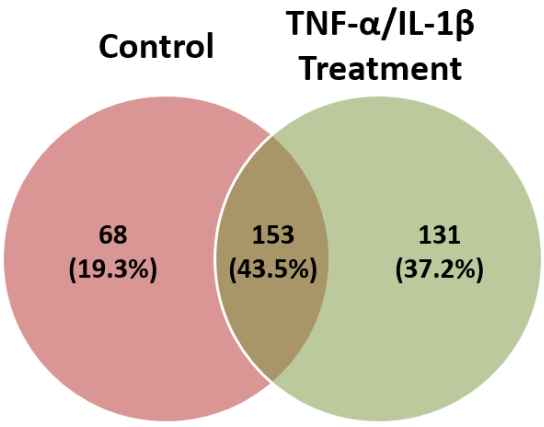

B

	No. Proteins Identified/Media Sample	
	Mean	Median
Control	124	112
TNF-α/IL-1β Treatment	189	191

Figure 8. Number of proteins identified within culture media for (A) combined and (B) individual sample time points for controls and TNF-α/IL-1β treated *ex-vivo* equine cartilage. Combined time points, n=5/group, Individual time points, n=15/group.

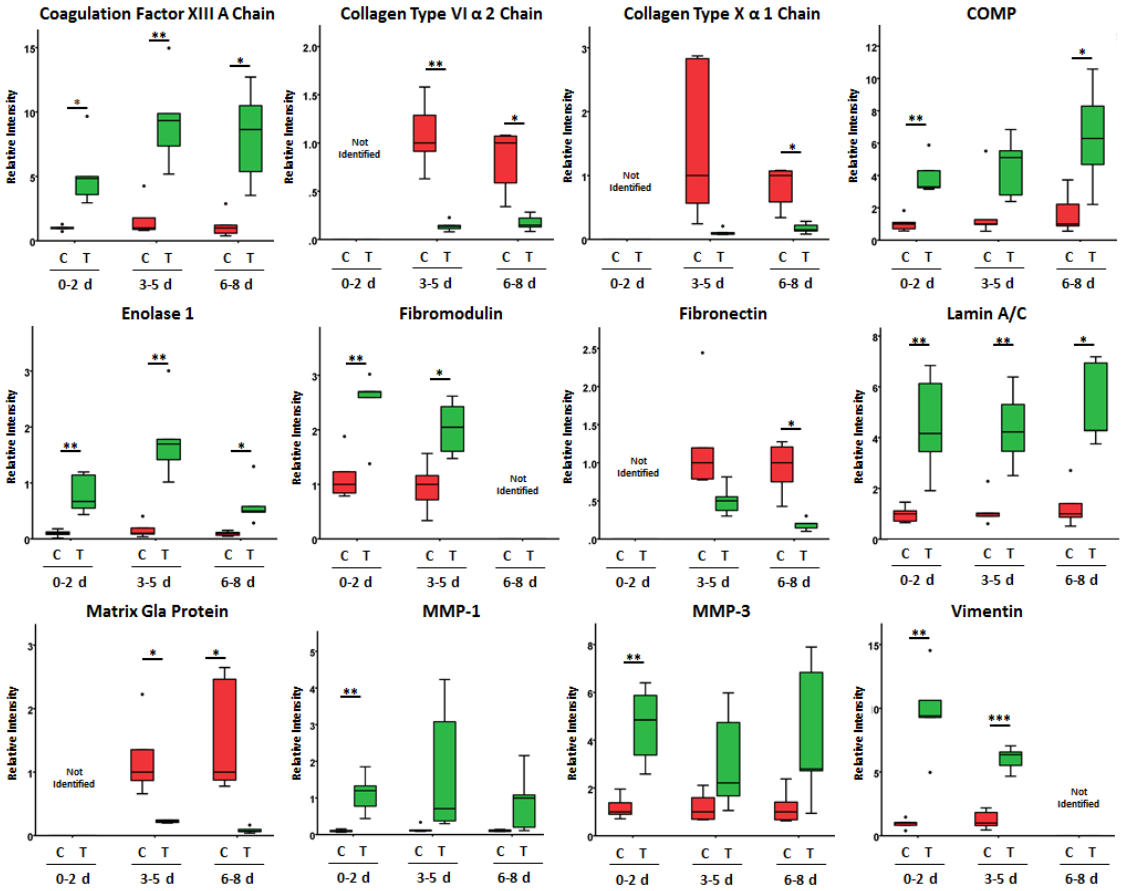

Figure 9. Boxplots of differentially abundant proteins within the culture media following incubation of *ex-vivo* equine cartilage for control samples (C, red) and following TNF-α/IL-1β treatment (T, green), at 0-2, 3-5 and 6-8 days (d). Protein abundances shown as relative intensities. t-test: * = $p < 0.05$, ** = $p < 0.01$ and *** = $p < 0.001$. Control (n=5) and TNF-α/IL-1β treatment (n=5) for each separate time point.

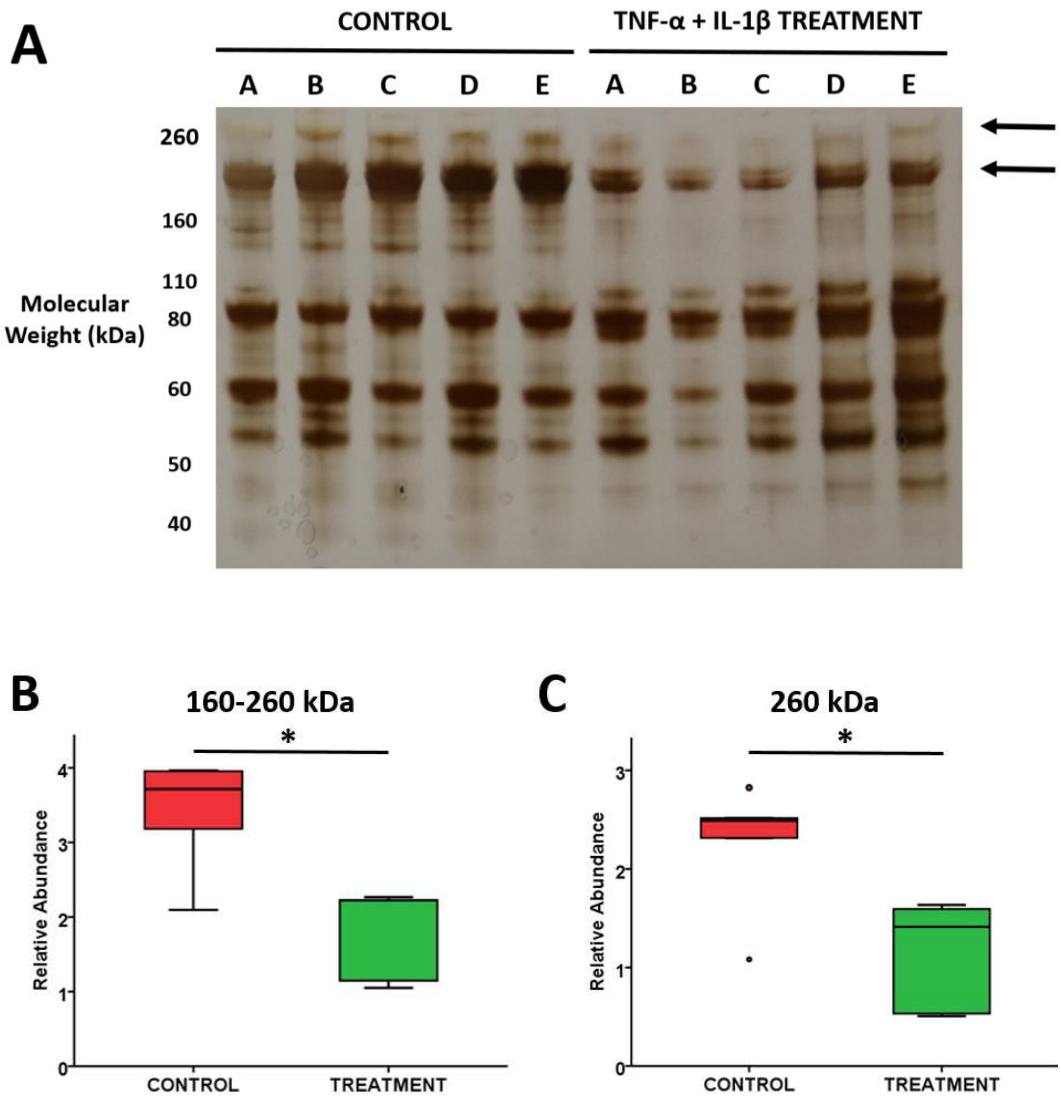

Figure 10. (A) Silver stain identifying media protein profiles (combined for all time points) following incubation of *ex-vivo* equine cartilage for control and TNF-α/IL-1β treated samples. Arrows indicate differentially secreted proteins at approximately 160-260 kDa and 260 kDa. Relative abundances of bands at (B) 160-260 kDa and (C) 260 kDa calculated using densitometry, n=5/group. t-test: * = $p < 0.05$.

4.4.2.2. Semi-Tryptic Peptides

PCA of all identified semi-tryptic peptides within combined control and combined treated samples identified far less variation within the treatment group (Figure 11). This was also identified for all time points analysed individually (Supplementary Figure 5). In total, nine potential novel OA neopeptides were identified which were

elevated in treated media samples (Table 2). These included semi-tryptic peptides of extracellular matrix proteins aggrecan, cartilage intermediate layer protein, collagen type VI α 2 chain and vimentin.

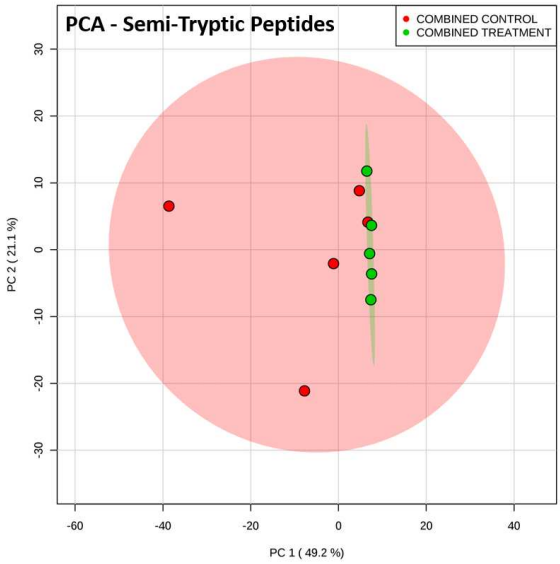

Figure 11. Principal component analysis (PCA) of semi-tryptic peptide profiles within culture media of control (red, n=5) and TNF-α/IL-1β treated (green, n=5) *ex-vivo* equine cartilage. Time points pooled for each individual donor.

Table 2. Potential Osteoarthritis Neopeptides. Semi-tryptic peptides of extracellular matrix related and unknown proteins, identified within culture media, with an increased abundance following TNF-α/IL-1β treatment of *ex-vivo* equine cartilage.

Time Point	Protein	Accession Number	Neopeptide Sequence	Previous Amino Acid	Following Amino Acid	Fold Change	p-value
0-2 Days	Aggrecan	F7C3C6	TYGVRPSSETYDVY	R	C	3.6	7.76E-05
3-5 Days	Cartilage intermediate layer protein	F7C2J3	AIGVPQPYLNK	N	L	2.2	1.83E-04
	Unknown	N/A	NGPTESTFSTSWK	C	G	5.4	2.24E-04
	Unknown	N/A	LVIIR	N	K	4.9	3.05E-04
	Vimentin	F7B5C4	RQVDQLTNDK	L	A	2.7	4.09E-04
Combined	Unknown	N/A	AFDQLR	H	N	6.4	3.05E-04
	Collagen type VI α 2 chain	F7CGV8	KQNVVPTVVAV	R	G	6.5	3.85E-04
	Unknown	N/A	DGAFLLR	E	Q	11.7	4.10E-04
	Unknown	N/A	SILGVR	M	S	5.6	4.61E-04

4.4.2.3. Pathway Analysis

In total, 36 biological pathways were identified which are potentially involved within OA pathogenesis (Table 3). The 'biosynthesis of amino acids' and 'carbon metabolism' pathways were both highly represented by metabolites and proteins across all three time points. Additionally, 'ABC Transporters', 'alanine, aspartate and glutamate metabolism' and 'aminoacyl-tRNA biosynthesis' were well represented by metabolites across all time points and 'fructose and mannose metabolism' and 'glycolysis/gluconeogenesis' by proteins across all time points.

Table 3. Pathway analysis for differentially abundant metabolites and proteins identified in cartilage and culture media following TNF-α/IL-1β treatment of *ex-vivo* equine cartilage.

		METABOLITES				PROTEINS		
Pathway ID	Pathway Description	DA Cartilage Metabolites	DA Media Metabolites			DA Media Proteins		
			(0-2 Days)	(3-5 Days)	(6-8 Days)	(0-2 Days)	(3-5 Days)	(6-8 Days)
1210	2-Oxocarboxylic acid metabolism			2	3			
2010	ABC Transporters	5	3	3	3			
250	Alanine, aspartate and glutamate metabolism		2	3	2	4		
520	Amino sugar and nucleotide sugar metabolism					6		
970	Aminoacyl-tRNA biosynthesis	2	2	2	2			
4612	Antigen processing and presentation					5		
330	Arginine and proline metabolism					4		
1230	Biosynthesis of amino acids	2	3	3	4	13	13	9
1200	Carbon metabolism		2	3	2	13	12	7
4610	Complement and coagulation cascades						6	6
270	Cysteine and methionine metabolism					4	4	
4512	ECM-receptor interaction						7	
4510	Focal adhesion					7	9	
51	Fructose and mannose metabolism					5	4	3
52	Galactose metabolism	2				3		
480	Glutathione metabolism					5	4	
260	Glycine, serine and threonine metabolism	2				4	4	
10	Glycolysis / Gluconeogenesis					12	11	8
630	Glyoxylate and dicarboxylate metabolism			2				
4978	Mineral absorption	2			2			
670	One carbon pool by folate					4		
40	Pentose and glucuronate interconversions					5		
30	Pentose phosphate pathway					7	7	3
4151	PI3K-Akt signaling pathway						9	
640	Propanoate metabolism					3	3	
4974	Protein digestion and absorption	2	2	2	2		5	5
4141	Protein processing in endoplasmic reticulum					8		
5205	Proteoglycans in cancer					7		
230	Purine metabolism					12	7	
620	Pyruvate metabolism					5	5	
4810	Regulation of actin cytoskeleton					9	7	
5150	Staphylococcus aureus infection						4	4
500	Starch and sucrose metabolism					5		
430	Taurine and hypotaurine metabolism			2				
290	Valine, leucine and isoleucine biosynthesis				2			
280	Valine, leucine and isoleucine degradation				2			

DA = differentially abundant

4.5. Discussion

In this study TNF-α/IL-1β treatment of *ex-vivo* equine cartilage explants was used to model OA to gain a greater understanding of OA pathogenesis and identify potential OA markers. ^{1}H NMR metabolomic analysis of extracted cartilage metabolites (following 8 days incubation) was undertaken in addition to ^{1}H NMR metabolomic and LC-MS/MS proteomic analysis of culture media at 0-2, 3-5 and 6-8 days.

4.5.1. MMPs, COMP and Fibronectin

Within culture media, following TNF-α/IL-1β treatment, elevations in endopeptidases MMP-1 and MMP-3 at 0-2 days, with a similar trend at both other time points, were identified as expected (Mackay *et al.*, 1992). Elevated MMP-1 activity has previously been identified within equine OA SF with general MMP activity also found to be correlated to severity of cartilage damage (van den Boom *et al.*, 2005; Brama *et al.*, 2004). Also, as previously reported, elevations in the non-collagenous ECM protein COMP were also identified within the TNF-α/IL-1β equine OA model, with COMP considered a marker of cartilage breakdown (Svala *et al.*, 2015; Tseng *et al.*, 2009). Clinically, elevated COMP levels have been identified within human OA SF, although within equine OA, one study identified reduced levels with COMP unable to stage the disease (Balakrishnan *et al.*, 2014; Taylor *et al.*, 2006). Fibronectin was identified as a key discriminator between control and treatment groups with reduced secreted fibronectin identified within the media following TNF-α/IL-1β treatment. Additionally, a protein band of molecular weight 160-260 kDa was identified as reduced in treated media compared to control samples via 1D SDS PAGE which may be representing fibronectin (250 kDa), although further techniques, i.e. Western blotting or MS/MS analysis of an in-gel tryptic digest, are required to confirm this (Peffers, 2013; Stashak and Theoret, 2011). However, elevated levels of fibronectin have previously been identified within OA SF with fibronectin found to localise at sites of cartilage degeneration and subsequently secreted into the ECM by equine chondrocytes (Lust *et al.*, 1987; Murray *et al.*, 2000). The reasons for this possible discrepancy in results between this study and previous studies is currently not known and requires further

investigation. It may be that within this study fibronectin has undergone post translational modifications following treatment which may not have been identified via the PEAKS® identification algorithm or resulted in peptides which subsequently did not 'fly' well during MS analysis and thus were subsequently not identified.

4.5.2. Glucose

Following TNF-α/IL-1β treatment, elevations of glucose within the cartilage were identified. This is supported by a previous study which demonstrated that TNF-α and IL-1β upregulate glucose transport in chondrocytes through upregulation of glucose transporter (GLUT)1 and GLUT9 mRNA synthesis with increased levels of glycosylated GLUT1 incorporated into the plasma membrane (Shikhman *et al.*, 2001). This influx in glucose is likely, at least in part, to be due to the increased energy requirement following cytokine stimulation in the production of MMPs and secretion of Il-6, Il-8, hematopoietic colony-stimulating factor and prostaglandin E_2 (Hernvann *et al.*, 1996).

4.5.3. Alanine, Arginine, Choline and Citrate

Alanine, arginine, choline and citrate were all identified to be differentially abundant within culture media following TNF-α/IL-1β treatment at the earliest time point, 0-2 days.

Within this study, arginine levels were initially identified as being decreased following treatment at the earliest time point. A recent study of human plasma also identified arginine to be depleted in knee OA (Zhang *et al.*, 2016). The authors proposed this is due to an increased activity of the conversion of arginine to ornithine resulting in an imbalance between cartilage repair and degradation. This is supported by a recent learning and network approach of OA associated metabolites in which arginine and ornithine appeared in about 30% and 25% of the generated models studied (Hu *et al.*, 2018). In addition to this, a reduction in arginine may be reflective of an increased production of nitric oxide (L-arginine being converted to NOH-arginine and subsequently L-citrulline and nitric oxide) as identified in human OA cartilage (Abramson, 2008; Loeser *et al.*, 2002).

A ^{1}H NMR metabolomics study of equine SF also identified elevated levels of choline in OA (Lacitignola *et al.*, 2008). However, elevated levels of alanine and citrate were also identified whilst these were found to be decreased within our study.

Across the whole study, alanine was found to be a central component in discriminating control and treatment groups. Alanine levels were depleted in treated cartilage extracts compared to controls, with PLS-DA identifying alanine as the fourth most important component in discriminating control and treated cartilage samples. Reduced alanine levels were also identified in human OA cartilage using HRMAS NMR spectroscopy (Shet *et al.*, 2012). Within culture media, at all three time points alanine was depleted in treated samples and KEGG pathway analysis revealed the 'alanine, aspartate and glutamate metabolism' pathway to be well represented by both metabolites and proteins. Alanine has previously been identified as a key component of the metabolic urinary OA profile of guinea pigs (Lamers *et al.*, 2003).

4.5.4. Collagen Degradation

Isoleucine was elevated within media during the latter stages of the model (6-8 days). Elevated isoleucine levels have previously been reported within SF of a canine OA model and human OA serum (Damyanovich *et al.*, 1999; Zhai *et al.*, 2010). Borel *et al.* previously identified elevations of peaks within ^{1}H HRMAS NMR spectra of OA cartilage which could be attributed to isoleucine (Borel *et al.*, 2009). Thus the elevations seen in isoleucine may be reflective of cartilage collagen breakdown (Zhai *et al.*, 2010). However, within this study, although a higher abundance was recorded for isoleucine in treated compared to control cartilage, this did not reach statistical significance. However, elevations in glutamate were identified within culture media at 3-5 days, which may be resultant of the catabolism of collagenous proline through proline oxidase (Phang *et al.*, 2015). Reduced levels of collagen type VI α 2 chain and collagen type X α 1 chain were identified at 3-5 and 6-8 days following cytokine treatment. This may reflect a reduction in collagen synthesis which has previously been identified within other collagen types following TNF-α/IL-1β stimulation (Stevens *et al.*, 2009). Therefore these results provide evidence of a

disruption in collagen homeostasis and suggest that collagens are being degraded within the model sooner than the 14-28 days previously reported within other *ex-vivo* cartilage OA models (Milner *et al.*, 2001, 2006).

4.5.5. Coagulation Factor XIII A Chain, Enolase 1, Fibromodulin, Lamin A/C and Vimentin

Coagulation factor XIII A chain, enolase 1, fibromodulin, lamin A/C and vimentin were all identified as being differentially abundant within the culture media at the earliest time point; 0-2 days.

Coagulation factor XIII is a heterotetrameric protein complex which crosslinks fibrin polymers through covalent bonds (Gupta *et al.*, 2016). Coagulation factor XIII A chain immunostaining was previously found to be elevated within human articular knee cartilage following IL-1β stimulation (Johnson *et al.*, 2001). Sanchez *et al.* identified increased expression of coagulation factor XIII A chain in osteoblasts within the sclerotic zone of OA subchondral bone (Sanchez *et al.*, 2008). Clinically, remodelling of the subchondral bone is likely to be closely related to cartilage degradation (Day *et al.*, 2004). Within hypertrophic chondrocytes, Nurminkaya *et al.* concluded that cell death and lysis were responsible for the externalisation of the protein (Nurminkaya *et al.*, 1998). However, coagulation factor XIII A chain has also been identified within articular cartilage vesicles, although the underlying externalisation mechanism remains unknown (Rosenthal *et al.*, 2001).

Enolase 1 is a multifunctional glycolytic enzyme which has previously been shown to have increased abundance within an equine articular cartilage model stimulated with IL-1β, as well as increased expression on the cell surface of immune cells during rheumatoid arthritis (RA) (Lee *et al.*, 2018; Peffers, 2013). Lee *et al.* identified apolipoprotein B within RA SF to be a specific ligand to enolase 1, provoking an inflammatory response. Elevated levels of apolipoprotein B have also been associated with human knee OA (Sánchez-Enríquez *et al.*, 2008). Thus lipid metabolism may operate through this mechanism to regulate chronic inflammation in OA as well as RA (Lee *et al.*, 2018).

Fibromodulin is a small leucine-rich repeat proteoglycan which interacts with collagen fibrils and influences fibrillogenesis rate and fibril structure (Roughley *et al.*, 1996). Experimental mice which lack biglycan and fibromodulin have been shown to develop OA in multiple joints (Ameye *et al.*, 2002; Wadhwa *et al.*, 2005). Neopeptides generated from fibromodulin degradation have also been identified as potential markers of equine articular cartilage degradation (Peffers *et al.*, 2016).

Within our study, higher levels of Lamin A/C (intermediate filament protein) were identified within treated media samples (Swift and Discher, 2014). Lamin A/C has also been identified as being upregulated in human OA cartilage and elevated levels have been implicated in dysregulation of chondrocyte autophagy in ageing and OA (Attur *et al.*, 2012; de Figueroa *et al.*, 2017). Thus our results support these studies, with chondrocyte autophagy targeting a potential novel therapeutic route.

Vimentin is a multifunctional intermediate filament protein (Ivaska *et al.*, 2007). Within chondrocytes it has been shown that vimentin is likely to be involved in mechanotransduction (Langelier *et al.*, 2000). Our results are supported by a previous study which identified elevated levels of cleaved vimentin within human OA cartilage with distortion of the vimentin network evident (Lambrecht *et al.*, 2008).

4.5.6. Semi-Tryptic Peptides and Neopeptides

Due to an elevation in enzymatic activity and breakdown of cartilage during OA, potential biomarkers include ECM degradation fragments (Lotz *et al.*, 2013). PCA identified that the semi-tryptic peptide profiles generated from treated equine cartilage was less variable than that of the controls, demonstrating the TNF-α/IL-1β treatment is driving the semi-tryptic peptide profile within the model. Within this study we have identified several semi-tryptic peptides (potential neopeptides) which were identified as being elevated following treatment compared to controls, including degradation products from ECM proteins aggrecan, cartilage intermediate layer protein, vimentin and collagen type VI. None of these potential neopeptides have previously been identified within the literature (Peffers, 2013; Peffers *et al.*, 2014; Peffers, McDermott, *et al.*, 2015; Peffers *et al.*, 2016).

4.5.7. Further Work

Additional MS based metabolomics analysis of the culture media within this study may be beneficial as NMR and MS are complementary techniques and would therefore expand the number of identified/quantified metabolites, additionally identifying potential lipid and carbohydrate profiles of interest (Anderson, Phelan, *et al.*, 2018; Beltran *et al.*, 2012; Marshall and Powers, 2017; Mickiewicz, Kelly, *et al.*, 2015). In order to confirm the differentially abundant proteins within this study, validation using an orthologous technique e.g. western blotting or enzyme-linked immunosorbent assays is required. Further validation of potential neopeptides could also be carried out through multiple reaction monitoring using a triple-quadrupole mass spectrometer (Parker and Borchers, 2014). Following this, development of monoclonal antibodies specific to neopeptides of interest would enable simpler monitoring of neopeptide abundance in *in vitro*, *ex-vivo* and clinical environments (Caterson *et al.*, 1985). Following validations, monitoring the differentially abundant metabolites, proteins and neopeptides within this study within longitudinal SF samples from OA horses would identify translation of these findings to a clinical setting and the eventual generation of 'bedside' tests.

4.5.8. Conclusion

In conclusion, this is the first study to use a multi 'omics' approach to simultaneously investigate the metabolomic profile of *ex-vivo* cartilage and metabolomic/proteomic profiles of culture media using the TNF-α/IL-1β *ex-vivo* OA cartilage model. We have identified a panel of metabolites and proteins which are differentially abundant within an early phase of the OA model, 0-2 days, which may provide further information on the underlying disease pathogenesis and well as potential to translate to clinical markers. This study has also identified a panel of potential, ECM derived, neopeptides which have potential to help enable OA stratification as well as provide potential novel therapeutic targets.

4.6. Ethics

Cartilage samples were collected as a by-product of the agricultural industry. The Animals (Scientific Procedures) Act 1986, Schedule 2, does not define collection

from these sources as scientific procedures and ethical approval was therefore not required.

4.7. Funding

Mr James Anderson is funded through a Horse Trust PhD studentship (G1015) and Professor Mandy Peffers funded through a Wellcome Trust Intermediate Clinical Fellowship (107471/Z/15/Z). Software licenses for data analysis used in the Shared Research Facility for NMR metabolomics were funded by the MRC Clinical Research Capabilities and Technologies Initiative (MR/M009114/1).

4.8. Acknowledgements

The authors would like to thank staff at F Drury and Sons abattoir, Swindon for their assistance in sample collection and members of the Centre for Protein Research, University of Liverpool including Professor Rob Beynon and Dr Philip Brownridge.

4.9. Supplementary Information

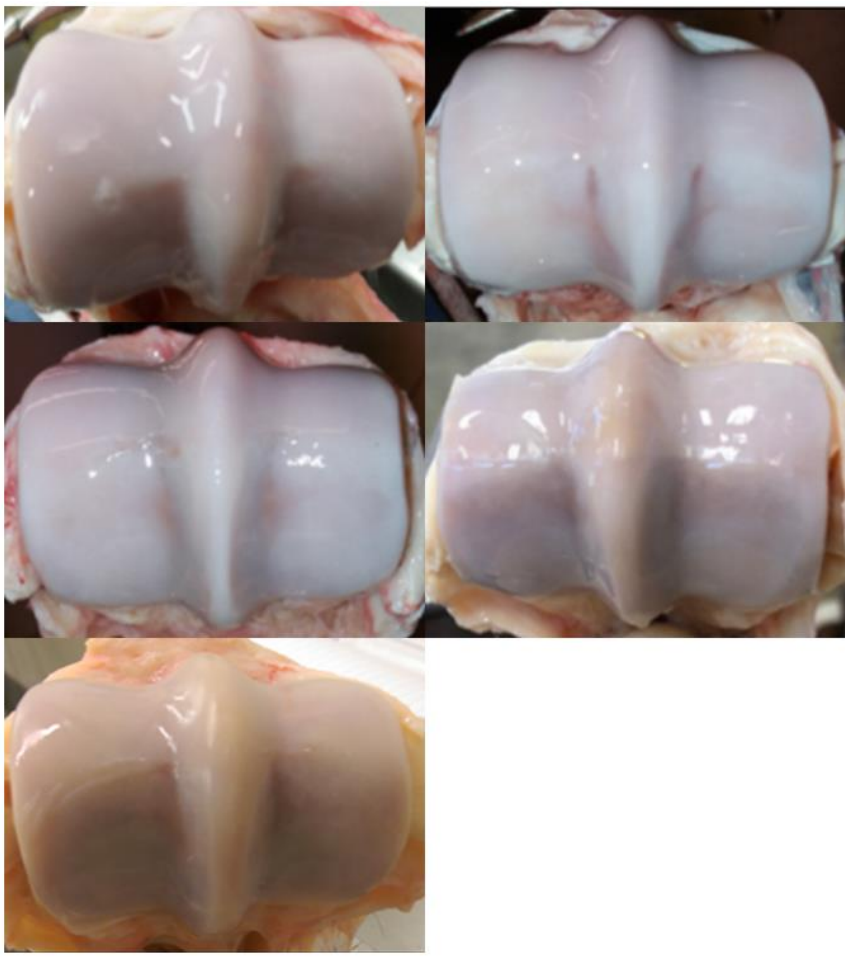

Supplementary Figure 1. Five post mortem equine metacarpophalangeal joints used for *ex-vivo* cartilage culture. Cartilage collected from all joints was considered macroscopically normal with a score of 0 according to the OARSI histopathology initiative scoring system for horses.

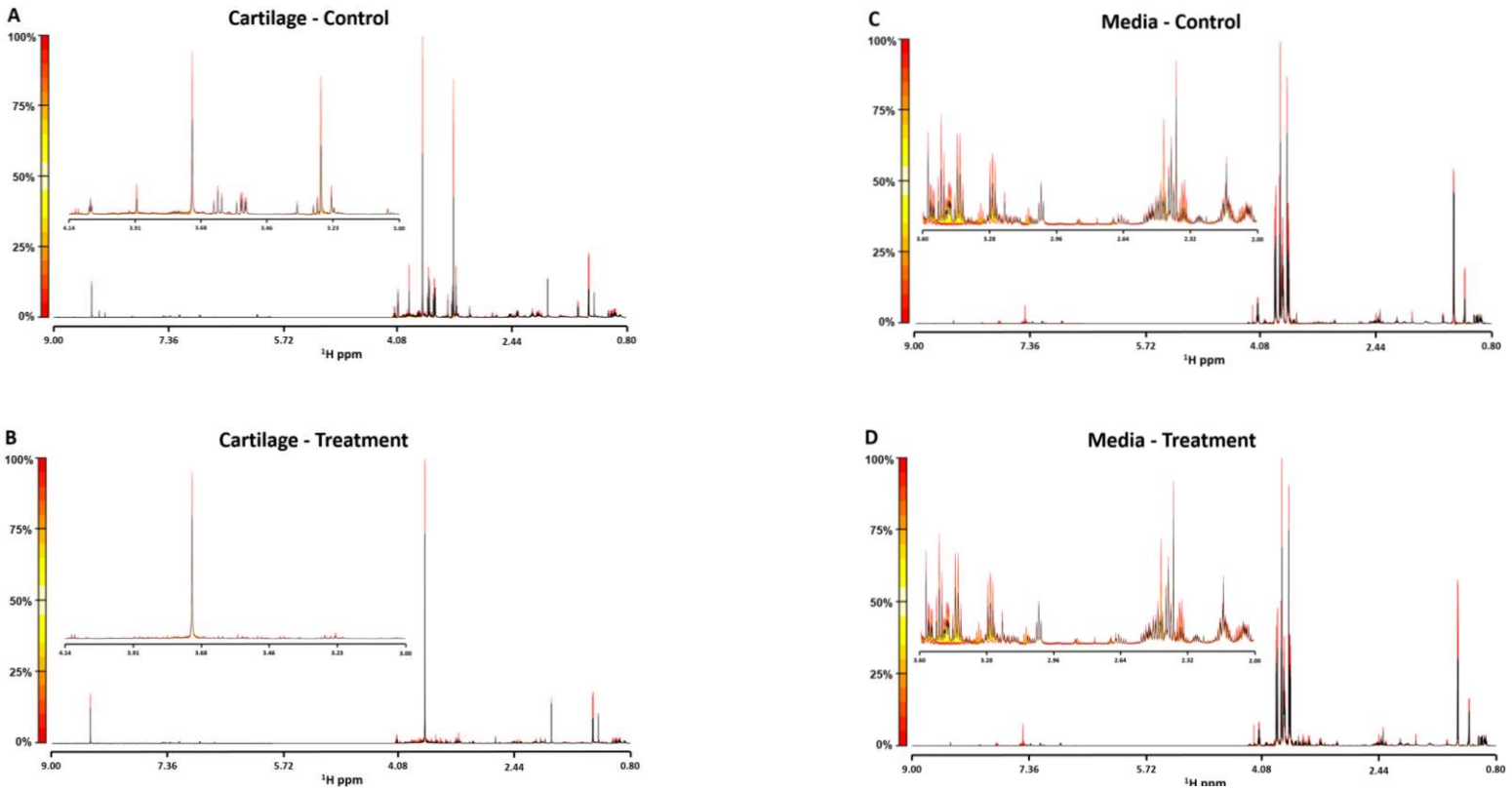

Supplementary Figure 2. 1D ^{1}H nuclear magnetic resonance spectral quantile plots of (A) cartilage, 8 days in control media (B) cartilage, 8 days in TNF-α/IL-1β treated media (C) control media (all time points combined) and (D) TNF-α/IL-1β treated media (all time points combined). The median spectral plot is depicted by a black line and variation from the median shown as a yellow to red scale for both the full spectral range (9.00-0.80 ppm) and more detailed regions (4.14-3.00 ppm for cartilage and 3.60-2.00 ppm for media). Control (n=5) and TNF-α/IL-1β treatment (n=5).

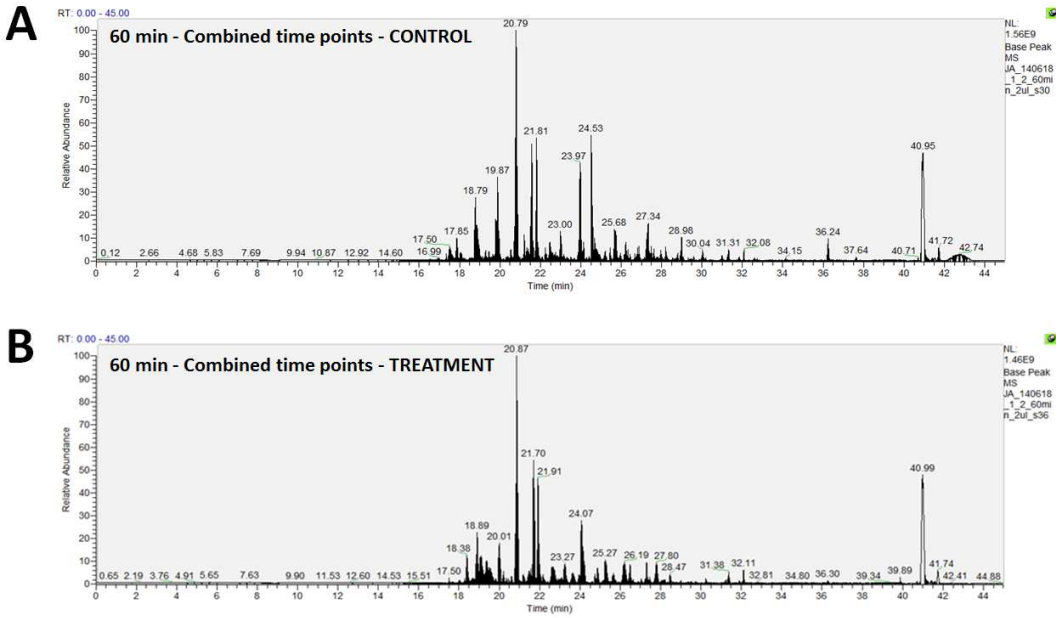

Supplementary Figure 3. Representative culture media ion chromatograms of combined time points for (A) control and (B) TNF-α/IL-1β treated equine *ex-vivo* cartilage explants using a 60 min liquid chromatography gradient.

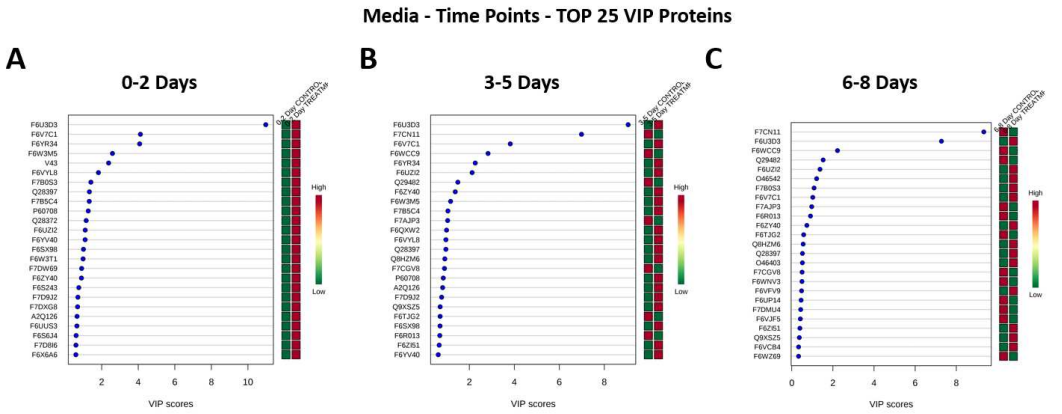

Supplementary Figure 4. Top 25 most influential differentially abundant proteins present within culture media at (A) 0-2 days, (B) 3-5 days and (C) 6-8 days following TNF-α/IL-1β treatment of *ex-vivo* equine cartilage. n=5 for each time point.

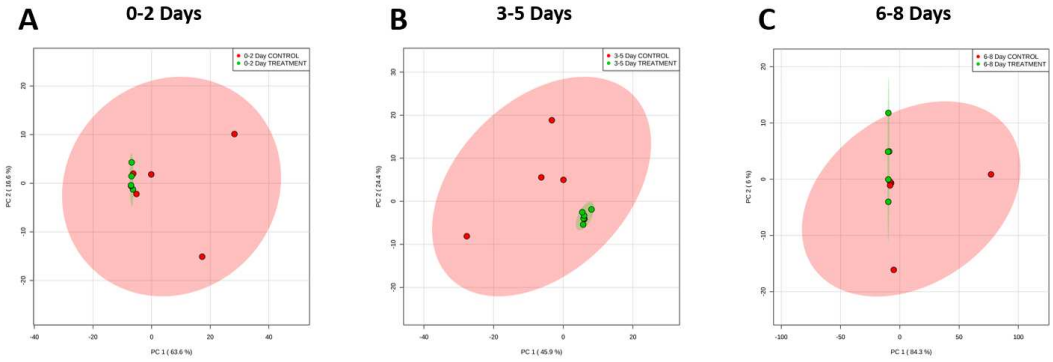

Supplementary Figure 5. Principal component analyses of semi-tryptic peptide profiles within culture media of control (red, n=5) and TNF-α/IL-1β treated (green, n=5) *ex-vivo* equine cartilage at (A) 0-2 days, (B) 3-5 days and (C) 6-8 days.

Supplementary Table 1. Proteins identified within culture media of control and TNF-α/IL-1β treated *ex-vivo* equine cartilage.

Media Samples Identified In	Accession Number	Family/Subfamily
Control Only	F6PLF6	2-Phosphoxylose Phosphatase 1
Control Only	F6R1X9	Actin, Alpha Cardiac Muscle 1
Control Only	F7CZ92	Actin, Alpha Skeletal Muscle
Control Only	F7CW82	Actin, Aortic Smooth Muscle
Control Only	F6Z8K0	Actin, Gamma-Enteric Smooth Muscle
Control Only	F7C2Y5	Adipocyte Enhancer-Binding Protein 1
Control Only	F6YRA8	ATP-Dependent rna Helicase Ddx60-Related
Control Only	F7CPZ3	Calsyntenin 1
Control Only	F6YQD9	Carboxypeptidase E
Control Only	F7CCP9	Cartilage Intermediate Layer Protein 2
Control Only	F6VF11	Chordin-Like Protein 2
Control Only	F6VP03	Collagen Type IX Alpha 3 Chain
Control Only	F6VBF7	Collagen Type XI Alpha 1 Chain
Control Only	F6U661	Collagen Type XI Alpha 1 Chain
Control Only	F6VAW6	Collagen Type XI Alpha 1 Chain
Control Only	F7BQD6	Complement C1S Subcomponent
Control Only	F6ZR63	Complement Factor H
Control Only	F7AU56	Complement Factor I

Control Only	F6Z7T9	Ectonucleotide Pyrophosphatase/Phosphodiesterase 2
Control Only	F6Z7X8	Ectonucleotide Pyrophosphatase/Phosphodiesterase Family Member 2
Control Only	F6Q4R1	Elongation Factor 1-Alpha 2
Control Only	F6WD07	Fibulin 7
Control Only	F7DHZ1	Gelsolin
Control Only	F7E2D1	Gelsolin
Control Only	F7D7T6	Heat Shock 70 KDa Protein 1-Like
Control Only	F6TWM4	Histone H2B
Control Only	F6WFI8	Histone H2B Type 1-A
Control Only	F7ASE9	Histone H2B Type 1-C/E/F/G/I
Control Only	F6VUX0	Histone H2B Type 1-D
Control Only	F7CJ51	Histone H2B Type 1-D
Control Only	F7E1X9	Histone H2B Type 1-H
Control Only	F6VYH8	Histone H2B Type 1-M
Control Only	F7DLL0	Histone H2B Type 1-N
Control Only	F6PWV1	Histone H2B Type 2-F
Control Only	Q95LJ1	Insulin-Like Growth Factor-Binding Protein 7
Control Only	F6SSR0	Integrin Beta-Like Protein 1
Control Only	F6QBB1	Inter-Alpha-Trypsin Inhibitor Heavy Chain H5
Control Only	F6ZEQ3	Keratin, Type I Cytoskeletal 16
Control Only	F7AGY4	Keratin, Type Ii Cytoskeletal 6B-Related
Control Only	F6ST15	Keratin-87 Protein-Related
Control Only	F6WZ08	Laminin Subunit Gamma-2
Control Only	Q8HZI9	Laminin Subunit Gamma-2
Control Only	F6W6E8	Latent Transforming Growth Factor Beta Binding Protein 1
Control Only	F6W6Y4	Latent-Transforming Growth Factor Beta-Binding Protein 1
Control Only	F6Z0F8	Latent-Transforming Growth Factor Beta-Binding Protein 3
Control Only	F6UXM7	Lysyl Oxidase Homolog 3
Control Only	O02722	Metalloproteinase Inhibitor 1
Control Only	F7BEE7	Metalloproteinase Inhibitor 2
Control Only	F7AEL9	Neuron Derived Neurotrophic Factor
Control Only	F7BQX4	Peptidylglycine Alpha-Amidating Monooxygenase
Control Only	F7BR00	Peptidylglycine Alpha-Amidating Monooxygenase
Control Only	F6ZCC8	Peptidyl-Glycine Alpha-Amidating Monooxygenase
Control Only	F7D1R1	Phosphoglycerate Kinase 1
Control Only	F6VTS1	Phospholipase A1 Member A
Control Only	F7CR03	Phospholipid Transfer Protein

Control Only	F7BKE1	Pigment Epithelium-Derived Factor
Control Only	F6R5Y2	Plasma Serine Protease Inhibitor
Control Only	F6V2X7	Procollagen-Lysine,2-Oxoglutarate 5-Dioxygenase 1
Control Only	F6VTD3	Proteoglycan 4
Control Only	F6XL03	Scrapie-Responsive Protein 1
Control Only	F6XVP2	Sparc-Related Modular Calcium-Binding Protein 1
Control Only	F6WQ44	Sulfhydryl Oxidase
Control Only	F6WR95	Sulfhydryl Oxidase 1
Control Only	O19011	Transforming Growth Factor Beta-1
Control Only	F7APU2	Uncharacterized Protein
Control Only	F6XLT6	Vascular Endothelial Growth Factor A
Control Only	Q9GKR0	Vascular Endothelial Growth Factor A
Control Only	F7AZP8	Xylosyltransferase 1
Treatment Only	F6T0A6	10 KDa Heat Shock Protein, Mitochondrial
Treatment Only	F6SP02	14-3-3 Protein Theta
Treatment Only	F7BFM4	60S Ribosomal Protein L10A
Treatment Only	F6T1A4	60S Ribosomal Protein L12
Treatment Only	F6Z421	60S Ribosomal Protein L12
Treatment Only	F7D917	6-Phosphogluconate Dehydrogenase, Decarboxylating
Treatment Only	F6YG82	78 KDa Glucose-Regulated Protein
Treatment Only	F6PH57	Actin-Related Protein 2/3 Complex Subunit 4
Treatment Only	F6W354	Actin-Related Protein 3
Treatment Only	F6UFV3	Adenosine Kinase
Treatment Only	F6TL52	Adenylate Kinase Isoenzyme 1
Treatment Only	F6SRP7	Adenylyl Cyclase-Associated Protein 1
Treatment Only	F7AJD4	AHNAK Nucleoprotein
Treatment Only	F7CBN0	Alcohol Dehydrogenase (NADP+)-Like Protein
Treatment Only	P19854	Alcohol Dehydrogenase Class-3
Treatment Only	F7DMQ3	Aldose Reductase
Treatment Only	F7E419	Annexin A8
Treatment Only	F6ZB53	Apurinic Or Apyrimidinic Site) Lyase;Apex1;Ortholog
Treatment Only	F6ZXT0	Atpase Inhibitor, Mitochondrial
Treatment Only	F7C555	Bifunctional Purine Biosynthesis Protein Purh
Treatment Only	F6YIU8	C-1-Tetrahydrofolate Synthase, Cytoplasmic
Treatment Only	F7D854	Catalase
Treatment Only	F6YF95	Cellular Nucleic Acid-Binding Protein
Treatment Only	F7CR22	Coatomer Subunit Delta
Treatment Only	F7DXG8	Cofilin-1
Treatment Only	F6ZNX3	Collagen Alpha-1
Treatment Only	F7DEW5	Coronin-1C

Treatment Only	F6S9Z1	C-X-C Motif Chemokine 5
Treatment Only	Q8MIN2	C-X-C Motif Chemokine 5
Treatment Only	F6XJR7	Cysteine And Glycine-Rich Protein 1
Treatment Only	F7B5P1	Cytosolic Non-Specific Dipeptidase
Treatment Only	F7B320	Dihydropyrimidinase-Related Protein 2
Treatment Only	A2Q127	Elongation Factor 1-Gamma
Treatment Only	F6XTN1	Eukaryotic Initiation Factor 4A-I
Treatment Only	F6YYS2	Eukaryotic Initiation Factor 4A-Ii
Treatment Only	F7BPT4	Ezrin
Treatment Only	F6ZYU6	Far Upstream Element-Binding Protein 1
Treatment Only	F7A984	Far Upstream Element-Binding Protein 2
Treatment Only	F7CS60	Fibronectin
Treatment Only	F7D2D9	Flavin Reductase
Treatment Only	F6RKC6	Four and A Half Lim Domains Protein 1
Treatment Only	F7CL92	Glutamine--Fructose-6-Phosphate Aminotransferase [Isomerizing] 1
Treatment Only	F6VSN2	Glutathione S-Transferase P
Treatment Only	F7BU09	Glutathione S-Transferase Pi 3
Treatment Only	F7DZD2	Glutathione S-Transferase Theta-1
Treatment Only	F6RV94	Glycogen Phosphorylase, Liver Form
Treatment Only	B7UBT6	Growth-Regulated Alpha Protein
Treatment Only	F6R8V8	Growth-Regulated Alpha Protein
Treatment Only	A2Q0Z1	Heat Shock Cognate 71 Kda Protein
Treatment Only	F7AUW2	Heat Shock Cognate 71 Kda Protein
Treatment Only	F7E3Y7	Heat Shock Protein Beta-1
Treatment Only	F6TF34	Heme Oxygenase 1
Treatment Only	F7A868	Heterogeneous Nuclear Ribonucleoprotein A1
Treatment Only	F6YZ44	Heterogeneous Nuclear Ribonucleoprotein A1-Related
Treatment Only	F6Z0C6	Heterogeneous Nuclear Ribonucleoprotein D
Treatment Only	F6WHS3	Heterogeneous Nuclear Ribonucleoprotein D0
Treatment Only	F6UQU2	Heterogeneous Nuclear Ribonucleoprotein D-Like
Treatment Only	F6Q4Q1	Heterogeneous Nuclear Ribonucleoprotein K
Treatment Only	F6RTD6	Heterogeneous Nuclear Ribonucleoprotein L
Treatment Only	F7BA08	Heterogeneous Nuclear Ribonucleoprotein R
Treatment Only	F6VYB1	Heterogeneous Nuclear Ribonucleoproteins A2/B1
Treatment Only	F6S2F8	Histone H1.2
Treatment Only	F7BCH1	Inhibin Beta A Chain
Treatment Only	P55102	Inhibin Beta A Chain
Treatment Only	F6QJ27	Isochorismatase Domain-Containing Protein 1
Treatment Only	F6R7J2	Isocitrate Dehydrogenase [Nadp] Cytoplasmic
Treatment Only	F6ZTT5	Keratin 33B

Treatment Only	F6PJX6	Keratin, Type I Cytoskeletal 13
Treatment Only	F6VNP6	Keratin, Type II Cuticular Hb5
Treatment Only	F6SHJ8	Keratin, Type II Cytoskeletal 2 Epidermal
Treatment Only	F7C7Y1	Keratin, Type II Cytoskeletal 73
Treatment Only	F7B232	Lambda-Crystallin Homolog
Treatment Only	F7DQB9	Lim and Cysteine-Rich Domains Protein 1
Treatment Only	F6PSB8	Lim and Sh3 Domain Protein 1
Treatment Only	C6L1J5	L-Lactate Dehydrogenase B Chain
Treatment Only	F7D144	Macrophage-Capping Protein
Treatment Only	F6SAI2	Matrilin-4
Treatment Only	F6WTM6	Matrix Metalloproteinase 1
Treatment Only	Q9XSZ5	Matrix Metalloproteinase 1
Treatment Only	F6U999	Mesencephalic Astrocyte-Derived Neurotrophic Factor
Treatment Only	Q9TUL9	Metalloproteinase Inhibitor 3
Treatment Only	F7DM22	Metallothionein
Treatment Only	P02801	Metallothionein-1B
Treatment Only	F6VKN2	Metallothionein-2
Treatment Only	F6PVJ6	Mimecan
Treatment Only	F7D7Z9	Multifunctional Protein Ade2
Treatment Only	F6X3K0	Nucleolin
Treatment Only	F6X6A6	Peptidyl-Prolyl Cis-Trans Isomerase-Related
Treatment Only	F7AXI9	Peroxiredoxin-6
Treatment Only	F7DQS6	Phosphoglycerate Mutase 1
Treatment Only	F7AGA5	Plastin-3
Treatment Only	F6WPZ3	Plectin
Treatment Only	F6WQ73	Plectin
Treatment Only	F6WQF0	Plectin
Treatment Only	F6WQW5	Plectin
Treatment Only	F6WXR4	Plectin
Treatment Only	F6WRA4	Plectin
Treatment Only	F6TQ92	Polyadenylate-Binding Protein 1
Treatment Only	F6UGL6	Polypyrimidine Tract-Binding Protein 1
Treatment Only	F6TEI8	Profilin-1
Treatment Only	F6UJ33	Profilin-1
Treatment Only	F6VS95	Protein Disulfide-Isomerase A6
Treatment Only	F6WPB4	Protein Dj-1
Treatment Only	F6UNB9	Protein S100-A1
Treatment Only	F7BND9	Protein S100-A11
Treatment Only	F7CB04	Protein Transport Protein Sec23A
Treatment Only	F7C108	Protein-Lysine 6-Oxidase
Treatment Only	F6WB51	Quinone Oxidoreductase

Treatment Only	F6Z4J4	Rab Gdp Dissociation Inhibitor Beta
Treatment Only	F6YRC5	Ras Gtpase-Activating-Like Protein Iqgap1
Treatment Only	F6XJB9	RNA-Binding Motif Protein, X Chromosome
Treatment Only	F7ASU6	Selenium Binding Protein 1
Treatment Only	F7CI32	Selenium Binding Protein 1
Treatment Only	F7DKR3	Selenium-Binding Protein 1
Treatment Only	F6XS05	S-Formylglutathione Hydrolase
Treatment Only	F6PZ47	Staphylococcal Nuclease Domain-Containing Protein 1
Treatment Only	F7E1X2	Stress-Induced-Phosphoprotein 1
Treatment Only	F6XC16	Synaptic Vesicle Membrane Protein Vat-1 Homolog
Treatment Only	F6UMQ4	Transforming Growth Factor Beta Induced
Treatment Only	F6QXN5	Transgelin-2
Treatment Only	F6TZS9	Triosephosphate Isomerase
Treatment Only	F6SAV5	Tubulin alpha chain
Treatment Only	F6ZSB4	Tubulin Alpha-1A Chain
Treatment Only	F7ANC9	Tubulin Alpha-1B Chain
Treatment Only	F6YRE0	Tubulin Alpha-1C Chain
Treatment Only	F7D253	UDP-Glucose 6-Dehydrogenase
Treatment Only	F6WHI8	UDP-N-Acetylglucosamine Pyrophosphorylase 1
Treatment Only	F6WI21	UDP-N-Acetylhexosamine Pyrophosphorylase
Treatment Only	F6VDK7	Uncharacterized Protein
Treatment Only	F6Y4I1	UTP--Glucose-1-Phosphate Uridylyltransferase
Treatment Only	F6VSD4	X-prolyl aminopeptidase 1
Control and Treatment	F7AYK2	72 KDa Type IV Collagenase
Control and Treatment	P60708	Actin, Cytoplasmic 1
Control and Treatment	F7AAK7	Actin, Cytoplasmic 2
Control and Treatment	F6UJD4	Adseverin
Control and Treatment	F7C3C6	Aggrecan Core Protein
Control and Treatment	F7C450	Alpha-2-Hs-Glycoprotein
Control and Treatment	F6V7C1	Alpha-Enolase
Control and Treatment	Q5VI84	Angiogenin
Control and Treatment	F7A971	Angiopoietin-Related Protein 4
Control and Treatment	Q8HZM6	Annexin A1
Control and Treatment	F6ZI51	Annexin A2-Related
Control and Treatment	F7C0I7	Basement Membrane-Specific Heparan Sulphate Proteoglycan Core Protein
Control and Treatment	Q0W9Q0	Beta-Defensin 4A
Control and Treatment	F6VYL8	Betaine--Homocysteine S-Methyltransferase
Control and Treatment	F6VUP8	Betaine--Homocysteine S-Methyltransferase 1
Control and Treatment	O46403	Biglycan
Control and Treatment	F7C2J3	Cartilage Intermediate Layer Protein 1

Control and Treatment	F6U3D3	Cartilage Oligomeric Matrix Protein
Control and Treatment	F6PQ46	Ceruloplasmin
Control and Treatment	F7AJP3	Chitotriosidase-1
Control and Treatment	F6WD70	Chondroadherin
Control and Treatment	Q29482	Clusterin
Control and Treatment	F6UZI2	Coagulation Factor XIII A Chain
Control and Treatment	F7DE18	Coiled-Coil Domain-Containing Protein 80
Control and Treatment	F6R4Y3	Collagen Alpha-1
Control and Treatment	F6UW03	Collagen Alpha-1
Control and Treatment	F6WCC9	Collagen Alpha-1
Control and Treatment	F6Y8T1	Collagen Alpha-1
Control and Treatment	F7A3F7	Collagen Alpha-1
Control and Treatment	F6RTL6	Collagen Alpha-2
Control and Treatment	F7BRR9	Collagen Alpha-2
Control and Treatment	F7CGV8	Collagen Alpha-2
Control and Treatment	F6R735	Collagen Alpha-3
Control and Treatment	F6RVX8	Collagen Type I Alpha 1 Chain
Control and Treatment	F6SSG3	Collagen Type I Alpha 1 Chain
Control and Treatment	F7D939	Collagen Type I Alpha 1 Chain
Control and Treatment	F7D9C7	Collagen Type I Alpha 1 Chain
Control and Treatment	F6RTH9	Collagen Type I Alpha 2 Chain
Control and Treatment	F6RTI8	Collagen Type I Alpha 2 Chain
Control and Treatment	F6RTJ6	Collagen Type I Alpha 2 Chain
Control and Treatment	F6RTN7	Collagen Type I Alpha 2 Chain
Control and Treatment	F6RTP3	Collagen Type I Alpha 2 Chain
Control and Treatment	F6RUA6	Collagen Type I Alpha 2 Chain
Control and Treatment	F6R528	Collagen type III alpha 1 chain
Control and Treatment	F6QAT0	Collagen type VI alpha 3 chain
Control and Treatment	F6TIN6	Complement C1Q Subcomponent Subunit A
Control and Treatment	F7BUV8	Complement C1Q Subcomponent Subunit B
Control and Treatment	F7DBT2	Complement C1Q Subcomponent Subunit C
Control and Treatment	F7BTW7	Complement C3
Control and Treatment	F6XSF7	Complement C4-A-Related
Control and Treatment	F6RMD0	Complement Factor B-Related
Control and Treatment	F6X0K3	Connective Tissue Growth Factor
Control and Treatment	F7CAX0	C-Type Lectin Domain Family 3 Member A
Control and Treatment	F6WCB7	Cytokine-Like Protein 1
Control and Treatment	O46542	Decorin
Control and Treatment	F7BQJ6	Elongation Factor 1-Alpha
Control and Treatment	A2Q0Z0	Elongation Factor 1-Alpha 1
Control and Treatment	F6RRD0	Elongation Factor 1-Alpha 1

Control and Treatment	F6UME7	Elongation Factor 1-Alpha 1
Control and Treatment	F6UUS3	Elongation Factor 2
Control and Treatment	F6QYS3	Extracellular Matrix Protein 1
Control and Treatment	F6W2Y1	Fibrinogen Gamma Chain
Control and Treatment	A2Q126	Fibromodulin
Control and Treatment	F7CN05	Fibronectin
Control and Treatment	F7CN11	Fibronectin
Control and Treatment	F7ABC9	Fibulin-1
Control and Treatment	F6SX98	Fructose-Bisphosphate Aldolase A
Control and Treatment	F6ZP69	Fructose-Bisphosphate Aldolase C
Control and Treatment	Q28372	Gelsolin
Control and Treatment	F6QIB2	Glia-Derived Nexin
Control and Treatment	F6YV40	Glyceraldehyde-3-Phosphate Dehydrogenase
Control and Treatment	F6ZD04	Glycogen Phosphorylase, Brain Form
Control and Treatment	F7AB03	Granulin Precursor
Control and Treatment	F7AS83	Granulins
Control and Treatment	F7DW69	Heat Shock 70 KDa Protein 1A-Related
Control and Treatment	F7DMY7	Heparan Sulfate Proteoglycan 2
Control and Treatment	F6TAH8	Hhip-Like Protein 2
Control and Treatment	F6SK17	Histone H2B Type 1-B
Control and Treatment	F6UGW9	Histone H2B Type 1-J
Control and Treatment	F7DIN7	Histone H2B Type 1-O
Control and Treatment	F7AHT9	Histone H2B Type 2-C-Related
Control and Treatment	F7AZR5	Histone H2B Type 2-E
Control and Treatment	F6PRL4	Histone H2B Type 3-B
Control and Treatment	F7A4V1	Histone H2B Type 3-B
Control and Treatment	F6VCB4	Histone H3
Control and Treatment	F6Y7V5	Histone H3.1
Control and Treatment	F7B238	Histone H3.1T
Control and Treatment	F6YXV8	Histone H3.3-Related
Control and Treatment	F7C964	Histone H3-Related
Control and Treatment	F6VFV9	Histone H4
Control and Treatment	Q28381	Hyaluronan And Proteoglycan Link Protein 1
Control and Treatment	F7DEB1	Insulin-Like Growth Factor-Binding Protein 6
Control and Treatment	F6TNR4	Keratin, Type I Cuticular Ha1
Control and Treatment	F6SS14	Keratin, Type I Cytoskeletal 10
Control and Treatment	F6WDW3	Keratin, Type I Cytoskeletal 10
Control and Treatment	F7ATL5	Keratin, Type I Cytoskeletal 14
Control and Treatment	F7B7X0	Keratin, Type II Cytoskeletal 1
Control and Treatment	F6W7V0	Keratin, Type II Cytoskeletal 5
Control and Treatment	F7D281	Keratin, Type II Cytoskeletal 6B-Related

Control and Treatment	F6YZV8	Keratin-87 Protein-Related
Control and Treatment	F7B0S3	Lactadherin
Control and Treatment	F6ZDB7	Latent-Transforming Growth Factor Beta-Binding Protein 2
Control and Treatment	F6VQL3	Leukocyte Cell-Derived Chemotaxin-2
Control and Treatment	F6W3T1	L-Lactate Dehydrogenase A Chain
Control and Treatment	F6SKT2	Lumican
Control and Treatment	F7CU94	Lysozyme C
Control and Treatment	F6S243	Macrophage Migration Inhibitory Factor
Control and Treatment	F6XSR3	Matrilin-3
Control and Treatment	F6R013	Matrix Gla Protein
Control and Treatment	F6T9W9	Matrix metalloproteinase 3
Control and Treatment	Q28397	Matrix metalloproteinase 3
Control and Treatment	F6VJF5	Melanoma-Derived Growth Regulatory Protein
Control and Treatment	F6QKR7	Myocilin
Control and Treatment	F6YY66	Nucleoside Diphosphate Kinase B
Control and Treatment	A5YBL8	Peptidyl-Prolyl Cis-Trans Isomerase B
Control and Treatment	F6S6J4	Peroxiredoxin-1
Control and Treatment	F6QXW2	Phosphatidylethanolamine-Binding Protein 1
Control and Treatment	F6X8Q2	Phosphoglucomutase-1
Control and Treatment	P00559	Phosphoglycerate Kinase 1
Control and Treatment	F6ZY40	Prelamin-A/C
Control and Treatment	F6WZ69	Procollagen C-Endopeptidase Enhancer 1
Control and Treatment	F6UP14	Procollagen C-Endopeptidase Enhancer 2
Control and Treatment	F6RZ46	Prolargin
Control and Treatment	F6VSN9	Protein Disulfide-Isomerase A3
Control and Treatment	F6W3M5	Pyruvate Kinase
Control and Treatment	F7C5F1	Retinoic Acid Receptor Responder Protein 2
Control and Treatment	F7ATC2	Ribonuclease 4
Control and Treatment	F6WNV3	Secreted Frizzled-Related Protein 3
Control and Treatment	F6T8U8	Semaphorin-3C
Control and Treatment	F7B812	Serine Protease Htra1
Control and Treatment	F6ZTA7	Serum Amyloid A Protein
Control and Treatment	F6ZL17	Serum amyloid A protein
Control and Treatment	F7DMJ7	Sushi Repeat-Containing Protein Srpx2
Control and Treatment	F6TVT0	Target of Nesh-Sh3
Control and Treatment	F6PN81	Tenascin
Control and Treatment	F7CCQ6	Tenascin-X
Control and Treatment	F6YR34	Thrombospondin-1
Control and Treatment	F7E0P3	Thrombospondin-4
Control and Treatment	F6U5V3	Transcobalamin-2

Control and Treatment	F6VB94	Transforming Growth Factor-Beta-Induced Protein Ig-H3
Control and Treatment	F7D9J2	Transketolase
Control and Treatment	F7DMU4	Tumour Necrosis Factor Receptor Superfamily Member 11B
Control and Treatment	Q28396	Type II collagen
Control and Treatment	F6SJK9	Uncharacterized Protein
Control and Treatment	F6SQQ0	Uncharacterized Protein
Control and Treatment	F6TTN2	Uncharacterized Protein
Control and Treatment	F6XIM5	Uncharacterized Protein
Control and Treatment	F6Y2J1	Uncharacterized Protein
Control and Treatment	F7CJG3	Uncharacterized Protein
Control and Treatment	F7E454	Uncharacterized Protein
Control and Treatment	F7B5C4	Vimentin
Control and Treatment	F6QP96	Vitrin
Control and Treatment	F7D8I6	Xanthine Dehydrogenase/Oxidase

5. Manuscript 4

^{1}H NMR Metabolomics Identifies Underlying Inflammatory Pathology in Osteoarthritis and Rheumatoid Arthritis Synovial Joints

James R Anderson[1], Susama Chokesuwattanaskul[2,3], Marie M Phelan[2,4], Tim JM Welting[5], Lu-Yun Lian[2], Mandy J Peffers[1], Helen L Wright[1]

[1]Institute of Ageing and Chronic Disease, University of Liverpool, Liverpool, UK
[2]Institute of Integrative Biology, University of Liverpool, Liverpool, UK
[3]Chulalongkorn University, Bangkok 10330, Thailand
[4]HLS Technology Directorate, University of Liverpool, Liverpool, UK
[5]Laboratory for Experimental Orthopedics, Department of Orthopedic Surgery, Maastricht University Medical Centre, 6229 HX Maastricht, The Netherlands

Keywords

Synovial Fluid, Metabolomics, Osteoarthritis, Rheumatoid Arthritis, Nuclear Magnetic Resonance

Declaration of Author Contributions

Dr Marie Phelan provided training in NMR spectral acquisition and training in/assistance with NMR spectral analysis. Dr Susama Chokesuwattanaskul acquired NMR spectra for rheumatoid arthritis synovial fluid samples and assisted with NMR spectral analysis. Dr Tim Welting provided osteoarthritis synovial fluid samples. Dr Helen Wright provided rheumatoid arthritis synovial fluid samples and undertook pathway and correlation analysis. Professor Lu-Yun Lian and Professor Mandy Peffers advised on interpretation of experimental results. All other experimental work was conducted by Mr James Anderson.

5.1. Abstract

Despite osteoarthritis (OA) and rheumatoid arthritis (RA) being typically age-related, their underlying aetiologies are markedly different. This study has used ^{1}H nuclear magnetic resonance (NMR) spectroscopy to identify differences in metabolite profiles in low volumes of OA and RA synovial fluid (SF). SF was aspirated from knee joints of 10 OA and 14 RA patients. 100 µl of SF was analysed using a 700 MHz Avance IIIHD Bruker NMR spectrometer with a TCI cryoprobe. Spectra were analysed by Chenomx, Bruker TopSpin and AMIX software. Statistical analysis was undertaken using Metaboanalyst. 50 metabolites were annotated, including amino acids, saccharides, nucleotides and soluble lipids. Discriminant analysis identified group separation between OA and RA cohorts, with 32 metabolites significantly different between OA and RA SF (false discovery rate < 0.05). Metabolites of glycolysis and the tricarboxylic acid cycle were lower in RA compared to OA; these results concur with higher levels of inflammation, synovial proliferation and hypoxia found in RA compared to OA. Elevated taurine in OA may indicate increased subchondral bone sclerosis. This study demonstrates that quantifiable differences in metabolite abundance can be measured in low volumes of SF by ^{1}H NMR spectroscopy, which may be clinically useful to aid diagnosis and improve understanding of disease pathogenesis.

5.2. Introduction

Osteoarthritis (OA) and rheumatoid arthritis (RA) are the two most common forms of arthritis, which lead to significant disability and substantial reduction in quality of life (Li *et al.*, 2016; Sprangers *et al.*, 2000). Despite both these chronic conditions being typically age-related with insidious onset, their underlying aetiologies are markedly different (Brouwers *et al.*, 2015; Majithia and Geraci, 2007). OA is a degenerative joint condition, primarily affecting the hands, hips and knees, with one-third of people in the UK aged over 45 (approximately 8.75 million) requiring treatment (Reynard and Loughlin, 2012). This disease is characterised by articular cartilage loss, synovial membrane dysfunction, subchondral bone sclerosis and osteophyte formation with the depletion of matrix proteins driven by proteases including multiple matrix metalloproteinases (MMPs) and a disintegrin and metalloproteinase with thrombospondin motifs (ADAMTSs) (Poole, 1999; Struglics *et al.*, 2006; Truong *et al.*, 2006). We have previously identified OA synovial fluid (SF) to be enriched in a number of proteins including S100-A10, Collagen type I and CD109 (Peffers, McDermott, *et al.*, 2015). RA is a systemic, inflammatory autoimmune disease that primarily affects the synovium of joints (Bartok and Firestein, 2010), presenting as a symmetric polyarthritis with an estimated prevalence of 0.5-1% of the adult population within developed countries (Davis and Matteson, 2012; Scott *et al.*, 2010). RA joints are marked by inflammation of the synovium and destruction of articular cartilage and underlying bone. The RA synovium becomes hyperplastic with infiltration by a variety of immunocompetent cells (activated neutrophils in particular) (Wright *et al.*, 2014). RA synovial fluid is enriched with cytokines, inflammatory mediators such as leukotrienes, and proteases that degrade the extracellular matrix (ECM) and hyaluronic acid (Wright *et al.*, 2012, 2014).

SF is located within the articular joint cavity, providing a pool of nutrients for surrounding tissues but primarily serving as a biological lubricant, containing molecules with low-friction and low-wear properties to articular surfaces (Blewis *et al.*, 2007). As a serum filtrate, not only does SF contain systemic protein/metabolite markers of disease, but also due to its close contact and near proximity to

numerous tissues found to be primarily altered during joint pathology (including synovial membrane, cartilage and bone), this biofluid holds significant potential in the discovery of biomarkers whose levels are altered at early stages of disease progression (Ruiz-Romero and Blanco, 2010).

Metabolomics systematically and comprehensively profiles metabolic changes within biological systems, including metabolic pathway analysis and abundance of unique biochemical molecules (Wang, Zhang, *et al.*, 2012). The small molecules investigated include secondary metabolites, metabolic intermediates and hormones, as well as other molecules involved in cellular signalling (Jukarainen, 2009). Few studies have investigated the whole profile of metabolites within human SF. A recent investigation analysing 10 ml of each SF sample by liquid chromatography coupled with mass spectrometry (MS) identified 21 differentially expressed metabolites between OA and RA SF (Kang *et al.*, 2015). These included a generally elevated level of lipid metabolites and phospholipids in RA patients compared to OA patients, although decreased levels of the phospholipid lysophosphatidylcholine was observed in OA. Nuclear magnetic resonance (NMR) spectroscopy is complementary to MS analysis and may offer advantages over MS in the metabolomic analysis of native samples, with a minimal level of sample preparation using a noninvasive and nondestructive method, subsequently producing results which are more reproducible and robust (Markley *et al.*, 2017). One limiting factor of NMR spectroscopy of SF has previously been the minimum volume required for analysis, with difficulties in analysing SF from normal human joints in which < 200 µl can be aspirated (Naughton *et al.*, 1993). Using the methods described in this study, it has been proved that analysable and reproducible ^{1}H NMR spectra can be produced from just 100 µl of SF, thus increasing the potential applications of this technique when sample volume is limited.

The aim of this study was to apply ^{1}H NMR to study human SF metabolomics, in order to provide novel insights on the underlying pathogenesis of OA and RA, and to optimise protocols for clinically relevant volumes of SF typically available in a clinical setting. This study describes protocols for human SF sampling and processing and presents a novel approach to inflammation analysis, carrying out full profile

metabolite NMR examination on low volumes (100 µl) of SF. This method of biofluid analysis enables further understanding of disease pathogenesis, inflammatory signatures and biomarkers, and may aid in both our comprehension of these conditions and progress toward an earlier diagnosis and/or prognostic indicators to stratify patients to treatment.

5.3. Methods

5.3.1. Sample Groups

RA patients (mean age 65.4 years) fulfilled the 1987 American College of Rheumatology (ACR) criteria for RA and were seropositive for rheumatoid factor (RF). OA patients (mean age 67.4 years) were diagnosed by radiographs using Kellgren and Lawrence score, and general orthopaedic guidelines carried out by an experienced orthopaedic knee surgeon. A diagnosis of RA was excluded for all OA patients. OA and RA groups were sex and age-matched to within 5 years of age. RA patients were receiving multiple therapies including disease-modifying antirheumatic drugs (DMARDs, typically methotrexate), tumour necrosis factor (TNF) inhibitors and/or prednisolone and had a mean disease duration of 13 years (range 0-35 years). OA patients were typically receiving nonsteroidal anti-inflammatory drugs (NSAIDs) and in end-stage disease.

5.3.2. Sample Collection

OA and RA SF from knee joints was aspirated into heparinized tubes and processed within 1 hr. Aliquots of whole SF were centrifuged at > 2000*g* for 5 min and cell-free SF decanted and frozen at -20°C.

5.3.3. Sample Preparation for NMR

100 µl of SF was thawed out over ice and diluted to a final volume containing 50% (v/v) SF, 40% (v/v) ddH_2O (18.2 MΩ), 10% (v/v) 1 M PO_4^{3-} pH 7.4 buffer (Na_2HPO_4, VWR, Pennsylvania, US; NaH_2PO_4, Sigma-Aldrich, Gillingham, UK) in deuterium oxide (^2H_2O) and 0.0025% (v/v) sodium azide (NaN_3, Sigma-Aldrich). Samples were vortexed for 1 min, centrifuged at 13000*g* and 4˚C for 2 min and 190 µl transferred into 3 mm outer diameter NMR tubes using a glass pipette.

5.3.4. NMR Setup Acquisition and Processing

SF samples were individually analysed using ^{1}H NMR spectroscopy on a 700 MHz NMR spectrometer Bruker Avance III HD with a TCI cryoprobe and chilled Sample-Jet autosampler. Software for acquisition and processing was carried out using Topsin 3.1 and IconNMR 4.6.7. 1D ^{1}H standard Carr-Purcell-Meiboom-Gill (CPMG)-type metabolomics experiments, with optimal water suppression via presaturation, were acquired with cpmgpr1d filters for small molecules via a CPMG sequence. Spectra were acquired at 37°C with 32 transients, a 15 ppm spectral width, 32 K points, 9.6 ms echo time and a 3.1 s interscan delay.

5.3.5. Spectra Processing and Quality Control

Spectra were assessed to conform to minimum reporting standards as outlined by the Metabolomics Society to ensure consistent line widths, baseline corrections and water suppression (Sumner *et al.*, 2007). As commonly used internal standards (trimethylsilyl propionate and 4,4-dimethyl-4-silapentane-1-sulfonic acid) are known to bind to some proteins including albumins, common in protein-rich fluids such as SF, spectra were indirectly referenced via an intrinsic metabolite whose shifts are unaffected by protein presence (glucose) (Beckonert *et al.*, 2007). All spectra passing appraisal were then divided into 'buckets' that were defined globally for all spectra by the peak limits using Amix software. Spectra were then prepared for statistical analysis by bucketing/binning according to spectral features or peaks; all peaks, both identified and unknown, were included in the bucket table.

5.3.6. Metabolite Annotation and Identification

Metabolites in the SF ^{1}H NMR spectra were initially tentatively annotated using the metabolite discovery software Chenomx (Chenomx, Canada) and, where possible, their identities confirmed using an in-house library of metabolite spectra (further details in Supplementary Table 1) (Salek *et al.*, 2013).

5.3.7. Metabolomics Statistical Analysis

Statistical analyses were performed using Metaboanalyst® (http://www.metaboanalyst.ca/) (Xia *et al.*, 2016). The bucketed experimental data

were normalised by the median and additionally Pareto scaled (for multivariate analysis). Univariate analysis was by t-test with application of a false discovery rate (FDR) adjusted p value of 0.05. Multivariate analysis was via unsupervised principal component analysis (PCA) followed by partial least squares discriminant analysis (PLS-DA) validated via leave one out cross-validation to automatically determine the optimal number of components for the model.

5.3.8. Metabolomics Pathway Analysis

Pathway analysis was carried out using the list of significantly differentially abundant metabolites between OA and RA SF using Metaboanalyst and with reference to the KEGG (Kyoto Encyclopedia of Genes and Genomes) metabolic pathway database (http://www.kegg.jp/kegg/pathway.html) for human metabolic pathways (Xia *et al.*, 2016). Pathway enrichment was determined by Hypergeometric test and reported with an FDR-adjusted p value. Pathway analysis was carried out by Dr Helen Wright.

5.3.9. Availability of Data and Materials

Metabolomics data have been deposited to the EMBL-EBI MetaboLights database and can be accessed at https://www.ebi.ac.uk/metabolights/MTBLS564.

5.4. Results

5.4.1 Metabolite Identification

NMR spectra for all cohorts showed a consistent set of metabolite signals present. NMR spectra of extracts were divided into individual spectral bins accounting for one or more multiplets. The number of spectral bins in each extract was 171, of which 126 (73.6%) were assigned to 50 metabolites. Quantile plots identifying the global variation of metabolite abundances within each cohort demonstrated much less variation within the OA cohort than the RA cohort, indicating a more homogeneous OA population (Figure 1). Fifty metabolites were annotated in total, including amino acids, saccharides, nucleotides and soluble lipids (Table 1).

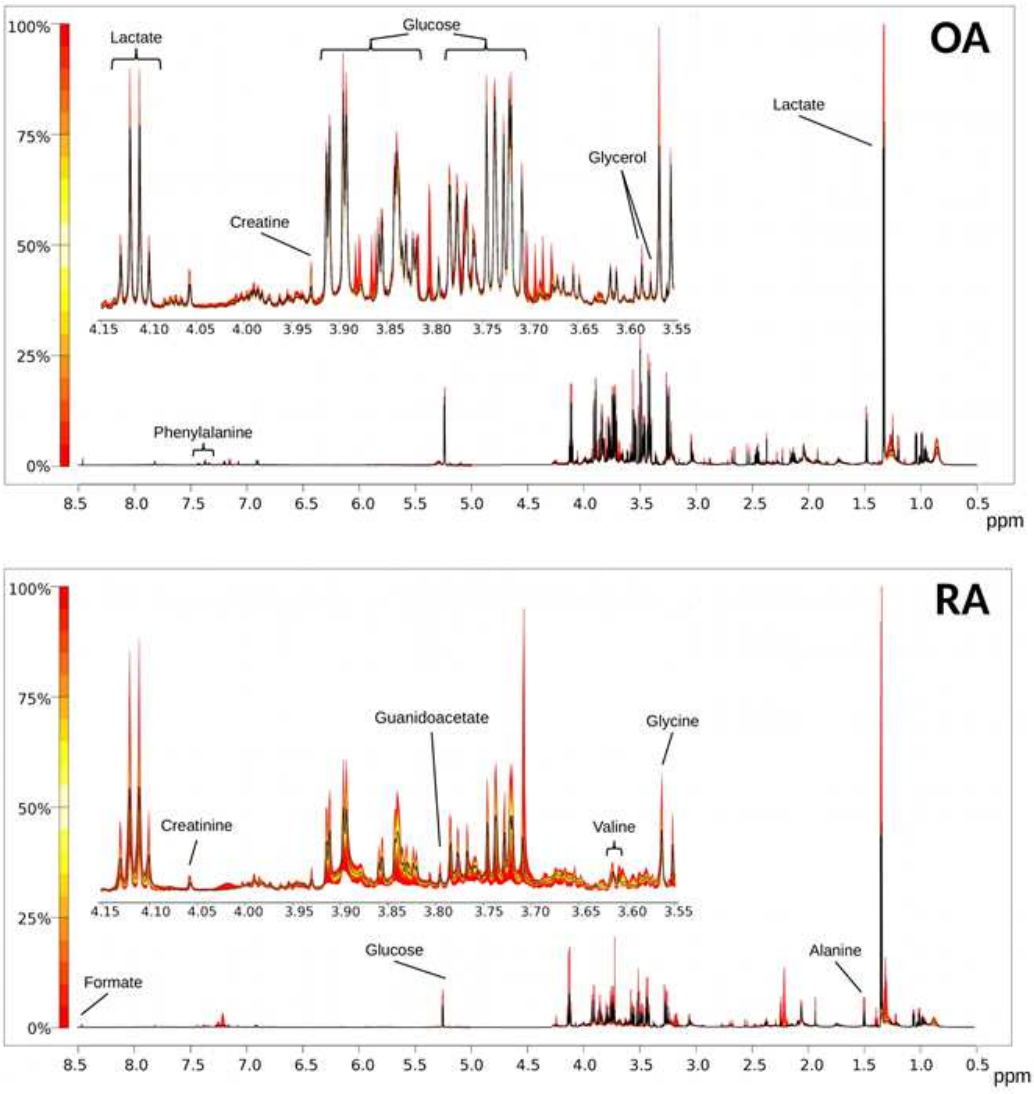

Figure 1. Quantile Plots of osteoarthritis (OA, n=10) and rheumatoid arthritis (RA, n=14) spectra depicting spectral variation within both pathological groups. The median spectral plot is depicted by a black line and variation from the median shown by a yellow to red scale for both the full spectral range (8.5 - 0.5 ppm) and a more detailed region (4.15 - 3.55 ppm). Peaks of interest are annotated as examples. Note multiple peaks for some metabolites, e.g. glucose.

Table 1. List of 50 Metabolites Detected in osteoarthritis and rheumatoid arthritis synovial fluid by ^{1}H NMR Spectroscopy

Amino Acids
2-Aminobutyrate, 5-Aminolevulinate, Alanine, Asparagine, Creatine, Creatinine, Glutamine, Glycine, Guanidoacetate, Histidine, Isoleucine, Leucine, Lysine, Methionine, n-Acetylamino acid, Ornithine, Phenylalanine, Proline, Sarcosine, Threonine, Tyrosine, Valine
Fatty and Organic Acids
2-Hydroxybutyrate, 3-Hydroxybutyrate, 3-Hydroxyisovalerate, Acetate, Acetoacetate, Carnitine, Citrate, Formate, Lactate, Malonate, Pyruvate, Taurine
Sugars
Acetylated-saccharide, Glucose, Glycerol, Mannose, Myoinositol
Other
Acetylcholine, Adenosine, Choline, Dimethylamine, Ethanol, Isopropanol, Mobile-lipid, o-Phosphocholine, Oxypurinol, sn-Glycero-3-phosphocholine, Xanthine

5.4.2. Univariate Comparison of Osteoarthritis and Rheumatoid Arthritis Synovial Fluid

Univariate analysis of the 171 spectral bins identified 91 significantly different bins (including 50 annotated) which corresponded to 32 metabolites which were significantly different (FDR < 0.05) between OA and RA SF. These included citrate, creatinine, glucose, glutamine, glycerol, pyruvate and taurine which were higher in OA (Table 2, Figure 2, Figure 3a). 3-hydroxybutyrate, acetate, isoleucine, leucine, sarcosine and threonine were higher in RA. Acetylated saccharides, an annotation that incorporates commonly acetylated molecules such as heparin and chondroitin sulphate, and monosaccharide subunits *N*-acetyl glucosamine and *N*-acetyl galactosamine, were also significantly higher in RA. No significant association was observed between metabolite profile or drug therapy in the RA patients, or with the length of disease activity.

5.4.3. Multivariate Analysis comparison of Osteoarthritis and Rheumatoid Arthritis Synovial Fluid

PCA analysis exhibited separation between OA and RA cohorts (Figure 3b). Regression analysis (PLS-DA, partial least square discriminant analysis) correctly distinguished between the two groups in five components (Figure 3c, $R^2 = 0.99$, $Q^2 = 0.95$).

Table 2. List of 32 significantly altered metabolites between osteoarthritis (OA) and rheumatoid arthritis (RA) synovial fluid (FDR < 0.05). Y = yes

Metabolite	HMDB Annotation	Higher in OA	Higher in RA	Fold Change OA vs RA	-log10 (p value)	FDR
2-Hydroxybutyrate	HMDB00008	Y		1.19	3.2495	$1.70x10^{-3}$
3-Hydroxybutyrate	HMDB00357	Y		1.59	2.3288	$1.02x10^{-2}$
3-Hydroxyisovalerate	HMDB00754	Y		2.22	7.6958	$6.85x10^{-7}$
Acetate	HMDB00042		Y	-1.69	2.6401	$5.56x10^{-3}$
Acetylcholine	HMDB00895	Y		1.57	3.9361	$5.32x10^{-4}$
Acetylated-saccharide	None		Y	-1.49	4.5038	$1.97x10^{-4}$
Adenosine	HMDB00050	Y		1.94	1.6375	$4.45x10^{-2}$
Alanine	HMDB00161	Y		1.42	2.79	$4.18x10^{-3}$
Asparagine	HMDB00168	Y		1.31	3.8413	$5.83x10^{-4}$
Citrate	HMDB00094	Y		1.67	5.972	$1.65x10^{-5}$
Creatinine	HMDB00562	Y		1.43	4.0608	$4.48x10^{-4}$
Glucose	HMDB00122	Y		1.82	4.2582	$3.03x10^{-4}$
Glutamine	HMDB00641	Y		1.80	9.7868	$9.26x10^{-9}$
Glycerol	HMDB00131	Y		1.42	2.6897	$5.18x10^{-3}$
Glycine	HMDB00123		Y	-1.64	3.9516	$5.28x10^{-4}$
Guanidoacetate	HMDB00128	Y		1.19	3.283	$1.61x10^{-3}$
Histidine	HMDB00177	Y		1.34	3.3713	$1.36x10^{-3}$
Isoleucine	HMDB00172		Y	-1.39	4.0006	$4.88x10^{-4}$
Leucine	HMDB00687		Y	-1.20	2.1407	$1.52x10^{-2}$
Mannose	HMDB00169	Y		1.73	3.5567	$9.85x10^{-4}$
Methionine	HMDB00696		Y	-1.30	2.8572	$3.69x10^{-3}$
Mobile-lipid	None	Y		1.96	4.7317	$1.42x10^{-4}$
Myoinositol	HMDB00211	Y		1.24	2.48	$7.61x10^{-3}$
n-Acetylamino acid	None	Y		1.11	2.5075	$7.24x10^{-3}$
Proline	HMDB00162	Y		1.26	3.1978	$1.85x10^{-3}$
Pyruvate	HMDB00243	Y		3.44	11.994	$8.61x10^{-11}$
Sarcosine	HMDB00271		Y	-1.56	4.6614	$1.51x10^{-4}$
sn-Glycero-3-phosphocholine	HMDB00086	Y		1.49	3.0967	$2.27x10^{-3}$
Taurine	HMDB00251	Y		1.26	2.2132	$1.32x10^{-2}$
Threonine	HMDB00167		Y	-1.22	1.6233	$4.50x10^{-2}$
Tyrosine	HMDB00158	Y		1.40	2.9942	$2.78x10^{-3}$
Valine	HMDB00883	Y		1.25	2.5638	$6.45x10^{-3}$

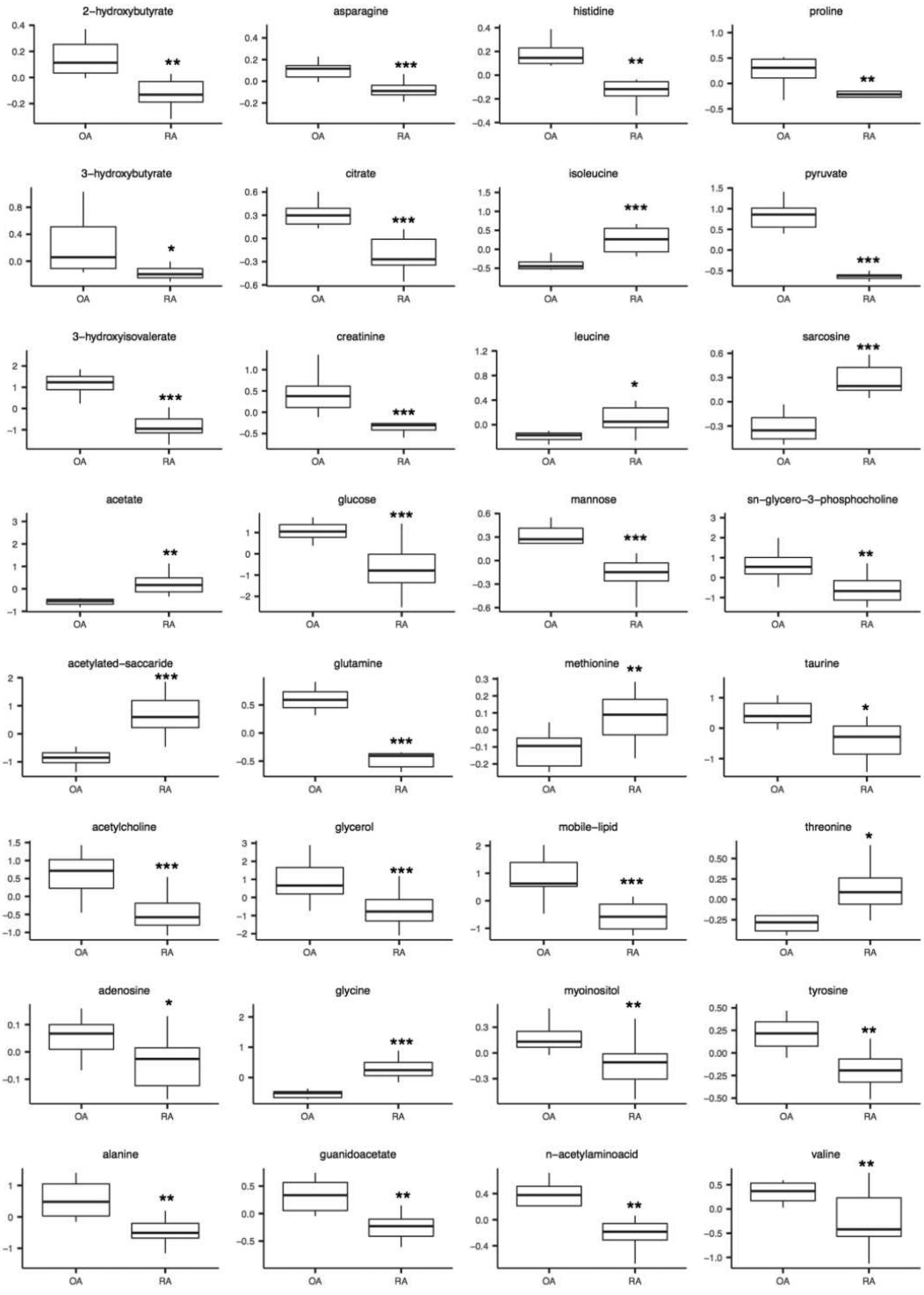

Figure 2. Boxplots of representative metabolites identified from univariate analysis as significantly different between osteoarthritis (OA, n=10) and rheumatoid arthritis (RA, n=14) synovial fluid (* = $p < 0.05$, ** = $p < 0.01$, *** = $p < 0.001$). Y-axis represents normalised peak intensity following median normalisation and Pareto scaling.

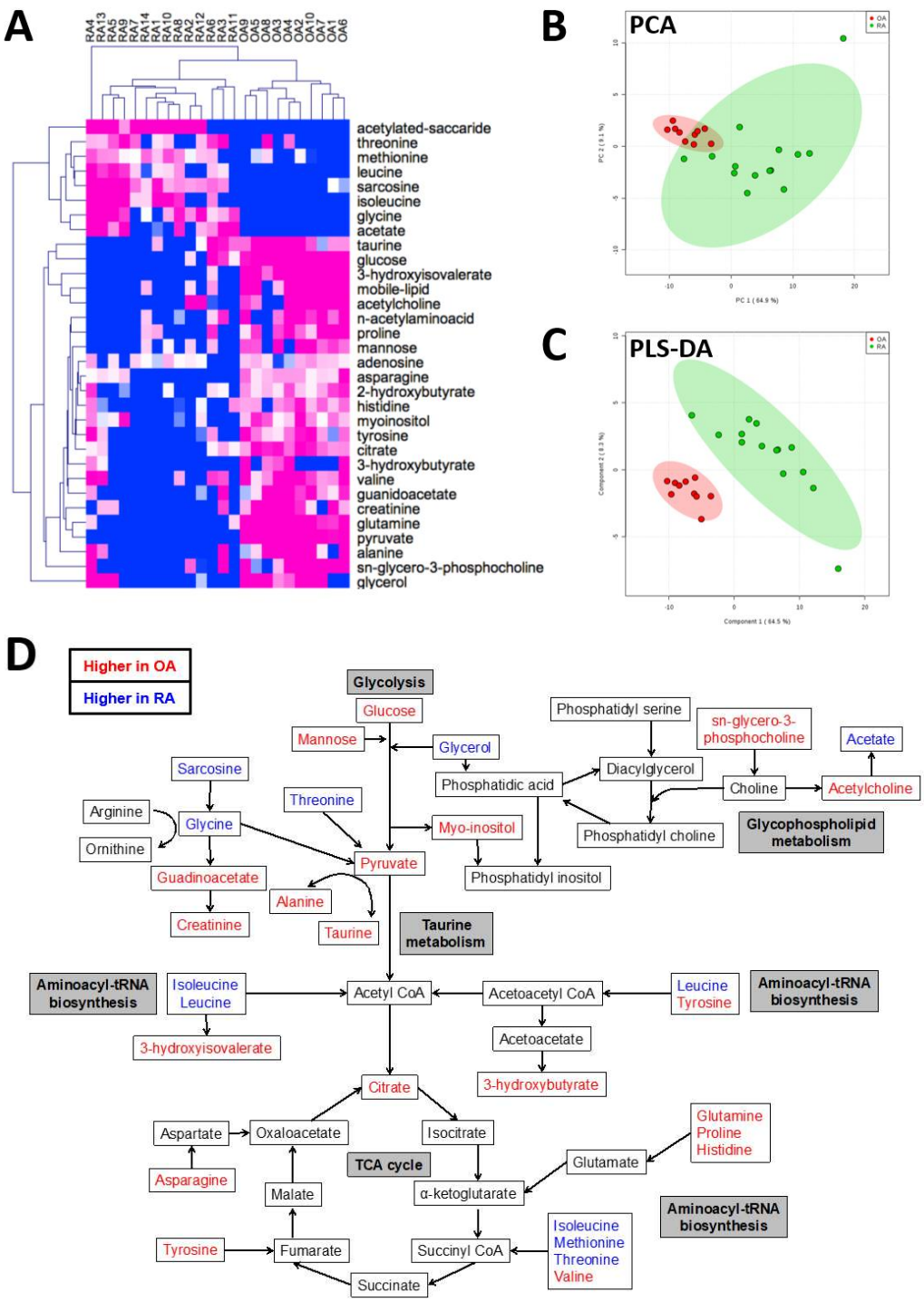

Figure 3. Comparison of NMR synovial fluid metabolomes between osteoarthritis (OA, n=10) and rheumatoid arthritis (RA, n=14). (A) Heatmap showing metabolites significantly different in OA and RA SF ($p < 0.05$). Blue = low, White = medium, Pink = high concentration. (B) Unsupervised PCA scores plot showing metabolite profile is more variable between RA (green) than OA synovial fluid (red). Shading represents 95% confidence region. (C) Supervised multivariate analysis by PLS-DA segregated RA (green) and OA (red) synovial fluid samples. Shading represents 95% confidence region. Scores plot is shown for components 1 and 2. (D) Pathway scheme depicting metabolite levels detected in RA and OA synovial fluid. Blue = higher in RA synovial fluid, Red = higher in OA synovial fluid.

5.4.4. Biological Context

In order to determine the metabolic pathways that were differently regulated between OA and RA, the list of 32 significantly different metabolites was uploaded into Metaboanalyst for Pathway Analysis. The results of this analysis are shown in Table 3 and include pathways relating to amino acid synthesis and degradation, taurine and hypotaurine metabolism and glycolysis. With reference to current understanding of metabolic pathways, results of the pathway analysis were combined into a single metabolic flow diagram (Figure 3d) to enable interpretation of the interactions between the metabolites and the different metabolic pathways (Berg *et al.*, 2012).

Table 3. Pathway analysis using Metaboanalyst and with reference to the KEGG database predicted the most enriched pathways from the list of metabolites that were significantly different between osteoarthritis and rheumatoid arthritis synovial fluid (FDR ≤ 0.1). Pathway enrichment was determined by Hypergeometric test and reported with an FDR-adjusted p value. The number of metabolites enriched in our dataset (hits) is shown compared with the total number of metabolites in the KEGG pathway.

Pathway	Total	Hits	$-\log_{10}$ (p value)	FDR
Aminoacyl-tRNA biosynthesis	75	12	24.693	1.51×10^{-9}
Nitrogen metabolism	39	6	12.124	2.17×10^{-4}
Valine, leucine and isoleucine biosynthesis	27	5	11.165	3.78×10^{-4}
Taurine and hypotaurine metabolism	20	4	9.3989	1.66×10^{-3}
Alanine, aspartate and glutamate metabolism	24	4	8.6483	2.81×10^{-3}
Glycine, serine and threonine metabolism	48	5	8.2939	3.24×10^{-3}
Arginine and proline metabolism	77	6	8.1678	3.24×10^{-3}
Galactose metabolism	41	4	6.5415	1.44×10^{-2}
Glycolysis or Gluconeogenesis	31	3	5.0818	5.52×10^{-2}
Valine, leucine and isoleucine degradation	40	3	4.3697	1.02×10^{-1}

Normalised levels of acetylated saccharide in RA SF correlated positively with serum levels of inflammatory markers (Figure 4), including the acute-phase protein C-related protein (CRP, g/L) (Pearson $R^2 = 0.78$, $p = 0.008$, $n = 10$), erythrocyte

sedimentation rate (ESR, mm/hr) (Pearson $R^2 = 0.62$, $p = 0.02$, $n = 13$) and rheumatoid factor (RF) titre (Pearson $R^2 = 0.618$, $p = 0.018$, $n = 14$).

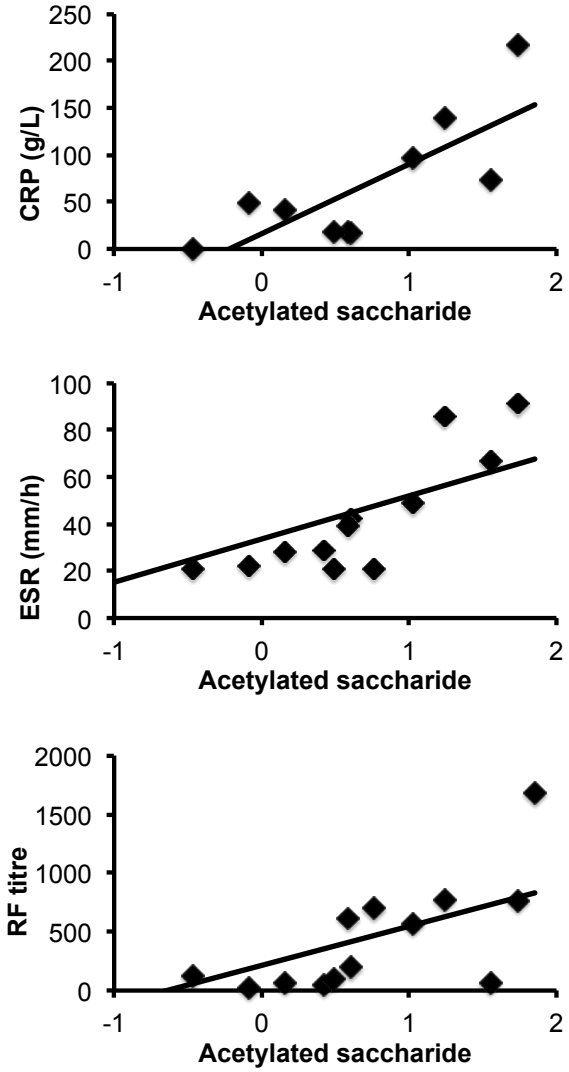

Figure 4. Correlation of acetylated saccharide with protein C-related protein (CRP), erythrocyte sedimentation rate (ESR) and rheumatoid factor (RF) titre in rheumatoid arthritis patients. Levels of acetylated saccharide (median normalised with Pareto scaling) in rheumatoid arthritis synovial fluid correlated positively with serum levels of CRP (Pearson $R^2 = 0.78$, $p = 0.008$, $n = 10$), ESR (Pearson $R^2 = 0.62$, $p = 0.02$, $n = 14$) and RF titre (Pearson $R^2 = 0.618$, $p = 0.018$, $n = 14$).

5.5. Discussion

In this study, OA and RA SF metabolomes were analysed using ^{1}H NMR spectroscopy. This study differs from previous ones in that this study has investigated the metabolome of SF, the biofluid that is in contact with all the tissues and cells at the site of disease manifestation and joint damage, thereby allowing analysis of the pathophysiology of the whole joint. To date, metabolomic studies in OA and RA have focused on biofluids, including urine, serum and SF using a number of different platforms including gas chromatography-mass spectrometry (GC-MS), liquid chromatography-mass spectrometry (LC-MS) and ^{1}H NMR spectroscopy (Cuppen *et al.*, 2016; Giera *et al.*, 2012; Hugle *et al.*, 2012; Kang *et al.*, 2015; Kapoor *et al.*, 2013; Kim *et al.*, 2017; Madsen *et al.*, 2011; Mickiewicz, Kelly, *et al.*, 2015; Priori *et al.*, 2015; Sumner *et al.*, 2007; Young *et al.*, 2013; Zhang *et al.*, 2014; Zhou *et al.*, 2016). These studies have provided insight into the metabolites found within human arthritic SF, and the different underlying cellular pathology of OA and RA joints. The RA synovial environment is characterised by proliferation of synovial fibroblasts and angiogenesis. Infiltration of immune cells, including neutrophils, macrophages, and T and B cells, drives inflammation within the joint, releasing proteases, cytokines, chemokines and lipid mediators that perpetuate inflammation leading to growth of an invasive, inflammatory pannus across the surface of the cartilage. Further dysregulation of neutrophils and osteoclasts within the pannus leads to degradation of the underlying cartilage matrix and bone erosion (Wright *et al.*, 2012, 2014). In contrast, while there is some evidence of mild to moderate inflammation and synovial hyperplasia within OA joints, this is markedly less than the levels observed in RA, with the population of infiltrating immune cells consisting mainly of T cells and macrophages (Berenbaum, 2013; de Lange-Brokaar *et al.*, 2012). Synovitis is not as common in OA, and the loss of articular cartilage and bone is caused by a dysregulation in proteases including MMPs leading to destruction of the cartilage ECM (Poole, 1999; Struglics *et al.*, 2006).

A common feature of previous studies investigating OA and RA SF metabolites is the activation of metabolic pathways controlling glycolysis and fatty acid metabolism; however most studies compare OA or RA serum metabolites to sera from healthy

individuals. This study presents a direct comparison of OA and RA metabolite profiles in SF using ^{1}H NMR spectroscopy and provides a novel insight into the differences in metabolic activity within joints of patients with two common forms of arthritis. In this study, 50 metabolites were identified in OA and RA SF: 22 amino acids, 5 sugars, 12 fatty and organic acids and 11 others. Multivariate analysis separated patient SF metabolite profiles based on the levels of 32 metabolites that were significantly different between OA and RA SF. These metabolites were associated with metabolic pathways controlling amino acid synthesis, taurine metabolism, glycophospholipid metabolism, glycolysis and the tricarboxylic acid (TCA) cycle. OA SF had significantly higher levels of substrates for glycolysis and the TCA cycle, including glucose, mannose, pyruvate and citrate. In addition, many amino acids, which feed into glycolysis and the TCA cycle, were higher in OA, including tyrosine, glutamine, proline, histidine, asparagine, taurine and alanine. We have previously identified altered glycolysis pathways in early OA using NMR metabolomics (Peffers, Riggs, *et al.*, 2015). Furthermore, several studies have identified altered status of glycolysis and glucose metabolism glycolytic proteins in OA. One study identified these changes in OA compared to normal cartilage (Guo *et al.*, 2008). In another study of an *in vitro* model of OA using cartilage explants and label-free MS proteomics, 13.8% of up-regulated proteins were related to glycolysis (Peffers, 2013).

A previous study of urine metabolomics found altered TCA cycle activity in OA (Li *et al.*, 2010). The authors hypothesised this was due to changes in cartilage metabolism which resulted in elevations of aconitic acid, isocitric acid and citrate in the urine of OA patients. In addition, a reduction in excretion of glutamine was suggestive of altered energy metabolism in chondrocytes (Li *et al.*, 2010). In our study we identified increased citrate and glutamine in OA SF compared to RA, suggestive of altered chondrocyte biology in OA joints. Chondrocytes are extremely dependent on glucose metabolism to drive the ECM biosynthetic machinery, requiring anaerobic glycolysis to generate ATP (Heywood *et al.*, 2010). Indeed, glycolysis constitutes 95% of their energy production (Heywood *et al.*, 2010). Adequate ATP is needed for chondrocytes to respond to stress thus, a high rate of

anaerobic glycolysis is essential for ATP generation. It is hypothesised that this increase in glycolysis is an attempt to increase ECM production in the face of MMP-driven degradation.

In this study, lower levels of substrates for glycolysis and the TCA cycle in RA SF were identified, suggesting even higher levels of anaerobic cellular metabolism within RA joints compared to OA. While the levels of lactate did not differ between OA and RA SF in this study, the ratio of lactate to glucose was significantly higher in RA, supporting this theory (Kramer, Ravi, *et al.*, 2014; Wright *et al.*, 2014). In RA sera, substrates of glycolysis including glucose, valine, alanine, glutamine and tyrosine increase in patients who respond to TNF-inhibitor therapy with etanercept, suggesting the levels of these metabolites increase when inflammation decreases (Priori *et al.*, 2015). A decrease in 3-hydroxybutyrate levels in RA sera in response to etanercept has also been reported (Priori *et al.*, 2015); again we observed lower levels of 3-hydroxybutyrate in RA SF compared to OA SF. Lower levels of glucose have been previously reported in RA serum compared to healthy individuals (Zhou *et al.*, 2016). Within the joint, lower glucose levels may be as a consequence of the increase in cellular metabolism in resident SF fibroblasts and infiltrating immune cells, particularly neutrophils, as these cells rely solely on glycolysis for energy production (Kramer, Ravi, *et al.*, 2014; Wright *et al.*, 2014). Increased hypoxia within RA joints has also been shown to promote glycolysis, and is strongly associated with synovial proliferation, whereas in OA, no association between synovial proliferation and hypoxia is evident (Biniecka *et al.*, 2016; Lee *et al.*, 2007). Interestingly, taurine was higher in OA versus RA SF, while ‘taurine and hypotaurine metabolism’ was identified in our pathway analysis. Previous metabolomics studies in RA have demonstrated that taurine is increased in RA versus control serum, and in RA SF compared to OA SF (Kang *et al.*, 2015; Young *et al.*, 2013). Taurine is involved in the pathogenesis of subchondral bone sclerosis, a feature of both RA and OA (Li *et al.*, 2014; Yang *et al.*, 2016). It is possible that the higher levels of taurine in OA SF identified in our study may be because of increased subchondral bone sclerosis in OA compared to RA samples, and in addition may be an indicator of the degree of subchondral bone sclerosis along with additional metabolites such as L-carnitine

and glycerophospholipids. Patients in our study were in end-stage OA and likely to have high levels of subchondral bone sclerosis associated with advanced disease, whereas in previous studies OA SF was collected from patients at an earlier stage of disease progression (Kang *et al.*, 2015).

A number of metabolites increased in RA SF indicated activation of ketosis, possibly due to the low glucose levels observed in RA. Metabolites including leucine, isoleucine and threonine were elevated in RA SF. Ketosis occurs via a shift in metabolism during glucose limitation: in the absence of glucose e.g. via dietary limitation or decreased mobilisation of glycogen stores, or during oxygen limitation, metabolism of stored lipids is stimulated to increase the supply of acetyl CoA. 3-Hydroxybutyrate, a key metabolite in ketosis, was previously identified as being elevated in RA serum compared to healthy controls (Priori *et al.*, 2015). Our study found levels of this metabolite to be lower in RA compared to OA SF. A number of lipid metabolites have previously been reported to be lower in RA biofluids, with a possible explanation being that lipids are a source of energy within the hypoxic joint (Young *et al.*, 2013). Alteration of lipid metabolism is associated with changes in membrane composition/permeability, gene expression and protein distribution and function, as well as in cellular functions such as cell growth, proliferation, differentiation, survival, apoptosis, and chemotaxis, implicated in the RA disease process (Guma *et al.*, 2016).

Metabolomic analysis of urine from RA patients prior to commencement of anti-TNF therapy identified higher histamine, glutamine and xanthurenic acid, along with lower levels of ethanolamine as biomarkers of a good response to therapy (Kapoor *et al.*, 2013). Serum metabolite biomarkers can also distinguish responders and nonresponders to methotrexate (Wang, Chen, *et al.*, 2012). A number of serum metabolites and metabolic pathways have been shown to correlate with markers of inflammation in RA, e.g. CRP, including metabolites associated with arginine metabolism (arginine and ornithine), tryptophan metabolism (serotonin and tryptophan) and branched-chain amino acids (isoleucine, leucine, and valine) (Cuppen *et al.*, 2016). We did not find correlation of these metabolites with markers of inflammation in RA SF in our study; however, we observed significant correlation

of acetylated-saccharide with serum CRP levels, ESR and RF titre. The assignment of this metabolite as 'acetylated saccharide' was based on comparison of 2D ^{1}H ^{13}C spectra to our in-house library of common acetylated molecules including acetylated heparin and acetylated chondroitin sulphate, and to monosaccharide subunits *N*-acetyl glucosamine and *N*-acetyl galactosamine (data not shown). While the precise acetylated saccharide cannot be definitively identified from this analysis alone, we are confident in our assignment of the NMR resonances to this class of acetylate-saccharide metabolites. The presence of these metabolites concurs with previous observation of a significant elevation in the activities of exoglycosidases (including β-D-glucuronidase and β-D-*N*-acetyl-glucosaminidase) in RA compared to OA SF (Ortutay *et al.*, 2003). These enzymes are responsible for the degradation of glycosaminoglycans (GAGs) such as heparan sulphate within the cartilage matrix, and of hyaluronic acid within SF, leading to the reduced viscosity of SF and irreversible damage to cartilage that is a hallmark of RA. Degradation of GAGs by β-D-glucuronidase and β-D-*N*-acetyl-glucosaminidase liberates both *N*-acetyl glucosamine monosaccharide and chondroitin sulphate (disaccharide of *N*-acetyl glucosamine and glucoronic acid). The likely source of exoglycosidases in RA SF is activated neutrophils (Wright *et al.*, 2014). Neutrophils are also the main source of SF myeloperoxidase, the enzyme responsible for the production of hypochlorous acid, which has also been implicated in the degradation of GAGs and the appearance of acetylated saccharides in SF (Schiller *et al.*, 1996). Interestingly, a strong correlation between β-D-*N*-acetyl-glucosaminidase activity and RF titre was previously reported (Ortutay *et al.*, 2003). Correlation of serum glycoprotein acetyls with CRP and disease activity has also been reported in RA sera (Kononoff *et al.*, 2015).

One limitation of our study was the heterogeneous nature of the RA patient cohort, which included patients at different stages of disease (from early RA with < 1 year diagnosis up to long-standing RA > 35 years diagnosis), and on a variety of different treatments including DMARDs such as methotrexate, biologic therapies and glucocorticoids. The heterogeneous nature of RA SFs was evident in the spectral analysis. Despite this, regression analysis (PLS-DA) was able to segregate OA and RA

SF samples with a high degree of accuracy. In addition, we were unable to include 'normal' SF samples from healthy donors in our study. Definition of normal SF, and in particular the ethical collection of such from living donors, is ambiguous and difficult. Post mortem SF cannot be defined as having a 'normal' metabolome due to the anaerobic changes that take place following death. It would be of great value for a future study of this kind to perform analysis of SF lipids in OA and RA; however this was outside the scope of our current study. Future studies should also correlate clinical markers of disease activity (e.g. tender and swollen joint counts, disease activity scores), radiographic changes and physical characteristics such as body mass index with SF metabolome profiles.

5.5.1. Conclusion

In summary, this study has made a direct comparison of SF from RA and OA and found that the metabolic pathways that differ most between the two forms of arthritis are glycolysis, amino acid biosynthesis and taurine and hypotaurine metabolism. In general, metabolites of glycolysis and the TCA cycle were higher in OA compared to RA; these results concur with higher level of inflammation, synovial proliferation and hypoxia found in RA compared to OA. Levels of taurine were also higher in OA indicating increased subchondral bone sclerosis compared to RA. The study has deepened our understanding of the metabolic differences (and hence pathophysiology) of these two forms of arthritis. This study also demonstrates the feasibility of performing ^{1}H NMR metabolomics on small clinical samples (100 µl), hence widening the applicability of the technology within a clinical setting. We speculate that the discriminative power of our approach to analysis of 100 µl SF using ^{1}H NMR spectroscopy may be sensitive enough to identify changes in disease progression that could inform the use of disease modifying therapies or measure the efficacy of future therapies on disease activity/progression in OA and RA.

5.6. Ethics

SF samples from patients with OA and RA were collected in accordance with the declaration of Helsinki. The study that collected OA SF was approved by Maastricht UMC Medical Ethical Committee, approval number 08-4-028, according to Dutch

law. The study that collected the RA SF was approved by Sefton Adult Ethics Committee; all patients gave written, informed consent.

5.7. Funding

Mr James Anderson is funded by The Horse Trust (Grant No G1015), Professor Mandy Peffers is funded by The Wellcome Trust (07471/Z/15/Z), Dr Helen Wright received funding from Arthritis Research UK (21430) and the University of Liverpool Technology Directorate, Professor Lu-Yun Lian received funding for equipment and software from The Medical Research Council (Grant No MR/M009114/1), Dr Susama Chokesuwattanaskul received funding from the 100th Anniversary Chulalongkorn University Fund for Doctoral Scholarship, the Overseas Research Experience Scholarship for Graduate Students, and Chulalongkorn University, Dr Tim Welting received funding from the Dutch Arthritis Foundation (15-3-403 and LLP14).

5.8. Acknowledgements

The authors would like to thank Dr RC Bucknall for assistance with collection of RA SF samples and Dr PJ Emans and Dr PZ Feczko for assistance with collection of OA SF samples.

5.9. Supplementary Information

Supplementary Table 1. List of 50 metabolites detected in osteoarthritis and rheumatoid arthritis synovial fluid by ^{1}H NMR spectroscopy, assignment levels according to the Metabolomics Society Initiative (Salek *et al.*, 2013).

Class	Metabolite Name	HMDB	Assignment Level	Chenomx Annotation (y/n)	Confirmed by in-house ^{1}H (n = no standard available; y = present)	Observed in in-house 2D HSQC (n1 = no standard available; n2 = below level of detection; y = present)
Amino Acids	2-Aminobutyrate	HMDB00650	2	y	n	n1
	5-Aminolevulinate	HMDB01149	2	y	n	n1
	Alanine	HMDB00161	1	y	y	y
	Asparagine	HMDB00168	2	y	n	n2
	Creatine	HMDB00064	1	y	y	y
	Creatinine	HMDB00562	1	y	y	n2
	Glutamine	HMDB00641	1	y	y	y
	Glycine	HMDB00123	1	y	y	y
	Guanidoacetate	HMDB00128	2	y	n	n1
	Histidine	HMDB00177	1	y	y	n2
	Isoleucine	HMDB00172	1	y	y	y
	Leucine	HMDB00687	1	y	y	y
	Lysine	HMDB00182	1	y	y	y
	Methionine	HMDB00696	1	y	y	n2
	n-acetylaminoacid	-	3	y	n	n1
	Ornithine	HMDB00214	1	y	y	n2
	Phenylalanine	HMDB00159	1	y	y	y
	Proline	HMDB00162	1	y	y	n2
	Sarcosine	HMDB00271	2	y	n	n2
	Threonine	HMDB00167	1	y	y	y
	Tyrosine	HMDB00158	1	y	y	n2
	Valine	HMDB00883	1	y	y	y
Fatty and Organic Acids	2-Hydroxybutyrate	HMDB00729	2	y	n	n1
	3-Hydroxybutyrate	HMDB00357	2	y	n	n1

	3-Hydroxyisovalerate	HMDB00754	2	y	n	n1
	Acetate	HMDB00042	1	y	y	y
	Acetoacetate	HMDB00060	2	y	n	n1
	Carnitine	HMDB00062	2	y	n	n1
	Citrate	HMDB00094	1	y	y	n2
	Formate	HMDB00142	2	y	n	n1
	Lactate	HMDB00190	1	y	y	y
	Malonate	HMDB00691	2	y	n	n2
	Pyruvate	HMDB00243	1	y	y	n2
	Taurine	HMDB00251	1	y	y	n2
Sugars	Acetylated-saccharide	-	3	y	y	y
	Glucose	HMDB00122	1	y	y	y
	Glycerol	HMDB00131	1	y	y	y
	Mannose	HMDB00169	1	y	y	y
	Myoinositol	HMDB00211	1	y	y	n2
Other	Acetylcholine	HMDB00895	2	y	n	n1
	Adenosine	HMDB00050	2	y	n	n1
	Choline	HMDB00097	1	y	y	y
	Dimethylamine	HMDB00087	1	y	y	y
	Ethanol	HMDB00108	1	y	y	y
	Isopropanol	HMDB00863	2	y	n	n1
	Mobile-lipid	-	3	y	n	n1
	o-Phosphocholine	HMDB01565	2	y	n	n2
	Oxypurinol	HMDB00086	2	y	n	n1
	sn-Glycero-3-phosphocholine	HMDB00086	2	y	n	n1
	Xanthine	HMDB00292	2	y	n	n2

Abbreviation: HSQC = Heteronuclear single quantum coherence

6. Manuscript 5

Synovial Fluid Metabolites Differentiate between Septic and Nonseptic Joint Pathologies

James R Anderson[1], Marie M Phelan[2,3], Peter D Clegg[1], Mandy J Peffers[1]* and Luis M Rubio-Martinez[1,4]*

[1]Institute of Ageing and Chronic Disease, University of Liverpool, Liverpool, UK
[2]Institute of Integrative Biology, University of Liverpool, Liverpool, UK
[3]HLS Technology Directorate, University of Liverpool, Liverpool, UK
[4]Institute of Veterinary Science, University of Liverpool, Leahurst Campus, Neston, UK

*corresponding authors

Keywords

Metabolomics, Equine, Synovial Fluid, Osteoarthritis, Osteochondrosis, Sepsis, Nuclear Magnetic Resonance

Declaration of Author Contributions

Dr Marie Phelan provided training in NMR spectral acquisition and training in NMR spectral analysis. Dr Luis Rubio-Martinez collected synovial fluid samples and co-supervised the study. Professor Peter Clegg and Professor Mandy Peffers also co-supervised the study and advised on experimental design. All other work was conducted by Mr James Anderson.

6.1. Abstract

Osteoarthritis (OA), osteochondrosis (OC) and synovial sepsis in horses cause loss of function and pain. Reliable biomarkers are required to achieve accurate and rapid diagnosis, with synovial fluid (SF) holding a unique source of biochemical information. Nuclear magnetic resonance (NMR) spectroscopy allows global metabolite analysis of a small volume of SF, with minimal sample preprocessing using a noninvasive and nondestructive method. Equine SF metabolic profiles from both nonseptic joints (OA and OC) and septic joints were analysed using 1D ^{1}H NMR spectroscopy. Univariate and multivariate statistical analyses were used to identify differential metabolite abundance between groups. Metabolites were annotated via ^{1}H NMR using 1D NMR identification software Chenomx, with identities confirmed using 1D ^{1}H and 2D ^{1}H ^{13}C NMR (Supplementary Figure 1). Multivariate analysis identified separation between septic and nonseptic groups. Acetate, alanine, citrate, creatine phosphate, creatinine, glucose, glutamate, glutamine, glycine, phenylalanine, pyruvate and valine were higher in the nonseptic group, while glycylproline was higher in sepsis. Multivariate separation was primarily driven by glucose; however, partial-least-squares discriminant analysis plots with glucose excluded demonstrated the remaining metabolites were still able to discriminate the groups. This study demonstrates that a panel of synovial metabolites can distinguish between septic and nonseptic equine SF, with glucose the principal discriminator.

6.2. Introduction

Conditions affecting the articular joints are common in horses resulting in loss of function, pain and/or subsequent inability to work, all of which represent economic and welfare concerns. These pathologies include osteoarthritis (OA), osteochondrosis (OC) and synovial sepsis, which can be life-threatening (Summerhays, 2000). Despite these conditions having a high prevalence and clinical relevance, diagnosis, staging, monitoring and determination of an accurate prognosis remain challenging for practising veterinarians. Therefore, in order to differentiate equine articular joint pathologies, there is a need to identify reliable biomarkers of disease. Synovial fluid (SF) is located within the articular joint cavity, providing a pool of nutrients for surrounding tissues but primarily serving as a biological lubricant, containing molecules with low-friction and low-wear properties to articular surfaces (Blewis *et al.*, 2007). As SF is in close proximity to articular tissues primarily altered during joint pathology, this biofluid is an important source of biomarker discovery (Mateos *et al.*, 2012; Ruiz-Romero and Blanco, 2010).

To date, no validated markers that are both sensitive and specific to synovial sepsis have been identified within veterinary medicine, making early diagnosis a challenge. Together with clinical examination, diagnosis is based on SF culture and intracellular bacteria identification (both low sensitivity) as well as total protein, total nucleated cell count and percentage of neutrophils whose results are open to interpretation and are affected by standard treatment protocols (Robinson *et al.*, 2017; Sanchez-Teran, Bracamonte, Hendrick, Burguess, *et al.*, 2016; Sanchez-Teran, Bracamonte, Hendrick, Riddell, *et al.*, 2016; Sanchez Teran *et al.*, 2012). Reduced levels of glucose in human and equine SF, due to an increase in synovial and neutrophil cell glycolytic activity in severe inflammation or infection, have previously been identified, with a serum-synovial glucose difference of > 2.2 mmol/L considered supportive of a diagnosis of synovial sepsis (Krey and Bailen, 1979; Roberts *et al.*, 1967). However, this parameter is nonspecific and can be influenced by multiple variables, including synovial necrosis, diet, pain and white blood cell count. Elevations in lactate during the acute infection phase have previously been identified in SF of septic human, canine and equine joints, due to an increase in the consumption of glucose and

subsequent production of lactate within an anaerobic environment (Gobelet and Gerster, 1984; Proot *et al.*, 2015; Tulamo *et al.*, 1989). However, other studies have not been able to differentiate septic and nonseptic arthropathies based on lactate levels alone (Arthur *et al.*, 1983; Washington, 1980). Synovial D-lactate (produced via bacterial fermentation and a stereoisomer of mammalian L-lactate) was recently found to be unable to aid diagnosis of equine synovial sepsis (Robinson *et al.*, 2017).

At present, no specific biomarkers have been identified for equine OA with none currently used as a diagnostic aid in clinical practice. Potential OA markers of interest include cartilage oligomeric matrix protein (COMP) and matrix metalloproteinases (MMPs), which have both been identified as elevated in human OA SF (Balakrishnan *et al.*, 2014). Although detection of active MMPs in horses has demonstrated important potential in diagnosis, conversely, decreased levels of COMP have been identified in equine OA and found unable to stage the disease (Taylor *et al.*, 2006; Zrimsek *et al.*, 2007). In equine OC, elevated levels of a C-propeptide of cartilage type II procollagen and osteocalcin have shown potential as a diagnostic aid, although these markers have not translated to clinical practice (Billinghurst *et al.*, 2004; Donabedian *et al.*, 2008; Laverty *et al.*, 2000). However, these protein markers identify pathology following significant cartilage degradation and bone remodelling opposed to an early disease state where potential intervention would prove most beneficial.

Metabolomics encompasses the comprehensive profiling of metabolic changes, including the study of metabolic pathways and quantification of unique biochemical molecules, within living systems (Wang, Zhang, *et al.*, 2012). These small molecule metabolites include metabolic intermediates, secondary metabolites, hormones and other signalling molecules (Jukarainen, 2009). A major advantage of nuclear magnetic resonance (NMR) spectroscopy over other techniques, that is, mass spectrometry, is the analysis of native samples with a minimal level of sample preparation using a noninvasive and nondestructive method, subsequently producing results which are more reproducible and robust (Keun and Athersuch, 2011). Thus this methodology holds huge potential in the analysis of biofluids to characterise the global metabolic profiles of various pathologies (de Sousa *et al.*,

2017). Hugle *et al.* previously carried out NMR spectroscopy using human SF, identifying that septic arthritis SF could be distinguished from nonseptic arthritis SF via principal component analysis (PCA), although they were unable to identify the specific metabolites responsible for this discrimination (Hugle *et al.*, 2012). To date, only one peer reviewed publication has used NMR to investigate the whole metabolic profile of equine SF, comparing normal and osteoarthritic SF (Lacitignola *et al.*, 2008). Lacitignola *et al.* identified ten differentially abundant metabolites which included elevated levels of glucose and lactate in OA. No studies have analysed equine SF using NMR to investigate synovial sepsis or OC, concurrently analysed the metabolic profiles of multiple equine articular pathologies or used multivariate analysis to investigate the metabolic profile as a whole.

In this study we have used global metabolite identification using ^{1}H NMR to identify potential metabolite biomarkers that allow differentiation between equine articular joint pathologies, potentially aiding accurate diagnosis.

6.3. Methods

6.3.1. Patient Groups and Synovial Fluid Collection

Following ethical approval and owner consent, excess aspirated SF (collected during clinical diagnostic investigations) was analysed from joints of horses presenting to The Philip Leverhulme Equine Hospital, University of Liverpool between 2014 and 2016. SF was aspirated for diagnostic purposes from the affected joints at the start of surgical arthroscopy under general anaesthesia with 500 µl of excess SF submitted for NMR metabolomic analysis. Pathological joints included the femorotibial, glenohumeral, metacarpophalangeal, metatarsophalangeal and tarsocrural joints. Horses were divided into two main groups of joint pathology, septic and nonseptic. The septic group was subdivided into six horses with synovial sepsis following a local penetrating wound and one foal diagnosed with synovial sepsis secondary to haematogenous spread. The nonseptic group consisted of four horses diagnosed with OA, two with meniscal tears and concurrent OA (MT) and six with OC. Diagnoses were determined via a combination of radiography, ultrasonography, arthroscopy and SF total protein, cytology and/or bacterial culture

as previously described (Robinson *et al.*, 2017). SF was immediately placed into uncoated 1.5 ml collection tubes and processed within 1 hr of collection. Particulate and cells were removed from the SF by centrifugation (4^{o}C, 2540*g* for 5 min) and then the cell-free supernatant transferred to a clean uncoated 1.5 ml collection tube, snap-frozen using liquid nitrogen and stored at -80^{o}C. Samples were spun to ensure removal of cellular debris which was critical to eliminate variance due to bacterial contamination in septic joints. To ascertain the most reproducible and robust collection protocol, biologically identical SF underwent ± centrifugation and supernatant removal followed by freezing using various methods at different temperatures. Multivariate statistical analysis of these samples indicated that the above method was most robust at reducing variance due to sample handling/processing (Chapter 2).

6.3.2. Sample Preparation

NMR samples were prepared within 48 hrs of acquisition. A 300 µl sample of thawed SF was diluted to a final volume containing 50% (v/v) SF, 40% (v/v) dd $^{1}H_2O$ (18.2 MΩ), 10% (v/v) 1 M PO_4^{3-} pH 7.4 buffer (Na_2HPO_4, VWR International Ltd., Radnor, Pennsylvania, USA and NaH_2PO_4, Sigma-Aldrich, Gillingham, UK) in deuterium oxide ($^{2}H_2O$, Sigma-Aldrich) and 0.0025% (v/v) sodium azide (NaN_3, Sigma-Aldrich). Samples were vortexed for 1 min, centrifuged at 13,000*g* and 4˚C for 2 min and 590 µl transferred (taking care not to disturb any pelleted material) into 5 mm outer diameter NMR tubes using a glass pipette.

6.3.3. NMR Acquisition

All SF samples were analysed individually. One dimensional ^{1}H NMR spectra, with Carr-Purcell-Meiboom-Gill (CPMG) filter to attenuate signals from macromolecules such as albumins, were acquired using a standard vendor pulse sequence (cpmgpr1d) on a 600 MHz NMR Bruker Avance III spectrometer with a TCI cryoprobe and chilled Sample-Jet autosampler. Spectra were acquired at 25˚C, with a 4 s interscan delay, 32 transients and a 15 ppm spectral width. Software for acquisition and processing was carried out using Topsin 3.1 and IconNMR 4.6.7 with

automated phasing and baseline correction and a standard vendor processing routine (exponential window function with 0.3 Hz line broadening).

6.3.4. Metabolite Annotation and Identification

All spectra were scrutinised to ensure spectra met community recommended quality control criteria prior to inclusion in statistical analysis (Sumner *et al.*, 2007). Quality control criteria included a flat baseline, water signal less than 0.4 ppm wide and line-width half heights of representative beta anomeric glucose doublet all within one standard deviation. Spectra were then divided into spectral regions or 'buckets' according to metabolite annotation from Chenomx NMR Suite 8.2 (330-mammalian metabolite library) with buckets attributed to multiple metabolites where peaks were found to overlap. Each spectrum was divided into 306 buckets with the intensity of each bucket divided by the bucket width to negate the intensity variance. Buckets were normalised to the median and Pareto scaled prior to statistical treatment. Metabolites annotated in Chenomx were also confirmed by a mixture of ^{1}H 1D NMR and, where possible, to in-house 2D ^{1}H ^{13}C Heteronuclear Single Quantum Coherence NMR standards. Spectra and metabolite assignments including HMDB IDs and annotation level are all available in the Metabolights repository (www.ebi.ac.uk/metabolights/MTBLS543) and shown in Table 2 (Salek *et al.*, 2013). Among the metabolites identified was ethanol, likely through contamination during SF aspiration following surgical sterilisation. Therefore, for multivariate analysis the buckets attributed to ethanol were omitted.

6.3.5. Statistical Analysis

SF spectra were divided into two groups: nonseptic and septic. Further separation of the groups was not possible due to limited sample number in this study. t-tests and partial-least-squares discriminant analysis (PLS-DA) were carried out using MetaboAnalyst 3.5 (http://www.metaboanalyst.ca) which uses the R package of statistical computing software (Xia *et al.*, 2016). For t-tests, $p < 0.05$ was considered statistically significant following correction for multiple testing using the Benjamini-Hochberg false discovery rate method (Benjamini and Hochberg, 1995). Box plots were carried out using the software package SPSS 22. Quantile and PCA plots were

produced using standard analytical routines in the software package R (https://cran.r-project.org/).

6.4. Results

6.4.1. Group Limitations

The patient groups were restricted to two main groups; septic or nonseptic (Table 1) due to a lack of sufficient cases of differing subdiagnoses. The joints from which each sample was collected were noted, however, without a larger study size no separate grouping for differing joints was attempted.

Table 1. Further clinical characteristics of group patients.

	Main Groups		Subgroups				
			Septic		Nonseptic		
	Septic	Nonseptic	Wound Sepsis	Haematogenous Sepsis	OA	MT with OA	OC
Number	7	12	6	1	4	2	6
Mean Age	6 years 10 months	7 years 7 months	7 years 11 months	0 years 2 months	10 years 6 months	12 years 0 months	4 years 6 months
Sex	7M	6F, 6M	6M	1M	1F, 3M	1F, 1M	4F, 2M
Joint	1 x GH 1 x MCP 1 x MTP 4 x TC	2 x GH 3 x MCP 4 x FT 1 x MTP 2 x TC	1 x MCP 1 x MTP 4 x TC	1 x GH	2 x GH 1 x FT 1 x MTP	2 x FT	3 x MCP 1 x FT 2 x TC

Abbreviations: Groups, OA = Osteoarthritis, MT = Meniscal tear and concurrent OA, OC = Osteochrondrosis; Sex, M = Male, F = Female; Joints, GH = Glenohumeral, MCP = Metacarpophalangeal. FT = Femorotibial, MTP = Metatarsophalangeal and TC = Tarsocrural.

6.4.2. Metabolite Annotation and Identification

NMR spectra for all groups showed a consistent set of metabolite signals present with multiple metabolites identified from 1D multiplet pattern overlap (Figure 1). The metabolite abundances within the septic group were less variable than the nonseptic group, which is perhaps expected given the nonseptic group included samples from two separate diagnoses (OA and OC). Of the 306 spectral bins in each extract, 203 (66%) were annotated to 71 metabolites, with identification confirmed for 55 of these metabolites (Table 2).

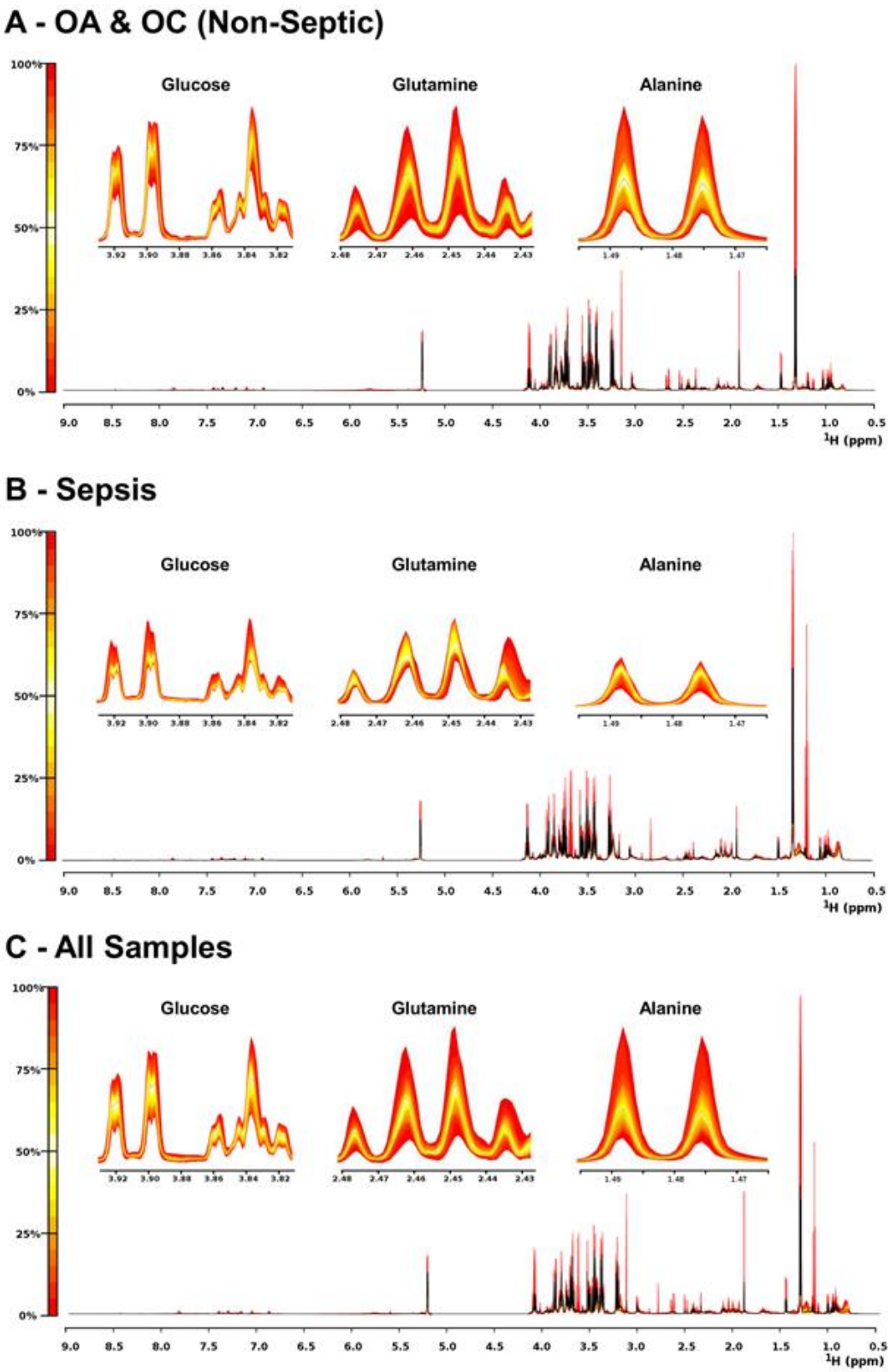

Figure 1. Quantile plots of osteoarthritis (OA)/osteochondrosis (OC) (nonseptic, n=12), sepsis (n=7) and all spectra (n=19) depicting the median spectral plot (black line) and variation from the median within each group (yellow to red scale) for the full spectral range (9.0 - 0.5 ppm) and more detailed regions depicting selected peaks from three differentially abundant metabolites, glucose, glutamine and alanine. Variation within the full spectra can most clearly be seen at 0.8 ppm.

Table 2. Metabolites annotated in synovial fluid by Chenomx, metabolites subsequently identified using an in-house library are indicated by the Metabolomics Standards Initiative (MSI) level 1 (Salek *et al.*, 2013).

Database Identifier	Metabolite Identification	Reliability
HMDB00001	1-Methylhistidine	MS Level 2
HMDB59655	2-Hydroxyglutarate	MS Level 2
HMDB11743	2-Phenylpropionate	MS Level 2
HMDB00357	3-Hydroxybutyrate	MS Level 2
HMDB00355	3-Hydroxymethylglutarate	MS Level 2
HMDB01149	5-Aminolevulinate	MS Level 2
HMDB00042	Acetate	MS Level 1
HMDB00060	Acetoacetate	MS Level 2
HMDB01890	Acetylcysteine	MS Level 2
HMDB01432	Agmatine	MS Level 2
HMDB00729	Alpha-Hydroxyisobutyrate	MS Level 2
HMDB00186	Alpha-Lactose	MS Level 2
HMDB00043	Betaine	MS Level 1
HMDB00030	Biotin	MS Level 1
HMDB00094	Citrate	MS Level 1
HMDB00064	Creatine	MS Level 1
HMDB00562	Creatinine	MS Level 1
HMDB00143	D-Galactose	MS Level 2
HMDB00122	D-Glucose	MS Level 1
HMDB00108	Ethanol	MS Level 1
HMDB00142	Formate	MS Level 2
HMDB00663	Glucarate	MS Level 2
HMDB01401	Glucose 6-phosphate	MS Level 2
HMDB00131	Glycerol	MS Level 1
HMDB00123	Glycine	MS Level 1
HMDB00721	Glycylproline	MS Level 2
HMDB00128	Guanidoacetate	MS Level 2
HMDB00870	Histamine	MS Level 2
HMDB00764	Hydrocinnamate	MS Level 2
HMDB00678	Isovalerylglycine	MS Level 2
HMDB00190	Lactate	MS Level 1
HMDB00161	L-Alanine	MS Level 1
HMDB00646	L-Arabinose	MS Level 2
HMDB00062	L-Carnitine	MS Level 2
HMDB00174	L-Fucose	MS Level 2
HMDB00148	L-Glutamate	MS Level 1
HMDB00641	L-Glutamine	MS Level 1
HMDB00177	L-Histidine	MS Level 1

HMDB00687	L-Leucine	MS Level 1
HMDB00159	L-Phenylalanine	MS Level 1
HMDB00167	L-Threonine	MS Level 2
HMDB00158	L-Tyrosine	MS Level 1
HMDB00883	L-Valine	MS Level 1
HMDB01389	Melatonin	MS Level 2
HMDB01238	N-Acetylserotonin	MS Level 2
HMDB02055	o-Cresol	MS Level 2
HMDB00210	Pantothenic acid	MS Level 2
HMDB00821	Phenylacetylglycine	MS Level 2
HMDB01511	Phosphocreatine	MS Level 2
HMDB00239	Pyridoxine	MS Level 2
HMDB00243	Pyruvate	MS Level 1
HMDB00635	Succinylacetone	MS Level 2
HMDB00262	Thymine	MS Level 1
HMDB01878	Thymol	MS Level 2
HMDB00294	Urea	MS Level 1

6.4.3. Statistical Analysis and Differentially Abundant Metabolites

Of the 306 identified peaks, 180 were found to be differentially abundant between septic and nonseptic groups when analysed using a univariate t-test, $p < 0.05$, with 98 peaks assigned to 26 different metabolites (Supplementary Table 1).

Unsupervised multivariate analysis (PCA) identified clear variance between spectra from septic and nonseptic joint pathologies, forming two distinct clusters (Figure 2). Ninety-five percent of the variance was explained by seven principal components (PCs) with PC1 and PC2 explaining a combined 71.89% of variance within the data. Although the analysis between groups was limited to a binary diagnosis (septic vs nonseptic) to explore the variance in metabolite profile for SF aspirated from horses with differing underlying conditions, the PCA score plots were coloured in terms of either main diagnosis (Binary) or subdiagnosis (five groups). Within the nonseptic group, samples obtained from joints with OA and associated meniscal tears were found to cluster together. In addition, despite a separate aetiology, SF obtained from a foal with haematogenous sepsis clustered with SF collected from joints diagnosed with sepsis subsequent to penetrating wounds.

Supervised multivariate discriminant analysis using PLS-DA plots of the known metabolites indicated that the variance was heavily influenced by glucose (Figure 3a and b), with 23 of the 25 most influential buckets attributed to glucose peaks. The optimal model comprised two components with reasonable predictive power (R^2 = 0.85, Q^2 = 0.72). Omitting glucose signals from the analysis gave rise to a somewhat lower predictive model (R^2 = 0.70, Q^2 = 0.45, fit with 1 component) (Figure 3c). From the glucose free model, metabolites acetate, glycylproline, glycine, citrate, creatinine and alanine were among the most influential (Figure 3d).

Both univariate and multivariate analysis were compared to identify differentially abundant metabolites. Metabolite peaks identified as either significantly different ($p < 0.05$) via t-test or in the top 25 variables of influence (VIP) via glucose excluded PLS-DA were then attributed to a genuine differentially abundant metabolite change if the individual metabolite peak changes correlated. In total a panel of 13 metabolites were identified as being differentially abundant between septic and nonseptic groups. Acetate, alanine, citrate, creatine phosphate, creatinine, glucose, glutamate, glutamine, glycine, phenylalanine, pyruvate and valine were higher in the nonseptic group whilst glycylproline was higher in synovial sepsis (Figure 4).

PCA analysis of OA and OC subgroups suggested that, bar one sample, they may cluster separately and may therefore demonstrate distinctive metabolomes. However, with this modest group size no significant differences in metabolites ($p < 0.05$) were identified by univariate analysis (data not shown).

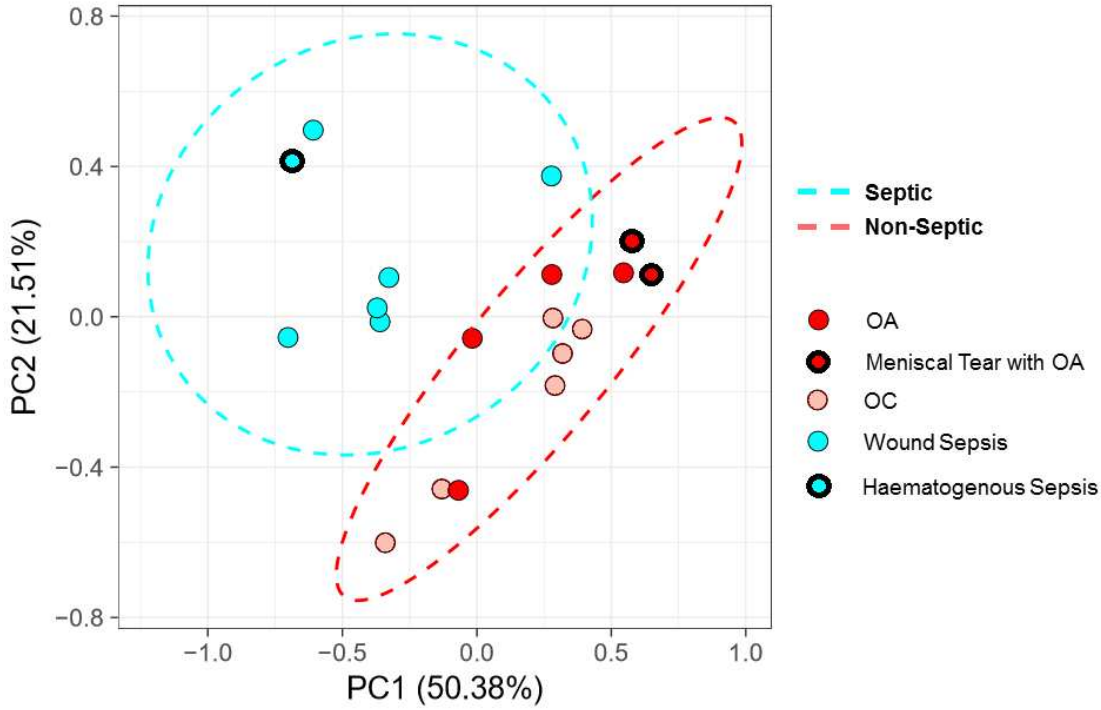

Figure 2. Principal component analysis (PCA) scores plot of septic (blue, n=7) and nonseptic (red, n=12) synovial fluid ^{1}H NMR metabolomes. Samples with meniscal tear or haematogenous sepsis subdiagnoses for osteoarthritis (OA) and sepsis, respectively, are highlighted in each group with a thick black outline, osteochondrosis (OC) are distinguished from OA by highlight shade.

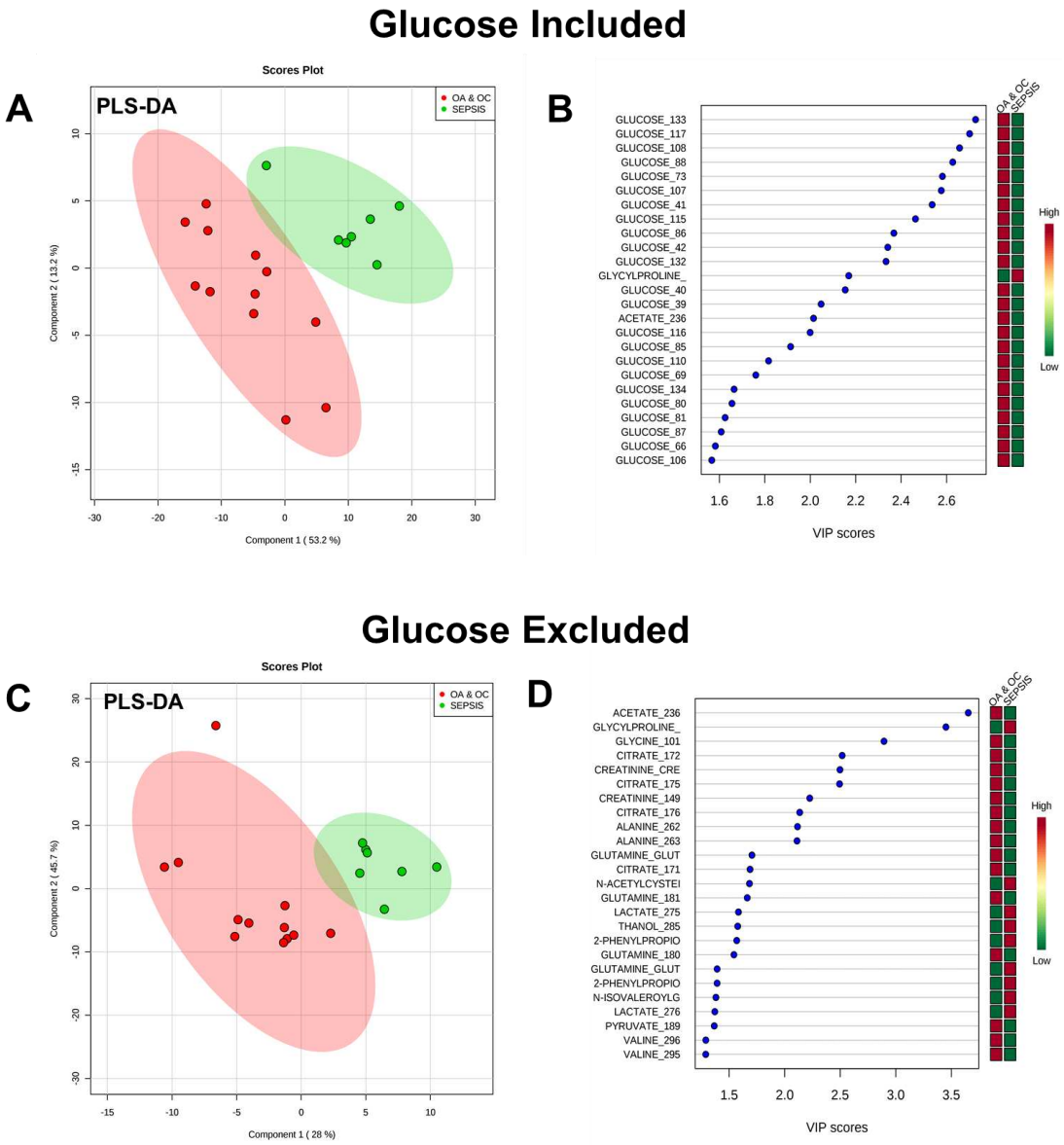

Figure 3. (a) PLS-DA plots of osteoarthritis (OA)/osteochondrosis (OC) (n=12) versus sepsis (n=7) using only metabolite annotated buckets: first two components shown out of a total of two components used to fit the model (R^2 = 0.85, Q^2 = 0.72). (b) VIP scores for the 25 most influential buckets of PLS-DA. (c) PLS-DA plots of OA/OC versus sepsis using only metabolite annotated/identified buckets with all glucose buckets excluded: first two components shown. It should be noted that only one component was used to fit the model (R^2 = 0.70, Q^2 = 0.45). (d) VIP scores for the 25 most influential buckets of glucose-excluded PLS-DA.

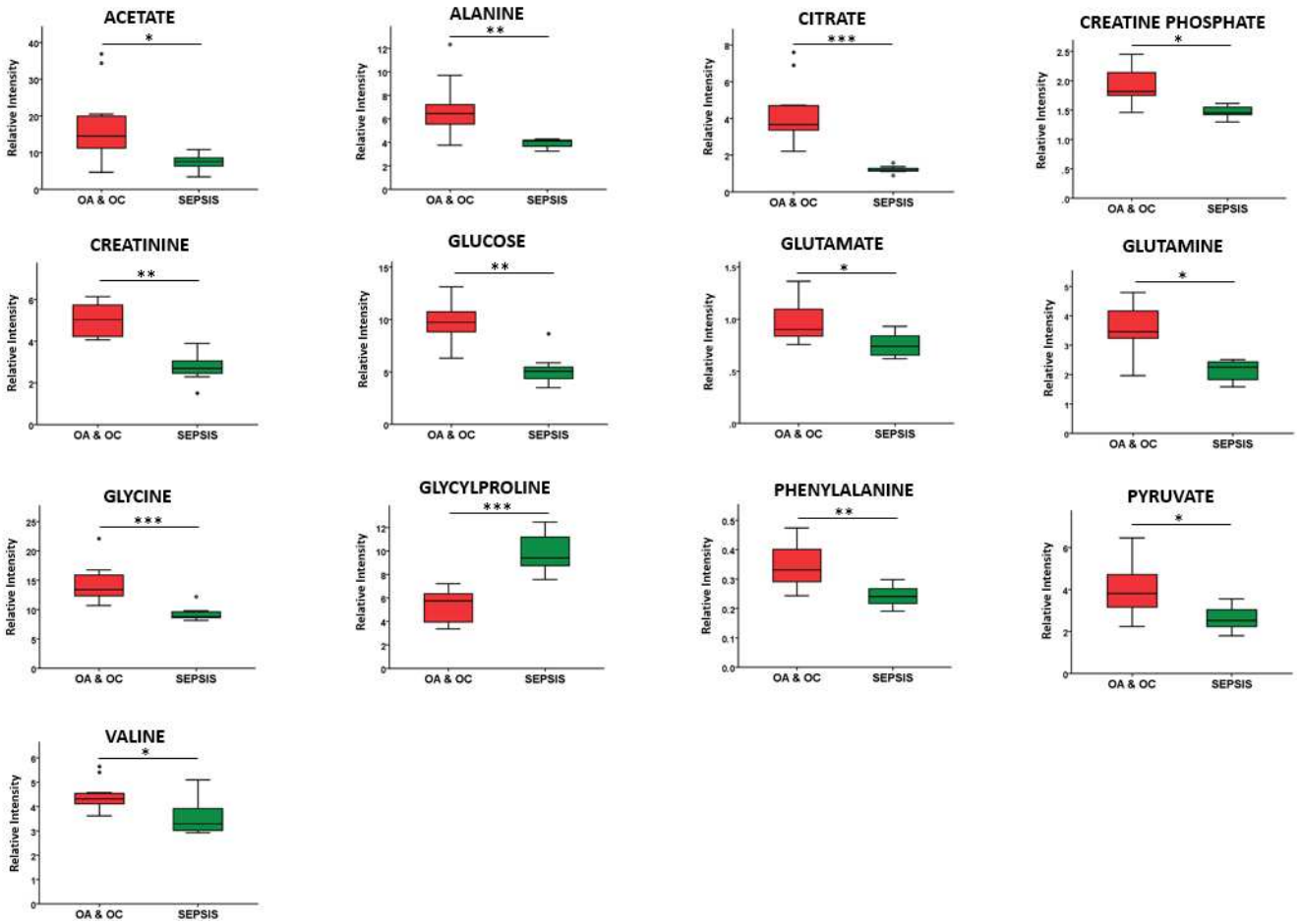

Figure 4. Boxplots of key synovial metabolites differentiating septic (n=7) and nonseptic (osteoarthritis (OA) and osteochondrosis (OC), n=12) articular pathologies, shown as relative intensities corresponding to the most representative peak for each metabolite. t-test: * = $p < 0.05$, ** = $p < 0.01$ and *** = $p < 0.001$.

6.5. Discussion

Despite OA, OC and synovial sepsis having a high prevalence and clinical relevance, diagnosis, staging, monitoring and determination of an accurate prognosis remain challenging for practising veterinarians. Therefore, to differentiate equine articular joint pathologies, there is a need to identify reliable biomarkers of disease. To aid equine synovial sepsis diagnosis, currently recognised markers of glucose and lactate are considered to be nonspecific and unreliable respectively (Arthur *et al.*, 1983; Tulamo *et al.*, 1989). In addition, clinically assessing response to treatment of septic joints can be challenging, with differentiating horses with continued lameness from a nonresolving sepsis to those with a resolving sepsis but ongoing significant inflammation, difficult. Therefore, reliable metabolic markers of sepsis may aid as part of a longitudinal clinical assessment.

In this study it has been shown that the metabolite profile of equine SF is able to discriminate between septic and nonseptic joint pathologies. A panel of 13 metabolites was identified which were differentially abundant between these two groups. These metabolites may in turn prove beneficial in an equine clinical setting as a diagnostic aid as well as monitoring response to treatment and assessing prognosis. Ideally this could be carried out through field tests, similar to those produced and used for equine biofluids for metabolites glucose and lactate, urinalysis and the protein inflammatory marker serum amyloid A (Hackett and McCue, 2010; Kobayashi, 2007; Savage, 2008; Stack *et al.*, 2014). No metabolite abundances were identified to be statistically different between OA and OC subgroups. However, the PCA analysis suggested that, bar one sample, OC and OA metabolite profiles were different and thus may demonstrate distinctive metabolomes sufficient to apply robust statistical models such as PLS-DA. This can only be tested with a larger sample size which was not possible on this modest subset of patients.

The PLS-DA VIP scores revealed spectral peaks assigned to glucose were highly represented as a discriminant of joint sepsis (23/25 of the most influential peaks). Reduced levels of glucose in human and equine SF, due to an increase in synovial

and neutrophil cell glycolytic activity in severe inflammation or infection, have previously been identified, with a serum-synovial glucose difference of >2.2 mmol/L considered supportive of a diagnosis of synovial sepsis (Krey and Bailen, 1979; Roberts *et al.*, 1967). Glucose is, however, a nonspecific parameter and can be influenced by multiple other variables (Tulamo *et al.*, 1989). However, PLS-DA analysis with all glucose influenced spectral peaks omitted revealed there to still be a modest separation between the groups, thus indicating the differentiated metabolomes are driven by a panel of metabolites and potential septic markers, opposed to glucose alone.

Previous studies have described mixed results as to whether elevated synovial lactate can be used to help distinguish synovial sepsis (Arthur *et al.*, 1983; Gobelet and Gerster, 1984; Tulamo *et al.*, 1989; Washington, 1980). In this study we did not identify lactate abundance to be different between the septic and nonseptic groups, therefore providing further evidence that lactate is an unreliable marker for synovial sepsis. ^{1}H NMR spectroscopy is not able to distinguish D-lactate from L-lactate and consequently we are unable to draw any conclusions on the specific levels of bacterially derived D-lactate within the groups.

In this study the majority of differentially abundant metabolites were found to be reduced in sepsis compared to the nonseptic group. However, glycylproline was elevated in synovial sepsis. Glycylproline is a dipeptide end product of the catabolism of collagen (Le *et al.*, 1999). Following synovial infection and an insufficient immunological response, collagen catabolism is upregulated through a high cytokine concentration increasing the release of matrix metalloproteinases and other collagen-degrading enzymes from within the host (Shirtliff and Mader, 2002). Elevated levels in markers of collagen destruction in synovial sepsis over nonseptic joint pathologies have been identified previously, with one study demonstrating increased synovial levels of the collagen degradation marker cross-linked C-telopeptide fragments of type II collagen (CTX-II) in longitudinal samples of a patient with septic arthritis compared to osteoarthritic patients' SF (Lohmander *et al.*, 2003). Thus glycylproline, in combination with other metabolite/protein derived markers of collagen catabolism, may aid clinical diagnosis of synovial sepsis.

Following on from this study, further investigation using mass spectrometry analysis would complement these results as the identified degradation of extracellular matrix may provide lipid and carbohydrate profiles of interest.

All raw NMR spectral data and associated annotations that contributed to this study have been deposited with the open access online repository Metabolights, curated by the European Bioinformatics Institute (EBI), including acquisition and processing parameters with all metabolites identified clearly reported. The authors feel this transparent, gold standard approach to data submission to independent bioinformatics specialists, such as the EBI, should be further encouraged within the NMR metabolomics field, in line with other 'omics' journal submissions.

6.5.1. Study Limitations

Modest sample size prohibited further analysis of metabolome differences between OA and OC or between wound sepsis and haematogenous sepsis. Similarly, SF with OA and associated meniscal tears were found to cluster together although we are unable to conclude that SF collected from femorotibial joints with meniscal tears form a distinct metabolome as only two samples were available for inclusion within this study. This is of particular interest as a diagnostic aid for meniscal tears would have a practical clinical implication within veterinary medicine which could also translate to human medicine. It is our hope that additional studies will provide further information and enable more stringent analyses to be undertaken. Furthermore, because of limited sample size, SF was aspirated from a range of joints which may lead to variation in data due to biomechanical differences between joints. Again, a larger sample size would enable a greater understanding as to what influence joint location has on the metabolome and a stricter control of site of sample collection (if necessary) and thus enable further information to be extracted from the metabolic profiles. In addition, during the joint pathologies studied there are likely to be changes to management of the animal, particularly exercise and diet, which may alter the metabolome of SF, although this influence is likely to be minimal compared to the significant metabolic influence of the localised joint pathology.

During this study we were unable to compare the SF of the joint pathologies of interest to a normal group. In equine clinical practice only pathological joints are aspirated during diagnostic investigations. Post mortem SF cannot be defined as having a normal metabolome due to the anaerobic changes that take place following death, including artefactual changes in the abundance of glucose and lactate, two key metabolites of interest during sepsis.

6.5.2. Conclusion

This paper is the first to use NMR-led metabolomics to analyse equine SF with multiple pathologies and demonstrates that NMR-led metabolomics is an effective technique for analysis of equine SF collected within a clinical veterinary environment. Furthermore, this study demonstrates a panel of synovial metabolites that can distinguish between septic and nonseptic equine SF, with glucose the principal discriminator. To translate this into a diagnostic aid, a wider study with participants with less common diagnoses is required to improve the diagnostic power.

6.6. Ethics

University of Liverpool Ethics approval ref: VREC175

6.7. Funding

The project was funded by a Veterinary School Research Project Support Grant (VSRP VET016) and the Technology Directorate voucher scheme (www.liverpool.ac.uk/technology-directorate), University of Liverpool. Professor Mandy Peffers is funded through a Wellcome Trust Intermediate Clinical Fellowship (107471/Z/15/Z) and Mr James Anderson through a Horse Trust PhD studentship (G1015). Software licences for data analysis used in the Shared Research Facility for NMR metabolomics were funded by the MRC Clinical Research Capabilities and Technologies Initiative (MR/M009114/1).

6.8. Acknowledgements

The authors are grateful for the use of R scripts written by Dr A Grauslys, Dr E

Caamano Gutierrez (Computational Biology Facility) and Mr R Grosman (NMR metabolomics facility) at the University of Liverpool and staff at the Philip Leverhulme Equine Hospital, University of Liverpool, for their involvement with sample collection.

6.9. Supplementary Information

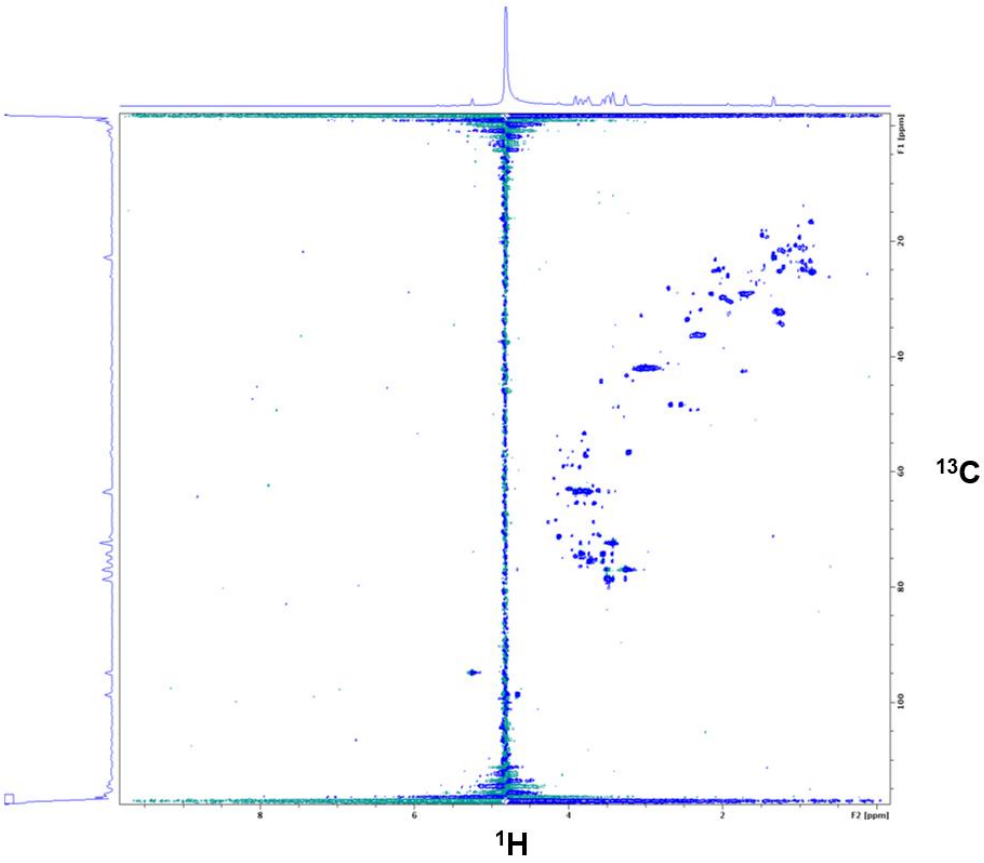

Supplementary Figure 1. Equine synovial fluid 2D NMR ^{1}H ^{13}C Heteronuclear Single Quantum Coherence (HSQC) spectrum used for metabolite identifications. x axis = ^{1}H, y axis = ^{13}C. n = 1.

Supplementary Table 1. Statistically significant differentially abundant peaks between septic and non-septic equine synovial fluid. t-test, $p < 0.05$.

Metabolite	Pattern File Peak Number	Peak Number	p value	Fold Change	Mean Fold Change	Median Fold Change
2-HYDROXYGLUTARATE	207	1	4.09E-06	0.61	0.61	0.61
3-HYDROXY-3-METHYLGLUTARATE	183	1	0.00723	1.56	1.56	1.56
3-HYDROXYBUTYRATE	188	1	0.00207	1.42	1.42	1.42
ACETATE	236	1	0.01926	2.32	2.32	2.32
AGMATINE	148	1	0.00388	1.26	1.26	1.26
ALANINE	262	1	0.00510	1.74	1.74	1.74
ALANINE	263	2	0.00400	1.75		
BIOTIN	209	1	0.00005	0.57	0.71	0.73
BIOTIN	210	2	0.00390	0.77		
BIOTIN	211	3	0.02578	0.82		
BIOTIN	267	4	0.00244	0.70		
CITRATE	171	1	0.00051	1.88	3.75	4.13
CITRATE	172	2	0.00011	3.49		
CITRATE	175	3	0.00014	4.76		
CITRATE	176	4	0.00011	4.86		
CREATINE PHOSPHATE	60	1	0.02617	1.23	1.26	1.26
CREATINE PHOSPHATE	61	2	0.00196	1.29		
CREATININE	53	1	0.00598	1.35	1.60	1.60
CREATININE	149	2	5.75E-06	1.84		
GLUCOSE	39	1	0.00247	1.93	1.88	1.91
GLUCOSE	40	2	0.00109	2.04		
GLUCOSE	41	3	0.00313	1.97		
GLUCOSE	42	4	0.00800	1.93		
GLUCOSE	65	5	0.01642	1.69		
GLUCOSE	66	6	0.00436	1.82		
GLUCOSE	68	7	0.01392	1.69		
GLUCOSE	69	8	0.00466	1.84		
GLUCOSE	70	9	0.03247	1.49		
GLUCOSE	71	10	0.00210	1.70		
GLUCOSE	72	11	0.00173	1.64		
GLUCOSE	73	12	0.00149	1.89		
GLUCOSE	74	13	0.00303	1.80		

GLUCOSE	75	14	0.00509	1.75		
GLUCOSE	80	15	0.00055	1.85		
GLUCOSE	81	16	0.00009	1.84		
GLUCOSE	83	17	0.00012	1.76		
GLUCOSE	84	18	0.00014	1.71		
GLUCOSE	85	19	0.00104	1.85		
GLUCOSE	86	20	0.00127	1.91		
GLUCOSE	87	21	0.00209	1.85		
GLUCOSE	88	22	0.00183	1.93		
GLUCOSE	89	23	0.00208	1.81		
GLUCOSE	102	24	0.00173	1.87		
GLUCOSE	103	25	0.00115	1.94		
GLUCOSE	104	26	0.00254	1.87		
GLUCOSE	105	27	0.00129	1.91		
GLUCOSE	106	28	0.00234	1.88		
GLUCOSE	107	29	0.00168	1.95		
GLUCOSE	108	30	0.00163	1.98		
GLUCOSE	109	31	0.00133	2.00		
GLUCOSE	110	32	0.00153	2.00		
GLUCOSE	111	33	0.00128	2.05		
GLUCOSE	112	34	0.00137	2.02		
GLUCOSE	113	35	0.00135	2.05		
GLUCOSE	114	36	0.00115	1.95		
GLUCOSE	115	37	0.00150	1.95		
GLUCOSE	116	38	0.00056	2.06		
GLUCOSE	117	39	0.00110	2.00		
GLUCOSE	118	40	0.00037	2.02		
GLUCOSE	119	41	0.00097	1.98		
GLUCOSE	132	42	0.00010	1.98		
GLUCOSE	133	43	0.00101	1.93		
GLUCOSE	134	44	0.00255	1.69		
GLUCOSE-6-PHOSPHATE	58	1	0.00119	1.37		
GLUCOSE-6-PHOSPHATE	129	2	0.00784	1.36	1.38	1.37
GLUCOSE-6-PHOSPHATE	130	3	0.00227	1.41		
GLUTAMATE	197	1	0.01746	1.29	1.29	1.29
GLUTAMINE	180	1	0.00037	1.66		
GLUTAMINE	181	2	0.00018	1.69	1.34	1.5
GLUTAMINE	182	3	0.04998	1.33		

GLUTAMINE	219	4	0.00001	0.66		
GLYCINE	101	1	0.00091	1.53	1.53	1.53
GLYCYLPROLINE	232	1	0.00017	0.77	0.66	0.66
GLYCYLPROLINE	233	2	7.46E-06	0.54		
HISTIDINE	143	1	0.00353	1.31	1.28	1.28
HISTIDINE	144	2	0.00079	1.25		
LEUCINE	244	1	0.00824	1.27	1.25	1.25
LEUCINE	246	2	0.04653	1.23		
N-ACETYLCYSTEINE	222	1	0.00011	0.65	0.65	0.65
N-ISOVALEROYLGLYCINE	304	1	0.00224	0.80	0.80	0.80
N-PHENYLACETYLGLYCINE	10	1	0.00180	0.55	0.55	0.55
PHENYLALANINE	4	1	0.00291	1.42	1.46	1.49
PHENYLALANINE	5	2	0.00344	1.49		
PHENYLALANINE	6	3	0.00413	1.49		
PI-METHYLHISTIDINE	137	1	0.02448	0.74	0.72	0.74
PI-METHYLHISTIDINE	139	2	0.02026	0.77		
PI-METHYLHISTIDINE	140	3	0.02210	0.66		
PYRUVATE	189	1	0.01229	1.53	1.53	1.53
TYROSINE	21	1	0.01954	1.23	1.45	1.49
TYROSINE	22	2	0.00066	1.41		
TYROSINE	28	3	0.00001	1.58		
TYROSINE	29	4	0.00003	1.57		
VALINE	203	1	0.01526	0.83	1.14	1.21
VALINE	204	2	0.00804	0.82		
VALINE	295	3	0.00179	1.40		
VALINE	296	4	0.00143	1.40		
VALINE	299	5	0.03166	1.19		
VALINE	300	6	0.01854	1.23		

7. Manuscript 6

The Synovial Fluid Proteome Differentiates between Septic and Nonseptic Articular Pathologies

James R Anderson[1], Aibek Smagul[1], Deborah Simpson[2], Peter D Clegg[1], Luis M Rubio-Martinez[1,3], Mandy J Peffers[1]

[1]Institute of Ageing and Chronic Disease, University of Liverpool, Liverpool, UK
[2]Centre for Proteome Research, Institute of Integrative Biology, University of Liverpool, Liverpool, UK
[3]Institute of Veterinary Science, University of Liverpool, Leahurst Campus, Neston, UK

Keywords

Synovial Fluid, Arthropathy, Osteoarthritis, Osteochondrosis, Synovial Sepsis, Equine

Declaration of Author Contributions

Mr Aibek Smagul conducted work using Ingenuity Pathway Analysis software. Dr Deborah Simpson prepared synovial fluid samples and undertook mass spectrometry. Dr Luis Rubio-Martinez collected synovial fluid samples and co-supervised the study. Professor Peter Clegg and Professor Mandy Peffers also co-supervised the study and advised on experimental design. All other work was conducted by Mr James Anderson.

7.1. Abstract

Articular conditions are common in horses and can result in loss of function, pain and/or inability to work. Common conditions include osteoarthritis, osteochondrosis and synovial sepsis, which can be life-threatening, but despite the high clinical prevalence of these conditions, rapid and specific diagnosis, monitoring and prognostication remains a challenge for practicing veterinarians. Synovial fluid from a range of arthropathies was enriched for low abundance proteins using combinatorial peptide ligand ProteoMiner™ beads and analysed via liquid chromatography-tandem mass spectrometry. Changes in protein abundances were analysed using label-free quantification. Principal component analysis of differentially expressed proteins identified groupings associated with joint pathology. Findings were validated using ELISA. Lactotransferrin (LTF) abundance was increased in sepsis compared to all other groups and insulin-like growth factor-binding protein 6 (IGFBP6) abundance decreased in sepsis compared to other disease groups. Pathway analysis identified upregulation of the complement system in synovial joint sepsis and the downregulation of eukaryotic translation initiation factors and mTOR signalling pathways in both osteoarthritis and osteochondrosis compared to the healthy group. Overall, we have identified a catalogue of proteins which we propose to be involved in osteoarthritis, osteochondrosis and synovial sepsis pathogenesis.

7.2. Introduction

Articular conditions are common in horses and can result in loss of function, pain and/or inability to work, which are important welfare concerns. The most common conditions include osteoarthritis (OA), osteochondrosis (OC) and synovial sepsis, which can be life-threatening (Rubio-Martínez *et al.*, 2012). Despite the high clinical prevalence of these conditions, rapid and specific diagnosis, monitoring and prognostication remains a challenge for practicing veterinarians, thus, identification of reliable biomarkers of disease is required. Synovial fluid (SF) is in direct contact with articular structures and represents an important source of biomarker discovery. SF is located within the articular joint cavity, providing a pool of nutrients for surrounding tissues but primarily serving as a biological lubricant, containing molecules including hyaluronan with low-friction and low-wear properties to articular surfaces (Dicker *et al.*, 2014). As SF is in close proximity to articular tissues primarily altered during joint pathology, this biofluid is an important first approach source for biomarker discovery (Mateos *et al.*, 2012; Ruiz-Romero and Blanco, 2010).

Total protein content in synovial fluid is associated with presence of articular pathology and is one of the parameters most commonly used in equine clinical practice to enable diagnosis and to monitor horses with synovial sepsis (Frisbie, 2006). Problematically there are large overlaps in the ranges of SF total protein content among arthropathies, and total protein content is also affected by articular diagnostic procedures and treatments (Sanchez-Teran, Bracamonte, Hendrick, Riddell, *et al.*, 2016). This situation can lead to erroneous interpretations and clinical decisions, representing an important welfare risk to the horse. More specific proteins such as the acute phase inflammatory protein serum amyloid A has been investigated as a potential biomarker of articular conditions in horses; however, it is easily affected by the systemic condition of the patient, and therefore, can be unreliable for specific diagnosis (Jacobsen, Thomsen, *et al.*, 2006; Sinovich *et al.*, 2018).

Proteomics encompasses the comprehensive profiling of protein contents. The SF proteome is dependent upon articular disease and its characterization has allowed the differentiation of OA and rheumatoid arthritis (RA) in man (Mateos *et al.*, 2012). A recent study has identified a subset of proteins differentially expressed in OA versus normal equine joints (Peffers, McDermott, *et al.*, 2015). Although an increase in total protein is a well-known feature of synovial sepsis, the protein profile in synovial sepsis has not been investigated. Identification of a characteristic proteomic profile in synovial sepsis would increase the understanding of the molecular basis of the condition and enable the identification of potential biomarkers for early diagnosis and treatment of this disease.

A previous study has investigated the equine SF profile in OA and OC compared to healthy donors using 2D-gel electrophoresis with subsequent mass spectrometry analysis of in-gel tryptic digests (Chiaradia *et al.*, 2012). However, few studies have investigated the proteomic profile of equine SF using high mass resolution mass spectrometer of in-solution tryptic digestions and, to our knowledge, none have investigated protein profile changes in septic SF in any species (Jacobsen, Niewold, *et al.*, 2006; Peffers, McDermott, *et al.*, 2015). In this study we have used mass spectrometry and label-free quantification to identify potential protein biomarkers that allow differentiation between equine articular joint pathologies, potentially aiding accurate diagnosis and enabling increased understanding of the effect of septic synovitis on the joint environment. Identification of characteristic proteomic profiles in synovial sepsis would increase the understanding of the molecular basis of the condition and allow the determination of potential biomarkers for early diagnosis and treatment of the disease. We hypothesised that proteomic profile characteristics will distinguish septic from non-septic equine arthropathies and between the non-septic common arthropathies OC and OA. The objective of the study was to identify possible synovial biomarkers in equine arthropathies.

7.3. Methods

All chemicals were supplied by Sigma-Aldrich (Gillingham, UK) unless otherwise stated.

7.3.1. Sample Collection

Following ethical approval and owner consent, excess aspirated SF (collected during clinical diagnostic investigations) was analysed from joints of horses presenting to The Philip Leverhulme Equine Hospital, University of Liverpool between 2014 and 2016, diagnosed with clinical OA, OC and synovial sepsis. Clinical diagnoses were determined via a combination of radiography, ultrasonography, arthroscopy and SF analysis and/or bacterial culture as previously described (Robinson *et al.*, 2017). SF was aspirated for diagnostic purposes from the affected joints during patient examinations or at the start of surgical arthroscopy under general anaesthesia. SF was immediately placed into EDTA-containing tubes (BD Vacutainer, Belliver Industrial Estate, Plymouth, UK) with particulate and cells removed from the SF by centrifugation (4^{o}C, 2540*g* for 4 min). The cell-free supernatant was transferred to a clean uncoated 1.5 ml collection tube, snap-frozen using liquid nitrogen and stored at -80°C. SF was collected from the distal interphalangeal, femorotibial, glenohumeral, intercarpal, metacarpophalangeal, metatarsophalangeal, patellofemoral and tarsocrural joints.

Eight healthy SF samples were obtained from the metacarpophalangeal joint of mixed breeds of horses from an abattoir with no gross joint changes, with a total score of 0 according to the Mcilwraith *et al.* gross scoring system, scored by two independent assessors (McIlwraith *et al.*, 2010). Samples were collected as a by-product of the agricultural industry and processed within 12 hours of euthanasia. The Animals (Scientific Procedures) Act 1986, Schedule 2, does not define collection from these sources as scientific procedures and ethical approval was therefore not required. Post mortem SF samples were processed using identical protocols as for clinically collected hospital samples. Final groups consisted of OA (n=4), OC (n=8), synovial sepsis (n=7) and healthy (n=8) (full details in Supplementary Table 1).

7.3.2. Synovial Fluid Preparation

SF was thawed and treated with 1 µg/ml hyaluronidase as previously described and centrifuged at 10000*g* for 10 min to remove any particulates (Peffers, McDermott, *et al.*, 2015). Protein concentrations of SF were determined by Bradford assay

(Thermo Scientific, USA). A volume of sample equivalent to 5 mg of protein was added to 10 µl of beads (Peffers, McDermott, *et al.*, 2015). SF samples were enriched for low abundance proteins using ProteoMiner™ beads (BioRad, UK) according to the manufacturer's instructions. Beads were re-suspended in 80 µl of 25 mM ammonium bicarbonate and 5 µl of 1% (w/v) Rapigest SF (Waters, UK) added and the sample heated at 80°C for 10 min. On-bead trypsin digestion was undertaken (Peffers, McDermott, *et al.*, 2015).

7.3.3. LC-MS/MS and Label-Free Quantification

Tryptic digests (diluted 5-fold in 0.1% (v/v) trifluoroacetic acid (TFA) and 3% (v/v) acetonitrile) were subjected to liquid chromatography tandem mass spectrometry (LC-MS/MS) using a 2 hr gradient and analysed individually. Data-dependent LC-MS/MS analyses were conducted on a Q Exactive^{TM} HF quadrupole-Orbitrap mass spectrometer (Thermo Scientific, Hemel Hempstead, UK) coupled to a Dionex Ultimate 3000 RSLC nano-liquid chromatograph (Thermo Scientific). Sample digests were loaded onto a trapping column (Acclaim PepMap 100 C18, 75 µm x 2 cm, 3 µm packing material, 100 Å) using a loading buffer of 0.1% (v/v) TFA and 2% (v/v) acetonitrile in water for 7 min at a flow rate of 12 µl min^{-1}. The trapping column was then set in-line with an analytical column (EASY-Spray PepMap RSLC C18, 75 µm x 50 cm, 2 µm packing material, 100 Å) and the peptides eluted using a linear gradient of 96.2% A (0.1% (v/v) formic acid):3.8% B (0.1 % (v/v) formic acid in water:acetonitrile (80:20) (v/v)) to 50% A:50% B over 90 min at a flow rate of 300 nl min^{-1}, followed by washing at 1 % A:99% B for 5 min and re-equilibration of the column to starting conditions. The column was maintained at 40°C and the effluent introduced directly into the integrated nano-electrospray ionisation source operating in positive ion mode. The mass spectrometer was operated in data-dependent acquisition (DDA) mode with survey scans between *m/z* 350-2000 acquired at a mass resolution of 60,000 (full width at half maximum) at *m/z* 200. The maximum injection time was 100 ms, and the automatic gain control was set to 3e^6. The 12 most intense precursor ions with charge states of between 2+ and 5+ were selected for MS/MS with an isolation window of 2 *m/z* units. Fragmentation of the peptides was by higher-energy collisional dissociation using normalised collision

energy of 30%. Dynamic exclusion of *m/z* values to prevent repeated fragmentation of the same peptide was used with an exclusion time of 20 s.

For label-free quantification, the raw files of the acquired spectra were analysed by ProgenesisQI™ software (Waters, Manchester, UK) which aligns the files and then peak picks for quantification by peptide abundance (Peffers, McDermott, *et al.*, 2015). Briefly, the top five spectra for each feature were exported from ProgenesisQI™ and utilised for peptide identification with our local Mascot server (Version 2.6.2), searching against the Unihorse database with carbamidomethyl cysteine as a fixed modification and methionine oxidation as a variable modification, peptide mass tolerance of 10 ppm and MS/MS tolerance of 0.01 Da. In this study, differentially expressed (DE) proteins are defined as those with a > 2 fold change in expression, with a false discovery rate (FDR) adjusted p value of < 0.05 and identified with at least two unique peptides

Proteomic data has been deposited in the PRIDE ProteomeXchange and can be accessed using the identifier PXD011276 (Vizcaíno *et al.*, 2016).

7.3.4. Pathway and Network Analysis Comparing Sepsis, OA or OC to Healthy

Network analysis, canonical pathways and upregulated regulators were analysed using Ingenuity Pathway Analysis (IPA, Qiagen, USA). Proteins with an FDR adjusted p value of < 0.05 and with 2 or more unique peptides were used for analysis, uncharacterised proteins were not included to the analysis. Gene names from the lists generated by ProgenesisQI™ were uploaded to IPA, unmapped genes were converted manually to human orthologues. IPA analysis was conducted by Mr Aibek Smagul.

7.3.5. Validation of Mass Spectrometry using ELISA

The differentially expressed proteins lactotransferrin (LTF) and insulin-like growth factor-binding protein 6 (IGFBP6) were selected to validate mass spectrometry findings as they could be measured using available enzyme linked immunosorbent assays (ELISAs) that were compatible with equine samples. Commercially available kits were used for both equine LTF (MBS902183, MyBioSource Inc., San Diego,

California, USA) and equine IGFBP6 (abx574245, Abbexa Ltd, Cambridge, UK), using sandwich and competitive inhibition ELISA methodology respectively. For IGFBP6 analysis, hyaluronidase treated/Costar processed native SF was diluted 1/10 whereas for LTF analysis SF was undiluted. 5-6 dependent cohort SF samples were tested per group. 100 µl aliquots of each sample were analysed in duplicate, with the absorbance measured at 450 nm and protein concentrations calculated from standard curves.

7.3.6. Additional Statistical Analyses

Principal component analysis (PCA) plots and heat map analysis were produced using MetaboAnalyst 4.0 (Chong *et al.*, 2018). The Venn diagram was produced using the online tool Venny 2.1 and box plots constructed using SPSS 24. Statistical analysis of SF protein concentration, LTF and IGFBP6 abundances were performed in Minitab version 17. These were conducted via ANOVA, using Tukey post hoc testing, with a p value of < 0.05 considered statistically significant, following correction for multiple testing.

7.4. Results

7.4.1. Protein Concentration of Synovial Fluid with Different Arthropathies

The SF protein assay demonstrated that protein concentration was dependant on the type of arthropathy, with septic SF having the highest protein concentration (Figure 1).

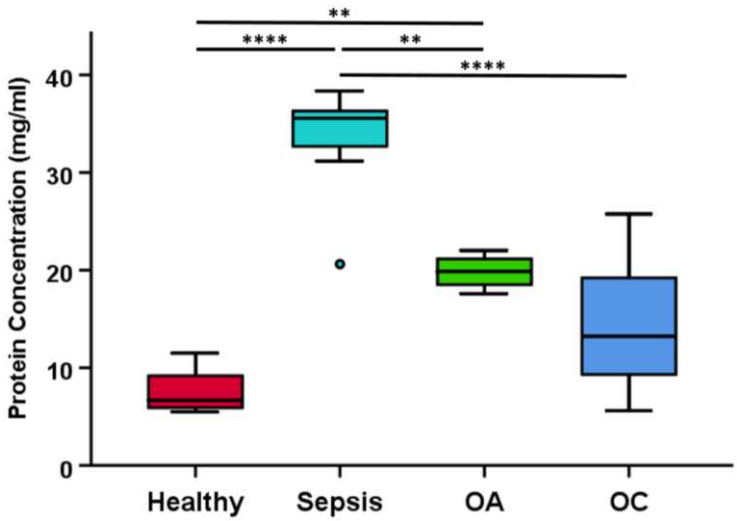

Figure 1. Synovial fluid protein concentrations in equine arthropathies. Protein concentrations of synovial fluid were determined by Bradford assay. Healthy (n=8), osteoarthritis (OA, n=4), osteochondrosis (OC, n=8), sepsis (n=7). Significant changes are demonstrated following analysis using ANOVA with Tukey's multiple comparison; ** $p < 0.01$, **** $p < 0.0001$.

7.4.2. Differential Abundance of Proteins in Osteoarthritis, Osteochondrosis and Sepsis compared to Healthy Synovial Fluid

From the aggregate data file produced from all samples 1,385 protein families, at a 1% FDR, were identified. ProgenesisQI™ identified 750 proteins DE when all groups were compared using a 4-way analysis (> 2-fold change, FDR < 0.05 and identified with at least two unique peptides). The number of protein identifications in each analysed group are shown in Figure 2a. The number of DE proteins in 2-way contrasts is shown in Table 1 and multivariate 2-way comparisons of protein profiles shown in Figure 2b. Unsupervised multivariate analysis (PCA) demonstrated clear variance between groups in the 4-way analysis (Figure 3a).

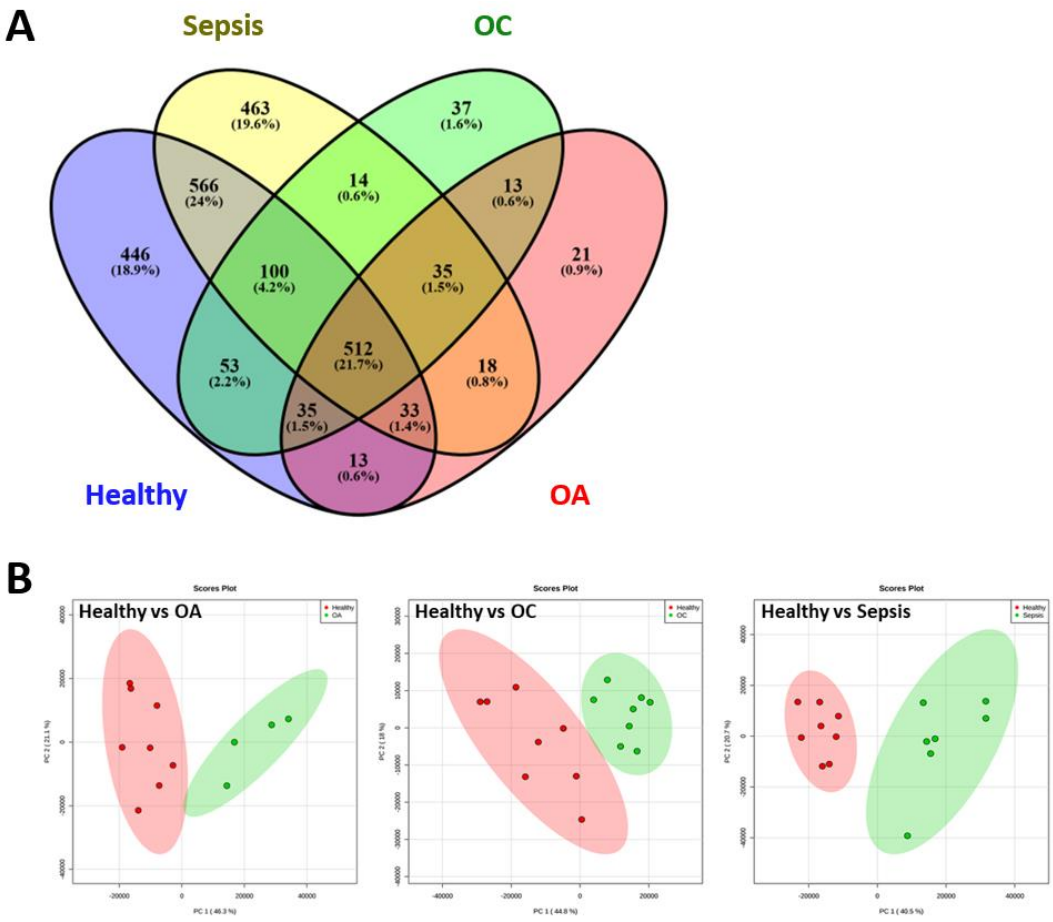

Figure 2. (A) Venn diagram of protein identifications for each analysed group. A minimum of 2 unique peptides were required for protein identification, with a 1% FDR correction applied. (B) Principal component analysis plots of healthy versus osteoarthritis (OA), healthy versus osteochondrosis (OC) and healthy versus sepsis (FDR < 0.05, > 2-fold change and identified with at least two unique peptides). Healthy (n=8), osteoarthritis (OA, n=4), osteochondrosis (OC, n=8), sepsis (n=7).

Table 1. Number of differentially expressed (DE) proteins in two-way comparisons.

Contrast	Number of Proteins DE	Increased	Decreased
Healthy versus Sepsis	386	205	181
Healthy versus OA	430	331	99
Healthy versus OC	539	474	65
OA versus Sepsis	53	22	31
OC versus Sepsis	454	75	379
OA versus OC	0	0	0

Differentially expressed proteins were filtered to include proteins identified with two or more peptides, q < 0.05 and > 2-fold change in expression. Osteoarthritis = OA, Osteochondrosis = OC.

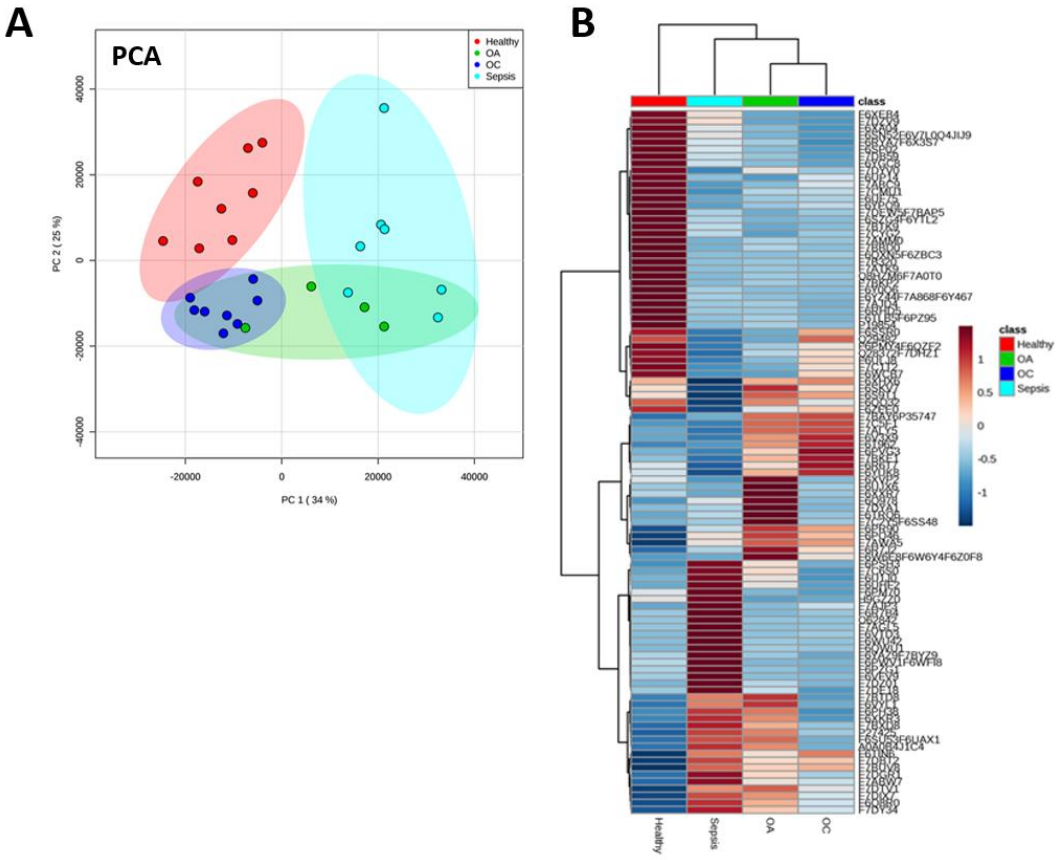

Figure 3. Principal component analysis (PCA) and heat map analysis of healthy (n=8), osteoarthritis (OA, n=4), osteochondrosis (OC, n=8) and sepsis (n=7) synovial fluid samples. (A) Principal component analysis of proteins (FDR < 0.05, > 2-fold change and identified with at least two unique peptides) revealed the greatest variability was due to the type of arthropathy distinguished by shading (healthy; red, OA; green, OC; blue, sepsis; turquoise). (B) Heat maps of the top 100 differentially expressed proteins show distinguishable profiles based on arthropathy type. Each column indicates a different sample group. Each row indicates one protein. Red shading indicates increased expression and blue decreased expression.

7.4.3. Canonical Pathways and Network Analysis of Osteoarthritis, Osteochondrosis and Sepsis Synovial Fluid

Canonical pathway analysis was undertaken on differentially abundant synovial proteins comparing either OA, OC or sepsis to healthy. When comparing sepsis and healthy samples, it revealed the predicted upregulation of coagulation system ($p = 7.94 \times 10^{-23}$), acute phase response signalling ($p = 3.98 \times 10^{-19}$), LXR/RXR activation ($p = 2.51 \times 10^{-17}$), extrinsic and intrinsic prothrombin activation pathways ($p = 2 \times 10^{-16}$ and $p = 1 \times 10^{-14}$), complement system ($p = 3.16 \times 10^{-11}$), neuroprotective role of THOP1 in Alzheimer's disease ($p = 1.55 \times 10^{-6}$) and OA pathway ($p = 7.08 \times 10^{-6}$); and downregulation of inhibition of matrix metalloproteases ($p = 2.51 \times 10^{-15}$) (Figure 4a). Pathway analysis of OA versus healthy demonstrated upregulation of the coagulation system ($p = 5.01 \times 10^{-17}$), complement system ($p = 1.58 \times 10^{-16}$), extrinsic and intrinsic prothrombin activation pathways ($p = 5.01 \times 10^{-12}$ and $p = 2 \times 10^{-11}$) (Figure 4b). Comparison of differentially abundant proteins in OC compared to healthy samples demonstrated an upregulation in complement system ($p = 2 \times 10^{-16}$) and RhoGDI signalling ($p = 5.62 \times 10^{-9}$) (Figure 4c). Downregulated canonical pathways of OA and OC versus healthy had a substantial overlap including acute phase response (OA: $p = 6.31 \times 10^{-15}$, OC: $p = 7.94 \times 10^{-11}$), EIF2 signalling (OA: $p = 7.94 \times 10^{-15}$, OC: $p = 1.26 \times 10^{-23}$), actin cytoskeleton signalling (OA: $p = 7.94 \times 10^{-13}$, OC: $p = 1 \times 10^{-12}$), regulation of eIF4 and p7056K signalling (OA: $p = 7.94 \times 10^{-13}$, OC: $p = 3.98 \times 10^{-15}$), mTOR signalling (OA: $p = 1.58 \times 10^{-11}$, OC: $p = 3.16 \times 10^{-13}$), leukocyte extravasation signalling (OA: $p = 3.98 \times 10^{-11}$, OC: $p = 3.98 \times 10^{-11}$), signalling by Rho family GTPases (OA: $p = 2.82 \times 10^{-10}$, OC: $p = 1.82 \times 10^{-9}$), p7056K signalling (OA: $p = 8.91 \times 10^{-9}$, OC: $p = 1.15 \times 10^{-9}$) and protein kinase A signalling (OA: $p = 1.02 \times 10^{-8}$, OC: $p = 4.9 \times 10^{-8}$). IGF-1 signalling ($p = 3.16 \times 10^{-11}$) and ephrin B signalling ($p = 1.91 \times 10^{-9}$) were downregulated pathways in OA only; and Fcy receptor-moderated phagocytosis in macrophages and monocytes ($p = 1.91 \times 10^{-10}$), production of nitric oxide and reactive oxygen species in macrophages ($p = 2.88 \times 10^{-8}$) downregulated in OC only.

Figure 4. Canonical pathways of differentially abundant proteins in equine synovial fluid of (A) sepsis, (B) osteoarthritis and (C) osteochondrosis compared to healthy samples. Bars represent the significance of the canonical pathway, calculated by a right-sided Fisher's exact test. The tallest bars represent the canonical pathways that are the least likely to have been identified due to random chance. Upregulated canonical pathways are shown in orange and downregulated pathways in blue. Ratio = number of proteins within the dataset mapping to the pathway divided by the total number of proteins within the pathway.

Compared to healthy SF, septic SF exhibited upregulation in cellular movement, haematological system development, inflammatory response, cell-to-cell signalling and immune cell trafficking (Figure 5). This was in direct contrast to OA and OC in which these pathways were downregulated. Similarities between groupings of canonical pathways in OA and OC were identified. The groups of organismal injury and abnormalities, and cancer had the highest overlap in OA versus healthy and OC versus healthy. These were predicted to be upregulated in OA compared to healthy and further upregulated in OC versus healthy.

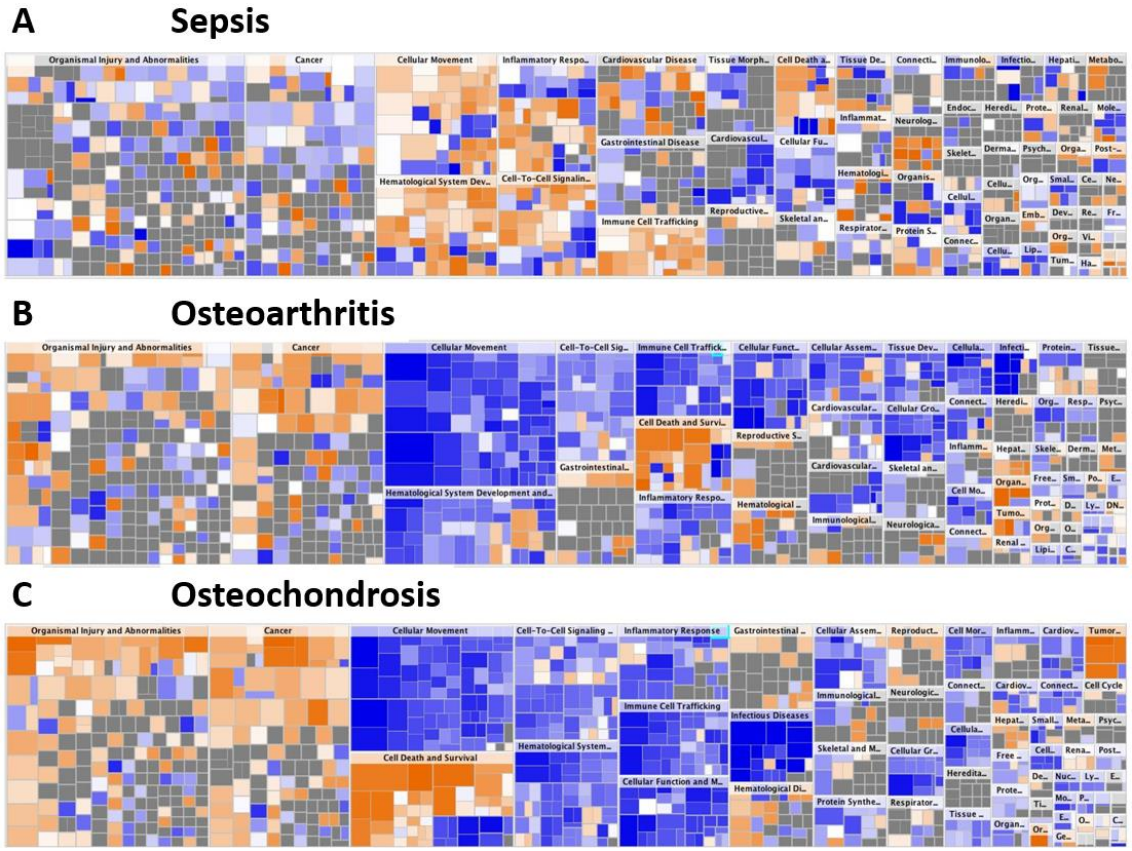

Figure 5. Heat map identifying canonical pathway groupings for molecular and cellular functions altered in equine synovial fluid of (A) sepsis, (B) osteoarthritis and (C) osteochondrosis compared to healthy. Squares are coloured according to their Z score, with orange upregulated in the disease state and blue downregulated, with the colour intensity indicating prediction strength. Z scores represent whether the up- or downregulation of the proteins within that function will lead to activation (positive Z score) or inhibition (negative Z score) of the function.

More detailed pathway analysis of differentially abundant proteins in healthy versus septic SF predicted the upregulation of immune response in cells ($p = 1.45 \times 10^{-3}$). The network of molecules included amyloid precursor protein (APP), 26s proteasome, LTF, DNM1L, HSP90, HSP90AA1, PIN1 and OTUB1 (Figure 6).

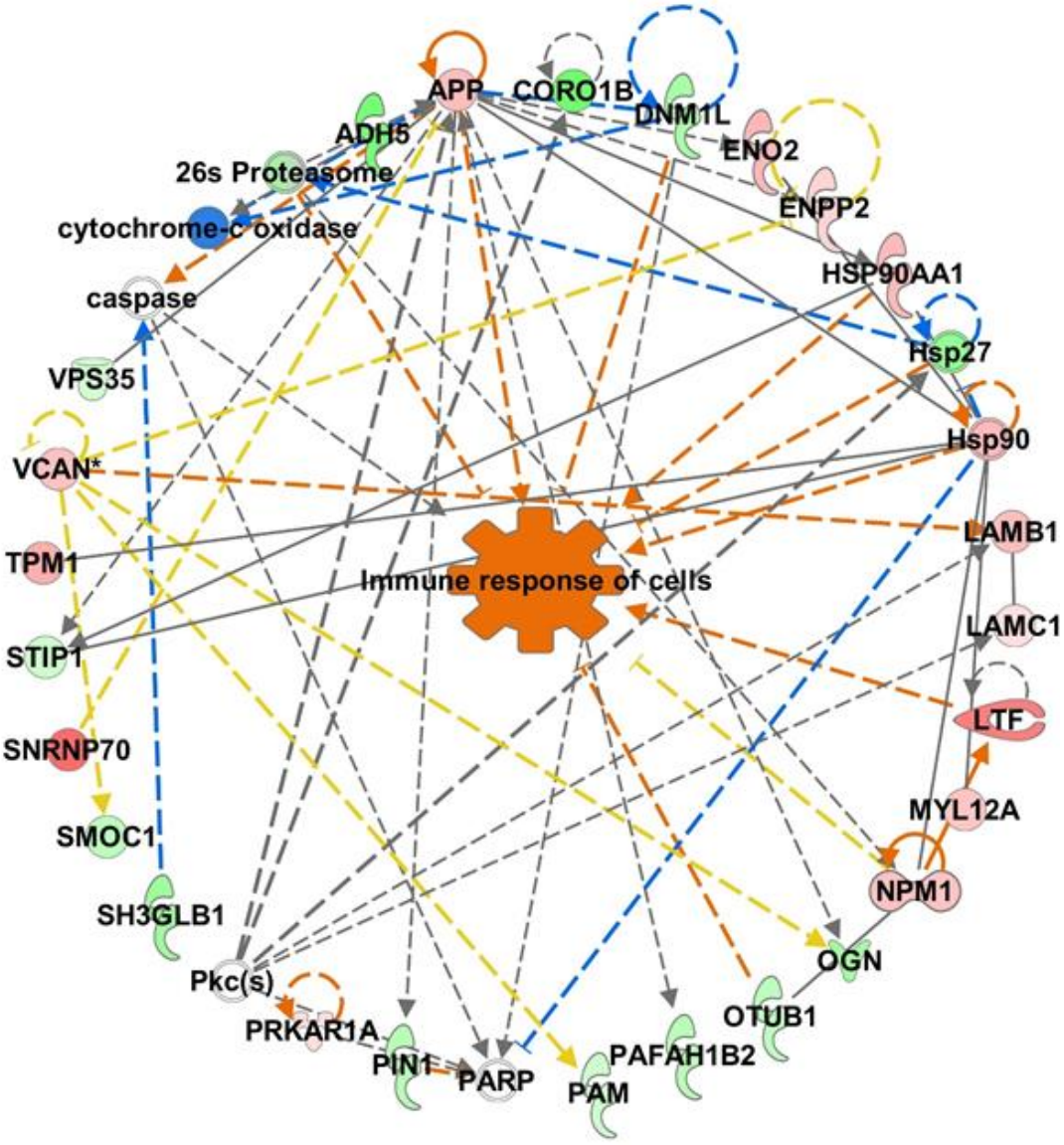

Figure 6. Network involved in the immune response of cells mapped from the differential abundant proteins of septic equine synovial fluid. Red nodes represent greater protein abundance in sepsis; green nodes represent lower protein abundance in sepsis; and white nodes represent molecules mapped to this network but not present in the dataset. Orange arrows represent predicted activation, blue arrows predicted inhibition and yellow arrows indicate results inconsistent with the state of downstream molecules.

7.4.4. ELISA Validation of LTF and IGFBP6

LTF ELISA assay results corroborated mass spectrometry findings with a statistically elevated abundance present within septic SF samples compared to all other groups (Figure 7). IGFBP6 ELISA results produced a similar trend to that identified via mass spectrometry; however, these results were not of statistical significance.

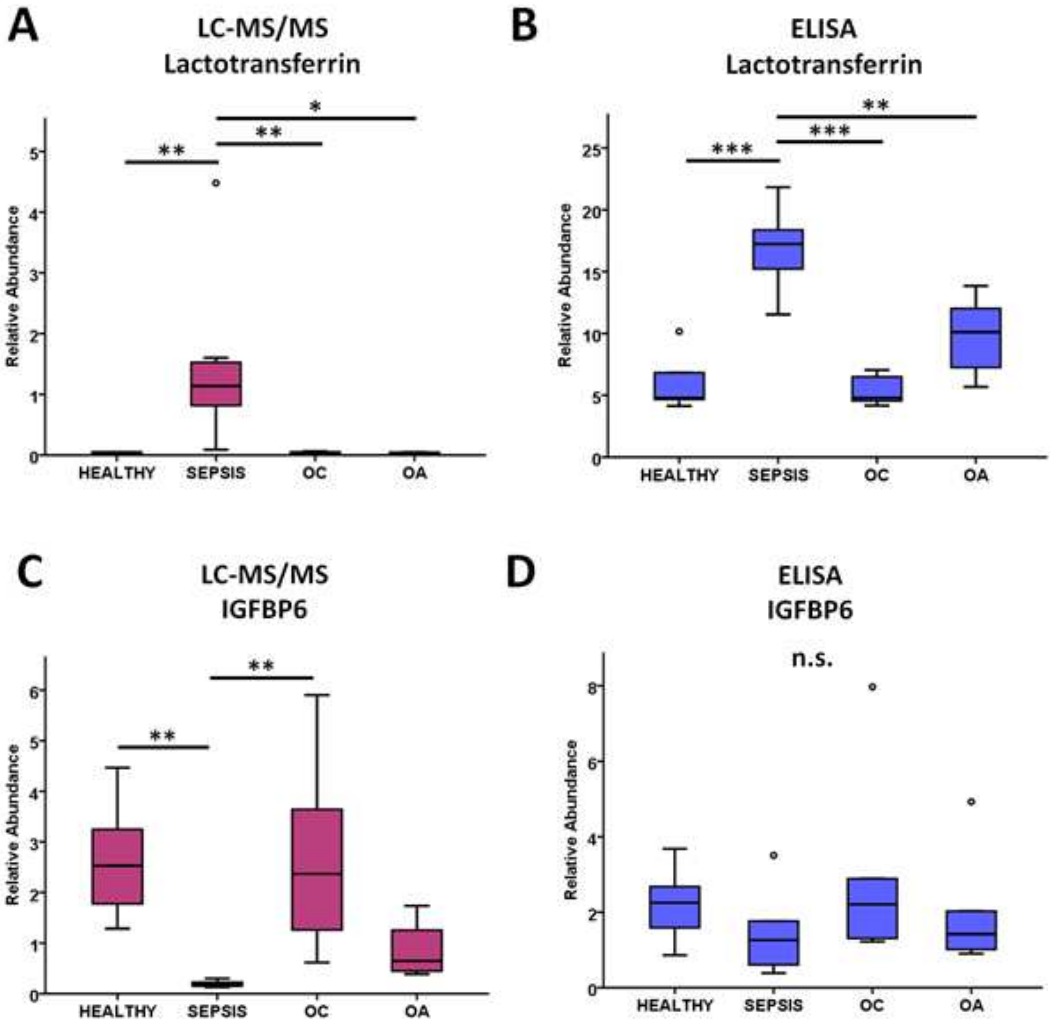

Figure 7. ELISA validation of LC-MS/MS results for lactotransferrin (A and B) and insulin-like growth factor binding protein 6 (IGFBP6) (C and D). IGFBP6 normalised to total protein. LC-MS/MS, n=4-8/group, ELISA: n=5-6/group. * = $p < 0.05$, ** = $p < 0.01$, *** = $p < 0.001$. OA = osteoarthritis, OC = osteochondrosis, n.s. = non-significant.

7.5. Discussion

Articular pathologies have an important clinical relevance in horses; however, to date the veterinary practitioner can find it difficult to achieve a timely diagnosis and prognostication of these conditions in horses affected by joint pathologies. This study has confirmed that SF protein concentration is associated with the type of arthropathy and has identified pathways and possible markers that may enable further understanding, together with rapid and accurate identification of these conditions in horses and potentially other species. For the first time the study of the proteomic profile of SF has identified potential SF markers of synovial sepsis. The proteomic profile can discriminate between septic and non-septic articular pathologies, and between non-septic conditions such as OC and OA. The implications highlighted by protein changes attributable to different pathways has increased our knowledge on articular pathophysiology.

Within this study, elevated synovial levels of lactotransferrin (LTF) were identified within the sepsis group compared to the other pathologies. LTF, also known as lactoferrin, is an 80 kDa multifunctional glycoprotein, abundant in various biofluids, primarily transporting iron ions, but also exhibiting anti-microbial, anti-inflammatory, and immune modulatory effects (Albar *et al.*, 2014; Paramasivam *et al.*, 2002; Ye *et al.*, 2014). LTF provides anti-bacterial action against various bacterial species, inhibiting the growth of *Staphylococcus epidermidis*, antibiotic-resistant *Klebseilla* and *Staphylococcus aureus in vitro* and reducing blood and hepatic infection severity following *Escherichia coli* enteral infection in rats (Edde *et al.*, 2001; Nibbering *et al.*, 2001; Pammi and Abrams, 2015; Valenti and Antonini, 2005). LTF is present within specific granules of neutrophils with elevations in LTF levels potentially representing a marker of neutrophil granulocyte activation (Afeltra *et al.*, 1997). LTF levels within human SF have been found to be closely correlated to the level of SF neutrophilia, indicating the degree of inflammatory response (Bennett and Skosey, 1977). Various studies on SF from RA patients have identified increased synovial levels of LTF (Abbink *et al.*, 1991; Caccavo *et al.*, 2003; Decoteau *et al.*, 1972). LTF has been found to activate expression of bone morphogenetic protein 7 (BMP7) within porcine articular chondrocytes, through the mitogen-

activated protein kinase ERK pathway (Zhang *et al.*, 2013). As BMP7 has an important role in maintaining homeostasis of articular cartilage, the authors propose LTF exhibits a protective function following inflammation within the joint. During synovial sepsis, there is an upregulation of collagen catabolism due to an increased cytokine concentration leading to the release of matrix metalloproteinases (Shirtliff and Mader, 2002). Thus, following synovial sepsis the release of LTF from neutrophil granulocytes may have a multi-functional role, both providing a direct antibacterial function and enabling a degree of chondroprotection. Clinically, LTF diet supplementation of neonates has demonstrated an ability to reduce the occurrence of late onset sepsis (Baveye *et al.*, 1999; Baynes and Bezwoda, 1994; Kruzel *et al.*, 2002; Pammi and Abrams, 2015). However, elevations in synovial LTF levels have not previously been identified as a marker of synovial sepsis.

In this study, reduced SF IGFBP6 was identified within the sepsis group compared to other joint pathologies. This protein is involved in cartilage and bone homeostasis but is also expressed in the synovium, particularly in RA versus OA in people (Alunno *et al.*, 2017). IGFBP6 is a 30 kDa protein which is secreted into extracellular regions where it can subsequently interact with insulin growth factors (IGFs). IGFBP6, unlike other IGFBPs, binds to IGF2 with higher affinity than IGF1, inhibiting IGF2 activity (Aboalola and Han, 2017). IGFBP6 has previously been identified in human SF, with synovial levels decreased in RA compared to OA (Alunno *et al.*, 2017). Postoperative sepsis significantly alters the growth hormone/IGF axis, reducing GH-dependent molecule secretion (i.e. IGFBP3) and increasing GH-independent molecule secretion (i.e. IGFBP6) (Nedic *et al.*, 2013). However, decreased levels of synovial IGFBP6 have not previously been identified for synovial sepsis in horses. IGFBPs are known regulators of insulin resistance, with increased serum IGFBP6 levels identified within type 1 diabetes, and thus high systemic glucose (Lu *et al.*, 2012). Reduced synovial glucose concentrations is a known clinical parameter associated with synovial sepsis (Anderson, Phelan, *et al.*, 2018). Thus, the localised reduced abundance of IGFBP6 may be reflective or the decreased synovial glucose levels.

Protein differences were greatest between synovial sepsis and other groups, probably reflecting the more distant pathological pathways implicated. Pathway analysis of DE proteins in sepsis compared to healthy revealed upregulation of several canonical pathways including the coagulation system, acute phase response signalling and complement system. Systemic inflammation results in activation of coagulation, due to tissue factor-mediated thrombin generation, downregulation of physiological anticoagulant mechanisms, and inhibition of fibrinolysis (Levi *et al.*, 2003). In healthy SF, coagulation proteins have a low abundance with the elevated SF levels identified within sepsis in our study probably due to thrombin activation and coagulation, also reported in inflamed human joints (So *et al.*, 2003). In an equine model of joint inflammation, changes in fibrinogen and thrombin/antithrombin have also been reported (Andreassen *et al.*, 2017). The upregulation in sepsis of the acute phase response signalling pathway supports findings of our group, and others, that acute phase proteins such as serum amyloid A increase in equine joint sepsis (Jacobsen and Kjelgaard-Hansen, 2008; Robinson *et al.*, 2017).

The upregulation of the complement system in joint sepsis is not unexpected. The complement system is one of the key players in the defence against infections (Blom, 2017). Its activation during the innate immune response leads to the generation of several proteins that contribute to the lysis and opsonisation of microorganisms, regulate inflammatory reactions and bridge innate immunity with the subsequent adaptive immune response. Depletion in the complement system in animal models increases the severity of septic arthritis (Sakiniene *et al.*, 1999).

Interestingly, eukaryotic translation initiation factors (EIF2) and mTOR signalling were downregulated pathways in both OA and OC compared to healthy SF. OC is a juvenile osteoarticular disorder affecting several mammalian species. In horses, it is a multifactorial disease with focal disruption of endochondral ossification leading to the development of osteoarticular lesions (Olsson and Reiland, 1978). Nevertheless, OC pathophysiology is poorly understood. Protein synthesis requires cooperation among a large number of polypeptides including ribosomal proteins, modification enzymes and ribosome associated translation factors. The initiation phase of

protein synthesis requires a set of EIFs. A reduction in these proteins in OA and OC is interesting as in both conditions there is an imbalance between cartilage protein anabolism and catabolism leading to a net loss of cartilage. However, there is an increase in mTOR in end-stage OA with mTOR important in maintaining cartilage homeostasis (Zhang *et al.*, 2015). Furthermore, signalling through mTOR is an important link between synovitis and structural damage in inflammatory arthritis (Cejka *et al.*, 2010). In OA and OC, proteins in the SF in our study may be derived from cartilage, subchondral bone or synovium. Further studies are required to determine the relevance of these changes at the SF proteome level to the pathogenesis of these diseases since mTOR inhibition protects cartilage from experimental OA (Olsson and Reiland, 1978).

Using IPA we have identified a number of proteins requiring further investigation as potential biomarkers of disease and/or therapeutic targets. For example, Nuclear factor (erythroid-derived 2) (NFE2L2) was identified as the most significantly inhibited upstream regulator in OC. Interestingly, although also identified as a potential upstream inhibitory regulator in OA, the effect in OC was much more significant. This master regulator of redox homeostasis regulates the expression of antioxidant proteins that protect against oxidative damage triggered by injury and inflammation. It has a potentially protective role in joint inflammation and degeneration (Maicas *et al.*, 2011). We have therefore identified a catalogue of proteins for future studies.

Healthy SF samples were collected following euthanasia whilst samples from the pathological groups were predominantly collected from live horses during clinical examination. Thus, it cannot be ruled out that differentially abundant proteins identified within the healthy group may be resultant of post mortem change. However, post mortem processing took place within 12 hours of euthanasia and therefore the impact on the synovial proteome is likely to be minimal. Due to the limited sample sizes included within this study, SF aspirated from various joints was included. However, despite the inclusion of analysis of SF from multiple sites, the clear separation identified in the proteomic profiles of different joint diseases strengthens the conclusion that the differentially expressed proteins are resultant

of the joint pathology opposed to joint location. Additionally, horses with different pathologies investigated within this study may experience changes in management, including diet and exercise, which may subsequently influence synovial protein composition. However, these systemic effects are likely to have a limited effect on the synovial proteome compared to the more significant impact of local joint pathology.

Within this study, ELISA validations of LTF and IGFBP6 synovial abundances were undertaken on the same samples as those used for mass spectrometry analysis due to limited availability of additional SF samples. Thus, to confirm the results of this study identifying these as potential synovial sepsis markers, further validation needs to be undertaken using an independent cohort before these proteins are investigated further.

7.5.1. Conclusion

This study has identified that the equine SF proteome exhibits distinctive profile changes between OA, OC, synovial sepsis and healthy joints. Elevated synovial abundance of LTF and decreased IGFBP6 were both found to distinguish synovial sepsis from all other study groups. Thus, these protein markers may have a future role in clinical practice to enable an earlier and reliable diagnosis of synovial sepsis.

7.6. Ethics

University of Liverpool Ethics approval ref: VREC175

7.7. Funding

The project was funded by a Veterinary School Research Project Support Grant (VSRP VET032) and the Technology Directorate voucher scheme (www.liverpool.ac.uk/technology-directorate), University of Liverpool. Mr James Anderson is funded by the Horse Trust (G1015). Professor Mandy Peffers is funded by a Wellcome Trust Clinical Intermediate Fellowship (107471/Z/15/Z). Mr Aibek Smagul is funded by a Kazakhstan President's Bolashak Scholarship.

7.8. Acknowledgements

The authors would like to thank The Centre for Proteome Research at the University of Liverpool for their invaluable advice on proteomic techniques and approaches and staff at the Philip Leverhulme Equine Hospital, University of Liverpool, for their involvement with sample collection.

7.9. Supplementary Information

Supplementary Table 1. Further Clinical Characteristics of Group Patients.

Group	Left/Right	Fore/Hind Limb	Joint	Age	Sex	Breed
Sepsis	R	H	TC	3 years 0 months	F	Thoroughbred
	R	H	TC	15 years 1 months	M	Thoroughbred
	L	F	IC	14 years 0 months	M	Arab
	L	F	DIP	16 years 0 months	F	Irish Sports
	L	F	DIP	19 years 11 months	M	Cob
	L	H	MTP	11 years 0 months	M	Thoroughbred
	R	H	TC	6 years 0 months	M	Irish Sports
Osteochondrosis	L	H	TC	5 years 3 months	M	Sports horse
	R	H	TC	8 years 0 months	M	Warmblood
	R	H	TC	5 years 5 months	M	Arab
	L	H	TC	6 years 2 months	M	Arab Cross
	L	H	FP	5 years 5 months	F	Apaloosa
	R	H	TC	7 years 0 months	M	Dutch Warmblood
	R	F	MCP	7 years 4 months	M	Warmblood
	L	H	MFT	6 years 0 months	F	Cob
Osteoarthritis	R	F	Shoulder	8 years 9 months	M	Welsh D
	R	H	TC	13 years 5 months	F	Irish Sports
	R	H	FP	9 years 7 months	M	Irish Sports
	R	F	MFT	8 years 0 months	M	Welsh D
Healthy	U	F	MCP	5 years 0 months	M	Thoroughbred
	U	F	MCP	16 years 0 months	M	Thoroughbred
	L	F	MCP	8 years 0 months	U	Thoroughbred
	L	F	MCP	3 years 0 months	U	Thoroughbred
	U	F	MCP	8 years 0 months	U	Unknown
	U	F	MCP	8 years 0 months	U	Unknown
	U	F	MCP	18 years 0 months	U	Unknown
	U	F	MCP	4 years 0 months	U	Unknown

Abbreviations: Joint, TC = Tarsocrural, IC = Intercarpal, DIP = Distal interphalageal, MCP = Metacarpophalangeal, MTP = Metatarsophalangeal, FP = Femoropatellar, MFT = Medial femorotibial (stifle - corresponds with the 'human knee'), Shoulder = Corresponds to the 'human' Glenohumeral joint, L = Left, R = Right, F = Forelimb, H = Hindlimb, U = Unknown; Sex, F = Female, M = Male, U = Unknown.

8. General Discussion

Osteoarthritis (OA) and rheumatoid arthritis (RA) are the most common arthropathies in people, causing limited mobility, pain and subsequent reduction in quality of life, resulting in a substantial impact on human society (Fusco *et al.*, 2017). Conditions affecting articular joints are also common in horses, including OA, osteochondrosis (OC) and synovial sepsis (Caron and Genovese, 2003; Summerhays, 2000). Despite their high prevalence and clinical relevance, diagnosis, staging, monitoring and determination of an accurate prognosis remain a challenge (Anderson, Phelan, *et al.*, 2018). Thus, there is a need to identify reliable biomarkers of disease. The development of 'omics' technologies, such as metabolomics and proteomics, has provided global analysis of biological tissues and fluids, enabling discovery of potential disease biomarkers as well as providing a greater understanding of their underlying pathogenesis (Carlyle *et al.*, 2018; Wang, Zhang, *et al.*, 2012). This thesis has optimised collection and processing protocols for analysis of synovial fluid (SF) using nuclear magnetic resonance (NMR) led metabolomics and mass spectrometry (MS) led proteomics. Human OA and RA SF metabolomes were compared using NMR, equine OA stratified via NMR metabolomic and MS proteomic SF analysis, equine SF metabolite and protein profiles compared between septic and common nonseptic joint pathologies and NMR metabolomic and MS proteomic analysis undertaken on an *ex-vivo* equine cartilage OA explant model.

8.1. Synovial Fluid Collection and Processing Optimisation

NMR and MS approaches provide comprehensive metabolite and protein/peptide profiling of complex biological samples respectively (Beckonert *et al.*, 2007; Beltran *et al.*, 2012; Hsueh *et al.*, 2014; Mahendran *et al.*, 2017). However, the large protein concentration dynamic range present within SF leads to various challenges associated with proteome analysis (Puangpila *et al.*, 2015). ProteoMiner™ protein enrichment columns contain beads bound to randomised hexapeptides which, following saturation, compress the protein concentration dynamic range of complex biological samples (Fonslow *et al.*, 2011; Righetti and Boschetti, 2008). However, to

date, there are no agreed standardised published protocols available for collection and processing of SF for these platforms with reproducibility of on-bead digestions of ProteoMiner™ columns, yet to be investigated.

This thesis has identified that for optimal reproducibility of SF NMR metabolomics analysis, SF should first be centrifuged at 2,540*g* and 4°C for 5 min and then snap frozen in liquid nitrogen. For proteomic analysis, treatment of SF with 1 µg/ml hyaluronidase and rotational incubation at 37°C for 1 hr provided sufficient enzymatic activity to enable efficient centrifugation through a 0.22 µm pore cellulose acetate membrane. Lys-C endopeptidase pre-digestion greatly improved on-bead tryptic protein digestion when used in conjunction with small-capacity ProteoMiner™ column kits for low abundant protein enrichment, resulting in a reduction of undigested proteins bound to ProteoMiner™ beads, a reduction in the number of peptide missed cleavages, improved reproducibility of tryptic peptide quantification and an increased number of protein identifications. To maximise protein identifications using ProteoMiner™ columns, a 4hr Lys-C pre-digestion + 16hr tryptic digestion followed by a 2hr trypsin supplementation would be recommended. For semi-tryptic peptide identification, a 16hr + 2hr tryptic digestion of native SF and a 4hr on-bead tryptic digestion were found to be the most reproducible. The optimised protocols examined during this thesis can subsequently be used for future SF NMR-led metabolomics and LC-MS/MS-led proteomic studies to ensure high levels of technical reproducibility, enabling more reliable results and maximising the value of SF samples and instrument time available.

Due to silver stain analysis of tryptic digests of native SF indicating complete protein digestion, the effect of Lys-C endopeptidase pre-digestion in conjunction with tryptic digestion of native SF was not investigated. Thus, following on from this work, it may be of interest to investigate this further as Lys-C pre-digestion may improve native SF digestion reproducibility and increase the number of protein identifications. Additionally, Lys-C pre-digestion may improve proteomic analysis of culture media e.g. when used in conjunction with *ex-vivo* cartilage cultures.

8.2. Osteoarthritis Stratification - Metabolomics and Proteomics

To assess the stratification of OA according to the SF metabolome and proteome, two sample sets were analysed. The University of Liverpool biobank SF was obtained from a commercial abattoir with horses sampled of mixed breed and sex and representing naturally occurring OA. Hong Kong Jockey Club (HKJC) SF samples were exclusively from Thoroughbred racehorses with a high prevalence of palmar/plantar osteochondral disease (POD), providing a model for subchondral bone mediated OA. OA stratification of post mortem equine SF according to its metabolome was limited, with unsupervised multivariate analysis of biobank samples not indicating any separation according to microscopic or macroscopic OA scoring. However, when stratified according to macroscopic grade, glutamate levels were found to be differentially abundant, with lower levels identified at higher OA grades. For the HKJC cohort, when stratified according to macroscopic OA pathology, three metabolites were found to be differentially abundant, with 2-aminobutyrate, alanine and creatine levels increasing with OA severity.

When assessing the SF proteome, for both the biobank and HKJC groups, when categorised according to macroscopic OA severity, principal component analysis (PCA) identified that increased OA severity resulted in less variation between samples, indicating that OA is driving the SF OA proteome. For the biobank cohort, eight proteins discriminated between OA severities including immunoglobulin kappa constant and lipopolysaccharide binding protein (LBP) which decreased with increasing OA severity and apolipoprotein A1 which increased for mild and moderate OA grades.

LBP is an endogenous protein which binds to lipopolysaccharides and catalytically delivers monomeric liposaccharides to cluster of differentiation 14 (CD14) protein (Citronberg *et al.*, 2016; Ranoa *et al.*, 2013). Recently, increased plasma LBP levels have been described to predict knee OA progression (Huang *et al.*, 2018). It has previously been identified that mononuclear cell activation, induced by lipopolysaccharides, is enhanced by low LBP concentrations (Lamping *et al.*, 1998). Activation of monocytes and macrophages by lipopolysaccharides leads to the

secretion of tumour necrosis factor-α (TNF-α) and interleukin-1β (IL-1β), two pro-inflammatory cytokines which are central to OA pathogenesis (Schumann *et al.*, 1994; Wojdasiewicz *et al.*, 2014). Thus, decreasing synovial LBP levels may have a role in OA development. With CD14 also identified as a key variable within the biobank and HKJC combined model, this provides further support that this pathway is involved in equine OA pathogenesis.

Elevations of apolipoprotein A1 have previously been identified in OA SF of horses and dogs (Chiaradia *et al.*, 2012; Shahid, 2018). Apolipoprotein A1 is the primary protein component of high density lipoproteins (HDLs) and involved in HDL binding to adenosine triphosphate (ATP)-binding cassette (ABC) transporters as well as being a lecithin cholesterol acyl transferase cofactor (Luc *et al.*, 1996; Rader, 2003; Ramella *et al.*, 2018; Silver *et al.*, 2001). Apolipoprotein A1 has been found to induce the expression of interleukin-6, matrix metalloproteinase (MMP)-1 and MMP-3 in chondrocytes and synoviocytes through toll-like receptor 4 with the same study identifying a dissociation between the relationship of apolipoprotein A1 and HDLs in OA SF (de Seny *et al.*, 2015). Thus, this study provides further evidence that OA is a metabolic syndrome with disruption of lipid homeostasis due to alterations to apolipoprotein activity (de Seny *et al.*, 2015).

Within the HKJC cohort, gelsolin abundance decreased with OA severity. This result is supported by a mouse model whereby gelsolin knockout mice resulted in arthritis exacerbation (Aidinis *et al.*, 2005). Additionally, within a mouse model of pain and acute inflammation, exogenous delivery of gelsolin was identified to have effective analgesic and anti-inflammatory properties (Gupta *et al.*, 2015). Exogenous gelsolin administration has also been shown to have chondroprotective properties, nullifying the effect of IL-1β and OA SF on anabolic gene expression and increased glycosaminoglycan deposition in chondrocytes and protection of the integrity of murine cartilage following intra-articular injection (Kaneva *et al.*, 2017). Therefore, gelsolin has potential as a biomarker of equine OA as well as an OA therapeutic target, and potential analgesic.

Although both the biobank and HKJC datasets produced a degree of OA stratification, markers of interest were generally distinct. This may be reflective of the more severe OA phenotype demonstrated by the HKJC horses, whilst markers identified within the biobank represented a subtler grade of OA. Alternatively, the differences in markers identified may be due to the varying OA aetiologies, with the biobank representing a naturally occurring OA whilst the HKJC horses demonstrated a POD model for subchondral bone mediated OA, which is associated with trauma and overload (Barr, 2010). Additionally, the biobank cohort was on average an older, mixed breed donor group compared to the younger, Thoroughbred HKJC cohort which may also account for differences between the datasets.

Both metabolomic and proteomic multivariate analysis of longitudinal culture media samples following TNF-α and IL-1β treatment of *ex-vivo* equine cartilage identified discrete groupings between control and treatment groups. This was evident for all analysed time points. Overall, the top five metabolites and proteins driving this discrimination were alanine, glutamate, pyroglutamate, citrate and glutamine and cartilage oligomeric matrix protein, fibronectin, enolase 1, thrombospondin and collagen X α 1 respectively. This model identified changes in the abundance of various molecules which were consistent with collagen degradation. Isoleucine was elevated within media during the latter stages of the model with elevated isoleucine levels previously reported within SF of a canine OA model and human OA serum (Damyanovich *et al.*, 1999; Zhai *et al.*, 2010). Borel *et al.* previously identified elevations of peaks within ^{1}H High resolution magical angle spinning NMR spectra of OA cartilage which could be attributed to isoleucine (Borel *et al.*, 2009). Thus the elevations seen in isoleucine may be reflective of cartilage collagen breakdown (Zhai *et al.*, 2010). However, within this study, although a higher abundance was recorded for isoleucine in treated compared to control cartilage, this did not reach statistical significance. However, elevations in glutamate were identified within culture media at 3-5 days, which may be resultant of the catabolism of collagenous proline through proline oxidase (Phang *et al.*, 2015). Reduced levels of collagen type VI α 2 chain and collagen type X α 1 chain were identified at 3-5 and 6-8 days following cytokine treatment. This may reflect a

reduction in collagen synthesis which has previously been identified within other collagen types following TNF-α/IL-1β stimulation (Stevens *et al.*, 2009). Therefore these results provide evidence of a disruption in collagen homeostasis and suggest that collagens are being degraded within the model sooner than the 14-28 days previously reported within other *ex-vivo* cartilage OA models (Milner *et al.*, 2001, 2006).

Although the TNF-α/IL-1β *ex-vivo* equine cartilage OA model identified a number of molecules of interest which were consistent with the equine OA SF samples, there were some discrepancies in the trends identified for these molecules between the experiments. The TNF-α/IL-1β model has become an established model for investigating OA pathology within *ex-vivo* studies, with elevations in TNF-α and IL-1β regularly identified within OA SF, although this model requires further refinement (Westacott *et al.*, 1990; Williams, 2014). Cartilage explant experiments allow investigation of chondrocytes in situ within their natural extracellular matrix (ECM) environment, although a limitation can be cell death at the edge of the explant (Johnson *et al.*, 2016). As OA is a disease of the whole joint, an improvement to this model would be to replace *ex-vivo* cartilage explants with osteochondral (cartilage and bone) plugs, treated with TNF-α/IL-1β or OA SF, to retain subchdrondral bone/cartilage communication (Cope *et al.*, 2019).

8.3. Human Osteoarthritis and Rheumatoid Arthritis

1D ^{1}H NMR spectroscopy of human SF was able to discriminate between OA and RA according to their metabolome. The metabolic pathways that differed the most between these two forms of arthritis were glycolysis, amino acid biosynthesis and taurine and hypotaurine metabolism. In general, metabolites of glycolysis and the tricarboxylic acid (TCA) cycle were higher in OA compared to RA, concurring with the higher levels of inflammation, synovial proliferation and hypoxia identified in RA compared to OA. Levels of taurine were also higher in OA indicating increased subchondral bone sclerosis in comparison to RA. Previously, one limiting factor of NMR spectroscopy of SF has been the minimum volume required for analysis, with difficulties in analysing SF from normal human joints in which < 200 µl can be

aspirated (Naughton *et al.*, 1993). Using the methods described within this thesis, it has been demonstrated that analysable and reproducible ^{1}H NMR spectra can be produced from just 100 µl of SF, thus increasing the potential applications of this technique when sample volume is limited.

8.4. Synovial Sepsis

This thesis has identified a panel of metabolites and proteins within equine SF which are able to distinguish synovial sepsis from other joint pathologies. Although reduced glucose abundance was the principal metabolite discriminant, a partial least squares discriminant analysis (PLS-DA) model with glucose removed revealed there to still be a modest separation between septic and nonseptic disease groups, thus indicating the differentiated metabolomes are driven by a panel of metabolites (potential septic markers) opposed to glucose alone.

Pathway analysis was not conducted on the metabolomic dataset as the number of differentially abundant metabolites was relatively small (thirteen) and subsequently this analysis was deemed unreliable. However, undertaking further computational analysis, combining the metabolomic and proteomic datasets (as in chapter 3) would complement the analysis already undertaken within this thesis, identifying a focused, combined synovial sepsis panel which is the most significant in discriminating disease groups as well as strengthening pathway analysis. Additionally, further 'omics' investigations, i.e. transcriptomics and lipidomics, of the same sample set would substantiate this work further.

The identified metabolite and protein synovial sepsis panel may also have translational potential to aid diagnosis in human medicine. However, in people, as RA is a risk factor for septic arthritis, joint infections complicate RA with diagnosis often delayed, resulting in increased morbidity and mortality (Al-Ahaideb, 2008; Goldenberg, 1989). Thus, septic markers would need to be able to discriminate septic joint pathology from autoimmune disease. As autoimmune joint disease was not a comparative study group to equine synovial sepsis within this thesis, as this is not diagnosed or considered to occur in horses, and human sepsis SF was

unavailable for comparison to human OA and RA SF, it is currently unknown whether this panel of molecules would be able to discriminate RA from sepsis. Thus, further analysis would need to be carried out on human SF with these associated pathologies in order to qualify this.

8.5. *Alanine*

Elevated levels of alanine have previously been identified within OA SF of both dogs and horses (Damyanovich *et al.*, 1999; Lacitignola *et al.*, 2008). As alanine is one of the main amino acid residues which constitutes collagen, it is likely that increased alanine abundance identified within OA SF is resultant of degradation of the cartilage collagen framework, subsequently releasing alanine into the surrounding SF (Huster *et al.*, 2004; Shet *et al.*, 2012). This is supported by another study, using high resolution magic angle spinning NMR spectroscopy, identifying depleted alanine abundance within human OA cartilage (Shet *et al.*, 2012). These results are supported by this thesis within chapters 3, 4, 5 and 6.

8.5.1. Equine Osteoarthritis Stratification - Alanine

Stratification of equine OA using SF for the HKJC dataset identified increasing alanine levels with increased severity. Although univariate analysis for the biobank dataset did not identify elevated levels of alanine with increasing OA severity, computational analysis integrating both proteomic and metabolomic datasets identified alanine to be the third most important variable driving the model. Additionally, combining metabolomic and proteomic datasets for both the biobank and HKJC datasets via discriminant analysis of principal components (DAPC) modelling identified alanine to be the third most important discriminant for linear discriminant 1.

Metabolite extraction of *ex-vivo* equine cartilage following 8 day TNF-α and IL-1β treatment identified reduced levels of alanine compared to control samples, with alanine the fourth most influential variable during supervised multivariate analysis, supporting the previous work by Shet *et al.* (Shet *et al.*, 2012). Over the same period, within associated culture media, alanine abundance was found to be the

most important variable in discriminating control from treated samples. However, unexpectedly, decreased alanine abundance was identified within treated culture media compared to control samples at all analysed time points. This may be due to the highly inflammatory environment of the TNF-α and IL-1β model leading to further degradation of alanine, particularly given the greater discrepancy between alanine abundances at later time points. It would therefore be of interest to repeat this study, applying TNF-α and IL-1β treatments separately to identify whether this has an effect on alanine media levels.

8.5.2. Equine Synovial Sepsis vs Nonseptic Synovial Fluid - Alanine

Elevated levels of alanine were identified within nonseptic articular pathology (OA and OC) SF compared to septic SF. Additionally, with the principal septic metabolite discriminator glucose removed from supervised multivariate analysis, alanine was identified as the sixth most important variable in discriminating between these two groups. However, this study was unable to separate OA and OC based on their synovial metabolome, restricted by the low sample number. Therefore, higher powered studies are required to identify whether the SF metabolome, in particular alanine, is able to distinguish OA from OC.

8.5.3. Human Osteoarthritis vs Rheumatoid Arthritis Synovial Fluid - Alanine

Elevated alanine levels were identified within human OA SF compared to RA with the 'alanine, aspartate and glutamate metabolism' pathway identified as differentially altered between the conditions. Additionally, many other amino acids which feed into glycolysis and the TCA cycle were higher in OA, including tyrosine, glutamine, proline, histidine, asparagine and taurine. Previously, a study of urine metabolomics identified altered TCA cycle activity in OA, hypothesising this was resultant of changes to cartilage metabolism, with glycolysis constituting 95% of chondrocyte energy production (Heywood *et al.*, 2010; Li *et al.*, 2010).

Although degradation of articular cartilage is present within both OA and RA, with overlap in the molecular mechanistic steps leading to cartilage ECM destruction, different pathways are also involved (Pap and Korb-Pap, 2015). Within OA, cartilage

damage leads to and combines with inflammatory processes resulting in altered chondrocyte phenotype and expression of ECM-degrading enzymes. During RA, fibroblast-like synoviocytes are activated, invade and breakdown ECM with resultant inflammatory molecules stimulating further fibroblast-like synoviocyte activity. Thus, these different cartilage breakdown mechanisms may result in differences in which alanine is first released into the SF as well as subsequently degraded. Therefore, chapter 5 has provided further evidence that elevated alanine SF levels may aid OA diagnosis and differentiation from other articular pathologies.

Overall, the results from this thesis have identified that alanine has potential as a diagnostic aid for OA and as a marker of OA severity to assist stratification.

8.6. Neopeptides

Increased activity of MMPs, a disintegrin and metalloproteinase with thrombospondin motifs (ADAMTS), cathepsins and serine proteases during OA leads to cartilage breakdown and the generation of OA-specific peptide degradation products (neopeptides) (Ben-Aderet *et al.*, 2015; Peffers *et al.*, 2016; Polur *et al.*, 2010). Proteomic analysis of culture media within the *ex-vivo* equine cartilage TNF-α/IL-1β OA model identified various potential novel biomarkers of early OA, including neopeptides generated from aggrecan, cartilage intermediate layer protein, vimentin and collagen type VI α 2 chain.

Although univariate analysis of equine SF did not identify any differentially abundant neopeptides, for the HKJC cohort, the semi-tryptic profile was most consistent between samples in the groups with the most severe OA and synovitis pathology. This suggests, as expected, the OA phenotype is driving the semi-tryptic peptide profile, most likely due to an increase in enzymatic activity leading to ECM degradation fragments (Lotz *et al.*, 2013). However, this was not evident within the biobank SF sample set. This may be because OA pathology identified within this group was far subtler than that identified within the HKJC samples and thus the level of pathology present was not severe enough to drive a global change within the semi-tryptic peptide profile.

As the *ex-vivo* equine cartilage OA model neopeptides were not identified as differentially abundant within equine SF of different OA severity grades, it would be of interest to use a targeted MS approach to undertake absolute quantification via multiple reaction monitoring (MRM) using a triple-quadrupole mass spectrometer to validate these findings within the culture media (Parker and Borchers, 2014). Additionally, the more targeted MRM approach could also be applied to the SF samples, to quantify these semi-tryptic peptides of interest which may not have been quantified during analysis of the global proteome.

8.7. Uncharacterised Proteins

Proteomic analysis of equine SF identified several proteins which were able to discriminate a healthy phenotype from early OA changes. Although these proteins were largely uncharacterised, basic local alignment search tool (BLAST) analysis of the amino acid sequences of three uncharacterised proteins (F6TED1, H9GZU9 and H9GZS6), decreasing in abundance with OA severity, identified high levels of similarity to immunoglobulin gamma 1 heavy chain constant region and immunoglobulin kappa chain V-III region MOPC 63 proteins. However, this could be taken further by conducting 3D computational modelling of these proteins to help confirm function and potential interactions with other proteins/molecules, as well as undertaking solid-state NMR (Zhao, 2011).

8.8. Equine Osteoarthritis Pathway Analysis

8.8.1. Complement and Coagulation Cascades

KEGG (Kyoto Encyclopedia of Genes and Genomes) protein pathway analysis, applied when stratifying equine OA using post mortem SF, identified the 'complement and coagulation cascades' pathway to be altered during OA pathology. This was supported by Ingenuity Pathway Analysis of differentially abundant proteins between clinical OA and healthy equine SF collected from live horses in which the 'coagulation system' and 'complement system' were the top two implemented pathways. Additionally, KEGG protein pathway analysis of culture media within the *ex-vivo* equine cartilage TNF-α/IL-1β OA model identified various proteins involved in the 'complement and coagulation cascades' pathway which

were differentially abundant between control and treatment groups. The complement system is an important component of the innate immune response, encompassing various roles including opsonisation initiation, pathogen phagocytosis, the inflammatory response and terminating within cell lysis (Horwitz *et al.*, 2019; Silawal *et al.*, 2018). However, there is a growing body of evidence which has identified a role of complement activation within OA pathogenesis, further supported by this thesis (Silawal *et al.*, 2018). Complement has been identified to have a role in the degradation of cartilage ECM, synovitis and osteophyte formation, with complement split fragment C3a found to upregulate gene expression of TNF-α and IL-1β, pro-inflammatory cytokines central to OA pathogenesis (Silawal *et al.*, 2018; Wojdasiewicz *et al.*, 2014). Additionally, within this thesis, various equine synovial immunoglobulins were identified as being differentially abundant according to OA severity, with immunoglobulins known to regulate complement binding (Miletic and Frank, 1995). Therefore, targeting the complement cascade may provide a novel therapeutic target for OA treatment.

Within experimental arthritis models, coagulation and fibrinolysis pathways are known to play a role within disease pathogenesis, with these cascades also found to be activated within both the joint and circulation of degenerative and inflammatory arthropathies (So *et al.*, 2003). Within the synovium of patients diagnosed with OA, the coagulation factor fibrinogen is present throughout the tissue with elevations in tissue factor, a coagulation initiator, identified near endothelial cells (Weinberg *et al.*, 1991). Previously, fibrinogen has been identified as a potential target for arthritis therapy, with removal of fibrinogen-leukocyte integrin receptor αMβ2 interactions limiting inflammatory processes whilst maintaining normal fibrinogen coagulation function (Raghu and Flick, 2011). Thus, these pathways may also hold potential as a novel target for OA therapy.

8.8.2. ABC Transporters

Metabolite pathway analysis identified the 'ABC transporters' pathway to be altered during OA pathology when stratifying equine OA using post mortem SF and within the *ex-vivo* equine cartilage TNF-α/IL-1β OA model. ABC transporters utilise ATP

hydrolysis to import or export molecules across cell membranes (Rees *et al.*, 2009). ABC exporters have an important role in the export of cholesterol, fatty acid and lipids from cells, with dysregulation of this pathway underlying numerous diseases. The Wnt/β-catenin signalling cascade, with a proposed central role within OA pathogenesis, has previously been identified as a regulator of ABC transporters (Takamatsu *et al.*, 2014). Additionally, the ABC transporter MRP5 has been found to be the principal exporter of hyaluronan from its site of synthesis within the cell to the ECM (Schulz *et al.*, 2007).

8.9. Further Work

8.9.1. Synovial Sepsis - Bacterial Species

Whilst obtaining a diagnosis of synovial sepsis in horses, sensitivity of bacterial culture is low, with just 32% of septic SF samples resulting in a positive bacterial culture (Robinson *et al.*, 2017; Taylor *et al.*, 2010). Within this thesis, both metabolite and protein septic SF profiles were able to discriminate equine synovial sepsis from nonseptic articular pathologies. However, in order to take this work further, it would be of interest to identify whether the septic SF metabolome and proteome, when analysed either independently or collectively, are able to discern joint infections derived from separate microbiological species, their associated markers/molecular profiles and whether these profiles can be used to predict antimicrobial sensitivity. Thus, this may provide an additional diagnostic aid which is clinically applicable.

8.9.2. Longitudinal Synovial Fluid Studies

During this thesis, longitudinal culture media samples were analysed within the *ex-vivo* equine cartilage TNF-α/IL-1β OA model. However, SF analysis was restricted to cross-sectional samples across each studied population with longitudinal SF samples unavailable. Therefore, in order to further the analysis of SF markers identified within this thesis, longitudinal samples taken at set time points during disease progression would confirm differential abundance of these markers during OA or synovial sepsis within individual horses. For OA stratification, these longitudinal SF samples could be aspirated during naturally occurring OA in addition to an

experimental OA model i.e. following carpal groove-defect surgery (Maninchedda *et al.*, 2015). For synovial sepsis, longitudinal analysis may provide further information as to what stage of disease the identified septic markers' abundances change. Additionally, longitudinal synovial sepsis SF samples may identify whether these markers can differentiate horses with continued lameness from a nonresolving sepsis compared to those with a resolving sepsis but ongoing significant inflammation, whether they can assess effectiveness of novel therapeutics and whether they have a role as a prognostic indicator.

8.9.3. Monoclonal Antibodies

Following MRM validation of OA-specific neopeptides of interest identified within the *ex-vivo* equine cartilage OA model, and additional MRM validation within stratified equine OA SF, the next step would be to develop/produce monoclonal antibodies using the methodology developed by Professor Bruce Caterson (Caterson *et al.*, 1985). Additionally, monoclonal antibodies could also be developed for proteins/unique peptides of proteins which this thesis has identified as candidates for aids in equine OA stratification, e.g. immunoglobulin kappa constant and uncharacterised proteins F6TED1, H9GZU9 and H9GZS6. The production of these antibodies would subsequently have the potential to develop clinical 'bedside' tests to assess OA severity, allowing a potentially more bespoke, timely and appropriate management protocol.

8.9.4. Clinical Trials

Before their potential use in clinical trials, markers of interest identified within this study, in particular for the stratification of equine OA and diagnosis of equine synovial sepsis, would need to undergo further validation and subsequently have clinically applicable assays developed. The assays developed for these markers may then have a potential role in investigating response to novel therapeutics, providing an earlier diagnostic aid and have a role as a prognostic indicator.

8.9.5. Lipid Analysis

A growing body of evidence is supporting the theory that disruption of lipid

homeostasis has a role to play in OA pathogenesis (de Seny *et al.*, 2015). Alteration of lipid metabolism is associated with changes in membrane composition/permeability, gene expression and protein distribution and function, as well as in cellular functions such as cell growth, proliferation, differentiation, survival, apoptosis, and chemotaxis (Guma *et al.*, 2016). Additionally, differential biofluid abundance of lipids has been identified between RA and OA, as well as healthy controls (Kang *et al.*, 2015; Young *et al.*, 2013). Within this thesis, apolipoprotein A1, apolipoprotein A2, apolipoprotein C2, enolase 1 and lipoprotein binding protein were found to be key discriminants between OA severity grades with mobile-lipids and metabolites involved in glycophospholipid metabolism (acetylcholine, acetate and sn-glycero-3-phosphocholine) key in distinguishing OA from RA. Therefore, for both conditions it would be of interest to further interrogate SF and serum, using both NMR and MS based approaches, to undertake lipidomic studies to further investigate lipid profiles. Additionally, with obesity a known risk factor for OA, it would also complement the work carried out within this thesis to undertake metabolomic, proteomic and lipidomic analysis of SF and serum of obese individuals and those with a healthy body mass index in order to further understand the underlying pathogenesis (Xia *et al.*, 2014).

8.9.6. Pain Markers

Within SF proteomics, the identification of early biomarkers for orthopaedic pathologies has been a key objective, with markers which can predict clinical prognosis and monitor therapeutic effects growing areas of interest. In addition, an exciting potential area of research is the identification of protein biomarkers of musculoskeletal pain within SF (Peffers *et al.*, 2019). Factors of interest include nerve growth factor, a neuromediator, which is likely to be a key regulator involved in inflammatory and neuropathic pain, and the neurotransmitter substance P, which has been suggested as a potential biomarker for pain in chronic equine OA joints (de Grauw, van de Lest, *et al.*, 2006; Isola *et al.*, 2011). This is an exciting area of research, which will undoubtedly develop over the coming years, potentially providing a panel of pain markers which may have potential to deliver a more bespoke, clinical analgesic therapeutic plan, identifying pain pathways implicated

for individuals, generating novel therapeutic targets for the next generation of analgesics, and a potential pain panel to quantifiably monitor the effectiveness of future analgesics. Additionally, within the equine field, this research area may play an important role in an earlier recognition of pain, identification of subclinical pain and subsequent improvements in quality of life and performance.

8.10. Conclusion

Within this thesis, protocols for collection and processing of SF for NMR metabolomic and LC-MS/MS proteomic analysis have been optimised. Lys-C endopeptidase pre-digestion was identified to greatly improve on-bead tryptic protein digestion when used in conjunction with small-capacity ProteoMiner™ column kits for low abundant protein enrichment. Equine OA was stratified using both metabolomic and proteomic SF profiles, identifying a panel of markers of interest which may be applicable to grading OA severity. This is the first study to undertake computational integration of NMR metabolomic and LC-MS/MS proteomic datasets. This thesis is also the first study to use a multi 'omics' approach to simultaneously investigate the metabolomic profile of *ex-vivo* cartilage and metabolomic/proteomic profiles of culture media using the TNF-α/IL-1β *ex-vivo* cartilage OA model. A panel of metabolites, proteins and neopeptides were identified which were differentially abundant within an early phase of this OA model and may provide further information on the underlying disease pathogenesis. A direct comparison of human SF from RA and OA identified that the metabolic pathways that differ most between these two forms of arthritis are glycolysis, amino acid biosynthesis and taurine and hypotaurine metabolism. This thesis has also identified a panel of metabolites and proteins within equine SF which are able to distinguish synovial sepsis from nonseptic joint pathologies, with glucose the principal metabolite discriminator.

References

Abbink, J.J., Kamp, A.M., Nieuwenhuys, E.J., Nuijens, J.H., Swaak, A.J.G. and Hack, C.E. (1991), "Predominant Role of Neutrophils in the Inactivation of α2-Macroglobulin in Arthritic Joints", *Arthritis & Rheumatism*, Vol. 34 No. 9, pp. 1139–1150.

Aboalola, D. and Han, V.K.M. (2017), "Insulin-Like Growth Factor Binding Protein-6 Alters Skeletal Muscle Differentiation of Human Mesenchymal Stem Cells", *Stem Cells International*, Vol. 2017, pp. 1–17.

Abramson, S.B. (2008), "Osteoarthritis and nitric oxide", *Osteoarthritis and Cartilage*, W.B. Saunders, Vol. 16, pp. S15–S20.

Afeltra, A., Caccavo, D., Ferri, G.M., Addessi, M.A., De Rosa, F.G., Amoroso, A. and Bonomo, L. (1997), "Expression of lactoferrin on human granulocytes: analysis with polyclonal and monoclonal antibodies", *Clin Exp Immunol*, Vol. 109, pp. 279–285.

Aidinis, V., Carninci, P., Armaka, M., Witke, W., Harokopos, V., Pavelka, N., Koczan, D., *et al.* (2005), "Cytoskeletal rearrangements in synovial fibroblasts as a novel pathophysiological determinant of modeled rheumatoid arthritis.", *PLoS Genetics*, Public Library of Science, Vol. 1 No. 4, pp. 455–466.

Al-Ahaideb, A. (2008), "Septic arthritis in patients with rheumatoid arthritis.", *Journal of Orthopaedic Surgery and Research*, BioMed Central, Vol. 3, p. 33.

Albar, A., Almehdar, H., Uversky, V. and Redwan, E. (2014), "Structural Heterogeneity and Multifunctionality of Lactoferrin", *Current Protein & Peptide Science*, Vol. 15 No. 8, pp. 778–797.

Altschul, S.F., Gish, W., Miller, W., Myers, E.W. and Lipman, D.J. (1990), "Basic local alignment search tool", *Journal of Molecular Biology*, Vol. 215 No. 3, pp. 403–410.

Alunno, A., Bistoni, O., Manetti, M., Cafaro, G., Valentini, V., Bartoloni, E., Gerli, R., *et al.* (2017), "Insulin-Like Growth Factor Binding Protein 6 in Rheumatoid Arthritis: A Possible Novel Chemotactic Factor?", *Frontiers in Immunology*, Vol. 8, p. 554.

Alwan, W.H., Carter, S.D., Bennett, D. and Edwards, G.B. (1991), "Glycosaminoglycans in horses with osteoarthritis", *Equine Veterinary Journal*, American Medical Association (AMA), Vol. 23 No. 1, pp. 44–47.

Alwan, W.H., Carter, S.D., Bennett, D., May, S.A. and Edwards, G.B. (1990), "Cartilage breakdown in equine osteoarthritis: measurement of keratan sulphate by an ELISA system.", *Research in Veterinary Science*, Vol. 49 No. 1, pp. 56–60.

Ameye, L., Aria, D., Jepsen, K., Oldberg, A., Xu, T. and Young, M.F. (2002), "Abnormal collagen fibrils in tendons of biglycan/fibromodulin-deficient mice lead to gait impairment, ectopic ossification, and osteoarthritis", *The FASEB Journal*, Federation of American Societies for Experimental Biology, Vol. 16 No. 7, pp. 673–680.

Anderson, J.R., Chokesuwattanaskul, S., Phelan, M.M., Welting, T.J.M., Lian, L.-Y., Peffers, M.J. and Wright, H.L. (2018), "1H NMR Metabolomics Identifies Underlying Inflammatory Pathology in Osteoarthritis and Rheumatoid Arthritis Synovial Joints", *Journal of Proteome Research*, American Chemical Society, Vol. 17 No. 11, pp. 3780–3790.

Anderson, J.R., Phelan, M.M., Clegg, P.D., Peffers, M.J. and Rubio-Martinez, L.M. (2018), "Synovial Fluid Metabolites Differentiate between Septic and Nonseptic Joint Pathologies", *Journal of Proteome Research*, American Chemical Society, Vol. 17 No. 8, pp. 2735–2743.

Anderson, N.L. and Anderson, N.G. (2002), "The human plasma proteome: history, character, and diagnostic prospects", *Mol Cell Proteomics*, Vol. 1 No. 11, pp. 845–867.

Andreassen, S.M., Vinther, A.M.L., Nielsen, S.S., Andersen, P.H., Tnibar, A., Kristensen, A.T. and Jacobsen, S. (2017), "Changes in concentrations of haemostatic and inflammatory biomarkers in synovial fluid after intra-articular injection of lipopolysaccharide in horses.", *BMC Veterinary Research*, BioMed Central, Vol. 13 No. 1, p. 182.

Arai, K., Misumi, K., Carter, S.D., Shinbara, S., Fujiki, M. and Sakamoto, H. (2005), "Analysis of cartilage oligomeric matrix protein (COMP) degradation and synthesis in equine joint disease", *Equine Veterinary Journal*, American Medical Association (AMA), Vol. 37 No. 1, pp. 31–36.

Arai, K., Tagami, M., Hatazoe, T., Nishimatsu, E., Shimizu, Y., Fujiki, M. and Misumi, K. (2008), "Analysis of cartilage oligomeric matrix protein (COMP) in synovial fluid, serum and urine from 51 racehorses with carpal bone fracture.", *The Journal of Veterinary Medical Science*, Vol. 70 No. 9, pp. 915–21.

Ariza-Suárez, Á.C., Stanek, C., Edinger, J. and Buchner, H. (2017), "Measurement of Metalloproteinase-3 levels in synovial fluid from horses as biomarker of joint disease", *Revista Electrónica de Veterinaria*, Vol. 18 No. 10, pp. 1–11.

"Arthritis Research UK". (2018), *What Is Rheumatoid Arthritis?*, available at: https://www.arthritisresearchuk.org/arthritis-information/conditions/rheumatoid-arthritis/what-is-rheumatoid-arthritis.aspx (accessed 13 September 2018).

Arthur, R.E., Stern, M., Galeazzi, M., Baldassare, A.R., Weiss, T.D., Rogers, J.R. and Zuckner, J. (1983), "Synovial fluid lactic acid in septic and nonseptic arthritis", *Arthritis & Rheumatism*, John Wiley & Sons, Inc., Vol. 26 No. 12, pp. 1499–

1505.

Aşkın, A., Özkan, A., Tosun, A., Demirdal, Ü.S. and İsnaç, F. (2017), “Quality of life and functional capacity are adversely affected in osteoarthritis patients with neuropathic pain”, *The Kaohsiung Journal of Medical Sciences*, No longer published by Elsevier, Vol. 33 No. 3, pp. 152–158.

Attur, M., Ben-Artzi, A., Yang, Q., Al-Mussawir, H.E., Worman, H.J., Palmer, G. and Abramson, S.B. (2012), “Perturbation of nuclear lamin A causes cell death in chondrocytes.”, *Arthritis and Rheumatism*, NIH Public Access, Vol. 64 No. 6, pp. 1940–9.

Baccarin, R.Y.A., Rasera, L., Machado, T.S.L. and Michelacci, Y.M. (2014), “Relevance of synovial fluid chondroitin sulphate as a biomarker to monitor polo pony joints.”, *Canadian Journal of Veterinary Research = Revue Canadienne de Recherche Veterinaire*, Canadian Veterinary Medical Association, Vol. 78 No. 1, pp. 50–60.

Balakrishnan, L., Nirujogi, R.S., Ahmad, S., Bhattacharjee, M., Manda, S.S., Renuse, S., Kelkar, D.S., *et al.* (2014), “Proteomic analysis of human osteoarthritis synovial fluid”, *Clin Proteomics*, Vol. 11 No. 1, p. 6.

Barksby, H.E., Milner, J.M., Patterson, A.M., Peake, N.J., Hui, W., Robson, T., Lakey, R., *et al.* (2006), “Matrix metalloproteinase 10 promotion of collagenolysis via procollagenase activation: Implications for cartilage degradation in arthritis”, *Arthritis & Rheumatism*, John Wiley & Sons, Ltd, Vol. 54 No. 10, pp. 3244–3253.

Barr, E.D. (2010), *The Association of Bone and Cartilage in Matrix Proteolysis of Articular Cartilage, and Its Role in Palmar/Plantar Osteochondral Disease in the Thoroughbred Racehorse*, University of Liverpool.

Barr, E.D., Pinchbeck, G.L., Clegg, P.D., Boyde, A. and Riggs, C.M. (2009), “Post mortem evaluation of palmar osteochondral disease (traumatic osteochondrosis) of the metacarpo/metatarsophalangeal joint in Thoroughbred racehorses.”, *Equine Veterinary Journal*, Vol. 41 No. 4, pp. 366–71.

Bartok, B. and Firestein, G.S. (2010), “Fibroblast-like synoviocytes: key effector cells in rheumatoid arthritis”, *Immunol Rev*, Vol. 233 No. 1, pp. 233–255.

Baveye, S., Elass, E., Mazurier, J., Spik, G. and Legrand, D. (1999), “Lactoferrin: A Multifunctional Glycoprotein Involved in the Modulation of the Inflammatory Process”, *Clinical Chemistry and Laboratory Medicine*, Vol. 37 No. 3, pp. 281–6.

Bay-Jensen, A.C., Reker, D., Kjelgaard-Petersen, C.F., Mobasheri, A., Karsdal, M.A., Ladel, C., Henrotin, Y., *et al.* (2016), “Osteoarthritis year in review 2015: soluble biomarkers and the BIPED criteria”, *Osteoarthritis Cartilage*, Vol. 24 No. 1, pp. 9–20.

Baynes, R.D. and Bezwoda, W.R. (1994), “Lactoferrin and the Inflammatory Response”, Springer, Boston, MA, pp. 133–141.

Becker, E.D. (2000), “High resolution NMR : theory and chemical applications”, Third., Academic Press, pp. 1–424.

Beckonert, O., Keun, H.C., Ebbels, T.M.D., Bundy, J., Holmes, E., Lindon, J.C. and Nicholson, J.K. (2007), “Metabolic profiling, metabolomic and metabonomic procedures for NMR spectroscopy of urine, plasma, serum and tissue extracts”, *Nature Protocols*, Nature Publishing Group, Vol. 2 No. 11, pp. 2692–2703.

Beltran, A., Suarez, M., Rodríguez, M.A., Vinaixa, M., Samino, S., Arola, L., Correig, X., *et al.* (2012), “Assessment of Compatibility between Extraction Methods for NMR- and LC/MS-Based Metabolomics”, *Analytical Chemistry*, American Chemical Society, Vol. 84 No. 14, pp. 5838–5844.

Ben-Aderet, L., Merquiol, E., Fahham, D., Kumar, A., Reich, E., Ben-Nun, Y., Kandel, L., *et al.* (2015), “Detecting cathepsin activity in human osteoarthritis via activity-based probes”, *Arthritis Research & Therapy*, BioMed Central, Vol. 17 No. 1, p. 69.

Benjamini, Y. and Hochberg, Y. (1995), “Controlling the False Discovery Rate: A Practical and Powerful Approach to Multiple Testing”, *Journal of the Royal Statistical Society. Series B (Methodological)*, WileyRoyal Statistical Society, Vol. 57, pp. 289–300.

Bennett, R.M. and Skosey, J.L. (1977), “Lactoferrin and lysozyme levels in synovial fluid”, *Arthritis & Rheumatism*, Wiley-Blackwell, Vol. 20 No. 1, pp. 84–90.

Berenbaum, F. (2013), “Osteoarthritis as an inflammatory disease (osteoarthritis is not osteoarthrosis!)”, *Osteoarthritis Cartilage*, Vol. 21 No. 1, pp. 16–21.

Berg, J.M., Tymoczko, J.L. and Stryer, L. (2012), *Biochemistry: International Edition*, 7th editio., W.H. Freeman, Basingstoke.

Berger, M.J., Kean, C.O., Goela, A. and Doherty, T.J. (2012), “Disease severity and knee extensor force in knee osteoarthritis: data from the Osteoarthritis Initiative.”, *Arthritis Care & Research*, NIH Public Access, Vol. 64 No. 5, pp. 729–34.

Bertone, A.L., Palmer, J.L. and Jones, J. (2001), “Synovial fluid cytokines and eicosanoids as markers of joint disease in horses”, *Veterinary Surgery*, Wiley/Blackwell (10.1111), Vol. 30 No. 6, p. ajvet0300528.

Bertuglia, A., Pagliara, E., Grego, E., Ricci, A. and Brkljaca-Bottegaro, N. (2016), “Pro-inflammatory cytokines and structural biomarkers are effective to categorize osteoarthritis phenotype and progression in Standardbred racehorses over five years of racing career.”, *BMC Veterinary Research*, BioMed Central, Vol. 12 No. 1, p. 246.

Billinghurst, R.C. (2002), “Biomarkers of joint disease”, in Robinson, N.E. (Ed.), *Current Therapy in Equine Medicine*, 5th ed., W.B. Saunders Co., Philadelphia, pp. 513–520.

Billinghurst, R.C., Brama, P.A.J., van Weeren, P.R., Knowlton, M.S. and McIlwraith, C.W. (2004), “Evaluation of serum concentrations of biomarkers of skeletal metabolism and results of radiography as indicators of severity of osteochondrosis in foals.”, *American Journal of Veterinary Research*, Vol. 65 No. 2, pp. 143–50.

Biniecka, M., Canavan, M., McGarry, T., Gao, W., McCormick, J., Cregan, S., Gallagher, L., *et al.* (2016), “Dysregulated bioenergetics: a key regulator of joint inflammation”, *Ann Rheum Dis*, Vol. 75 No. 12, pp. 2192–2200.

Blaum, B. (2010), *Glycosaminoglycan-Protein Interactions and Human Complement Factor H*, University of Edinburgh.

Blewis, M.E., Nugent-Derfus, G.E., Schmidt, T.A., Schumacher, B.L. and Sah, R.L. (2007), “A model of synovial fluid lubricant composition in normal and injured joints”, *Eur Cell Mater*, Vol. 13, pp. 26–39.

Blom, A.M. (2017), “The role of complement inhibitors beyond controlling inflammation”, *Journal of Internal Medicine*, John Wiley & Sons, Ltd (10.1111), Vol. 282 No. 2, pp. 116–128.

Bohnen, N., Terwel, D., Markermk, M., Haaf, J.A. Ten and Jolles, J. (1992), “Pitfalls in the Measurement of Plasma Osmolality Pertinent to Research in Vasopressin and Water Metabolism”, *Clinical Chemistry*, Vol. 38 No. 1, pp. 2278–2280.

Bonassar, L.J., Frank, E.H., Murray, J.C., Paguio, C.G., Moore, V.L., Lark, M.W., Sandy, J.D., *et al.* (1995), “Changes in cartilage composition and physical properties due to stromelysin degradation”, *Arthritis & Rheumatism*, John Wiley & Sons, Ltd, Vol. 38 No. 2, pp. 173–183.

van den Boom, R., van der Harst, M.R., Brommer, H., Brama, P.A.J., Barneveld, A., van Weeren, P.R. and De Groot, J. (2005), “Relationship between synovial fluid levels of glycosaminoglycans, hydroxyproline and general MMP activity and the presence and severity of articular cartilage change on the proximal articular surface of P1”, *Equine Veterinary Journal*, American Medical Association (AMA), Vol. 37 No. 1, pp. 19–25.

Borel, M., Pastoureau, P., Papon, J., Madelmont, J.C., Moins, N., Maublant, J. and Miot-Noirault, E. (2009), “Longitudinal Profiling of Articular Cartilage Degradation in Osteoarthritis by High-Resolution Magic Angle Spinning ^{1}H NMR Spectroscopy: Experimental Study in the Meniscectomized Guinea Pig Model”, *Journal of Proteome Research*, American Chemical Society, Vol. 8 No. 5, pp. 2594–2600.

Brama, P.A., TeKoppele, J.M., Beekman, B., van Weeren, P.R. and Barneveld, A.

(1998), “Matrix metalloproteinase activity in equine synovial fluid: influence of age, osteoarthritis, and osteochondrosis.”, *Annals of the Rheumatic Diseases*, BMJ Publishing Group, Vol. 57 No. 11, pp. 697–9.

Brama, P.A.J., Boom, R., DEGroot, J., Kiers, G.H. and Weeren, P.R. (2004), “Collagenase-1 (MMP-1) activity in equine synovial fluid: influence of age, joint pathology, exercise and repeated arthrocentesis”, *Equine Veterinary Journal*, American Medical Association (AMA), Vol. 36 No. 1, pp. 34–40.

Brink, H.F., Buschmann, M.D. and Rosen, B.R. (1988), “NMR chemical shift imaging.”, *Computerized Medical Imaging and Graphics : The Official Journal of the Computerized Medical Imaging Society*, Vol. 13 No. 1, pp. 93–104.

Brommer, H., van Weeren, P.R. and Brama, P.A. (2003), “New approach for quantitative assessment of articular cartilage degeneration in horses with osteoarthritis”, *Am J Vet Res*, Vol. 64 No. 1, pp. 83–87.

Brouwers, H., von Hegedus, J., Toes, R., Kloppenburg, M. and Ioan-Facsinay, A. (2015), “Lipid mediators of inflammation in rheumatoid arthritis and osteoarthritis”, *Best Pract Res Clin Rheumatol*, Vol. 29 No. 6, pp. 741–755.

Brown, M.P., West, L.A., Merritt, K.A. and Plaas, A.H. (1998), “Changes in sulfation patterns of chondroitin sulfate in equine articular cartilage and synovial fluid in response to aging and osteoarthritis.”, *American Journal of Veterinary Research*, Vol. 59 No. 6, pp. 786–91.

Buckwalter, J.A., Mankin, H.J. and Grodzinsky, A.J. (2005), “Articular cartilage and osteoarthritis.”, *Instructional Course Lectures*, Vol. 54, pp. 465–80.

Caccavo, D., Garzia, P., Sebastiani, G.D., Ferri, G.M., Galluzzo, S., Vadacca, M., Rigon, A., *et al.* (2003), “Expression of lactoferrin on neutrophil granulocytes from synovial fluid and peripheral blood of patients with rheumatoid arthritis.”, *The Journal of Rheumatology*, The Journal of Rheumatology, Vol. 30 No. 2, pp. 220–4.

Carlyle, B., Trombetta, B., Arnold, S., Carlyle, B.C., Trombetta, B.A. and Arnold, S.E. (2018), “Proteomic Approaches for the Discovery of Biofluid Biomarkers of Neurodegenerative Dementias”, *Proteomes*, Multidisciplinary Digital Publishing Institute, Vol. 6 No. 3, p. 32.

Caron, J. and Genovese, R. (2003), “Principles and practices of joint disease treatment”, in Ross, M. and Dyson, S. (Eds.), *Diagnosis and Management of Lameness in the Horse*, 2nd ed., W.B. Saunders, Philadelphia, pp. 746–764.

Caterson, B., Baker, J.R., Christnerg, J.E., Leell, Y. and Lentzn, M. (1985), “Monoclonal Antibodies as Probes for Determining the Microheterogeneity of the Link Proteins of Cartilage Proteoglycan”, *The Journal of Biological Chemistry*, Vol. 260 No. 19.

Catterall, J.B., Rowan, A.D., Sarsfield, S., Saklatvala, J., Wait, R. and Cawston, T.E. (2006), "Development of a novel 2D proteomics approach for the identification of proteins secreted by primary chondrocytes after stimulation by IL-1 and oncostatin M", *Rheumatology*, Oxford University Press, Vol. 45 No. 9, pp. 1101–1109.

Cavill, R., Jennen, D., Kleinjans, J. and Briedé, J.J. (2016), "Transcriptomic and metabolomic data integration", *Briefings in Bioinformatics*, Oxford University Press, Vol. 17 No. 5, pp. 891–901.

Cejka, D., Hayer, S., Niederreiter, B., Sieghart, W., Fuereder, T., Zwerina, J. and Schett, G. (2010), "Mammalian target of rapamycin signaling is crucial for joint destruction in experimental arthritis and is activated in osteoclasts from patients with rheumatoid arthritis", *Arthritis & Rheumatism*, John Wiley & Sons, Ltd, Vol. 62 No. 8, pp. 2294–2302.

De Ceuninck, F., Dassencourt, L. and Anract, P. (2004), "The inflammatory side of human chondrocytes unveiled by antibody microarrays", *Biochemical and Biophysical Research Communications*, Academic Press, Vol. 323 No. 3, pp. 960–969.

Chiaradia, E., Pepe, M., Tartaglia, M., Scoppetta, F., D'Ambrosio, C., Renzone, G., Avellini, L., *et al.* (2012), "Gambling on putative biomarkers of osteoarthritis and osteochondrosis by equine synovial fluid proteomics", *Journal of Proteomics*, Vol. 75 No. 14, pp. 4478–4493.

Chong, J., Soufan, O., Li, C., Caraus, I., Li, S., Bourque, G., Wishart, D.S., *et al.* (2018), "MetaboAnalyst 4.0: towards more transparent and integrative metabolomics analysis", *Nucleic Acids Research*, Oxford University Press, Vol. 46 No. W1, pp. W486–W494.

Christians, U., Klawitter, J., Klepacki, J. and Klawitter, J. (2017), "The Role of Proteomics in the Study of Kidney Diseases and in the Development of Diagnostic Tools", in Edelstein, C.L. (Ed.), *Biomarkers of Kidney Disease*, 2nd ed., Elsevier, pp. 119–223.

Cillero-Pastor, B., Ruiz-Romero, C., Caramés, B., López-Armada, M.J. and Blanco, F.J. (2010), "Proteomic analysis by two-dimensional electrophoresis to identify the normal human chondrocyte proteome stimulated by tumor necrosis factor α and interleukin-1β", *Arthritis & Rheumatism*, Wiley-Blackwell, Vol. 62 No. 3, pp. 802–814.

Citronberg, J.S., Wilkens, L.R., Lim, U., Hullar, M.A.J., White, E., Newcomb, P.A., Le Marchand, L., *et al.* (2016), "Reliability of plasma lipopolysaccharide-binding protein (LBP) from repeated measures in healthy adults.", *Cancer Causes & Control : CCC*, NIH Public Access, Vol. 27 No. 9, pp. 1163–6.

Ciurtin, C., Cojocaru, V.M., Miron, I.M., Preda, F., Milicescu, M., Bojinca, M., Costan, O., *et al.* (2006), "Correlation between different components of synovial fluid

and pathogenesis of rheumatic diseases", *Rom J Intern Med*, Vol. 44 No. 2, pp. 171–181.

Cleary, O.B., Trumble, T.N., Merritt, K.A. and Brown, M.P. (2010), "Effect of exercise and osteochondral injury on synovial fluid and serum concentrations of carboxy-terminal telopeptide fragments of type II collagen in racehorses.", *American Journal of Veterinary Research*, Vol. 71 No. 1, pp. 33–40.

Clegg, P.D., Coughlan, A.R., Riggs, C.M. and Carter, S.D. (1997), "Matrix metalloproteinases 2 and 9 in equine synovial fluids", *Equine Veterinary Journal*, American Medical Association (AMA), Vol. 29 No. 5, pp. 343–348.

Cooke, T.D., Hurd, E.R., Jasin, H.E., Bienenstock, J. and Ziff, M. (1975), "Identification of immunoglobulins and complement in rheumatoid articular collagenous tissues", *Arthritis & Rheumatism*, John Wiley & Sons, Ltd, Vol. 18 No. 6, pp. 541–551.

Cope, P.J., Ourradi, K., Li, Y. and Sharif, M. (2019), "Models of osteoarthritis: the good, the bad and the promising", *Osteoarthritis and Cartilage*, W.B. Saunders, Vol. 27 No. 2, pp. 230–239.

Cuppen, B. V, Fu, J., van Wietmarschen, H.A., Harms, A.C., Koval, S., Marijnissen, A.C., Peeters, J.J., *et al.* (2016), "Exploring the Inflammatory Metabolomic Profile to Predict Response to TNF-alpha Inhibitors in Rheumatoid Arthritis", *PLoS One*, Vol. 11 No. 9, p. e0163087.

Dagleish, M.P., Wakeman, K.D. and McDiarmid, A.M. (2003), "A preliminary evaluation of the use of equine neutrophil elastase 2A concentration in synovial fluid as a marker for joint inflammation in horses", *Equine Veterinary Journal*, American Medical Association (AMA), Vol. 35 No. 6, pp. 623–626.

Damyanovich, A.Z., Staples, J.R., Chan, A.D. and Marshall, K.W. (1999), "Comparative study of normal and osteoarthritic canine synovial fluid using 500 MHz 1H magnetic resonance spectroscopy", *J Orthop Res*, Vol. 17 No. 2, pp. 223–231.

Damyanovich, A.Z., Staples, J.R. and Marshall, K.W. (2000), "The effects of freeze/thawing on human synovial fluid observed by 500 MHz 1H magnetic resonance spectroscopy.", *The Journal of Rheumatology*, Vol. 27 No. 3, pp. 746–52.

Davidson, R., Gardner, S., Jupp, O., Bullough, A., Butters, S., Watts, L., Donell, S., *et al.* (2017), "Isothiocyanates are detected in human synovial fluid following broccoli consumption and can affect the tissues of the knee joint.", *Scientific Reports*, Nature Publishing Group, Vol. 7 No. 1, p. 3398.

Davis, J.M. and Matteson, E.L. (2012), "My Treatment Approach to Rheumatoid Arthritis", *Mayo Clin Proc*, Vol. 87 No. 7, pp. 659–673.

Day, J.S., Van Der Linden, J.C., Bank, R.A., Ding, M., Hvid, I., Sumner, D.R. and Weinans, H. (2004), "Adaptation of subchondral bone in osteoarthritis.", *Biorheology*, Vol. 41 No. 3–4, pp. 359–68.

Decoteau, E., Yurchak, A.M., Partridge, R.E.H. and Tomasi, T.B. (1972), "Lactoferrin in synovial fluid of patients with inflammatory arthritis", *Arthritis & Rheumatism*, Wiley-Blackwell, Vol. 15 No. 3, pp. 324–325.

Demarque, D.P., Crotti, A.E.M., Vessecchi, R., Lopes, J.L.C. and Lopes, N.P. (2016), "Fragmentation reactions using electrospray ionization mass spectrometry: an important tool for the structural elucidation and characterization of synthetic and natural products", *Natural Product Reports*, Royal Society of Chemistry, Vol. 33 No. 3, pp. 432–455.

Dicker, K.T., Gurski, L.A., Pradhan-Bhatt, S., Witt, R.L., Farach-Carson, M.C. and Jia, X. (2014), "Hyaluronan: a simple polysaccharide with diverse biological functions.", *Acta Biomaterialia*, NIH Public Access, Vol. 10 No. 4, pp. 1558–70.

Dieplinger, H. and Dieplinger, B. (2015), "Afamin — A pleiotropic glycoprotein involved in various disease states", *Clinica Chimica Acta*, Vol. 446, pp. 105–110.

Dieterle, F., Ross, A., Schlotterbeck, G. and Senn, H. (2006), "Probabilistic Quotient Normalization as Robust Method to Account for Dilution of Complex Biological Mixtures. Application in 1H NMR Metabonomics", American Chemical Society, available at:https://doi.org/10.1021/AC051632C.

DiNubile, M.J., Stossel, T.P., Ljunghusen, O.C., Ferrara, J.L.M. and Antin, J.H. (2002), "Prognostic implications of declining plasma gelsolin levels after allogeneic stem cell transplantation.", *Blood*, American Society of Hematology, Vol. 100 No. 13, pp. 4367–71.

Donabedian, M., Weeren, P.R., Perona, G., Fleurance, G., Robert, C., Leger, S., Bergero, D., *et al.* (2008), "Early changes in biomarkers of skeletal metabolism and their association to the occurrence of osteochondrosis (OC) in the horse", *Equine Veterinary Journal*, American Medical Association (AMA), Vol. 40 No. 3, pp. 253–259.

Duffy, J.M., Grimshaw, J., Guthrie, D.J., McNally, G.M., Mollan, R.A., Spedding, P.L., Trocha-Grimshaw, J., *et al.* (1993), "1H-nuclear magnetic resonance studies of human synovial fluid in arthritic disease states as an aid to confirming metabolic activity in the synovial cavity.", *Clinical Science (London, England : 1979)*, Portland Press Limited, Vol. 85 No. 3, pp. 343–51.

Edde, L., Hipolito, R.B., Hwang, F.F.Y., Headon, D.R., Shalwitz, R.A. and Sherman, M.P. (2001), "Lactoferrin protects neonatal rats from gut-related systemic infection", *American Journal of Physiology-Gastrointestinal and Liver Physiology*, American Physiological SocietyBethesda, MD , Vol. 281 No. 5, pp. G1140–G1150.

Eichner, J., Rosenbaum, L., Wrzodek, C., Häring, H.-U., Zell, A. and Lehmann, R. (2014), "Integrated enrichment analysis and pathway-centered visualization of metabolomics, proteomics, transcriptomics, and genomics data by using the InCroMAP software", *Journal of Chromatography B*, Vol. 966, pp. 77–82.

Escalona, E. (2015), *Metabonomic Characterisation of the Thoroughbred Racehorse*, Imperial College London.

Fanigliulo, A., Cabooter, D., Bellazzi, G., Allieri, B., Rottigni, A. and Desmet, G. (2011), "Kinetic performance of reversed-phase C18 high-performance liquid chromatography columns compared by means of the Kinetic Plot Method in pharmaceutically relevant applications", *Journal of Chromatography A*, Elsevier, Vol. 1218 No. 21, pp. 3351–3359.

Fenn, J.B., Mann, M., Meng, C.K., Wong, S.F. and Whitehouse, C.M. (1989), "Electrospray ionization for mass spectrometry of large biomolecules.", *Science (New York, N.Y.)*, American Association for the Advancement of Science, Vol. 246 No. 4926, pp. 64–71.

Fernandes, J.C., Martel-Pelletier, J. and Pelletier, J.-P. (2002), "The role of cytokines in osteoarthritis pathophysiology.", *Biorheology*, Vol. 39 No. 1–2, pp. 237–46.

Fernandez-Costa, C., Calamia, V., Fernandez-Puente, P., Capelo-Martinez, J.L., Ruiz-Romero, C. and Blanco, F.J. (2012), "Sequential depletion of human serum for the search of osteoarthritis biomarkers", *Proteome Sci*, Vol. 10 No. 1, p. 55.

Fietz, S., Einspanier, R., Hoppner, S., Hertsch, B. and Bondzio, A. (2008), "Determination of MMP-2 and -9 activities in synovial fluid of horses with osteoarthritic and arthritic joint diseases using gelatin zymography and immunocapture activity assays", *Equine Veterinary Journal*, American Medical Association (AMA), Vol. 40 No. 3, pp. 266–271.

de Figueroa, P.L., Nogueira-Recalde, U., Osorio, F., Lotz, M., Lopez-Otin, C., Blanco, F.J. and Carames, B. (2017), "Deficient Autophagy Induces Lamin a/C Accumulation in Aging and Osteoarthritis", *American College of Rheumatology*, Vol. 69 No. Supplement 10.

Fonslow, B.R., Carvalho, P.C., Academia, K., Freeby, S., Xu, T., Nakorchevsky, A., Paulus, A., *et al.* (2011), "Improvements in Proteomic Metrics of Low Abundance Proteins through Proteome Equalization Using ProteoMiner Prior to MudPIT", *Journal of Proteome Research*, American Chemical Society, Vol. 10 No. 8, pp. 3690–3700.

Freeby, S., Walker, J., Paulus, A., Smith, K., Liu, N. and Academia, K. (2010), "Enrichment of Medium- and Low-abundance Proteins in Sample Types Using Proteominer Technology", *Bio-Rad Laboratories*, pp. 1–6.

Frisbie, D. (2006), "Synovial Joint Biology and Pathobiology", in Auer, J. and Stick, J. (Eds.), *Equine Surgery*, 3rd ed., Elsevier Inc, St Louis, pp. 1096–1114.

Frisbie, D., Al-Sobayil, F., Billinghurst, R. and McIlwraith, C. (2002), "Serum Markers Differentiate Exercise from Pathology and Correlate to Clinical Parameters of Pain in an Osteoarthritic Model", available at: http://www.ors.org/Transactions/49/0751.pdf (accessed 3 January 2019).

Frisbie, D.D., Al-Sobayil, F., Billinghurst, R.C., Kawcak, C.E. and McIlwraith, C.W. (2008), "Changes in synovial fluid and serum biomarkers with exercise and early osteoarthritis in horses", *Osteoarthritis and Cartilage*, Vol. 16 No. 10, pp. 1196–1204.

Frisbie, D.D., Al-Sobayil, F.A., Billinghurst, R.C. and McIlwraith, C.W. (2003), "Synovial fluid biomarkers distinguish exercise from osteoarthritic pathology.", *Proceedings of the 49th Annual Convention of the American Association of Equine Practitioners, New Orleans, Louisiana, USA, 21-25 November 2003*, American Association of Equine Practitioners (AAEP), pp. 116–117.

Frisbie, D.D., Ray, C.S., Ionescu, M., Poole, A.R., Chapman, P.L. and McIlwraith, C.W. (1999), "Measurement of synovial fluid and serum concentrations of the 846 epitope of chondroitin sulfate and of carboxy propeptides of type II procollagen for diagnosis of osteochondral fragmentation in horses.", *American Journal of Veterinary Research*, Vol. 60 No. 3, pp. 306–9.

Fuller, C.J., Barr, A.R., Sharif, M. and Dieppe, P.A. (2001), "Cross-sectional comparison of synovial fluid biochemical markers in equine osteoarthritis and the correlation of these markers with articular cartilage damage", *Osteoarthritis and Cartilage*, W.B. Saunders, Vol. 9 No. 1, pp. 49–55.

Furka, A., Sebestyen, F., Asgedom, M. and Dibo, G. (1991), "General method for rapid synthesis of multicomponent peptide mixtures", *Int J Pept Protein Res*, Vol. 37 No. 6, pp. 487–493.

Fusco, M., Skaper, S.D., Coaccioli, S., Varrassi, G. and Paladini, A. (2017), "Degenerative Joint Diseases and Neuroinflammation", *Pain Practice*, John Wiley & Sons, Ltd (10.1111), Vol. 17 No. 4, pp. 522–532.

García-Alcalde, F., García-López, F., Dopazo, J. and Conesa, A. (2011), "Paintomics: a web based tool for the joint visualization of transcriptomics and metabolomics data.", *Bioinformatics (Oxford, England)*, Oxford University Press, Vol. 27 No. 1, pp. 137–9.

Garner, B.C., Kuroki, K., Stoker, A.M., Cook, C.R. and Cook, J.L. (2013), "Expression of proteins in serum, synovial fluid, synovial membrane, and articular cartilage samples obtained from dogs with stifle joint osteoarthritis secondary to cranial cruciate ligament disease and dogs without stifle joint arthritis", *Am J Vet Res*, Vol. 74 No. 3, pp. 386–394.

Gibson, D.S. and Rooney, M.E. (2007), "The human synovial fluid proteome: A key factor in the pathology of joint disease", *Proteomics - Clinical Applications*, Wiley-Blackwell, Vol. 1 No. 8, pp. 889–899.

Gibson, K.T., Hodge, H. and Whittem, T. (1996), “Inflammatory mediators in equine synovial fluid”, *Australian Veterinary Journal*, Wiley/Blackwell (10.1111), Vol. 73 No. 4, pp. 148–151.

Giera, M., Ioan-Facsinay, A., Toes, R., Gao, F., Dalli, J., Deelder, A.M., Serhan, C.N., *et al.* (2012), “Lipid and lipid mediator profiling of human synovial fluid in rheumatoid arthritis patients by means of LC-MS/MS”, *Biochim Biophys Acta*, Vol. 1821 No. 11, pp. 1415–1424.

Glatter, T., Ludwig, C., Ahrné, E., Aebersold, R., Heck, A.J.R. and Schmidt, A. (2012), “Large-Scale Quantitative Assessment of Different In-Solution Protein Digestion Protocols Reveals Superior Cleavage Efficiency of Tandem Lys-C/Trypsin Proteolysis over Trypsin Digestion”, *Journal of Proteome Research*, American Chemical Society, Vol. 11 No. 11, pp. 5145–5156.

Gobelet, C. and Gerster, J.C. (1984), “Synovial fluid lactate levels in septic and non-septic arthritides.”, *Annals of the Rheumatic Diseases*, Vol. 43 No. 5, pp. 742–5.

Gobezie, R., Kho, A., Krastins, B., Sarracino, D.A., Thornhill, T.S., Chase, M., Millett, P.J., *et al.* (2007), “High abundance synovial fluid proteome: distinct profiles in health and osteoarthritis”, *Arthritis Res Ther*, Vol. 9 No. 2, p. R36.

Goldenberg, D.L. (1989), “Infectious arthritis complicating rheumatoid arthritis and other chronic rheumatic disorders”, *Arthritis & Rheumatism*, John Wiley & Sons, Ltd, Vol. 32 No. 4, pp. 496–502.

Goldring, S.R. and Goldring, M.B. (2004), “The Role of Cytokines in Cartilage Matrix Degeneration in Osteoarthritis”, *Clinical Orthopaedics and Related Research*, Vol. 427S, pp. 27–36.

de Grauw, J.C., Brama, P.A., Wiemer, P., Brommer, H., van de Lest, C.H. and van Weeren, P.R. (2006), “Cartilage-derived biomarkers and lipid mediators of inflammation in horses with osteochondritis dissecans of the distal intermediate ridge of the tibia”, *American Journal of Veterinary Research*, Vol. 67 No. 7, pp. 1156–1162.

de Grauw, J.C., Donabédian, M., van de Lest, C.H.A., Perona, G., Robert, C., Lepage, O., Martin-Rosset, W., *et al.* (2011), “Assessment of synovial fluid biomarkers in healthy foals and in foals with tarsocrural osteochondrosis”, *The Veterinary Journal*, W.B. Saunders, Vol. 190 No. 3, pp. 390–395.

de Grauw, J.C., van de Lest, C.H.A. and van Weeren, P.R. (2009), “Inflammatory mediators and cartilage biomarkers in synovial fluid after a single inflammatory insult: a longitudinal experimental study.”, *Arthritis Research & Therapy*, BioMed Central, Vol. 11 No. 2, p. R35.

de Grauw, J.C., van de Lest, C.H.A., van Weeren, R., Brommer, H. and Brama, P.A.J. (2006), “Arthrogenic lameness of the fetlock: synovial fluid markers of inflammation and cartilage turnover in relation to clinical joint pain”, *Equine*

Veterinary Journal, American Medical Association (AMA), Vol. 38 No. 4, pp. 305–311.

Griffin, T.M. and Guilak, F. (2008), "Why is obesity associated with osteoarthritis? Insights from mouse models of obesity", *Biorheology*, IOS Press, Vol. 45 No. 3–4, pp. 387–398.

Guan, S. and Marshall, A.G. (1996), "Stacked-Ring Electrostatic Ion Guide", *American Society for Mass Spectrometry*, Vol. 7, pp. 101–106.

Guma, M., Tiziani, S. and Firestein, G.S. (2016), "Metabolomics in rheumatic diseases: desperately seeking biomarkers", *Nat Rev Rheumatol*, Vol. 12 No. 5, pp. 269–281.

Guo, D., Tan, W., Wang, F., Lv, Z., Hu, J., Lv, T., Chen, Q., *et al.* (2008), "Proteomic analysis of human articular cartilage: identification of differentially expressed proteins in knee osteoarthritis", *Joint Bone Spine*, Vol. 75 No. 4, pp. 439–444.

Gupta, A.K., Parasar, D., Sagar, A., Choudhary, V., Chopra, B.S., Garg, R., Ashish, *et al.* (2015), "Analgesic and Anti-Inflammatory Properties of Gelsolin in Acetic Acid Induced Writhing, Tail Immersion and Carrageenan Induced Paw Edema in Mice.", *PloS One*, Public Library of Science, Vol. 10 No. 9, p. e0135558.

Gupta, S., Biswas, A., Akhter, M.S., Krettler, C., Reinhart, C., Dodt, J., Reuter, A., *et al.* (2016), "Revisiting the mechanism of coagulation factor XIII activation and regulation from a structure/functional perspective", *Scientific Reports*, Nature Publishing Group, Vol. 6 No. 1, p. 30105.

Hackett, E.S. and McCue, P.M. (2010), "Evaluation of a Veterinary Glucometer for Use in Horses", *Journal of Veterinary Internal Medicine*, Vol. 24 No. 3, pp. 617–621.

Haltmayer, E., Schwendenwein, I. and Licka, T.F. (2017), "Course of serum amyloid A (SAA) plasma concentrations in horses undergoing surgery for injuries penetrating synovial structures, an observational clinical study.", *BMC Veterinary Research*, BioMed Central, Vol. 13 No. 1, p. 137.

Hartwig, S., Czibere, A., Kotzka, J., Passlack, W., Haas, R., Eckel, J. and Lehr, S. (2009), "Combinatorial hexapeptide ligand libraries (ProteoMiner): an innovative fractionation tool for differential quantitative clinical proteomics", *Arch Physiol Biochem*, Vol. 115 No. 3, pp. 155–160.

Havliš, J. and Shevchenko, A. (2004), "Absolute Quantification of Proteins in Solutions and in Polyacrylamide Gels by Mass Spectrometry", *Analytical Chemistry*, Vol. 76 No. 11, pp. 3029–3036.

Heijink, A., Gomoll, A.H., Madry, H., Drobnič, M., Filardo, G., Espregueira-Mendes, J. and Van Dijk, C.N. (2012), "Biomechanical considerations in the pathogenesis of osteoarthritis of the knee.", *Knee Surgery, Sports Traumatology,*

Arthroscopy : Official Journal of the ESSKA, Springer, Vol. 20 No. 3, pp. 423–35.

Hernvann, A., Jaffray, P., Hilliquin, P., Cazalet, C., Menkes, C.-J. and Ekindjian, O.G. (1996), "Interleukin-1β-mediated glucose uptake by chondrocytes. Inhibition by cortisol", *Osteoarthritis and Cartilage*, W.B. Saunders, Vol. 4 No. 2, pp. 139–142.

Heumann, D., Bas, S., Gallay, P., Le Roy, D., Barras, C., Mensi, N., Glauser, M.P., *et al.* (1995), "Lipopolysaccharide binding protein as a marker of inflammation in synovial fluid of patients with arthritis: correlation with interleukin 6 and C-reactive protein.", *The Journal of Rheumatology*, Vol. 22 No. 7, pp. 1224–9.

Heywood, H.K., Knight, M.M. and Lee, D.A. (2010), "Both superficial and deep zone articular chondrocyte subpopulations exhibit the Crabtree effect but have different basal oxygen consumption rates", *J Cell Physiol*, Vol. 223 No. 3, pp. 630–639.

Honsawek, S., Wilairatana, V., Udomsinprasert, W., Sinlapavilawan, P. and Jirathanathornnukul, N. (2015), "Association of plasma and synovial fluid periostin with radiographic knee osteoarthritis: Cross-sectional study", *Joint Bone Spine*, Elsevier Masson, Vol. 82 No. 5, pp. 352–355.

de Hoog, C.L. and Mann, M. (2004), "Proteomics.", *Annual Review of Genomics and Human Genetics*, Vol. 5 No. 1, pp. 267–93.

Horwitz, J.K., Chun, N.H. and Heeger, P.S. (2019), "Complement and Transplantation", *Clinics in Laboratory Medicine*, Vol. 39 No. 1, pp. 31–43.

Hsieh, E.J., Bereman, M.S., Durand, S., Valaskovic, G.A. and Maccoss, M.J. (2013), "Effects of Column and Gradient Lengths on Peak Capacity and Peptide Identification in Nanoflow LC-MS/MS of Complex Proteomic Samples", *J. Am. Soc. Mass Spectrom*, Vol. 24, pp. 148–153.

Hsueh, M.-F., Önnerfjord, P. and Kraus, V.B. (2014), "Biomarkers and proteomic analysis of osteoarthritis", *Matrix Biology*, Elsevier, Vol. 39, pp. 56–66.

Hu, T., Oksanen, K., Zhang, W., Randell, E., Furey, A., Sun, G. and Zhai, G. (2018), "An evolutionary learning and network approach to identifying key metabolites for osteoarthritis.", *PLoS Computational Biology*, Public Library of Science, Vol. 14 No. 3, p. e1005986.

Huang, Z.Y., Perry, E., Huebner, J.L., Katz, B., Li, Y.-J. and Kraus, V.B. (2018), "Biomarkers of inflammation – LBP and TLR- predict progression of knee osteoarthritis in the DOXY clinical trial", *Osteoarthritis and Cartilage*, available at:https://doi.org/10.1016/j.joca.2018.08.005.

Hugle, T., Kovacs, H., Heijnen, I.A., Daikeler, T., Baisch, U., Hicks, J.M. and Valderrabano, V. (2012), "Synovial fluid metabolomics in different forms of arthritis assessed by nuclear magnetic resonance spectroscopy", *Clin Exp*

Rheumatol, Vol. 30 No. 2, pp. 240–245.

Hui, A.Y., McCarty, W.J., Masuda, K., Firestein, G.S. and Sah, R.L. (2012), "A systems biology approach to synovial joint lubrication in health, injury, and disease", *Wiley Interdisciplinary Reviews: Systems Biology and Medicine*, Wiley-Blackwell, Vol. 4 No. 1, pp. 15–37.

Hulme, C.H., Wilson, E.L., Peffers, M.J., Roberts, S., Simpson, D.M., Richardson, J.B., Gallacher, P., *et al.* (2017), "Autologous chondrocyte implantation-derived synovial fluids display distinct responder and non-responder proteomic profiles.", *Arthritis Research & Therapy*, BioMed Central, Vol. 19 No. 1, p. 150.

Hunt, I. (n.d.). "Nuclear Magnetic Resonance (NMR) Spectroscopy", *Department of Chemistry, University of Calgary*, available at: http://www.chem.ucalgary.ca/courses/350/Carey5th/Ch13/ch13-nmr-1.html (accessed 10 September 2018).

Hunter, D.J., Nevitt, M., Losina, E. and Kraus, V. (2014), "Biomarkers for osteoarthritis: current position and steps towards further validation.", *Best Practice & Research. Clinical Rheumatology*, Elsevier, Vol. 28 No. 1, pp. 61–71.

Huster, D., Schiller, J., Naji, L., Kaufmann, J. and Arnold, K. (2004), "NMR Studies of Cartilage – Dynamics, Diffusion, Degradation", Springer, Berlin, Heidelberg, pp. 465–503.

van Iersel, M.P., Kelder, T., Pico, A.R., Hanspers, K., Coort, S., Conklin, B.R. and Evelo, C. (2008), "Presenting and exploring biological pathways with PathVisio.", *BMC Bioinformatics*, BioMed Central, Vol. 9, p. 399.

Ireland, J.L., Clegg, P.D., McGowan, C.M., McKane, S.A., Chandler, K.J. and Pinchbeck, G.L. (2012), "Disease prevalence in geriatric horses in the United Kingdom: veterinary clinical assessment of 200 cases", *Equine Vet J*, Vol. 44 No. 1, pp. 101–106.

Ireland, J.L., Clegg, P.D., McGowan, C.M., Platt, L. and Pinchbeck, G.L. (2011), "Factors associated with mortality of geriatric horses in the United Kingdom", *Prev Vet Med*, Vol. 101 No. 3–4, pp. 204–218.

Isola, M., Ferrari, V., Miolo, A., Stabile, F., Bernardini, D., Carnier, P. and Busetto, R. (2011), "Nerve growth factor concentrations in the synovial fluid from healthy dogs and dogs with secondary osteoarthritis", *Veterinary and Comparative Orthopaedics and Traumatology*, Schattauer GmbH, Vol. 24 No. 4, pp. 279–284.

Ito, H., Kambe, H., Kimura, Y., Nakamura, H., Hayashi, E., Kishimoto, T., Kishimoto, S., *et al.* (1992), "Depression of plasma gelsolin level during acute liver injury.", *Gastroenterology*, Vol. 102 No. 5, pp. 1686–92.

Ivaska, J., Pallari, H.-M., Nevo, J. and Eriksson, J.E. (2007), "Novel functions of

vimentin in cell adhesion, migration, and signaling", *Experimental Cell Research*, Academic Press, Vol. 313 No. 10, pp. 2050–2062.

Jacobsen, S. and Kjelgaard-Hansen, M. (2008), "Evaluation of a commercially available apparatus for measuring the acute phase protein serum amyloid A in horses.", *The Veterinary Record*, British Medical Journal Publishing Group, Vol. 163 No. 11, pp. 327–30.

Jacobsen, S., Niewold, T.A., Halling-Thomsen, M., Nanni, S., Olsen, E., Lindegaard, C. and Andersen, P.H. (2006), "Serum amyloid A isoforms in serum and synovial fluid in horses with lipopolysaccharide-induced arthritis", *Veterinary Immunology and Immunopathology*, Elsevier, Vol. 110 No. 3–4, pp. 325–330.

Jacobsen, S., Thomsen, M.H. and Nanni, S. (2006), "Concentrations of serum amyloid A in serum and synovial fluid from healthy horses and horses with joint disease", *American Journal of Veterinary Research*, American Veterinary Medical Association 1931 North Meacham Road, Suite 100, Schaumburg, IL 60173-4360 USA 847-925-8070 847-925-1329 avmajournals@avma.org , Vol. 67 No. 10, pp. 1738–1742.

Jean, Y.-H., Wen, Z.-H., Chang, Y.-C., Huang, G.-S., Lee, H.-S., Hsieh, S.-P. and Wong, C.-S. (2005), "Increased concentrations of neuro-excitatory amino acids in rat anterior cruciate ligament-transected knee joint dialysates: A microdialysis study", *Journal of Orthopaedic Research*, Wiley-Blackwell, Vol. 23 No. 3, pp. 569–575.

Jekel, P.A., Weijer, W.J. and Beintema, J.J. (1983), "Use of endoproteinase Lys-C from Lysobacter enzymogenes in protein sequence analysis", *Analytical Biochemistry*, Academic Press, Vol. 134 No. 2, pp. 347–354.

Ji, J., Zhang, L., Zhang, Q., Yin, R., Fu, T., Li, L. and Gu, Z. (2017), "Functional disability associated with disease and quality-of-life parameters in Chinese patients with rheumatoid arthritis.", *Health and Quality of Life Outcomes*, BioMed Central, Vol. 15 No. 1, p. 89.

Johnson, C.I., Argyle, D.J. and Clements, D.N. (2016), "In vitro models for the study of osteoarthritis", *The Veterinary Journal*, W.B. Saunders, Vol. 209, pp. 40–49.

Johnson, K., Hashimoto, S., Lotz, M., Pritzker, K. and Terkeltaub, R. (2001), "Interleukin-1 induces pro-mineralizing activity of cartilage tissue transglutaminase and factor XIIIa.", *The American Journal of Pathology*, American Society for Investigative Pathology, Vol. 159 No. 1, pp. 149–63.

Johnson, W.E., Li, C. and Rabinovic, A. (2007), "Adjusting batch effects in microarray expression data using empirical Bayes methods", *Biostatistics*, Oxford University Press, Vol. 8 No. 1, pp. 118–127.

Jouglin, M., Robert, C., Valette, J.-P., Gavard, F., Quintin-Colonna, F. and Denoix, J.-M. (2000), "Metalloproteinases and tumor necrosis factor-alpha activities in

synovial fluids of horses: correlation with articular cartilage alterations", *Veterinary Research*, EDP Sciences, Vol. 31 No. 5, pp. 507–515.

Jukarainen, N. (2009), *NMR Metabolomics Techniques and Mathematical Tools as an Aid in Neurological Diagnosis*, University of Kuopio.

Kamm, J.L., Frisbie, D.D., McIlwraith, C.W. and Orr, K.E. (2013), "Gene biomarkers in peripheral white blood cells of horses with experimentally induced osteoarthritis", *American Journal of Veterinary Research*, American Veterinary Medical Association 1931 North Meacham Road, Suite 100, Schaumburg, IL 60173-4360 USA 847-925-8070 847-925-1329 avmajournals@avma.org, Vol. 74 No. 1, pp. 115–121.

Kaneva, M.K., Greco, K. V, Headland, S.E., Montero-Melendez, T., Mori, P., Greenslade, K., Pitzalis, C., *et al.* (2017), "Identification of Novel Chondroprotective Mediators in Resolving Inflammatory Exudates.", *Journal of Immunology (Baltimore, Md. : 1950)*, American Association of Immunologists, Vol. 198 No. 7, pp. 2876–2885.

Kang, J.-S. (2012), *Principles and Applications of LC-MS/MS for the Quantitative Bioanalysis of Analytes in Various Biological Samples*, available at: www.intechopen.com (accessed 21 September 2018).

Kang, K.Y., Lee, S.H., Jung, S.M., Park, S.H., Jung, B.H. and Ju, J.H. (2015), "Downregulation of Tryptophan-related Metabolomic Profile in Rheumatoid Arthritis Synovial Fluid", *J Rheumatol*, Vol. 42 No. 11, pp. 2003–2011.

Kapoor, S.R., Filer, A., Fitzpatrick, M.A., Fisher, B.A., Taylor, P.C., Buckley, C.D., McInnes, I.B., *et al.* (2013), "Metabolic profiling predicts response to anti-tumor necrosis factor alpha therapy in patients with rheumatoid arthritis", *Arthritis Rheum*, Vol. 65 No. 6, pp. 1448–1456.

Karas, M. and Hillenkamp, F. (1988), "Laser desorption ionization of proteins with molecular masses exceeding 10,000 daltons.", *Analytical Chemistry*, Vol. 60 No. 20, pp. 2299–301.

Kawcak, C.E., Frisbie, D.D., Werpy, N.M., Park, R.D. and McIlwraith, C.W. (2008), "Effects of exercise vs experimental osteoarthritis on imaging outcomes", *Osteoarthritis and Cartilage*, W.B. Saunders, Vol. 16 No. 12, pp. 1519–1525.

Kawcak, C.E., McIlwraith, C.W., Norrdin, R.W., Park, R.D. and Steyn, P.S. (2000), "Clinical effects of exercise on subchondral bone of carpal and metacarpophalangeal joints in horses.", *American Journal of Veterinary Research*, Vol. 61 No. 10, pp. 1252–8.

Keun, H.C. and Athersuch, T.J. (2011), "Nuclear magnetic resonance (NMR)-based metabolomics", *Methods Mol Biol*, Vol. 708, pp. 321–334.

Kim, S., Hwang, J., Kim, J., Ahn, J.K., Cha, H.-S. and Kim, K.H. (2017), "Metabolite

profiles of synovial fluid change with the radiographic severity of knee osteoarthritis.", *Joint, Bone, Spine : Revue Du Rhumatisme*, Vol. 84 No. 5, pp. 605–610.

Kirker-Head, C.A., Chandna, V.K., Agarwal, R.K., Morris, E.A., Tidwell, A., O'Callaghan, M.W., Rand, W., *et al.* (2000), "Concentrations of substance P and prostaglandin E2 in synovial fluid of normal and abnormal joints of horses.", *American Journal of Veterinary Research*, Vol. 61 No. 6, pp. 714–8.

Klammer, A.A. and MacCoss, M.J. (2006), "Effects of Modified Digestion Schemes on the Identification of Proteins from Complex Mixtures", *J Proteome Res*, Vol. 5 No. 3, pp. 695–700.

Kobayashi, M. (2007), "Simple Lactate Measurement in Horses Using a Portable Lactate Analyzer with Lancet Skin Punctures under Field Conditions", *J. Equine Sci*, Vol. 18 No. 1, pp. 5–11.

Kohl, S.M., Klein, M.S., Hochrein, J., Oefner, P.J., Spang, R. and Gronwald, W. (2012), "State-of-the art data normalization methods improve NMR-based metabolomic analysis", *Metabolomics*, Springer US, Vol. 8 No. S1, pp. 146–160.

Kononoff, A., Arstila, L., Kautiainen, H., Elfving, P., Savolainen, E., Niinisalo, H. and Kaipiainen-Seppanen, O. (2015), "Patient reported outcomes correlated with concentrations of glycoprotein acetyls in patients with early untreated rheumatoid arthritis", *Annals of Rheumatic Disease*, Vol. 74 No. 2, p. 430.1.

Kramer, C.M., Tsang, A.S., Koenig, T., Jeffcott, L.B., Dart, C.M. and Dart, A.J. (2014), "Survey of the therapeutic approach and efficacy of pentosan polysulfate for the prevention and treatment of equine osteoarthritis in veterinary practice in Australia", *Aust Vet J*, Vol. 92 No. 12, pp. 482–487.

Kramer, P.A., Ravi, S., Chacko, B., Johnson, M.S. and Darley-Usmar, V.M. (2014), "A review of the mitochondrial and glycolytic metabolism in human platelets and leukocytes: implications for their use as bioenergetic biomarkers.", *Redox Biology*, Elsevier, Vol. 2, pp. 206–10.

Krenn, V., Morawietz, L., Burmester, G.-R., Kinne, R.W., Mueller-Ladner, U., Muller, B. and Haupl, T. (2006), "Synovitis score: discrimination between chronic low-grade and high-grade synovitis", *Histopathology*, Wiley/Blackwell (10.1111), Vol. 49 No. 4, pp. 358–364.

Krey, P.R. and Bailen, D.A. (1979), "Synovial fluid leukocytosis. A study of extremes.", *The American Journal of Medicine*, Vol. 67 No. 3, pp. 436–42.

Kruzel, M.L., Harari, Y., Mailman, D. and Actor, J.K. (2002), "Differential effects of prophylactic, concurrent and therapeutic lactoferrin treatment on LPS-induced inflammatory responses in mice", *Clinical and Experimental Immunology*, Wiley/Blackwell (10.1111), Vol. 130 No. 1, pp. 25–31.

Kudo, A. and Kii, I. (2018), “Periostin function in communication with extracellular matrices.”, *Journal of Cell Communication and Signaling*, Springer, Vol. 12 No. 1, pp. 301–308.

Lacitignola, L., Fanizzi, F.P., Francioso, E. and Crovace, A. (2008), “1H NMR investigation of normal and osteo-arthritic synovial fluid in the horse”, *Veterinary and Comparative Orthopaedics and Traumatology*, Schattauer Publishers, Vol. 21 No. 1, pp. 85–88.

Lam, K.S., Salmon, S.E., Hersh, E.M., Hruby, V.J., Kazmierski, W.M. and Knapp, R.J. (1991), “A new type of synthetic peptide library for identifying ligand-binding activity”, *Nature*, Vol. 354 No. 6348, pp. 82–84.

Lambrecht, S., Verbruggen, G., Verdonk, P.C.M., Elewaut, D. and Deforce, D. (2008), “Differential proteome analysis of normal and osteoarthritic chondrocytes reveals distortion of vimentin network in osteoarthritis”, *Osteoarthritis and Cartilage*, W.B. Saunders, Vol. 16 No. 2, pp. 163–173.

Lamers, R.-J.A.N., DeGroot, J., Spies-Faber, E.J., Jellema, R.H., Kraus, V.B., Verzijl, N., TeKoppele, J.M., *et al.* (2003), “Identification of Disease- and Nutrient-Related Metabolic Fingerprints in Osteoarthritic Guinea Pigs”, *The Journal of Nutrition*, Oxford University Press, Vol. 133 No. 6, pp. 1776–1780.

Lamping, N., Dettmer, R., Schröder, N.W., Pfeil, D., Hallatschek, W., Burger, R. and Schumann, R.R. (1998), “LPS-binding protein protects mice from septic shock caused by LPS or gram-negative bacteria.”, *Journal of Clinical Investigation*, Vol. 101 No. 10, pp. 2065–2071.

de Lange-Brokaar, B.J., Ioan-Facsinay, A., van Osch, G.J., Zuurmond, A.M., Schoones, J., Toes, R.E., Huizinga, T.W., *et al.* (2012), “Synovial inflammation, immune cells and their cytokines in osteoarthritis: a review”, *Osteoarthritis Cartilage*, Vol. 20 No. 12, pp. 1484–1499.

Langelier, E., Suetterlin, R., Hoemann, C.D., Aebi, U. and Buschmann, M.D. (2000), “The Chondrocyte Cytoskeleton in Mature Articular Cartilage: Structure and Distribution of Actin, Tubulin, and Vimentin Filaments”, *Journal of Histochemistry & Cytochemistry*, SAGE PublicationsSage CA: Los Angeles, CA, Vol. 48 No. 10, pp. 1307–1320.

Laverty, S., Ionescu, M., Marcoux, M., Bouré, L., Doizé, B. and Poole, A.R. (2000), “Alterations in cartilage type-ii procollagen and aggrecan contents in synovial fluid in equine osteochondrosis”, *Journal of Orthopaedic Research*, Wiley-Blackwell, Vol. 18 No. 3, pp. 399–405.

Lawand, N.B., McNearney, T. and Westlund, K.N. (2000), “Amino acid release into the knee joint: key role in nociception and inflammation.”, *Pain*, Vol. 86 No. 1–2, pp. 69–74.

Lawrence, D., Bao, S., J. Canfield, P., Allanson, M. and Husband, A.J. (1998),

"Elevation of immunoglobulin deposition in the synovial membrane of dogs with cranial cruciate ligament rupture", *Veterinary Immunology and Immunopathology*, Elsevier, Vol. 65 No. 1, pp. 89–96.

Le, J., Perier, C., Peyroche, S., Rascle, F., Blanchon, M.A., Gonthier, R., Frey, J., *et al.* (1999), "Urine glycyl-L-proline increase and skin trophicity", *Amino Acids*, Springer-Verlag, Vol. 17 No. 3, pp. 315–322.

Lee, J.Y., Kang, M.J., Choi, J.Y., Park, J.S., Park, J.K., Lee, E.Y., Lee, E.B., *et al.* (2018), "Apolipoprotein B binds to enolase-1 and aggravates inflammation in rheumatoid arthritis.", *Annals of the Rheumatic Diseases*, BMJ Publishing Group Ltd, p. annrheumdis-2018-213444.

Lee, Y.A., Kim, J.Y., Hong, S.J., Lee, S.H., Yoo, M.C., Kim, K.S. and Yang, H.I. (2007), "Synovial proliferation differentially affects hypoxia in the joint cavities of rheumatoid arthritis and osteoarthritis patients", *Clin Rheumatol*, Vol. 26 No. 12, pp. 2023–2029.

Levi, M., Keller, T.T., van Gorp, E. and ten Cate, H. (2003), "Infection and inflammation and the coagulation system", *Cardiovascular Research*, Oxford University Press, Vol. 60 No. 1, pp. 26–39.

Ley, C., Ekman, S., Elmén, A., Nilsson, G. and Eloranta, M.-L. (2007), "Interleukin-6 and Tumour Necrosis Factor in Synovial Fluid from Horses with Carpal Joint Pathology", *Journal of Veterinary Medicine Series A*, John Wiley & Sons, Ltd (10.1111), Vol. 54 No. 7, pp. 346–351.

Li, G., Ma, Y., Cheng, T.S., Landao-Bassonga, E., Qin, A., Pavlos, N.J., Zhang, C., *et al.* (2014), "Identical subchondral bone microarchitecture pattern with increased bone resorption in rheumatoid arthritis as compared to osteoarthritis", *Osteoarthritis Cartilage*, Vol. 22 No. 12, pp. 2083–2092.

Li, H., Han, J., Pan, J., Liu, T., Parker, C.E. and Borchers, C.H. (2017), "Current trends in quantitative proteomics - an update", *Journal of Mass Spectrometry*, Wiley-Blackwell, Vol. 52 No. 5, pp. 319–341.

Li, H., Hao, Z., Zhao, L., Liu, W., Han, Y., Bai, Y. and Wang, J. (2016), "Comparison of molecular mechanisms of rheumatoid arthritis and osteoarthritis using gene microarrays", *Mol Med Rep*, Vol. 13 No. 6, pp. 4599–4605.

Li, L., Sun, C., Freeby, S., Yee, D., Kieffer-Jaquinod, S., Guerrier, L., Boschetti, E., *et al.* (2009), "Protein sample treatment with peptide ligand library: coverage and consistency", *Journal of Proteomics & Bioinformatice*, Vol. 2 No. 12, pp. 485–494.

Li, W., Gao, P., Zhi, Y., Xu, W., Wu, Y., Yin, J. and Zhang, J. (2015), "Periostin: its role in asthma and its potential as a diagnostic or therapeutic target.", *Respiratory Research*, BioMed Central, Vol. 16 No. 1, p. 57.

Li, X., Yang, S., Qiu, Y., Zhao, T., Chen, T., Su, M., Chu, L., *et al.* (2010), "Urinary metabolomics as a potentially novel diagnostic and stratification tool for knee osteoarthritis", *Metabolomics*, Vol. 6 No. 1, pp. 109–118.

Li, Y., Xu, L. and Olsen, B.R. (2007), "Lessons from genetic forms of osteoarthritis for the pathogenesis of the disease.", *Osteoarthritis and Cartilage*, NIH Public Access, Vol. 15 No. 10, pp. 1101–5.

Ling, W., Regatte, R.R., Schweitzer, M.E. and Jerschow, A. (2008), "Characterization of bovine patellar cartilage by NMR", *NMR in Biomedicine*, Wiley-Blackwell, Vol. 21 No. 3, pp. 289–295.

Little, C.B., Smith, M.M., Cake, M.A., Read, R.A., Murphy, M.J. and Barry, F.P. (2010), "The OARSI histopathology initiative – recommendations for histological assessments of osteoarthritis in sheep and goats", *Osteoarthritis and Cartilage*, W.B. Saunders, Vol. 18, pp. S80–S92.

Loeser, R.F., Carlson, C.S., Carlo, M. Del and Cole, A. (2002), "Detection of nitrotyrosine in aging and osteoarthritic cartilage: Correlation of oxidative damage with the presence of interleukin-1? and with chondrocyte resistance to insulin-like growth factor 1", *Arthritis & Rheumatism*, Wiley-Blackwell, Vol. 46 No. 9, pp. 2349–2357.

Lohmander, L.S., Atley, L.M., Pietka, T.A. and Eyre, D.R. (2003), "The release of crosslinked peptides from type II collagen into human synovial fluid is increased soon after joint injury and in osteoarthritis", *Arthritis & Rheumatism*, Wiley Subscription Services, Inc., A Wiley Company, Vol. 48 No. 11, pp. 3130–3139.

Lotz, M., Martel-Pelletier, J., Christiansen, C., Brandi, M.-L., Bruyère, O., Chapurlat, R., Collette, J., *et al.* (2013), "Value of biomarkers in osteoarthritis: current status and perspectives.", *Annals of the Rheumatic Diseases*, BMJ Publishing Group Ltd, Vol. 72 No. 11, pp. 1756–63.

Loziuk, P.L., Wang, J., Li, Q., Sederoff, R.R., Chiang, V.L. and Muddiman, D.C. (2013), "Understanding the Role of Proteolytic Digestion on Discovery and Targeted Proteomic Measurements Using Liquid Chromatography Tandem Mass Spectrometry and Design of Experiments", *Journal of Proteome Research*, American Chemical Society, Vol. 12 No. 12, pp. 5820–5829.

Lu, S., Purohit, S., Sharma, A., Zhi, W., He, M., Wang, Y., Li, C.-J., *et al.* (2012), "Serum insulin-like growth factor binding protein 6 (IGFBP6) is increased in patients with type 1 diabetes and its complications.", *International Journal of Clinical and Experimental Medicine*, e-Century Publishing Corporation, Vol. 5 No. 3, pp. 229–37.

Luc, G., Majd, Z., Poulain, P., Elkhalil, L. and Fruchart, J.C. (1996), "Interstitial fluid apolipoprotein A-II: an association with the occurrence of myocardial infarction.", *Atherosclerosis*, Vol. 127 No. 1, pp. 131–7.

Luo, Q., Qin, X., Qiu, Y., Hou, L. and Yang, N. (2018), "The change of synovial fluid proteome in rabbit surgery-induced model of knee osteoarthritis.", *American Journal of Translational Research*, e-Century Publishing Corporation, Vol. 10 No. 7, pp. 2087–2101.

Lust, G., Burton-Wurster, N. and Leipold, H. (1987), "Fibronectin as a marker for osteoarthritis.", *The Journal of Rheumatology*, Vol. 14 Spec No, pp. 28–9.

Ma, T.-W., Li, Y., Wang, G.-Y., Li, X.-R., Jiang, R.-L., Song, X.-P., Zhang, Z.-H., *et al.* (2017), "Changes in Synovial Fluid Biomarkers after Experimental Equine Osteoarthritis.", *Journal of Veterinary Research*, De Gruyter Open, Vol. 61 No. 4, pp. 503–508.

Mackay, A.R., Ballin, M., Pelina, M.D., Farina, A.R., Nason, A.M., Hartzler, J.L. and Thorgeirsson, U.P. (1992), "Effect of phorbol ester and cytokines on matrix metalloproteinase and tissue inhibitor of metalloproteinase expression in tumor and normal cell lines.", *Invasion & Metastasis*, Vol. 12 No. 3–4, pp. 168–84.

Madsen, R.K., Lundstedt, T., Gabrielsson, J., Sennbro, C.J., Alenius, G.M., Moritz, T., Rantapaa-Dahlqvist, S., *et al.* (2011), "Diagnostic properties of metabolic perturbations in rheumatoid arthritis", *Arthritis Res Ther*, Vol. 13 No. 1, p. R19.

Mahendran, S.M., Oikonomopoulou, K., Diamandis, E.P. and Chandran, V. (2017), "Synovial fluid proteomics in the pursuit of arthritis mediators: An evolving field of novel biomarker discovery", *Critical Reviews in Clinical Laboratory Sciences*, Taylor & Francis, Vol. 54 No. 7–8, pp. 495–505.

Maicas, N., Ferrándiz, M.L., Brines, R., Ibáñez, L., Cuadrado, A., Koenders, M.I., van den Berg, W.B., *et al.* (2011), "Deficiency of Nrf2 Accelerates the Effector Phase of Arthritis and Aggravates Joint Disease", *Antioxidants & Redox Signaling*, Mary Ann Liebert, Inc. 140 Huguenot Street, 3rd Floor New Rochelle, NY 10801 USA , Vol. 15 No. 4, pp. 889–901.

Majithia, V. and Geraci, S.A. (2007), "Rheumatoid Arthritis: Diagnosis and Management", *The American Journal of Medicine*, Vol. 120 No. 11, pp. 936–939.

Makarov, A. (2012), *Orbitrap Mass Spectrometry: Ultrahigh Resolution for Every Lab*.

Maninchedda, U., Lepage, O.M., Gangl, M., Hilairet, S., Remandet, B., Meot, F., Penarier, G., *et al.* (2015), "Development of an Equine Groove Model to Induce Metacarpophalangeal Osteoarthritis: A Pilot Study on 6 Horses", edited by Kerkis, I.*PLOS ONE*, Public Library of Science, Vol. 10 No. 2, p. e0115089.

Marhardt, K. and Muurahainen, N. (2015), "Development of a Disease-Modifying OA Drug (DMOAD) in Knee Osteoarthritis: The Example of Sprifermin", *Drug Research*, Georg Thieme Verlag KG, Vol. 65 No. S 01, pp. S13–S13.

Markley, J.L., Bruschweiler, R., Edison, A.S., Eghbalnia, H.R., Powers, R., Raftery, D. and Wishart, D.S. (2017), "The future of NMR-based metabolomics", *Curr Opin Biotechnol*, Vol. 43, pp. 34–40.

Marshall, D.D. and Powers, R. (2017), "Beyond the paradigm: Combining mass spectrometry and nuclear magnetic resonance for metabolomics", *Progress in Nuclear Magnetic Resonance Spectroscopy*, Pergamon, Vol. 100, pp. 1–16.

Mateos, J., Lourido, L., Fernandez-Puente, P., Calamia, V., Fernandez-Lopez, C., Oreiro, N., Ruiz-Romero, C., *et al.* (2012), "Differential protein profiling of synovial fluid from rheumatoid arthritis and osteoarthritis patients using LC-MALDI TOF/TOF", *J Proteomics*, Vol. 75 No. 10, pp. 2869–2878.

Mathiessen, A. and Conaghan, P.G. (2017), "Synovitis in osteoarthritis: current understanding with therapeutic implications.", *Arthritis Research & Therapy*, BioMed Central, Vol. 19 No. 1, p. 18.

McCoy, A.M., Toth, F., Dolvik, N.I., Ekman, S., Ellermann, J., Olstad, K., Ytrehus, B., *et al.* (2013), "Articular osteochondrosis: a comparison of naturally-occurring human and animal disease", *Osteoarthritis and Cartilage*, W.B. Saunders, Vol. 21 No. 11, pp. 1638–1647.

McHugh, M.L. (2012), "Interrater reliability: the kappa statistic", *Biochem Med (Zagreb)*, Vol. 22 No. 3, pp. 276–282.

McIlwraith, C.W. (2005), "Use of synovial fluid and serum biomarkers in equine bone and joint disease: a review", *Equine Vet J*, Vol. 37 No. 5, pp. 473–482.

McIlwraith, C.W., Frisbie, D.D., Kawcak, C.E., Fuller, C.J., Hurtig, M. and Cruz, A. (2010), "The OARSI histopathology initiative – recommendations for histological assessments of osteoarthritis in the horse", *Osteoarthritis and Cartilage*, W.B. Saunders, Vol. 18, pp. S93–S105.

McIlwraith, C.W., Kawcak, C.E., Frisbie, D.D., Little, C.B., Clegg, P.D., Peffers, M.J., Karsdal, M.A., *et al.* (2018), "Biomarkers for equine joint injury and osteoarthritis", *Journal of Orthopaedic Research*, Wiley-Blackwell, Vol. 36 No. 3, pp. 823–831.

McNearney, T., Speegle, D., Lawand, N., Lisse, J. and Westlund, K.N. (2000), "Excitatory amino acid profiles of synovial fluid from patients with arthritis.", *The Journal of Rheumatology*, Vol. 27 No. 3, pp. 739–45.

Meshitsuka, S., Yamazaki, E., Inoue, M., Hagino, H., Teshima, R. and Yamamoto, K. (1999), "Nuclear magnetic resonance studies of synovial fluids from patients with rheumatoid arthritis and osteoarthritis", *Clinica Chimica Acta*, Elsevier, Vol. 281 No. 1–2, pp. 163–167.

Michalski, A., Damoc, E., Hauschild, J.-P., Lange, O., Wieghaus, A., Makarov, A., Nagaraj, N., *et al.* (2011), "Mass spectrometry-based proteomics using Q

Exactive, a high-performance benchtop quadrupole Orbitrap mass spectrometer.", *Molecular & Cellular Proteomics : MCP*, American Society for Biochemistry and Molecular Biology, Vol. 10 No. 9, p. M111.011015.

Mickiewicz, B., Heard, B.J., Chau, J.K., Chung, M., Hart, D.A., Shrive, N.G., Frank, C.B., *et al.* (2015), "Metabolic profiling of synovial fluid in a unilateral ovine model of anterior cruciate ligament reconstruction of the knee suggests biomarkers for early osteoarthritis", *Journal of Orthopaedic Research*, Vol. 33 No. 1, pp. 71–77.

Mickiewicz, B., Kelly, J.J., Ludwig, T.E., Weljie, A.M., Wiley, J.P., Schmidt, T.A. and Vogel, H.J. (2015), "Metabolic analysis of knee synovial fluid as a potential diagnostic approach for osteoarthritis", *J Orthop Res*, Vol. 33 No. 11, pp. 1631–1638.

Mihara, E., Hirai, H., Yamamoto, H., Tamura-Kawakami, K., Matano, M., Kikuchi, A., Sato, T., *et al.* (2016), "Active and water-soluble form of lipidated Wnt protein is maintained by a serum glycoprotein afamin/α-albumin.", *ELife*, eLife Sciences Publications, Ltd, Vol. 5, available at:https://doi.org/10.7554/eLife.11621.

Miletic, V.D. and Frank, M.M. (1995), *Complement-Immunoglobulin Interactions*, *Current Opinion in Immunology*, Vol. 7.

Miller, R.E., Ishihara, S., Tran, P.B., Golub, S.B., Last, K., Miller, R.J., Fosang, A.J., *et al.* (2018), "An aggrecan fragment drives osteoarthritis pain through Toll-like receptor 2", *JCI Insight*, American Society for Clinical Investigation, Vol. 3 No. 6, pp. 1–9.

Milner, J.M., Elliott, S.-F. and Cawston, T.E. (2001), "Activation of procollagenases is a key control point in cartilage collagen degradation: Interaction of serine and metalloproteinase pathways", *Arthritis & Rheumatism*, Wiley-Blackwell, Vol. 44 No. 9, pp. 2084–2096.

Milner, J.M., Rowan, A.D., Cawston, T.E. and Young, D.A. (2006), "Metalloproteinase and inhibitor expression profiling of resorbing cartilage reveals pro-collagenase activation as a critical step for collagenolysis.", *Arthritis Research & Therapy*, BioMed Central, Vol. 8 No. 5, p. R142.

Mirgorodskaya, O.A., Kozmin, Y.P., Titov, M.I., Körner, R., Sönksen, C.P. and Roepstorff, P. (2000), "Quantitation of peptides and proteins by matrix-assisted laser desorption/ionization mass spectrometry using18O-labeled internal standards", *Rapid Communications in Mass Spectrometry*, Vol. 14 No. 14, pp. 1226–1232.

Misumi, K., Vilim, V., Clegg, P.D., Thompson, C.C.M. and Carter, S.D. (2001), "Measurement of cartilage oligomeric matrix protein (COMP) in normal and diseased equine synovial fluids", *Osteoarthritis and Cartilage*, Vol. 9 No. 2, pp. 119–127.

Misumi, K., Vilim, V., Hatazoe, T., Murata, T., Fujiki, M., Oka, T., Sakamoto, H., *et al.* (2002), "Serum level of cartilage oligomeric matrix protein (COMP) in equine osteoarthritis", *Equine Veterinary Journal*, American Medical Association (AMA), Vol. 34 No. 6, pp. 602–608.

Murray, R.C., Janicke, H.C., Henson, F.M. and Goodship, A. (2000), "Equine carpal articular cartilage fibronectin distribution associated with training, joint location and cartilage deterioration.", *Equine Veterinary Journal*, Vol. 32 No. 1, pp. 47–51.

Nagana Gowda, G.A. and Raftery, D. (2017), "Recent Advances in NMR-Based Metabolomics", *Analytical Chemistry*, American Chemical Society, Vol. 89 No. 1, pp. 490–510.

"National Cancer Institute". (2016), *What Is Cancer Proteomics?*, available at: http://proteomics.cancer.gov/whatisproteomics (accessed 1 May 2016).

Naughton, D., Whelan, M., Smith, E.C., Williams, R., Blake, D.R. and Grootveld, M. (1993), "An investigation of the abnormal metabolic status of synovial fluid from patients with rheumatoid arthritis by high field proton nuclear magnetic resonance spectroscopy", *FEBS Lett*, Vol. 317 No. 1–2, pp. 135–138.

Nedic, O., Malenkovic, V., Dukanovic, B. and Baricevic, I. (2013), "Ligand-Binding Activity and Immunoreactivity of Insulin-Like Growth Factor Binding Proteins in Patients with Colorectal Carcinoma and Postoperative Sepsis", *J Med Biochem*, Vol. 32, pp. 250–255.

Nibbering, P.H., Ravensbergen, E., Welling, M.M., van Berkel, L.A., van Berkel, P.H., Pauwels, E.K. and Nuijens, J.H. (2001), "Human lactoferrin and peptides derived from its N terminus are highly effective against infections with antibiotic-resistant bacteria.", *Infection and Immunity*, American Society for Microbiology (ASM), Vol. 69 No. 3, pp. 1469–76.

Nicholson, A.M., Trumble, T.N., Merritt, K.A. and Brown, M.P. (2010), "Associations of horse age, joint type, and osteochondral injury with serum and synovial fluid concentrations of type II collagen biomarkers in Thoroughbreds", *American Journal of Veterinary Research*, American Veterinary Medical Association 1931 North Meacham Road, Suite 100, Schaumburg, IL 60173-4360 USA 847-925-8070 847-925-1329 avmajournals@avma.org , Vol. 71 No. 7, pp. 741–749.

"Nuclear Magnetic Resonance Spectroscopy". (n.d.). *Sheffield Hallam University*, available at: https://teaching.shu.ac.uk/hwb/chemistry/tutorials/molspec/nmr1.htm# (accessed 11 September 2018).

Nurminskaya, M., Magee, C., Nurminsky, D. and Linsenmayer, T.F. (1998), "Plasma transglutaminase in hypertrophic chondrocytes: expression and cell-specific intracellular activation produce cell death and externalization.", *The Journal of Cell Biology*, The Rockefeller University Press, Vol. 142 No. 4, pp. 1135–44.

Ogata, H., Goto, S., Sato, K., Fujibuchi, W., Bono, H. and Kanehisa, M. (1999), "KEGG: Kyoto Encyclopedia of Genes and Genomes.", *Nucleic Acids Research*, Oxford University Press, Vol. 27 No. 1, pp. 29–34.

Oliveria, S.A., Felson, D.T., Cirillo, P.A., Reed, J.I. and Walker, A.M. (1999), "Body Weight, Body Mass Index, and Incident Symptomatic Osteoarthritis of the Hand, Hip, and Knee", *Epidemiology*, Lippincott Williams & Wilkins.

Olsson, S. and Reiland, S. (1978), "The nature of osteochondrosis in animals. Summary and conclusions with comparative aspects on osteochondritis dissecans in man.", *Acta Radiologica Supplement*, Vol. 358, pp. 299–306.

Ortutay, Z., Polgar, A., Gomor, B., Geher, P., Lakatos, T., Glant, T.T., Gay, R.E., *et al.* (2003), "Synovial fluid exoglycosidases are predictors of rheumatoid arthritis and are effective in cartilage glycosaminoglycan depletion", *Arthritis Rheum*, Vol. 48 No. 8, pp. 2163–2172.

Osborn, T.M., Verdrengh, M., Stossel, T.P., Tarkowski, A. and Bokarewa, M. (2008), "Decreased levels of the gelsolin plasma isoform in patients with rheumatoid arthritis.", *Arthritis Research & Therapy*, BioMed Central, Vol. 10 No. 5, p. R117.

Palmer, J.L., Bertone, A.L. and McClain, H. (1995), "Assessment of glycosaminoglycan concentration in equine synovial fluid as a marker of joint disease.", *Canadian Journal of Veterinary Research = Revue Canadienne de Recherche Veterinaire*, Canadian Veterinary Medical Association, Vol. 59 No. 3, pp. 205–12.

Pammi, M. and Abrams, S.A. (2015), "Oral lactoferrin for the prevention of sepsis and necrotizing enterocolitis in preterm infants", in Pammi, M. (Ed.), *Cochrane Database of Systematic Reviews*, John Wiley & Sons, Ltd, Chichester, UK, available at:https://doi.org/10.1002/14651858.CD007137.pub4.

Pap, T. and Korb-Pap, A. (2015), "Cartilage damage in osteoarthritis and rheumatoid arthritis—two unequal siblings", *Nature Reviews Rheumatology*, Nature Publishing Group, Vol. 11 No. 10, pp. 606–615.

Paramasivam, M., Saravanan, K., Uma, K., Sharma, S., Singh, T.. and Srinivasan, A. (2002), "Expression, purification, and characterization of equine lactoferrin in Pichia pastoris", *Protein Expression and Purification*, Academic Press, Vol. 26 No. 1, pp. 28–34.

Parker, C.E. and Borchers, C.H. (2014), "Mass spectrometry based biomarker discovery, verification, and validation - Quality assurance and control of protein biomarker assays", *Molecular Oncology*, Wiley-Blackwell, Vol. 8 No. 4, pp. 840–858.

Peffers, M., Jones, A.R., McCabe, A. and Anderson, J. (2017), "Neopeptide Analyser: A software tool for neopeptide discovery in proteomics data", *Wellcome Open*

Research, Vol. 2, p. 24.

Peffers, M., Riggs, C., Phelan, M. and Clegg, P. (2015), "Identification of Disease Specific Metabolic Fingerprints in Early Osteoarthritis", *Equine Veterinary Journal*, Vol. 47 No. S48, pp. 13–13.

Peffers, M.J. (2013), *Proteomic and Transcriptomic Signatures of Cartilage Ageing and Disease*, University of Liverpool.

Peffers, M.J., Cillero-Pastor, B., Eijkel, G.B., Clegg, P.D. and Heeren, R.M. (2014), "Matrix assisted laser desorption ionization mass spectrometry imaging identifies markers of ageing and osteoarthritic cartilage", *Arthritis Research & Therapy*, BioMed Central, Vol. 16 No. 3, p. R110.

Peffers, M.J., McDermott, B., Clegg, P.D. and Riggs, C.M. (2015), "Comprehensive protein profiling of synovial fluid in osteoarthritis following protein equalization", *Osteoarthritis Cartilage*, Vol. 23 No. 7, pp. 1204–1213.

Peffers, M.J., Smagul, A. and Anderson, J.R. (2019), "Proteomic analysis of synovial fluid: current and potential uses to improve clinical outcomes", *Expert Review of Proteomics*, Taylor & Francis, Vol. 16 No. 4, pp. 287–302.

Peffers, M.J., Thornton, D.J. and Clegg, P.D. (2016), "Characterization of neopeptides in equine articular cartilage degradation", *Journal of Orthopaedic Research*, Wiley-Blackwell, Vol. 34 No. 1, pp. 106–120.

Perkins, D.N., Pappin, D.J., Creasy, D.M. and Cottrell, J.S. (1999), "Probability-based protein identification by searching sequence databases using mass spectrometry data.", *Electrophoresis*, Vol. 20 No. 18, pp. 3551–67.

Phang, J.M., Liu, W., Hancock, C.N. and Fischer, J.W. (2015), "Proline metabolism and cancer: emerging links to glutamine and collagen.", *Current Opinion in Clinical Nutrition and Metabolic Care*, Wolters Kluwer Health, Vol. 18 No. 1, pp. 71–7.

Piepoli, T., Mennuni, L., Zerbi, S., Lanza, M., Rovati, L.C. and Caselli, G. (2009), "Glutamate signaling in chondrocytes and the potential involvement of NMDA receptors in cell proliferation and inflammatory gene expression", *Osteoarthritis and Cartilage*, Vol. 17 No. 8, pp. 1076–1083.

Piktel, E., Levental, I., Durnaś, B., Janmey, P., Bucki, R., Piktel, E., Levental, I., *et al.* (2018), "Plasma Gelsolin: Indicator of Inflammation and Its Potential as a Diagnostic Tool and Therapeutic Target", *International Journal of Molecular Sciences*, Multidisciplinary Digital Publishing Institute, Vol. 19 No. 9, p. 2516.

Pinchbeck, G.L., Clegg, P.D., Boyde, A. and Riggs, C.M. (2013), "Pathological and clinical features associated with palmar/plantar osteochondral disease of the metacarpo/metatarsophalangeal joint in Thoroughbred racehorses", *Equine Veterinary Journal*, American Medical Association (AMA), Vol. 45 No. 5, pp.

587–592.

Pisanu, S., Biosa, G., Carcangiu, L., Uzzau, S. and Pagnozzi, D. (2018), “Comparative evaluation of seven commercial products for human serum enrichment/depletion by shotgun proteomics”, *Talanta*, Elsevier, Vol. 185, pp. 213–220.

Polur, I., Lee, P.L., Servais, J.M., Xu, L. and Li, Y. (2010), “Role of HTRA1, a serine protease, in the progression of articular cartilage degeneration.”, *Histology and Histopathology*, NIH Public Access, Vol. 25 No. 5, pp. 599–608.

Poole, A.R. (1999), “An introduction to the pathophysiology of osteoarthritis”, *Front Biosci*, Vol. 4, pp. D662-70.

Porter, M. (2005), “Equine rehabilitation therapy for joint disease.”, *The Veterinary Clinics of North America. Equine Practice*, Elsevier, Vol. 21 No. 3, p. 599–607, vi.

Pottie, P., Presle, N., Terlain, B., Netter, P., Mainard, D. and Berenbaum, F. (2006), “Obesity and osteoarthritis: more complex than predicted!”, *Annals of the Rheumatic Diseases*, BMJ Publishing Group Ltd, Vol. 65 No. 11, pp. 1403–5.

Pretzel, D., Pohlers, D., Weinert, S. and Kinne, R.W. (2009), “In vitro model for the analysis of synovial fibroblast-mediated degradation of intact cartilage.”, *Arthritis Research & Therapy*, BioMed Central, Vol. 11 No. 1, p. R25.

Priori, R., Casadei, L., Valerio, M., Scrivo, R., Valesini, G. and Manetti, C. (2015), “(1)H-NMR-Based Metabolomic Study for Identifying Serum Profiles Associated with the Response to Etanercept in Patients with Rheumatoid Arthritis”, *PLoS One*, Vol. 10 No. 11, p. e0138537.

Proot, J.L.J., Vicente, F. de. and Sheahan, D.E. (2015), “Analysis of lactate concentrations in canine synovial fluid”, *Veterinary and Comparative Orthopaedics and Traumatology*, Schattauer GmbH, Vol. 28 No. 05, pp. 301–305.

Puangpila, C., Mayadunne, E. and El Rassi, Z. (2015), “Liquid phase based separation systems for depletion, prefractionation, and enrichment of proteins in biological fluids and matrices for in-depth proteomics analysis-An update covering the period 2011-2014”, *Electrophoresis*, Vol. 36 No. 1, pp. 238–252.

Rader, D.J. (2003), “Regulation of reverse cholesterol transport and clinical implications.”, *The American Journal of Cardiology*, Vol. 92 No. 4A, p. 42J–49J.

Raghu, H. and Flick, M. (2011), “Targeting the Coagulation Factor Fibrinogen for Arthritis Therapy”, *Current Pharmaceutical Biotechnology*, Vol. 12 No. 9, pp. 1497–1506.

Ralston, S.L., Pappalardo, L., Pelczer, I. and Spears4, P.F. (2011), *NMR-Based Metabonomic Analyses of Horse Serum: Detection of Metabolic Markers of*

Disease, available at: http://younghorse.rutgers.edu/RalstonetalRAAN2011.pdf (accessed 12 January 2019).

Ramella, N.A., Andújar, I., Ríos, J.L., Rosú, S.A., Tricerri, M.A. and Schinella, G.R. (2018), "Human apolipoprotein A-I Gly26Arg stimulation of inflammatory responses via NF-kB activation: Potential roles in amyloidosis?", *Pathophysiology : The Official Journal of the International Society for Pathophysiology*, available at:https://doi.org/10.1016/j.pathophys.2018.08.002.

Ranoa, D.R.E., Kelley, S.L. and Tapping, R.I. (2013), "Human lipopolysaccharide-binding protein (LBP) and CD14 independently deliver triacylated lipoproteins to Toll-like receptor 1 (TLR1) and TLR2 and enhance formation of the ternary signaling complex.", *The Journal of Biological Chemistry*, American Society for Biochemistry and Molecular Biology, Vol. 288 No. 14, pp. 9729–41.

Rattle, H. (1995), *An NMR Primer for Life Scientists*, Partnership Press, Fareham.

Rees, D.C., Johnson, E. and Lewinson, O. (2009), "ABC transporters: the power to change.", *Nature Reviews. Molecular Cell Biology*, NIH Public Access, Vol. 10 No. 3, pp. 218–27.

Reesink, H.L., Watts, A.E., Mohammed, H.O., Jay, G.D. and Nixon, A.J. (2017), "Lubricin/proteoglycan 4 increases in both experimental and naturally occurring equine osteoarthritis", *Osteoarthritis and Cartilage*, W.B. Saunders, Vol. 25 No. 1, pp. 128–137.

Rejnö, S. and Strömberg, B. (1978), "Osteochondrosis in the horse. II. Pathology.", *Acta Radiologica. Supplementum*, Vol. 358, pp. 153–78.

Reynard, L.N. and Loughlin, J. (2012), "Genetics and epigenetics of osteoarthritis", *Maturitas*, Vol. 71 No. 3, pp. 200–204.

Ribera, T., Monreal, L., Delgado, M.A., Ríos, J. and Prades, M. (2013), "Synovial fluid D-dimer concentration in horses with osteochondritis dissecans and osteoarthritis", *Veterinary and Comparative Orthopaedics and Traumatology*, Schattauer GmbH, Vol. 26 No. 01, pp. 54–60.

Righetti, P.G. and Boschetti, E. (2008), "The ProteoMiner and the FortyNiners: searching for gold nuggets in the proteomic arena", *Mass Spectrom Rev*, Vol. 27 No. 6, pp. 596–608.

Ritter, S.Y., Collins, J., Krastins, B., Sarracino, D., Lopez, M., Losina, E. and Aliprantis, A.O. (2014), "Mass spectrometry assays of plasma biomarkers to predict radiographic progression of knee osteoarthritis.", *Arthritis Research & Therapy*, BioMed Central, Vol. 16 No. 5, p. 456.

Ritter, S.Y., Subbaiah, R., Bebek, G., Crish, J., Scanzello, C.R., Krastins, B., Sarracino, D., *et al.* (2013), "Proteomic analysis of synovial fluid from the osteoarthritic

knee: comparison with transcriptome analyses of joint tissues.", *Arthritis and Rheumatism*, NIH Public Access, Vol. 65 No. 4, pp. 981–92.

Roberts, J.E., McLees, B.D. and Kerby, G.P. (1967), "Pathways of glucose metabolism in rheumatoid and nonrheumatoid synovial membrane.", *The Journal of Laboratory and Clinical Medicine*, Vol. 70 No. 3, pp. 503–11.

Robinson, C.S., Singer, E.R., Piviani, M. and Rubio-Martinez, L.M. (2017), "Are serum amyloid A or D-lactate useful to diagnose synovial contamination or sepsis in horses?", *The Veterinary Record*, BMJ Publishing Group, Vol. 181 No. 16, p. 425.

Roche, S., Tiers, L., Provansal, M., Piva, M.T. and Lehmann, S. (2006), "Interest of major serum protein removal for Surface-Enhanced Laser Desorption/Ionization - Time Of Flight (SELDI-TOF) proteomic blood profiling", *Proteome Sci*, Vol. 4, p. 20.

Rosen, E.P., Bokhart, M.T., Nazari, M. and Muddiman, D.C. (2015), "Influence of C-Trap Ion Accumulation Time on the Detectability of Analytes in IR-MALDESI MSI.", *Analytical Chemistry*, NIH Public Access, Vol. 87 No. 20, pp. 10483–90.

Rosenthal, A.K., Masuda, I., Gohr, C.M., Derfus, B.A. and Le, M. (2001), "The transglutaminase, Factor XIIIA, is present in articular chondrocytes", *Osteoarthritis and Cartilage*, W.B. Saunders, Vol. 9 No. 6, pp. 578–581.

Roughley, P.J., White, R.J., Cs-Szabó, G. and Mort, J.S. (1996), "Changes with age in the structure of fibromodulin in human articular cartilage", *Osteoarthritis and Cartilage*, W.B. Saunders, Vol. 4 No. 3, pp. 153–161.

Rousseau, J.C. and Delmas, P.D. (2007), "Biological markers in osteoarthritis", *Nat Clin Pract Rheumatol*, Vol. 3 No. 6, pp. 346–356.

Rousseau, J.C., Sornay-Rendu, E., Bertholon, C., Garnero, P. and Chapurlat, R. (2015), "Serum periostin is associated with prevalent knee osteoarthritis and disease incidence/progression in women: the OFELY study", *Osteoarthritis and Cartilage*, W.B. Saunders, Vol. 23 No. 10, pp. 1736–1742.

Rubio-Martínez, L.M., Elmas, C.R., Black, B. and Monteith, G. (2012), "Clinical use of antimicrobial regional limb perfusion in horses: 174 cases (1999–2009)", *Journal of the American Veterinary Medical Association*, Vol. 241 No. 12, pp. 1650–1658.

Ruiz-Romero, C. and Blanco, F.J. (2010), "Proteomics role in the search for improved diagnosis, prognosis and treatment of osteoarthritis", *Osteoarthritis Cartilage*, Vol. 18 No. 4, pp. 500–509.

Sakiniene, E., Bremell, T. and Tarkowski, A. (1999), "Complement depletion aggravates Staphylococcus aureus septicaemia and septic arthritis.", *Clinical and Experimental Immunology*, Wiley-Blackwell, Vol. 115 No. 1, pp. 95–102.

Salek, R.M., Steinbeck, C., Viant, M.R., Goodacre, R. and Dunn, W.B. (2013), "The role of reporting standards for metabolite annotation and identification in metabolomic studies.", *GigaScience*, Oxford University Press, Vol. 2 No. 1, p. 13.

Sánchez-Enríquez, S., Torres-Carrillo, N.M., Vázquez-Del Mercado, M., Salgado-Goytia, L., Rangel-Villalobos, H. and Muñoz-Valle, J.F. (2008), "Increase levels of apo-A1 and apo B are associated in knee osteoarthritis: lack of association with VEGF-460 T/C and +405 C/G polymorphisms", *Rheumatology International*, Springer-Verlag, Vol. 29 No. 1, pp. 63–68.

Sanchez-Teran, A.F., Bracamonte, J.L., Hendrick, S., Burguess, H.J., Duke-Novakovski, T., Schott, M., Hoff, B., *et al.* (2016), "Effect of Arthroscopic Lavage on Systemic and Synovial Fluid Serum Amyloid A in Healthy Horses", *Veterinary Surgery*, Wiley/Blackwell (10.1111), Vol. 45 No. 2, pp. 223–230.

Sanchez-Teran, A.F., Bracamonte, J.L., Hendrick, S., Riddell, L., Musil, K., Hoff, B. and Rubio-Martínez, L.M. (2016), "Effect of repeated through-and-through joint lavage on serum amyloid A in synovial fluid from healthy horses", *The Veterinary Journal*, W.B. Saunders, Vol. 210, pp. 30–33.

Sanchez, C., Deberg, M.A., Bellahcène, A., Castronovo, V., Msika, P., Delcour, J.P., Crielaard, J.M., *et al.* (2008), "Phenotypic characterization of osteoblasts from the sclerotic zones of osteoarthritic subchondral bone", *Arthritis & Rheumatism*, Wiley-Blackwell, Vol. 58 No. 2, pp. 442–455.

Sanchez Teran, A.F., Rubio-Martinez, L.M., Villarino, N.F. and Sanz, M.G. (2012), "Effects of repeated intra-articular administration of amikacin on serum amyloid A, total protein and nucleated cell count in synovial fluid from healthy horses.", *Equine Veterinary Journal. Supplement*, Vol. 44 No. 43, pp. 12–6.

Savage, C.J. (2008), "Urinary Clinical Pathologic Findings and Glomerular Filtration Rate in the Horse", *Veterinary Clinics of North America: Equine Practice*, Elsevier, Vol. 24 No. 2, pp. 387–404.

Savaryn, J.P., Toby, T.K. and Kelleher, N.L. (2016), "A researcher's guide to mass spectrometry-based proteomics.", *Proteomics*, NIH Public Access, Vol. 16 No. 18, pp. 2435–43.

Schiller, J., Arnhold, J., Sonntag, K. and Arnold, K. (1996), "NMR studies on human, pathologically changed synovial fluids: Role of hypochlorous acid", *Magnetic Resonance in Medicine*, John Wiley & Sons, Ltd, Vol. 35 No. 6, pp. 848–853.

Schiller, J., Huster, D., Fuchs, B., Naji, L., Kaufmann, J. and Arnold, K. (2004), "Evaluation of Cartilage Composition and Degradation by High-Resolution Magic-Angle Spinning Nuclear Magnetic Resonance", *Cartilage and Osteoarthritis*, Humana Press, New Jersey, pp. 267–286.

Schiller, J., Naji, L., Huster, D., Kaufmann, J. and Arnold, K. (2001), "1H and13C HR-

MAS NMR investigations on native and enzymatically digested bovine nasal cartilage", *Magma: Magnetic Resonance Materials in Physics, Biology, and Medicine*, Kluwer Academic Publishers, Vol. 13 No. 1, pp. 19–27.

Schiphof, D., Kerkhof, H.J.M., Damen, J., De Klerk, B.M., Hofman, A., Koes, B.W., Van Meurs, J.B.J., *et al.* (2013), "Factors for Pain in Patients With Different Grades of Knee Osteoarthritis", *Arthritis Care & Research*, Vol. 65 No. 5, pp. 695–702.

Schulz, T., Schumacher, U. and Prehm, P. (2007), "Hyaluronan export by the ABC transporter MRP5 and its modulation by intracellular cGMP.", *The Journal of Biological Chemistry*, American Society for Biochemistry and Molecular Biology, Vol. 282 No. 29, pp. 20999–1004.

Schumann, R., Rietschel, E. and Loppnow, H. (1994), "The role of CD14 and lipopolysaccharide-binding protein (LBP) in the activation of different cell types by endotoxin", *Medical Microbiology and Immunology*, Springer-Verlag, Vol. 183 No. 6, pp. 279–297.

Scott, D.L., Wolfe, F. and Huizinga, T.W. (2010), "Rheumatoid arthritis", *Lancet*, Vol. 376 No. 9746, pp. 1094–1108.

Scumaci, D., Oliva, A., Concolino, A., Curcio, A., Fiumara, C.V., Tammè, L., Campuzano, O., *et al.* (2018), "Integration of 'Omics' Strategies for Biomarkers Discovery and for the Elucidation of Molecular Mechanisms Underlying Brugada Syndrome", *PROTEOMICS - Clinical Applications*, Wiley-Blackwell, p. 1800065.

Seligner, B. and Kellner, R. (2006), "Biomarker Discovery in Renal Cell Carcinoma Applying Proteome-Based Studies in Combination with Serology", in Hamacher, M., Marcus, K., Stuhler, K., Van Hall, A., Warscheid, B. and Meyer, H.E. (Eds.), *Proteomics in Drug Research*, Wiley, Weinheim, p. 227.

Sellam, J. and Berenbaum, F. (2010), "The role of synovitis in pathophysiology and clinical symptoms of osteoarthritis", *Nature Reviews Rheumatology*, Nature Publishing Group, Vol. 6 No. 11, pp. 625–635.

de Seny, D., Cobraiville, G., Charlier, E., Neuville, S., Lutteri, L., Le Goff, C., Malaise, D., *et al.* (2015), "Apolipoprotein-A1 as a Damage-Associated Molecular Patterns Protein in Osteoarthritis: Ex Vivo and In Vitro Pro-Inflammatory Properties", edited by Feng, Y.*PLOS ONE*, Public Library of Science, Vol. 10 No. 4, p. e0122904.

Shahid, M. (2018), *Investigations on the Quantitative and Qualitative Protein Content in Serum and Synovial Fluid of Dogs with Osteoarthritis*, Freien Universität Berlin.

Shanfield, S., Campbell, P., Baumgarten, M., Bloebaum, R. and Sarmiento, A. (1988), "Synovial fluid osmolality in osteoarthritis and rheumatoid arthritis.", *Clinical Orthopaedics and Related Research*, No. 235, pp. 289–95.

Shen, Y., Jacobs, J.M., Camp 2nd, D.G., Fang, R., Moore, R.J., Smith, R.D., Xiao, W., *et al.* (2004), "Ultra-high-efficiency strong cation exchange LC/RPLC/MS/MS for high dynamic range characterization of the human plasma proteome", *Anal Chem*, Vol. 76 No. 4, pp. 1134–1144.

Shet, K., Siddiqui, S.M., Yoshihara, H., Kurhanewicz, J., Ries, M. and Li, X. (2012), "High-resolution magic angle spinning NMR spectroscopy of human osteoarthritic cartilage.", *NMR in Biomedicine*, NIH Public Access, Vol. 25 No. 4, pp. 538–44.

Shikhman, A.R., Brinson, D.C., Valbracht, J. and Lotz, M.K. (2001), "Cytokine regulation of facilitated glucose transport in human articular chondrocytes.", *Journal of Immunology (Baltimore, Md. : 1950)*, American Association of Immunologists, Vol. 167 No. 12, pp. 7001–8.

Shirtliff, M.E. and Mader, J.T. (2002), "Acute septic arthritis.", *Clinical Microbiology Reviews*, American Society for Microbiology (ASM), Vol. 15 No. 4, pp. 527–44.

Siepen, J.A., Keevil, E.-J., Knight, D. and Hubbard, S.J. (2007), "Prediction of missed cleavage sites in tryptic peptides aids protein identification in proteomics.", *Journal of Proteome Research*, Europe PMC Funders, Vol. 6 No. 1, pp. 399–408.

Silawal, S., Triebel, J., Bertsch, T. and Schulze-Tanzil, G. (2018), "Osteoarthritis and the Complement Cascade.", *Clinical Medicine Insights. Arthritis and Musculoskeletal Disorders*, SAGE Publications, Vol. 11, p. 1179544117751430.

da Silva, R.P., Clow, K., Brosnan, J.T. and Brosnan, M.E. (2014), "Synthesis of guanidinoacetate and creatine from amino acids by rat pancreas", *British Journal of Nutrition*, Cambridge University Press, Vol. 111 No. 04, pp. 571–577.

Silver, D.L., Wang, N., Xiao, X. and Tall, A.R. (2001), "High density lipoprotein (HDL) particle uptake mediated by scavenger receptor class B type 1 results in selective sorting of HDL cholesterol from protein and polarized cholesterol secretion.", *The Journal of Biological Chemistry*, Vol. 276 No. 27, pp. 25287–93.

Sinovich, M., Villarino, N., Singer, E., Robinson, C. and Rubio-Martinez, L. (2018), "Investigation of blood serum amyloid A concentrations in horses to differentiate synovial sepsis from inflammation and determine prognosis an response to treatment", *Veterinary Surgery*, Vol. 47, p. E26.

Skiöldebrand, E., Ekman, S., Mattsson Hultén, L., Svala, E., Björkman, K., Lindahl, A., Lundqvist, A., *et al.* (2017), "Cartilage oligomeric matrix protein neoepitope in the synovial fluid of horses with acute lameness: A new biomarker for the early stages of osteoarthritis", *Equine Veterinary Journal*, American Medical Association (AMA), Vol. 49 No. 5, pp. 662–667.

Skiöldebrand, E., Heinegård, D., Eloranta, M.-L., Nilsson, G., Dudhia, J., Sandgren, B. and Ekman, S. (2005), "Enhanced concentration of COMP (cartilage oligomeric matrix protein) in osteochondral fractures from racing Thoroughbreds",

Journal of Orthopaedic Research, John Wiley & Sons, Ltd, Vol. 23 No. 1, pp. 156–163.

Skiöldebrand, E., Lorenzo, P., Zunino, L., Rucklidge, G.J., Sandgren, B., Carlsten, J. and Ekman, S. (2001), "Concentration of collagen, aggrecan and cartilage oligomeric matrix protein (COMP) in synovial fluid from equine middle carpal joints.", *Equine Veterinary Journal*, Vol. 33 No. 4, pp. 394–402.

Snow, R.J. and Murphy, R.M. (2001), "Creatine and the creatine transporter: A review", *Molecular and Cellular Biochemistry*, Kluwer Academic Publishers, Vol. 224 No. 1/2, pp. 169–181.

So, A.K., Varisco, P.-A., Kemkes-Matthes, B., Herkenne-Morard, C., Chobaz-Peclat, V., Gerster, J.-C. and Busso, N. (2003), "Arthritis is linked to local and systemic activation of coagulation and fibrinolysis pathways", *Journal of Thrombosis and Haemostasis*, John Wiley & Sons, Ltd (10.1111), Vol. 1 No. 12, pp. 2510–2515.

Soul, J., Dunn, S.L., Anand, S., Serracino-Inglott, F., Schwartz, J.-M., Boot-Handford, R.P. and Hardingham, T.E. (2018), "Stratification of knee osteoarthritis: two major patient subgroups identified by genome-wide expression analysis of articular cartilage", *Annals of the Rheumatic Diseases*, BMJ Publishing Group Ltd, Vol. 77 No. 3, pp. 423–423.

de Sousa, E.B., Dos Santos, G.C., Duarte, M.E.L., Moura, V., Aguiar, D.P., Neto and Aguiar, D.P. (2017), "Metabolomics as a promising tool for early osteoarthritis diagnosis.", *Brazilian Journal of Medical and Biological Research = Revista Brasileira de Pesquisas Medicas e Biologicas*, Associação Brasileira de Divulgação Científica, Vol. 50 No. 11, p. e6485.

Sprangers, M.A., de Regt, E.B., Andries, F., van Agt, H.M., Bijl, R. V, de Boer, J.B., Foets, M., *et al.* (2000), "Which chronic conditions are associated with better or poorer quality of life?", *J Clin Epidemiol*, Vol. 53 No. 9, pp. 895–907.

Stack, J.D., Walshe, K., Steele, E., Cousty, M., Lechartier, A. and David, F. (2014), "Synovial Serum Amyloid A (SAA) Point-of-Care Test—A Valuable Aid to Immediate Diagnosis of Synovial Sepsis in Horses.", *Veterinary Surgery*, Vol. 43, p. E202.

Stashak, T.S. and Theoret, C. (2011), *Equine Wound Management*, John Wiley & Sons, available at: https://books.google.co.uk/books?id=XVwsA6d0INAC&pg=PT263&lpg=PT263&dq=equine+fibronectin+wound+management&source=bl&ots=0NdFYF3kav&sig=8jv-qPx68DTAiYcBBd4_IRuJKNo&hl=en&sa=X&ved=2ahUKEwiLmZm0m8HfAhWtzoUKHYQCAr0Q6AEwDXoECAMQAQ#v=onepage&q=equine fibronect (accessed 27 December 2018).

Stern, R. and Jedrzejas, M.J. (2006), "Hyaluronidases: their genomics, structures, and mechanisms of action.", *Chemical Reviews*, NIH Public Access, Vol. 106 No.

3, pp. 818–39.

Stevens, A.L., Wishnok, J.S., Chai, D.H., Grodzinsky, A.J. and Tannenbaum, S.R. (2008), “A sodium dodecyl sulfate-polyacrylamide gel electrophoresis-liquid chromatography tandem mass spectrometry analysis of bovine cartilage tissue response to mechanical compression injury and the inflammatory cytokines tumor necrosis factor α and interleukin”, *Arthritis & Rheumatism*, Wiley-Blackwell, Vol. 58 No. 2, pp. 489–500.

Stevens, A.L., Wishnok, J.S., White, F.M., Grodzinsky, A.J. and Tannenbaum, S.R. (2009), “Mechanical injury and cytokines cause loss of cartilage integrity and upregulate proteins associated with catabolism, immunity, inflammation, and repair.”, *Molecular & Cellular Proteomics : MCP*, American Society for Biochemistry and Molecular Biology, Vol. 8 No. 7, pp. 1475–89.

Struglics, A., Larsson, S., Pratta, M.A., Kumar, S., Lark, M.W. and Lohmander, L.S. (2006), “Human osteoarthritis synovial fluid and joint cartilage contain both aggrecanase- and matrix metalloproteinase-generated aggrecan fragments”, *Osteoarthritis Cartilage*, Vol. 14 No. 2, pp. 101–113.

Summerhays, G.E. (2000), “Treatment of traumatically induced synovial sepsis in horses with gentamicin-impregnated collagen sponges”, *Vet Rec*, Vol. 147 No. 7, pp. 184–188.

Sumner, L.W., Amberg, A., Barrett, D., Beale, M.H., Beger, R., Daykin, C.A., Fan, T.W., *et al.* (2007), “Proposed minimum reporting standards for chemical analysis Chemical Analysis Working Group (CAWG) Metabolomics Standards Initiative (MSI)”, *Metabolomics*, Vol. 3 No. 3, pp. 211–221.

Sundblad, L. (1950), “The Chemistry of Synovial Fluid with Special Regard to Hyaluronic Acid”, *Acta Orthopaedica Scandinavica*, Vol. 20 No. 2, pp. 105–113.

Svala, E., Jin, C., Rüetschi, U., Ekman, S., Lindahl, A., Karlsson, N.G. and Skiöldebrand, E. (2017), “Characterisation of lubricin in synovial fluid from horses with osteoarthritis”, *Equine Veterinary Journal*, American Medical Association (AMA), Vol. 49 No. 1, pp. 116–123.

Svala, E., Löfgren, M., Sihlbom, C., Rüetschi, U., Lindahl, A., Ekman, S. and Skiöldebrand, E. (2015), “An inflammatory equine model demonstrates dynamic changes of immune response and cartilage matrix molecule degradation in vitro”, *Connective Tissue Research*, Vol. 56 No. 4, pp. 315–325.

Swift, J. and Discher, D.E. (2014), “The nuclear lamina is mechano-responsive to ECM elasticity in mature tissue.”, *Journal of Cell Science*, Company of Biologists, Vol. 127 No. Pt 14, pp. 3005–15.

Szklarczyk, D., Franceschini, A., Wyder, S., Forslund, K., Heller, D., Huerta-Cepas, J., Simonovic, M., *et al.* (2015), “STRING v10: protein-protein interaction networks, integrated over the tree of life.”, *Nucleic Acids Research*, Oxford

University Press, Vol. 43 No. Database issue, pp. D447-52.

Tajika, Y., Moue, T., Ishikawa, S., Asano, K., Okumo, T., Takagi, H. and Hisamitsu, T. (2017), "Influence of Periostin on Synoviocytes in Knee Osteoarthritis.", *In Vivo (Athens, Greece)*, International Institute of Anticancer Research, Vol. 31 No. 1, pp. 69–77.

Takamatsu, A., Ohkawara, B., Ito, M., Masuda, A., Sakai, T., Ishiguro, N. and Ohno, K. (2014), "Verapamil Protects against Cartilage Degradation in Osteoarthritis by Inhibiting Wnt/β-Catenin Signaling", edited by Liu, C.*PLoS ONE*, Public Library of Science, Vol. 9 No. 3, p. e92699.

Tamer, T.M. (2013), "Hyaluronan and synovial joint: function, distribution and healing.", *Interdisciplinary Toxicology*, Slovak Toxicology Society, Vol. 6 No. 3, pp. 111–25.

Taylor, A.H., Mair, T.S., Smith, L.J. and Perkins, J.D. (2010), "Bacterial culture of septic synovial structures of horses: Does a positive bacterial culture influence prognosis?", *Equine Veterinary Journal*, American Medical Association (AMA), Vol. 42 No. 3, pp. 213–218.

Taylor, S.E., Weaver, M.P., Pitsillides, A.A., Wheeler, B.T., Wheeler-Jones, C.P.D., Shaw, D.J. and Smith, R.K.W. (2006), "Cartilage oligomeric matrix protein and hyaluronan levels in synovial fluid from horses with osteoarthritis of the tarsometatarsal joint compared to a control population.", *Equine Veterinary Journal*, Vol. 38 No. 6, pp. 502–7.

ThermoFisher. (n.d.). *Improved Sensitivity Through Enhanced Ion Transmission Using an S-Lens on the LTQ Velos Linear Ion Trap*, available at: www.thermo.com/velosPSB63058_E05/09S (accessed 6 January 2019).

Trumble, T.N., Brown, M.P., Merritt, K.A. and Billinghurst, R.C. (2008), "Joint dependent concentrations of bone alkaline phosphatase in serum and synovial fluids of horses with osteochondral injury: an analytical and clinical validation.", *Osteoarthritis and Cartilage*, Elsevier, Vol. 16 No. 7, pp. 779–86.

Trumble, T.N., Scarbrough, A.B. and Brown, M.P. (2009), "Osteochondral injury increases type II collagen degradation products (C2C) in synovial fluid of Thoroughbred racehorses.", *Osteoarthritis and Cartilage*, Elsevier, Vol. 17 No. 3, pp. 371–4.

Truong, L.-H., Kuliwaba, J.S., Tsangari, H. and Fazzalari, N.L. (2006), "Differential gene expression of bone anabolic factors and trabecular bone architectural changes in the proximal femoral shaft of primary hip osteoarthritis patients", *Arthritis Research & Therapy*, BioMed Central, London, Vol. 8 No. 6, pp. R188–R188.

Tseng, S., Reddi, A.H. and Di Cesare, P.E. (2009), "Cartilage Oligomeric Matrix Protein (COMP): A Biomarker of Arthritis.", *Biomarker Insights*, SAGE

Publications, Vol. 4, pp. 33–44.

Tulamo, R.-M., Bramlage, L.R. and Gabel, A.A. (1989), "The influence of corticosteroids on sequential clinical and synovial fluid parameters in joints with acute infectious arthritis in the horse", *Equine Veterinary Journal*, Blackwell Publishing Ltd, Vol. 21 No. 5, pp. 332–337.

Turlo, A.J., Cywinska, A., Rosevear, P., Eghbalnia, H., McIlwraith, C.W. and Frisbie, D.D. (2018), "Detecting biomarkers of musculoskeletal injury in racing Thoroughbreds with nuclear magnetic resonance metabolomics", *Equine Veterinary Journal*, American Medical Association (AMA), Vol. 50, p. 26.

Turmezei, T.D., Fotiadou, A., Lomas, D.J., Hopper, M.A. and Poole, K.E.S. (2014), "A new CT grading system for hip osteoarthritis", *Osteoarthritis and Cartilage*, W.B. Saunders, Vol. 22 No. 10, pp. 1360–1366.

Valenti, P. and Antonini, G. (2005), "Lactoferrin: an important host defence against microbial and viral attack", *Cellular and Molecular Life Sciences*, Birkhäuser-Verlag, Vol. 62 No. 22, pp. 2576–2587.

Vizcaíno, J.A., Csordas, A., del-Toro, N., Dianes, J.A., Griss, J., Lavidas, I., Mayer, G., *et al.* (2016), "2016 update of the PRIDE database and its related tools.", *Nucleic Acids Research*, Oxford University Press, Vol. 44 No. D1, pp. D447-56.

Wadhwa, S., Embree, M.C., Kilts, T., Young, M.F. and Ameye, L.G. (2005), "Accelerated osteoarthritis in the temporomandibular joint of biglycan/fibromodulin double-deficient mice", *Osteoarthritis and Cartilage*, W.B. Saunders, Vol. 13 No. 9, pp. 817–827.

Wang, J., Markova, D., Anderson, D.G., Zheng, Z., Shapiro, I.M. and Risbud, M. V. (2011), "TNF-α and IL-1β promote a disintegrin-like and metalloprotease with thrombospondin type I motif-5-mediated aggrecan degradation through syndecan-4 in intervertebral disc.", *The Journal of Biological Chemistry*, American Society for Biochemistry and Molecular Biology, Vol. 286 No. 46, pp. 39738–49.

Wang, X., Zhang, A., Han, Y., Wang, P., Sun, H., Song, G., Dong, T., *et al.* (2012), "Urine metabolomics analysis for biomarker discovery and detection of jaundice syndrome in patients with liver disease", *Mol Cell Proteomics*, Vol. 11 No. 8, pp. 370–380.

Wang, Z., Chen, Z., Yang, S., Wang, Y., Yu, L., Zhang, B., Rao, Z., *et al.* (2012), "(1)H NMR-based metabolomic analysis for identifying serum biomarkers to evaluate methotrexate treatment in patients with early rheumatoid arthritis", *Exp Ther Med*, Vol. 4 No. 1, pp. 165–171.

Washington, W.L. (1980), "Role of synovial fluid lactate in the immediate diagnosis of septic arthritis (abstract)", *Clin Res*, Vol. 28 No. 791A.

Weinberg, J.B., Pippen, A.M.M. and Greenberg, C.S. (1991), “Extravascular fibrin formation and dissolution in synovial tissue of patients with osteoarthritis and rheumatoid arthritis”, *Arthritis & Rheumatism*, John Wiley & Sons, Ltd, Vol. 34 No. 8, pp. 996–1005.

Wen, Z.-H., Chang, Y.-C. and Jean, Y.-H. (2015), “Excitatory amino acid glutamate: role in peripheral nociceptive transduction and inflammation in experimental and clinical osteoarthritis”, *Osteoarthritis and Cartilage*, Vol. 23 No. 11, pp. 2009–2016.

Westacott, C.I., Whicher, J.T., Barnes, I.C., Thompson, D., Swan, A.J. and Dieppe, P.A. (1990), “Synovial fluid concentration of five different cytokines in rheumatic diseases.”, *Annals of the Rheumatic Diseases*, BMJ Publishing Group Ltd, Vol. 49 No. 9, pp. 676–81.

Wilkins, M.R., Pasquali, C., Appel, R.D., Ou, K., Golaz, O., Sanchez, J.-C., Yan, J.X., *et al.* (1996), “From Proteins to Proteomes: Large Scale Protein Identification by Two-Dimensional Electrophoresis and Arnino Acid Analysis”, *Nature Biotechnology*, Nature Publishing Group, Vol. 14 No. 1, pp. 61–65.

Williams, A. (2014), *Proteomic Studies of an Explant Model of Equine Articular Cartilage in Response to Proinflammatory and Anti-Inflammatory Stimuli*, University of Nottingham, available at: http://eprints.nottingham.ac.uk/14371/1/AdamWilliams_Corrected_Thesis_Final.pdf.

Wluka, A.E., Lombard, C.B. and Cicuttini, F.M. (2013), “Tackling obesity in knee osteoarthritis”, *Nature Reviews Rheumatology*, Nature Publishing Group, Vol. 9 No. 4, pp. 225–235.

Wojdasiewicz, P., Poniatowski, Ł.A. and Szukiewicz, D. (2014), “The role of inflammatory and anti-inflammatory cytokines in the pathogenesis of osteoarthritis.”, *Mediators of Inflammation*, Hindawi, Vol. 2014, p. 561459.

Worley, B. and Powers, R. (2013), “Multivariate Analysis in Metabolomics”, *Current Metabolomics*, Vol. 1 No. 1, pp. 92–107.

Wright, H.L., Bucknall, R.C., Moots, R.J. and Edwards, S.W. (2012), “Analysis of SF and plasma cytokines provides insights into the mechanisms of inflammatory arthritis and may predict response to therapy.”, *Rheumatology (Oxford, England)*, Vol. 51, pp. 451–459.

Wright, H.L., Moots, R.J. and Edwards, S.W. (2014), “The multifactorial role of neutrophils in rheumatoid arthritis”, *Nat Rev Rheumatol*, Vol. 10 No. 10, pp. 593–601.

Wright, I. and Minshall, G. (2005), “Diagnosis and treatment of equine osteochondrosis”, *In Practice*, British Medical Journal Publishing Group, Vol. 27 No. 6, pp. 302–309.

Wu, Z., Huang, J., Huang, J., Li, Q. and Zhang, X. (2018), "Lys-C/Arg-C, a More Specific and Efficient Digestion Approach for Proteomics Studies", *Analytical Chemistry*, American Chemical Society, Vol. 90 No. 16, pp. 9700–9707.

Xia, B., Di Chen, Zhang, J., Hu, S., Jin, H. and Tong, P. (2014), "Osteoarthritis Pathogenesis: A Review of Molecular Mechanisms", *Calcified Tissue International*, Vol. 95 No. 6, pp. 495–505.

Xia, J., Fjell, C.D., Mayer, M.L., Pena, O.M., Wishart, D.S. and Hancock, R.E.W. (2013), "INMEX--a web-based tool for integrative meta-analysis of expression data.", *Nucleic Acids Research*, Oxford University Press, Vol. 41 No. Web Server issue, pp. W63-70.

Xia, J., Wishart, D.S., Xia, J. and Wishart, D.S. (2016), "Using MetaboAnalyst 3.0 for Comprehensive Metabolomics Data Analysis", *Current Protocols in Bioinformatics*, John Wiley & Sons, Inc., Hoboken, NJ, USA, p. 14.10.1-14.10.91.

Yahia, D. and El-Hakiem, M. (2014), "Biochemical Analysis of Synovial Fluid, Cerebrospinal Fluid and Vitreous Humor at Early Postmortem Intervals in Donkeys", *Journal of Advanced Veterinary Research*, Vol. 4 No. 1, pp. 6–11.

Yamanokuchi, K., Tagami, M., Nishimatsu, E., Shimizu, Y., Hirose, Y., Komatsu, K. and Misumi, K. (2009), "Sandwich ELISA system for cartilage oligomeric matrix protein in equine synovial fluid and serum", *Equine Veterinary Journal*, American Medical Association (AMA), Vol. 41 No. 1, pp. 41–46.

Yang, G., Zhang, H., Chen, T., Zhu, W., Ding, S., Xu, K., Xu, Z., *et al.* (2016), "Metabolic analysis of osteoarthritis subchondral bone based on UPLC/Q-TOF-MS", *Anal Bioanal Chem*, Vol. 408 No. 16, pp. 4275–4286.

Yang, M., Liu, Y., Dai, J., Li, L., Ding, X., Xu, Z., Mori, M., *et al.* (2018), "Apolipoprotein A-II induces acute-phase response associated AA amyloidosis in mice through conformational changes of plasma lipoprotein structure.", *Scientific Reports*, Nature Publishing Group, Vol. 8 No. 1, p. 5620.

Ye, Q., Zheng, Y., Fan, S., Qin, Z. and Li, N. (2014), "Lactoferrin Deficiency Promotes Colitis-Associated Colorectal Dysplasia in Mice", *PLoS ONE*, Vol. 9 No. 7, pp. 111–113.

Yin, H.L., Kwiatkowski, D.J., Mole, J.E. and Cole, F.S. (1984), "Structure and biosynthesis of cytoplasmic and secreted variants of gelsolin.", *The Journal of Biological Chemistry*, Vol. 259 No. 8, pp. 5271–6.

Young, S.P., Kapoor, S.R., Viant, M.R., Byrne, J.J., Filer, A., Buckley, C.D., Kitas, G.D., *et al.* (2013), "The impact of inflammation on metabolomic profiles in patients with arthritis", *Arthritis Rheum*, Vol. 65 No. 8, pp. 2015–2023.

Ytrehus, B., Carlson, C.S. and Ekman, S. (2007), "Etiology and Pathogenesis of Osteochondrosis", *Veterinary Pathology*, SAGE PublicationsSage CA: Los

Angeles, CA, Vol. 44 No. 4, pp. 429–448.

Zhai, G., Wang-Sattler, R., Hart, D.J., Arden, N.K., Hakim, A.J., Illig, T. and Spector, T.D. (2010), "Serum branched-chain amino acid to histidine ratio: a novel metabolomic biomarker of knee osteoarthritis.", *Annals of the Rheumatic Diseases*, BMJ Publishing Group Ltd, Vol. 69 No. 6, pp. 1227–31.

Zhang, C., Li, Y., Tang, W., Kamiya, N. and Kim, H. (2013), "Lactoferrin activates BMP7 gene expression through the mitogen-activated protein kinase ERK pathway in articular cartilage", *Biochemical and Biophysical Research Communications*, Vol. 431, pp. 31–35.

Zhang, W., Likhodii, S., Zhang, Y., Aref-Eshghi, E., Harper, P.E., Randell, E., Green, R., *et al.* (2014), "Classification of osteoarthritis phenotypes by metabolomics analysis", *BMJ Open*, Vol. 4 No. 11, p. e006286.

Zhang, W., Sun, G., Likhodii, S., Liu, M., Aref-Eshghi, E., Harper, P.E., Martin, G., *et al.* (2016), "Metabolomic analysis of human plasma reveals that arginine is depleted in knee osteoarthritis patients", *Osteoarthritis and Cartilage*, W.B. Saunders, Vol. 24 No. 5, pp. 827–834.

Zhang, Y., Vasheghani, F., Li, Y.-H., Blati, M., Simeone, K., Fahmi, H., Lussier, B., *et al.* (2015), "Cartilage-specific deletion of mTOR upregulates autophagy and protects mice from osteoarthritis.", *Annals of the Rheumatic Diseases*, BMJ Publishing Group Ltd, Vol. 74 No. 7, pp. 1432–40.

Zhao, X. (2011), "Protein Structure Determination by Solid-State NMR", Springer, Berlin, Heidelberg, pp. 187–213.

Zheng, K., Shen, N., Chen, H., Ni, S., Zhang, T., Hu, M., Wang, J., *et al.* (2017), "Global and targeted metabolomics of synovial fluid discovers special osteoarthritis metabolites", *Journal of Orthopaedic Research*, Wiley-Blackwell, Vol. 35 No. 9, pp. 1973–1981.

Zhou, J., Chen, J., Hu, C., Xie, Z., Li, H., Wei, S., Wang, D., *et al.* (2016), "Exploration of the serum metabolite signature in patients with rheumatoid arthritis using gas chromatography-mass spectrometry", *J Pharm Biomed Anal*, Vol. 127, pp. 60–67.

Zhou, M., Lucas, D.A., Chan, K.C., Issaq, H.J., Petricoin 3rd, E.F., Liotta, L.A., Veenstra, T.D., *et al.* (2004), "An investigation into the human serum 'interactome'", *Electrophoresis*, Vol. 25 No. 9, pp. 1289–1298.

Zhou, Y., Wang, T., Hamilton, J.L. and Chen, D. (2017), "Wnt/β-catenin Signaling in Osteoarthritis and in Other Forms of Arthritis.", *Current Rheumatology Reports*, NIH Public Access, Vol. 19 No. 9, p. 53.

Zrimsek, P., Kadunc Kos, V., Mrkun, J. and Kosec, M. (2007), "Diagnostic Value of Matrix Metalloproteinases MMP-2 and MMP-9 in Synovial Fluid for Identifying

Osteoarthritis in the Distal Interphalangeal Joint in Horses", *Acta Veterinaria Brno*, Vol. 76, pp. 87–95.

Publications

Anderson, J.R., Smagul, A., Simpson, D., Clegg, P.D., Rubio-Martinez, L.M. and Peffers, M.J. (2019), "The synovial fluid proteome differentiates between septic and nonseptic articular pathologies", *Journal of Proteomics*, Elsevier, Vol. 202, p. 103370. https://doi.org/10.1016/j.jprot.2019.04.020

Peffers, M.J., Smagul, A. and **Anderson, J.R.** (2019), "Proteomic analysis of synovial fluid: current and potential uses to improve clinical outcomes", *Expert Review of Proteomics*, Taylor & Francis, Vol. 16 No. 4, pp. 287–302. https://doi.org/10.1080/14789450.2019.1578214

Anderson, J.R., Chokesuwattanaskul, S., Phelan, M.M., Welting, T.J.M., Lian, L.-Y., Peffers, M.J. and Wright, H.L. (2018), "^{1}H NMR Metabolomics Identifies Underlying Inflammatory Pathology in Osteoarthritis and Rheumatoid Arthritis Synovial Joints", *Journal of Proteome Research*, American Chemical Society, Vol. 17 No. 11, pp. 3780–3790. https://doi.org/10.1021/acs.jproteome.8b00455

Anderson, J.R., Phelan, M.M., Clegg, P.D., Peffers, M.J. and Rubio-Martinez, L.M. (2018), "Synovial Fluid Metabolites Differentiate between Septic and Nonseptic Joint Pathologies", *Journal of Proteome Research*, American Chemical Society, Vol. 17 No. 8, pp. 2735–2743. https://doi.org/10.1021/acs.jproteome.8b00190

Peffers, M., Jones, A.R., McCabe, A. and **Anderson, J.** (2017), "Neopeptide Analyser: A software tool for neopeptide discovery in proteomics data", *Wellcome Open Research*, Vol. 2, p. 24. https://doi.org/10.12688/wellcomeopenres.11275.1

Journal of Proteomics 202 (2019) 103370

Contents lists available at ScienceDirect

Journal of Proteomics

journal homepage: www.elsevier.com/locate/jprot

The synovial fluid proteome differentiates between septic and nonseptic articular pathologies

James R. Anderson[a], Aibek Smagul[a], Deborah Simpson[b], Peter D. Clegg[a], Luis M. Rubio-Martinez[c,1], Mandy J. Peffers[a,*,1]

[a] Institute of Ageing and Chronic Disease, William Henry Duncan Building, 6 West Derby Street, Liverpool L7 8TX, UK
[b] Centre for Proteome Research, Institute of Integrative Biology, Biosciences Building, Crown Street, University of Liverpool, Liverpool L69 7ZB, UK
[c] Department of Equine Clinical Studies, Institute of Veterinary Science, Chester High Road, Neston CH64 7TE, UK

ARTICLE INFO

Keywords:
Synovial fluid
Arthropathy
Osteochondrosis
Osteoarthritis
Synovial sepsis,110 equine

ABSTRACT

Articular conditions are common in horses and can result in loss of function, chronic pain and/or inability to work. Common conditions include osteoarthritis, osteochondrosis and synovial sepsis, which can be life-threatening, but despite the high clinical prevalence of these conditions, rapid and specific diagnosis, monitoring and prognostication remains a challenge for practicing veterinarians. Synovial fluid from a range of arthropathies was enriched for low abundance proteins using combinatorial peptide ligand ProteoMiner™ beads and analysed via liquid chromatography-tandem mass spectrometry. Changes in protein abundances were analysed using label-free quantification. Principle component analysis of differentially expressed proteins identified groupings associated with joint pathology. Findings were validated using ELISA. Lactotransferrin (LTF) abundance was increased in sepsis compared to all other groups and insulin-like growth factor-binding protein 6 (IGFBP6) abundance decreased in sepsis compared to other disease groups. Pathway analysis identified upregulation of the complement system in synovial joint sepsis and the downregulation of eukaryotic translation initiation factors and mTOR signalling pathways in both OA and OC compared to the healthy group. Overall, we have identified a catalogue of proteins which we propose to be involved in osteoarthritis, osteochondrosis and synovial sepsis pathogenesis.

Significance: Osteoarthritis, osteochondrosis and synovial sepsis, which can be life-threatening, are common articular conditions in which rapid and specific diagnosis, monitoring and prognostication remains a challenge for practicing veterinarians. This study has identified that the equine synovial fluid proteome exhibits distinctive profile changes between osteoarthritis, osteochondrosis, synovial sepsis and healthy joints. Elevated synovial abundance of lactotransferrin and decreased insulin-like growth factor-binding protein 6 were both found to distinguish synovial sepsis from all other study groups. Thus, these protein markers may have a future role in clinical practice to enable an earlier and reliable diagnosis of synovial sepsis.

1. Introduction

Articular conditions are common in horses and can result in loss of function, chronic pain and/or inability to work, which are important welfare concerns. The most common conditions include osteoarthritis (OA), osteochondrosis (OC) and synovial sepsis, which can be life-threatening [1]. Despite the high clinical prevalence of these conditions, rapid and specific diagnosis, monitoring and prognostication remains a challenge for practicing veterinarians, thus, identification of reliable biomarkers of disease is required. Synovial fluid (SF) is in direct contact with articular structures and represents an important source of biomarker discovery. SF is located within the articular joint cavity, providing a pool of nutrients for surrounding tissues but primarily serving as a biological lubricant, containing molecules including hyaluronan with low-friction and low-wear properties to articular surfaces [2]. As SF is in close proximity to articular tissues primarily altered during joint pathology, this biofluid is an important first approach source for biomarker discovery [3,4].

Total protein content in synovial fluid is associated with presence of articular pathology and is one of the parameters most commonly used

* Corresponding author.
E-mail addresses: janders@liverpool.ac.uk (J.R. Anderson), aibek@liverpool.ac.uk (A. Smagul), dsimpson@liverpool.ac.uk (D. Simpson), pclegg@liverpool.ac.uk (P.D. Clegg), lrubio@liverpool.ac.uk (L.M. Rubio-Martinez), peffs@liv.ac.uk, peffs@liverpool.ac.uk (M.J. Peffers).
[1] Joint last author.

https://doi.org/10.1016/j.jprot.2019.04.020
Received 7 January 2019; Received in revised form 28 March 2019; Accepted 22 April 2019
Available online 25 April 2019

Journal of proteome research

Article

Cite This: J. Proteome Res. 2018, 17, 3780−3790

pubs.acs.org/jpr

^{1}H NMR Metabolomics Identifies Underlying Inflammatory Pathology in Osteoarthritis and Rheumatoid Arthritis Synovial Joints

James R. Anderson,[†,#] Susama Chokesuwattanaskul,[‡,§,#] Marie M. Phelan,[‡,∥] Tim J. M. Welting,[⊥] Lu-Yun Lian,[‡] Mandy J. Peffers,[†] and Helen L. Wright*[,†]

[†]Institute of Ageing and Chronic Disease, University of Liverpool, Liverpool L7 8TX, U.K.

[‡]Institute of Integrative Biology, University of Liverpool, Liverpool L69 7ZB, U.K.

[§]Chulalongkorn University, Bangkok 10330, Thailand

[∥]HLS Technology Directorate, University of Liverpool, Liverpool L7 8TX, U.K.

[⊥]Laboratory for Experimental Orthopedics, Department of Orthopedic Surgery, Maastricht University Medical Centre, 6229 HX Maastricht, The Netherlands

Supporting Information

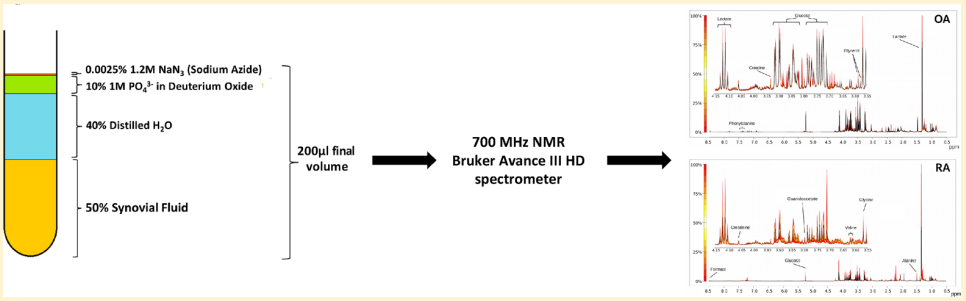

ABSTRACT: Despite osteoarthritis (OA) and rheumatoid arthritis (RA) being typically age-related, their underlying etiologies are markedly different. We used ^{1}H nuclear magnetic resonance (NMR) spectroscopy to identify differences in metabolite profiles in low volumes of OA and RA synovial fluid (SF). SF was aspirated from knee joints of 10 OA and 14 RA patients. 100 μL SF was analyzed using a 700 MHz Avance IIIHD Bruker NMR spectrometer with a TCI cryoprobe. Spectra were analyzed by Chenomx, Bruker TopSpin and AMIX software. Statistical analysis was undertaken using Metaboanalyst. 50 metabolites were annotated, including amino acids, saccharides, nucleotides and soluble lipids. Discriminant analysis identified group separation between OA and RA cohorts, with 32 metabolites significantly different between OA and RA SF (false discovery rate (FDR) < 0.05). Metabolites of glycolysis and the tricarboxylic acid cycle were lower in RA compared to OA; these results concur with higher levels of inflammation, synovial proliferation and hypoxia found in RA compared to OA. Elevated taurine in OA may indicate increased subchondral bone sclerosis. We demonstrate that quantifiable differences in metabolite abundance can be measured in low volumes of SF by ^{1}H NMR spectroscopy, which may be clinically useful to aid diagnosis and improve understanding of disease pathogenesis.

KEYWORDS: *synovial fluid, metabolomics, osteoarthritis, rheumatoid arthritis, nuclear magnetic resonance*

INTRODUCTION

Osteoarthritis (OA) and rheumatoid arthritis (RA) are the two most common forms of arthritis, which lead to significant disability and substantial reduction in quality of life.[1,2] Despite both these chronic conditions being typically age-related with insidious onset, their underlying etiologies are markedly different.[3,4] OA is a degenerative joint condition, primarily affecting the hands, hips and knees, with one-third of people in the UK aged over 45 (approximately 8.75 million) requiring treatment.[5] This disease is characterized by articular cartilage loss, synovial membrane dysfunction, subchondral bone sclerosis and osteophyte formation with the depletion of matrix proteins driven by proteases including multiple matrix metalloproteinases (MMPs) and a disintegrin and metalloproteinase with thrombospondin motifs (ADAMTSs[6−8]). We have identified OA synovial fluid (SF) to be enriched in a number of proteins including S100-A10, Collagen type I and CD109.[9] RA is a systemic, inflammatory autoimmune disease that primarily affects the synovium of joints,[10] presenting as a symmetric polyarthritis with an estimated prevalence of 0.5−1% of the adult population within developed countries.[11,12] RA joints

Received: June 14, 2018
Published: September 19, 2018

DOI: 10.1021/acs.jproteome.8b00455
J. Proteome Res. 2018, 17, 3780−3790

Journal of proteome research

Article

Cite This: J. Proteome Res. 2018, 17, 2735−2743

pubs.acs.org/jpr

Synovial Fluid Metabolites Differentiate between Septic and Nonseptic Joint Pathologies

James R. Anderson,[†] Marie M. Phelan,[‡,§] Peter D. Clegg,[†] Mandy J. Peffers,[*,†] and Luis M. Rubio-Martinez[*,⊥]

[†]Institute of Ageing and Chronic Disease, University of Liverpool, Liverpool L7 8TX, U.K.

[‡]Institute of Integrative Biology, University of Liverpool, Liverpool L69 7ZB, U.K.

[§]HLS Technology Directorate, University of Liverpool, Liverpool L69 3GB, U.K.

[⊥]Institute of Veterinary Science, University of Liverpool, Leahurst Campus, Neson CH64 7TE, U.K.

Supporting Information

ABSTRACT: Osteoarthritis (OA), osteochondrosis (OC), and synovial sepsis in horses cause loss of function and pain. Reliable biomarkers are required to achieve accurate and rapid diagnosis, with synovial fluid (SF) holding a unique source of biochemical information. Nuclear magnetic resonance (NMR) spectroscopy allows global metabolite analysis of a small volume of SF, with minimal sample preprocessing using a noninvasive and nondestructive method. Equine SF metabolic profiles from both nonseptic joints (OA and OC) and septic joints were analyzed using 1D ^{1}H NMR spectroscopy. Univariate and multivariate statistical analyses were used to identify differential metabolite abundance between groups. Metabolites were annotated via ^{1}H NMR using 1D NMR identification software Chenomx, with identities confirmed using 1D ^{1}H and 2D ^{1}H ^{13}C NMR. Multivariate analysis identified separation between septic and nonseptic groups. Acetate, alanine, citrate, creatine phosphate, creatinine, glucose, glutamate, glutamine, glycine, phenylalanine, pyruvate, and valine were higher in the nonseptic group, while glycylproline was higher in sepsis. Multivariate separation was primarily driven by glucose; however, partial-least-squares discriminant analysis plots with glucose excluded demonstrated the remaining metabolites were still able to discriminate the groups. This study demonstrates that a panel of synovial metabolites can distinguish between septic and nonseptic equine SF, with glucose the principal discriminator.

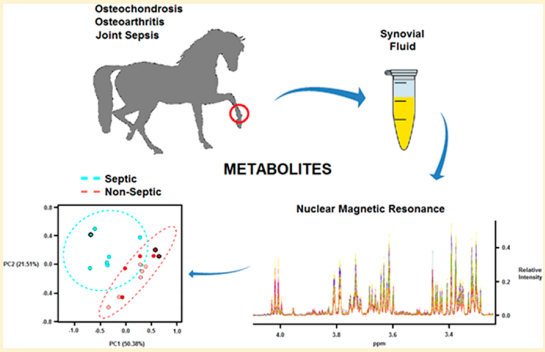

KEYWORDS: *metabolomics, equine, synovial fluid, osteoarthritis, osteochondrosis, sepsis, nuclear magnetic resonance*

INTRODUCTION

Conditions affecting the articular joints are common in horses resulting in loss of function, chronic pain, or subsequent inability to work, all of which represent economic and welfare concerns. These pathologies include osteoarthritis (OA), osteochondrosis (OC), and synovial sepsis, which can be life-threatening.[1] Despite these conditions having a high prevalence and clinical relevance, diagnosis, staging, monitoring, and determination of an accurate prognosis remain challenging for practising veterinarians. Therefore, to differentiate equine articular joint pathologies, there is a need to identify reliable biomarkers of disease. Synovial fluid (SF) is located within the articular joint cavity, providing a pool of nutrients for surrounding tissues but primarily serving as a biological lubricant, containing molecules with low-friction and low-wear properties to articular surfaces.[2] As SF is in close proximity to articular tissues primarily altered during joint pathology, this biofluid is an important source of biomarker discovery.[3,4]

To date, no validated markers that are both sensitive and specific to synovial sepsis have been identified within veterinary medicine, making early diagnosis a challenge. Together with clinical examination, diagnosis is based on SF culture and intracellular bacteria identification (both low sensitivity) as well as total protein, total nucleated cell count, and percentage of neutrophils whose results are open to interpretation and are affected by standard treatment protocols.[5−8] Reduced levels of glucose in human and equine SF, due to an increase in synovial and neutrophil cell glycolytic activity in severe inflammation or infection, have previously been identified, with a serum-synovial glucose difference of >2.2 mmol/L considered supportive of a diagnosis of synovial sepsis.[9,10] However, this parameter is nonspecific and can be influenced by multiple variables including synovial necrosis, diet, pain and white blood cell count. Elevations in lactate during the acute infection phase have previously been identified in SF of septic human, canine, and equine joints due to an increase in the consumption of glucose and subsequent production of lactate within an anaerobic environment.[11−13]

Received: March 21, 2018
Published: July 3, 2018

DOI: 10.1021/acs.jproteome.8b00190
J. Proteome Res. 2018, 17, 2735−2743

SOFTWARE TOOL ARTICLE

Neopeptide Analyser: A software tool for neopeptide discovery in proteomics data [version 1; referees: 2 approved]

Mandy Peffers [1], Andrew R. Jones[2], Antony McCabe[2], James Anderson[1]

[1]Institute of Ageing and Chronic Disease, University of Liverpool, Liverpool, L7 9TX, UK
[2]Institute of Integrative Biology, University of Liverpool, Liverpool, L69 7ZB, UK

v1 **First published:** 07 Apr 2017, **2**:24 (doi: 10.12688/wellcomeopenres.11275.1)
Latest published: 07 Apr 2017, **2**:24 (doi: 10.12688/wellcomeopenres.11275.1)

Abstract

Experiments involving mass spectrometry (MS)-based proteomics are widely used for analyses of connective tissues. Common examples include the use of relative quantification to identify differentially expressed peptides and proteins in cartilage and tendon. We are working on characterising so-called 'neopeptides', i.e. peptides formed due to native cleavage of proteins, for example under pathological conditions. Unlike peptides typically quantified in MS workflows due to the *in vitro* use of an enzyme such as trypsin, a neopeptide has at least one terminus that was not due to the use of trypsin in the workflow. The identification of neopeptides within these datasets is important in understanding disease pathology, and the development of antibodies that could be utilised as diagnostic biomarkers for diseases, such as osteoarthritis, and targets for novel treatments. Our previously described neopeptide data analysis workflow was laborious and was not amenable to robust statistical analysis, which reduced confidence in the neopeptides identified. To overcome this, we developed 'Neopeptide Analyser', a user friendly neopeptide analysis tool used in conjunction with label-free MS quantification tool Progenesis QIP for proteomics. Neopeptide Analyser filters data sourced from Progenesis QIP output to identify neopeptide sequences, as well as give the residues that are adjacent to the peptide in its corresponding protein sequence. It also produces normalised values for the neopeptide quantification values and uses these to perform statistical tests, which are also included in the output. Neopeptide Analyser is available as a Java application for Mac, Windows and Linux. The analysis features and ease of use encourages data exploration, which could aid the discovery of novel pathways in extracellular matrix degradation, the identification of potential biomarkers and as a tool to investigate matrix turnover. Neopeptide Analyser is available from https://github.com/PGB-LIV/neo-pep-tool/releases/.

Open Peer Review

Referee Status: ✓ ✓

	Invited Referees 1	2
version 1 published 07 Apr 2017	✓ report	✓ report

1 **Timothy E. Hardingham**, University of Manchester UK, **Jamie Soul**, University of Manchester UK

2 **Stephanie G. Dakin**, University of Oxford UK

Discuss this article

Comments (0)